PERFORMANCE OPTIMIZATION OF BLENDED BIOMASS PELLETS FROM CORN STOVER AND EUCALYPTUS SAWDUST USING LINEAR LOW-DENSITY POLYETHYLENE AS A BINDER

BY LAZARUS KIPROP LIMO

A THESIS SUBMITTED TO THE DEPARTMENT OF

MANUFACTURING, INDUSTRIAL AND TEXTILE ENGINEERING

SCHOOL OF ENGINEERING IN PARTIAL FULFILLMENT OF THE

REQUIREMENTS FOR THE DEGREE OF DOCTOR OF PHILOSOPHY

IN INDUSTRIAL ENGINEERING

MOI UNIVERSITY

DECLARATION

Declaration by the Candidate

This thesis is my original work and has not been presented at any other university for
the award of a doctoral degree or any other degree. No part of this thesis can be
reproduced without prior written permission from the author and/or Moi University.
Sign: Date:
Limo, Lazarus Kiprop
PHD/IE/5312/22
Declaration by the Supervisors
This thesis has been submitted for examination with our approval as University
Supervisors.
Sign: Date:
Prof. Diana Madara
Department of Manufacturing, Industrial and Textile Engineering
School of Engineering
Moi University,
Eldoret - Kenya.
Sign: Date:
Dr. Jerry Ochola
Department of Manufacturing, Industrial and Textile Engineering
School of Engineering
Moi University,
Eldoret - Kenya.

DEDICATION

To my family, who have continuously encouraged and supported me throughout this research.

ACKNOWLEDGEMENTS

My sincere thanks go to our omnipotent God, who has guided me this far and blessed me abundantly in my research. My supervisors, Prof. Diana Madara and Dr. Jerry Ochola, deserve special thanks for their advice as I continue with my research. I appreciate the technical staff at the Moi University departments of mechanical, production & energy engineering and manufacturing, textiles, and industrial engineering as well as KIRDI Nairobi for their guidance on how to conduct pellet production and testing and the best equipment to use given their availability and functional status. I would also like to express my sincere gratitude to the Manufacturing, Industrial and Textile Engineering Department staff, as well as to my fellow students, friends, and the school administration as a whole for their unwavering support throughout my PhD studies. Finally, special thanks go to Africa Centre of Excellence II (ACEII) for their full sponsorship of my PhD study.

ABSTRACT

Two significant biomass waste streams that are frequently disposed or underutilized are corn stovers and eucalyptus sawdust. Little research has been done on the impact of linear low-density polyethylene (LLDPE) binder on the qualities of blended pellets. Therefore, the main objective of this research was to undertake performance optimization of blended biomass pellets from corn stover and eucalyptus sawdust using linear low-density polyethylene as a binder. The specific objectives were: to perform proximate and ultimate analysis of corn stover and eucalyptus sawdust; to design and fabricate a single pellet press heated mould (SPP) and a pellet durability tester; to fabricate and torrefy blended pellets from corn stover and eucalyptus sawdust using LLDPE as a binder; to carry out characterization of the physical, mechanical and thermochemical properties of blended torrefied pellets and to optimize the pelleting process variables in terms of corn stover to eucalyptus sawdust ratio, the ratio of LLDPE binder and the torrefaction temperature. The Standard ASTM methods such as ASTM E871, E872, D1102 and D5373-02 were used to perform characterization of corn stover and eucalyptus sawdust. SPP heated mould was fabricated using stainless steel and incorporating heating mechanism and temperature controls. Pellet durability tester chamber was fabricated according to ISO 17831-1 standard. The fabricated SPP was used to fabricate the blended pellets and a modified tube furnace was used to torrefy the blended pellets. Taguchi multi-response optimization using grey relational analysis (GRA), through response graphs, ANOVA, contour and response surface plots were used to determine the impact of corn stover: eucalyptus sawdust ratio, LLDPE fraction, and torrefaction temperature variables, as well as their interaction effects, on the pellet properties. Proximate analysis of both feedstocks showed acceptable volatile matter, ash content and fixed carbon while moisture content was slightly lower for pellet production. While the ultimate analysis of both feedstocks indicated high carbon and hydrogen contents suitable for fuel applications. Additionally, the SPP fabricated was able to densify loosely packed ground feedstock to solid pellets, while the durability tester was able to perform tumbling at constant speed of 50 revolutions per minute. Also, the torrefaction of the blended pellets resulted in brownish to black pellets with maintained structural integrity. The optimal variables for blended pellet fabrication were; a 5:5 ratio of corn stover to eucalyptus sawdust, a 2% LLDPE ratio and a torrefaction temperature of 210°C. Consequently, the validation of blended pellet qualities resulted in particle density of 1074.75Kg/m³, bulk density of 633.2Kg/m³, durability index of 99.07%, Hardness of 1046.972N, Mass yield of 64.45%, higher heating value of 29.894MJ/Kg and Carbon dioxide emissions of 3.55% by volume. In addition, combustion emissions from the optimized blended pellet were: 44.3g/min for CO₂, 0.40g/min for CO and 7.55mg/min for particulate matter (PM2.5) by gravimetric method. LLDPE significantly influenced most of the properties evaluated. In conclusion, the suitability of corn stover and eucalyptus sawdust for pellet fuel production was guaranteed as demonstrated by their characterization results. From preliminary tests, the designs and fabrications made functioned as required and therefore can be used for production and evaluation of pellets. Furthermore, the validated optimal properties of the blended pellet were within the acceptable European guidelines EN 14961-6 international standard and other published literature for pellets with superior qualities for domestic as well as industrial applications as solid fuels. Furthermore, LLDPE proved to be a significant additive in the pellet blends as a binder. It is highly recommended that the optimized pellet produced be used in improved pellet cookstoves and industrial boilers since they have high energy output and enhanced mechanical properties and physical properties for ease of transportation to their destination of application.

TABLE OF CONTENTS

DECLARATION	ii
DEDICATION	iii
ACKNOWLEDGEMENTS	iv
ABSTRACT	v
TABLE OF CONTENTS	vi
LIST OF TABLES	xiii
LIST OF FIGURES AND PLATES	XV
ACRONYMS AND ABBREVIATIONS	XX
CHAPTER ONE: INTRODUCTION	1
1.1 Introduction	1
1.2 Background study	1
1.2.1 Pelleting and Briquetting Techniques for Production of Solid Biofuels	3
1.3 Problem Statement	6
1.4 Objectives	7
1.4.1 Main objective	7
1.4.2 Specific objectives	7
1.5 Research Justification	7
1.6 Scope and Limitations	9
1.7 Significance of the Study	9
1.8 Outline of the thesis	10
CHAPTER TWO: LITERATURE REVIEW	12
2.1 Introduction	12
2.2 Biomass	12
2.2.1 Characterization of biomass	13
2.2.1.1 Proximate analysis	15
2.2.1.2 Ultimate analysis	17
2.2.1.3 Higher Heating Value (HHV).	17
2.2.1.4 Prediction of biomass properties using proximate and ultimate analysis	sis 18
2.3 Biomass classification	20
2.4 Biomass as feedstock for biofuel production	21
2.4.1 Corn stover and Eucalyptus sawdust	22
2.4.2 Compositions of corn stover and eucalyptus sawdust	23

2.4.3 Energy from biomass	24
2.5 Densification of biomass residues	24
2.6 The pelletization process	25
2.7 Pellet production and important pellet properties as well as their process	
parameters	27
2.7.1 Pellet mills	27
2.7.2 Single pellet presses (SPP)	28
2.7.2.1 Design principles of single pellet presses	29
2.7.3 Process variables for pelletization	31
2.7.3.1 Moisture content	32
2.7.3.2 Particle size	33
2.7.3.3 Feedstock composition.	34
2.7.3.4 Machine-specific parameters	35
2.7.4 Fundamental pellet qualities (physico-mechanical properties of pellets)	37
2.7.4.1 Durability	37
2.7.4.2 Hardness	38
2.7.4.3 Bulk density	39
2.7.4.4 Particle density	39
2.7.4.5 Size of the pellets	40
2.8 Binders/Additives	40
2.9 Torrefaction.	41
2.9.1 Classification of torrefaction processes	43
2.9.2 Process variables for torrefaction	45
2.10 Combustion analyses of pellets	48
2.10.1 Combustion characteristics	48
2.10.1.1 Ultimate and proximate analyses and higher heating values (HHV).	48
2.10.1.2 Combustion emissions	48
2.11 Methods of Biomass Pellet Quality Enhancement	51
2.11.1 Use of woody biomass as an additive	51
2.11.2 Use of plastic additives	53
2.11.3 Use of TAP (Torrefaction After Pelletization)	53
2.11.4 Optimization as quality enhancement method	
2.12 Pellet quality standards	57
2.13 Literature review matrix: Summary and gaps	59

2.14 Design of experiments	60
2.14.1 Taguchi method	60
2.14.2 Steps in Taguchi Experimentation	61
2.14.3 Design of experiments using Orthogonal Arrays (OA)	62
2.14.3.1 Nomenclature of arrays in OA approach	62
2.14.3.2 Assignment of factors and interactions	63
2.14.4 Data analysis from Taguchi experiments	63
2.14.4.1 Regression analysis	64
2.14.4.2 Model adequacy checking	64
2.14.4.3 Taguchi multi-response optimization	66
CHAPTER THREE: METHODOLOGY	69
3.1 Introduction	69
3.2 Materials	69
3.3 Preparation of corn stover and eucalyptus sawdust	70
3.3.1 Removal of undesirable impurities	70
3.3.2 Size reduction of the raw materials	70
3.3.3 Drying	70
3.5 Determination of specific objectives of research	70
3.5.1 Perform characterization of corn stover and eucalyptus sawdust	71
3.5.1.1 Proximate analysis	71
3.5.1.2 Ultimate analysis	74
3.5.2 Design and Fabrication of Single Piston Pellet Press (SPP) heated mould	75
3.5.3 Design and Fabrication of durability tester	77
3.5.4 Fabrication and torrefaction of blended pellets from corn stover and	
eucalyptus sawdust using LLDPE as a binder	79
3.5.4.1 Experimental design.	79
3.5.4.2 Compaction of raw materials to pellets	80
3.5.4.3. Torrefaction of the blended pellet	81
3.5.5 Characterization of physical, mechanical and thermochemical properties of	f
blended torrefied pellets	83
3.5.5.1 Physical properties	83
3.5.5.2 Mechanical properties	86
3.5.5.3 Combustion properties	88
3.5.6 Optimization of pelleting process variables	89

3.5.6.1 The Pellet quality check against International Standard	89
3.7 Presentation of the results	90
3.7.1 Compositional analysis of feedstock	90
3.7.2 Pellet characteristics	91
3.7.2.1 Physico-mechanical and Combustion characteristics	91
CHAPTER FOUR: RESULTS, ANALYSIS AND DISCUSSION	92
4.1 Introduction	92
4.2 Proximate and Ultimate analysis of Cornstover and Eucalyptus sawdust	92
4.2.1 Proximate analysis	92
4.2.2 Ultimate analysis of corn stover and eucalyptus sawdust at ECO prend	uers ltd-
Nairobi	96
4.3 Fabrication of single pellet press and durability tester	99
4.3.1 Fabrication of single pellet press	99
4.3.2 Fabrication of durability tester	101
4.4 Fabrication and torrefaction of blended pellets	102
4.5 Characterization of blended torrefied pellets	103
4.5.1 Physical properties	103
4.5.1.1 Pellet particle density	103
4.5.1.2 Bulk density	111
4.5.2 Mechanical properties	120
4.5.2.1 Pellet durability index	120
4.5.2.2 Pellet Hardness	128
4.5.3 Torrefaction yields	136
4.5.3.1 Mass yields	136
4.5.4 Combustion properties	145
4.5.4.1 Higher heating value (HHV)	145
4.5.5 Emissions analysis	154
4.6 Taguchi multi-response optimization using grey relational analysis	163
4.6.1 Computation of signal-to-noise ratios (S/N), Normalized data (Z_{ij}), qu	ality
loss (Δ) and grey relational coefficient (GC _{ij}) of the responses	164
4.6.2 Computation of grey relational grade (Gi)	164
4.6.3 Optimization of design parameters	165
4.6.3.1 Multivariable linear regression model for grey relational grade (C	ii)166
4.6.3.2 Analysis of contour and surface plots for grey relational grade (G	i)168

4.6.3.3 Analysis of interactions of grey relational analysis (Gi)	169
4.7 Validation Test	172
4.7.1 Emissions test of optimized blended pellets using Laboratory Emissions	
Monitoring Systems (LEMS)	174
CHAPTER FIVE: CONCLUSIONS AND RECOMMENDATIONS	176
5.1 Introduction	176
5.2 Conclusions	176
5.3 Recommendations	180
REFERENCES	183
APPENDICES	208
Appendix 1: Biomass pelleting optimization studies	208
Appendix 2: Literature review matrix: Summary and gaps	210
Appendix 3: Using cone and quarter sampling method described above at KIRI	DI in
preparation for proximate analysis	213
Appendix 4: Using bomb calorimeter to determined HHV	213
Appendix 5 (a): Pellet particle density results (Y1)	214
Appendix 5 (b): Response Table for Signal to Noise Ratios for pellet particle	
density	215
Appendix 5 (c): Response Table for Means for pellet particle density	215
Appendix 6 (a): Bulk density results (Y2)	216
Appendix 6 (b): Response Table for Signal to Noise Ratios for pellet bulk dens	sity
	217
Appendix 6 (c): Response Table for Means for pellet bulk density	
Appendix 7 (a): Pellet durability index results (Y3)	218
Appendix 7 (b): Response Table for Signal to Noise Ratios for pellet durability	7
index	219
Appendix 7 (c): Response Table for Means for pellet durability index	219
Appendix 8 (a): Pellet hardness results (Y4)	220
Appendix 8 (b): Response Table for Signal to Noise Ratios for pellet hardness	221
Appendix 8 (c): Response Table for Means for pellet hardness	221
Appendix 9 (a): Pellet mass yield results (Y5)	222
Appendix 9 (b): Response Table for Signal to Noise Ratios for mass yield	
Appendix 9 (c): Response Table for Means for mass yield	
Appendix 10 (a): Pellet's higher heating values results (Y6)	224

Appendix	10 (c): Response Table for Signal to Noise Ratios for HHV(MJ/Kg	g)225
Appendix	10 (c): Response Table for Means for HHV(MJ/kg)	225
Appendix	11 (a): Carbon dioxide emissions results (Y7)	226
Appendix	11 (b): Response Table for Signal to Noise Ratios for carbon diox	ide
	emissions	227
Appendix	11 (c): Response Table for Means for carbon dioxide emissions	227
Appendix	12: Computation of signal to noise ratios (S/N), Normalized data	$(Z_{ij}),$
	quality loss (Δ) and grey relational coefficient (GC $_{ij}$) for pellet	particle
	density (Y1)	228
Appendix	13: Computation of signal to noise ratios (S/N), Normalized data	$(Z_{ij}),$
	quality loss (Δ) and grey relational coefficient (GC $_{ij}$) for bulk of	lensity
	(Y2)	229
Appendix	14: Computation of signal to noise ratios (S/N), Normalized data	$(Z_{ij}),$
	quality loss (Δ) and grey relational coefficient (GC $_{ij}$) for pellet	
	durability index (Y3).	230
Appendix	15: Computation of signal to noise ratios (S/N), Normalized data	$(Z_{ij}),$
	quality loss (Δ) and grey relational coefficient (GC $_{ij}$) for pellet	
	hardness (Y4).	231
Appendix	16: Computation of signal to noise ratios (S/N), Normalized data	$(Z_{ij}),$
	quality loss (Δ) and grey relational coefficient (GC $_{ij}$) for mass	yield
	(Y5)	232
Appendix	17: Computation of signal to noise ratios (S/N), Normalized data	$(Z_{ij}),$
	quality loss (Δ) and grey relational coefficient (GC $_{ij}$) for pellet	's
	higher heating value (Y6)	233
Appendix	18: Computation of signal to noise ratios (S/N), Normalized data	$(Z_{ij}),$
	quality loss (Δ) and grey relational coefficient (GC $_{ij}$) for pellet	's
	carbon dioxide emissions (Y7)	234
Appendix	19: Computation and ranking of grey relational grade from grey	
	relational coefficient of responses	235
Appendix	20 (a): Computed grey relational grade (Gi) and their signal to no	ise
	ratios (S/N)	236
Appendix	20 (b): Response Table for Signal to Noise Ratios for Gi	237
Appendix	20 (c): Response Table for Means for Gi	237
Appendix	21: Experimental set-up of emissions testing at LEMS	238

Appendix 22: Combustion of optimized blended pellet in a pellet stove	239
Appendix 23: Publications	240
Appendix 23: Antiplagiarism certificate	241

LIST OF TABLES

Table 2.1: Biomass compositions for woody, herbaceous, and waste materials; average
(standard deviation) number of samples
Table 2.2. Corn stover and Eucalyptus sawdust composition
Table 2.3. The standard methods for analyses of biomass fuels
Table 2.4 Research on effect of addition of woody biomass to herbaceous biomass fo
pelleting52
Table 2.5 Research on effect of plastic additives biomass pelleting54
Table 2.6: European normative guidelines for pellets produced from herbaceous and
fruit biomass and blends and mixtures59
Table 3.1 Design parameters and their levels
Table 3.2 Taguchi parameter experimental design .,
Table 3.3. European normative guidelines for pellets produced from herbaceous and
fruit biomass and blends and mixtures90
Table 3.4 Proximate and ultimate analysis of corn stover and eucalyptus sawdus
feedstock90
Table 3.5 Physico-mechanical and combustion characteristics of produced pellets 9
Table 4.1 Corn stover moisture content analysis
Table 4.2 Eucalyptus sawdust moisture content analysis
Table 4.3 Corn stover ash content analysis94
Table 4.4 Eucalyptus sawdust ash content analysis
Table 4.5 Corn stover volatile content analysis
Table 4.6 Eucalyptus sawdust volatile content analysis
Table 4.7 Ultimate analysis of Corn stover
Table 4.8 Ultimate analysis of Eucalyptus sawdust
Table 4.9 Summary of Proximate, Ultimate and Higher heating values
Table 4.10 Analysis of Variance of pellet particle density
Table 4.11 Model Summary statistics for pellet particle density
Table 4.12 Analysis of Variance of pellet bulk density
Table 4.13 Model Summary statistics of pellet bulk density
Table 4.14 Analysis of Variance of pellet durability index
Table 4.15 Model Summary statistics for pellet durability index
Table 4.16 Analysis of Variance of pellet hardness

Table 4.17 Model Summary statistics of pellet hardness	132
Table 4.18 Analysis of Variance for mass yield	139
Table 4.19 Model Summary statistics for pellets mass yield	141
Table 4.20 Analysis of Variance pellet higher heating values	148
Table 4.21 Model Summary statistics for higher heating values	150
Table 4.22 Analysis of Variance for carbon dioxide emissions	157
Table 4.23 Model Summary statistics for carbon dioxide emissions	159
Table 4.24 Parameters and their levels for optimum pellet production	166
Table 4.25 Optimum actual values of parameters for pellet production	166
Table 4.26 Confirmation experiments under optimal conditions	174
Table 4.27 Summary of optimized blended pellet properties	174

LIST OF FIGURES AND PLATES

Figure 1.1. Carbon cycle	3
Figure 1.2: a) Total primary energy supply and b) domestic biomass supply 2020	3
Figure 2.1. The most important biomass resources	13
Figure 2.2: Lignocellulosic biomass structure	15
Figure 2.3: Biomass types	21
Figure 2.4. Stages of the pelletization process.	25
Figure 2.5. Typical pellet mill designs a) ring die and b) flat die	28
Figure 2.6.Schematic illustration of pelleting using a single piston.	29
Figure 2.7 A schematic diagram showing the stages of torrefaction	43
Figure 2. 8: Conceptual framework	60
Figure 3.1 Coning and quartering method of sampling	71
Figure 3.2: 3-Dimensional CAD drafting of single pellet press (SPP) heated mould	.76
Figure 3.3: Orthographic views with dimensions of the die, piston and backstop	76
Figure 3.4: Circuit diagram of temperature control of the heated die	77
Figure 3.5: Durability tester tumbling box	78
Figure 3.6 Schematic diagram of a single die pellet press	81
Figure 3.7: Biomass pellet orientation during compressive strength testing	87
Figure 4.1: Fabricated die, piston and backstop	100
Figure 4.2: Picture of SPP and all its accessories in their working position	100
Figure 4.3: Hydraulic press and heated mould in operation	101
Figure 4.4: Pellets produced in the fabricated die	101
Figure 4.5: Fabricated pellet durability tester	102
Figure 4.6: Fabricated and torrefied blended biomass pellets	102
Figure 4.7 Response graph for main effects plot for, a) means and b) SN ratios for pe	ellet
particle density	105
Figure 4.8 Pareto chart of the standardized effects of pellet particle density	106
Figure 4.9 Standardized residuals plot for pellet particle density (Y1)	108
Figure 4.10 Contour plots for pellet particle density (Y1): a) corn stover to eucaly	ptus
sawdust ratio (X1) vs linear low-density polyethylene (X2), b) corn stove	r to
eucalyptus sawdust ratio (X1) vs torrefaction temperature (X3), c) linear	low
density polyethylene (X2) vs torrefaction temperature (X3)	109
Figure 4.11 Response surface plots for pellet particle density (Y1): a) corn stove	r to
eucalyptus sawdust ratio (X1) vs linear low-density polyethylene (X2), b) c	corn

stover to eucalyptus sawdust ratio (X1) vs torrefaction temperature (X3), of
linear low density polyethylene (X2) vs torrefaction temperature (X3)11
Figure 4.12 Interaction plot for pellet particle density (Y1)11
Figure 4.13 Response graph for main effects plot for, a) means and b) SN ratios for
pellet bulk density11
Figure 4.14 Pareto chart of the standardized effects of pellet bulk density11
Figure 4.15 Standardized residuals plot for pellet bulk density (Y2)11
Figure 4.16 Contour plots for pellet bulk density (Y2): a) corn stover to eucalyptu
sawdust ratio (X1) vs linear low density polyethylene (X2), b) corn stover
eucalyptus sawdust ratio (X1) vs torrefaction temperature (X3), c) linear lo
density polyethylene (X2) vs torrefaction temperature (X3)11
Figure 4.17 Response surface plots for pellet bulk density (Y2): a) corn stover
eucalyptus sawdust ratio (X1) vs linear low density polyethylene (X2), b) con
stover to eucalyptus sawdust ratio (X1) vs torrefaction temperature (X3),
linear low density polyethylene (X2) vs torrefaction temperature (X3)11
Figure 4.18 Interaction plots for pellet bulk density (Y2)
Figure 4.19 Response graph for main effects plot for, a) means and b) SN ratios for
pellet durability index
Figure 4.20 Pareto chart of the standardized effects of pellet durability index (Y3). 12
Figure 4.21 Standardized residuals plot for pellet durability index (Y3)
Figure 4.22 Contour plots for pellet durability index (Y3): a) corn stover to eucalyptu
sawdust ratio (X1) vs linear low-density polyethylene (X2), b) corn stover
eucalyptus sawdust ratio (X1) vs torrefaction temperature (X3), c) linear lo
density polyethylene (X2) vs torrefaction temperature (X3)
Figure 4.23 Response surface plots for pellet durability index (Y3): a) corn stover
eucalyptus sawdust ratio (X1) vs linear low-density polyethylene (X2), b) con
stover to eucalyptus sawdust ratio (X1) vs torrefaction temperature (X3),
linear low density polyethylene (X2) vs torrefaction temperature (X3) 12
Figure 4.24 Interaction plot for pellet durability index
Figure 4.25 Response graph for main effects plot for, a) means and b) SN ratios for
pellet hardness
Figure 4.26 Pareto chart of the standardized effects of pellet hardness
Figure 4.27 Standardized residuals plot for pellet hardness (Y4).

Figure 4.28 Contour plots for pellet hardness (Y4): a) corn stover to eucalyptus sawdust
ratio (X1) vs linear low density polyethylene (X2), b) corn stover to eucalyptus
sawdust ratio (X1) vs torrefaction temperature (X3), c) linear low-density
polyethylene (X2) vs torrefaction temperature (X3)
Figure 4.29 Response surface plots for pellet hardness (Y4): a) corn stover to
eucalyptus sawdust ratio (X1) vs linear low density polyethylene (X2), b) corn
stover to eucalyptus sawdust ratio (X1) vs torrefaction temperature (X3), c)
linear low-density polyethylene (X2) vs torrefaction temperature (X3) 135
Figure 4.30 Interaction plot for pellet hardness (Y4)
Figure 4.31 Response graph for main effects plot for, a) means and b) SN ratios for
pellet mass yield
Figure 4.32 Pareto chart of the standardized effects of pellets' mass yields
Figure 4.33 Standardized residuals plot for pellet mass yield
Figure 4.34 Contour plots for pellet mass yield (Y5): a) corn stover to eucalyptus
sawdust ratio (X1) vs linear low-density polyethylene (X2), b) corn stover to
eucalyptus sawdust ratio (X1) vs torrefaction temperature (X3), c) linear low
density polyethylene (X2) vs torrefaction temperature (X3)143
Figure 4.35 Response surface plots for pellet mass yield (Y5): a) corn stover to
eucalyptus sawdust ratio (X1) vs linear low-density polyethylene (X2), b) corn
stover to eucalyptus sawdust ratio (X1) vs torrefaction temperature (X3), c)
linear low density polyethylene (X2) vs torrefaction temperature (X3)144
Figure 4.36 Interaction plots for pellet mass yield
Figure 4.37 Response graph for main effects plot for, a) means and b) SN ratios for
pellet higher heating values
Figure 4.38 Pareto chart of the standardized effects of pellet higher heating values 149
Figure 4.39 Standardized residuals plot for HHV
Figure 4.40 Contour plots for pellet higher heating value (Y5): a) corn stover to
eucalyptus sawdust ratio (X1) vs linear low-density polyethylene (X2), b) corn
stover to eucalyptus sawdust ratio (X1) vs torrefaction temperature (X3), c)
linear low density polyethylene (X2) vs torrefaction temperature (X3)152
Figure 4.41 Response surface plots for pellet higher heating value (Y5): a) corn stover
to eucalyptus sawdust ratio (X1) vs linear low-density polyethylene (X2), b)
corn stover to eucalyptus sawdust ratio (X1) vs torrefaction temperature (X3),
c) linear low density polyethylene (X2) vs torrefaction temperature (X3)153

Figure 4.42 Interaction plots for HHV
Figure 4.43 Response graph for main effects plot for, a) means and b) SN ratios for
carbon dioxide emissions
Figure 4.44 Pareto chart of the standardized effects of carbon dioxide emissions 158
Figure 4.45 Standardized effects plot of residuals for carbon dioxide emissions 159
Figure 4.46 Contour plots for carbon dioxide emissions (Y7): a) corn stover to
eucalyptus sawdust ratio (X1) vs linear low-density polyethylene (X2), b) corn
stover to eucalyptus sawdust ratio (X1) vs torrefaction temperature (X3), c)
linear low density polyethylene (X2) vs torrefaction temperature (X3)161
Figure 4.47 Response surface plots for carbon dioxide emissions (Y7): a) corn stover
to eucalyptus sawdust ratio (X1) vs linear low-density polyethylene (X2), b)
corn stover to eucalyptus sawdust ratio (X1) vs torrefaction temperature (X3),
c) linear low density polyethylene (X2) vs torrefaction temperature (X3)162
Figure 4.48 Interaction plots for carbon dioxide emissions
Figure 4.49 A graph of grey relational grade and its corresponding S/N ratios 165
Figure 4.50 Main effects plot for (a) SN ratios and (b) means for grey relational grade
(Gi)166
Figure 4. 51 Standardized residuals plot for grey relational analysis (Gi)167
Figure 4. 52 Pareto chart of the standardized effects of grey relational grade (Gi) 168
Figure 4.53 Contour plots for grey relational grade - Gi (Y5): a) corn stover to
eucalyptus sawdust ratio (X1) vs linear low-density polyethylene (X2), b) corn
stover to eucalyptus sawdust ratio (X1) vs torrefaction temperature (X3), c)
linear low density polyethylene (X2) vs torrefaction temperature (X3) 170
Figure 4.54 Response surface plots for grey relational grade - Gi (Y5): a) corn stover
to eucalyptus sawdust ratio (X1) vs linear low-density polyethylene (X2), b)
corn stover to eucalyptus sawdust ratio (X1) vs torrefaction temperature (X3),
c) linear low density polyethylene (X2) vs torrefaction temperature (X3) 171
Figure 4.55 Analysis of interactions of grey relational analysis
Figure 4.56: CO2 and CO emissions during test
Figure 4.57: Particulate Matter (PM2.5) emissions rate during test
Plate 3.1: a) Corn stover b) Eucalyptus sawdust c) LLDPE pellets
Plate 3.2: Ground raw materials
Plate 3.3:Modified tube furnace to torrefaction equipment
Plate 3.4: Measuring pellet dimensions

Plate 3.5: Determination of bulk density	84
Plate 3. 6: Hardness testing in universal testing machine	87

ACRONYMS AND ABBREVIATIONS

ANOVA Analysis of variance

ASTM American society of testing and materials

BD Bulk density

CS Cornstover

D Pellet particle density

DOE Design of experiments

DU Durability of pellets

ESD Eucalyptus sawdust

EU European union

FC Fixed carbon

GRC Grey relational coefficient

GRG Grey relational grade

HHV Higher heating value

LG Linear graph

LHV Low heating value

LLDPE Linear low-density polyethylene

MSW Municipal solid waste

MY Mass yields

O/C Oxygen-to-carbon ratio

OA Orthogonal array

PDI Pellet durability index

PID Proportional Integral Derivative

SEM Scanning electron microscopy

VFD Variable frequency drive

%VOL Percent volume

WBA World bioenergy association

CHAPTER ONE: INTRODUCTION

1.1 Introduction

This chapter puts this research in the context of the broader study area of biomass pelletization and its significance. Biomass pellet enhancement technologies such as blending, use of binders and torrefaction are where this research was anchored. The problem statement, objectives, justification, scope, and limitations of this study are also presented in this section.

1.2 Background study

Mixtures of various biomass resources compressed into pellets for use as renewable energy sources are referred to as biomass pellet blends. A variety of organic resources, including wood, grasses, agricultural wastes, and even sawdust or paper pulp, can be incorporated into these blends (Frodeson & Tumuluru, 2023). The chemical and physical features of various biomass feedstocks can be complimented and coordinated by blending different feedstock types in order to optimize the pelletizing processes and qualities through blending (Pradhan et al., 2018). Blending is perceived to have potential in enhancing biomass pellet when sustainable, affordable and ecofriendly raw materials are utilized. Subsequently, blending emerges as a viable alternative for optimizing performance of production of biomass pellet fuels (Cui et al., 2021). Additionally, blending various materials and optimizing pelletizing variables appear to be viable approaches to producing quality pellets. The strength of biomass pellets and the durability of the bonds of biomass particles are the most desired parameters in pellets (Agu, 2018). Pelleting temperature is critical in promoting strong bonding by enhancing chemical restructuring of biomass particles (Anukam et al., 2021; Henriksen et al., 2008; Ma et al., 2021; Riva et al., 2019).

Utilization of biomass as renewable energy has, however, been faced with challenges such as: wide dispersion, irregular shape, low heating value, high moisture content (Ali et al., 2021; Li et al., 2016), low bulk density and others, consequently, leading to high handling, transportation and storage expenses (Ali et al., 2021; He et al., 2018). Drying, pelletizing and briquetting, torrefaction and use of binders are pretreatment and enhancement techniques of production of quality solid biomass fuels (He et al., 2018). Biomass does not increase the net atmospheric carbon dioxide as it is illustrated in the carbon cycle (see Figure 1.1) and it offers a variety of uses (Koondhar et al., 2021) through its derived products which include methanol, ethanol, biodiesel, Fischer-Tropsch hydrogen, methane, fuelwood, charcoal, pellets and other biofuels (Alizadeh et al., 2020; Ambaye et al., 2021). Cui et al. (2021) also observed that using biodegradable and agricultural wastes as fuel alternatives reduces emissions from landfills and combustion. In this scenario, biomass has a lot of potential as a long-term, renewable source of bioenergy, as demonstrated by the world bioenergy statistics 2022 (see Figure 1.2). Figure 1.2 illustrates that fossil fuel energy currently dominates world energy supply (Haq et al., 2021; Liu et al., 2022), standing at about 80% of the total primary energy supply while renewable energy accounts for 15% (Global Bioenergy Statistics 2022 World Bioenergy Association, 2022). From the statistics, biomass energy contributes to 63.2% of renewable energy and solid biomass fuels in which this research project is anchored accounts to 86% of the biomass energy (see Figure 1.2). The possibility of blended biomass pellets as a sustainable fuel source has been investigated in a number of studies. Gil et al. (2010) found that blends of sawdust from chestnut and pine trees were the most durable, while Zeng et al. (2016) and Zeng et al. (2018) both emphasized how blending may be used to lower emissions and improve pelletization. Wattana et al. (2017) further illustrated the potential of blended pellets by demonstrating how the combustion characteristics were enhanced by combining oil palm and para-rubber tree residue. Blending coal with Miscanthus biochar can increase fuel conversion rates, improve combustion characteristics, and decrease ignition and burnout temperatures (Li et al., 2018). All of these findings point to the potential of blended biomass pellets being a more effective and sustainable fuel source.

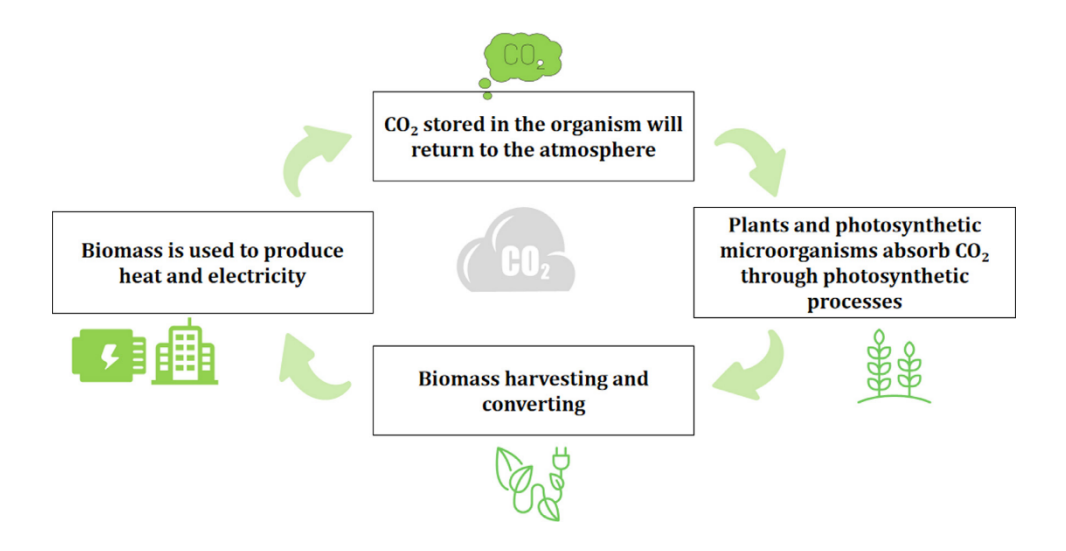


Figure 1.1. Carbon cycle (Cui et al., 2021)

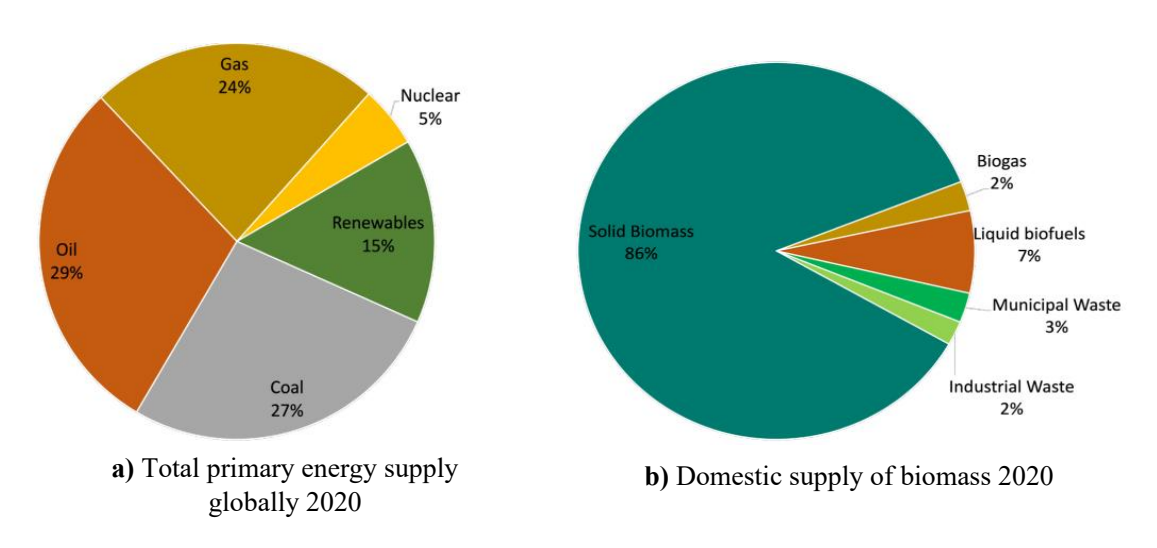


Figure 1.2: a) Total primary energy supply and b) domestic biomass supply 2020 (Global Bioenergy Statistics World Bioenergy Association, 2022).

1.2.1 Pelleting and Briquetting Techniques for Production of Solid Biofuels

Niedziółka et al. (2015) observed that agricultural biomass, especially cereal and other crop straw, requires a lot of transportation and storage space and possesses a low

calorific value per volume. Similarly, forestry residues are plentifully available at low cost (Arevalo-Gallegos et al., 2017). According to Myburg et al. (2014), eucalyptus species which yields eucalyptus sawdust through wood processing is the most widely planted wood because of its exceptional adaptation to many climates, quick growth, and great wood qualities. Demirbas et al. (2017) and Nunes et al. (2020) municipal solid wastes including waste plastics like LLDPE are classified as biomass and can be used as binders in solid biofuel production. This is because LLDPE has a low melting point (115–125 °C), which is essential to its ability to work as a binder because it melts and softens when heated and compressed during the pelletization process, effectively encasing and binding biomass particles. Due to the fact that the chemical makeup of straw varies depending on the plant species, region, and growing method, it should be handled carefully to maximize its energy efficiency. As a result, in an effort to increase the concentration of mass and energy per unit of volume and simplify the transportation and use of this type of biofuel, efforts are being made to condense these plant resources through briquetting or pelleting.

Solid fuels are frequently made from wood waste, agricultural and forestry wastes, energy crops, as well as other biomass feedstocks. He et al. (2018) and Sitek et al. (2021) discovered that compared to raw biomass fuels, biomass solid fuels emit very little particles and have a higher energy density. Furthermore, regular shape and dimensions allow for convenient handling, compact storage, and reliable feeding in large-scale applications.

There are many different types of biomass solid fuels, but the most popular solid biofuels types are pellets and briquettes (Pradhan et al., 2018b). Depending on the application, rod (block) fuels should have a diameter of more than 25 mm while pellet fuels should have a diameter of less than or equal to 25 mm (Cui et al., 2021). When

briquettes and pellets are compared, there are differences in production methods and market demands (Pradhan et al., 2018b). The size of the dies used in the two manufacturing processes is the key distinction between the two methods. Briquettes and pellets are produced densely from biomass resources at a predetermined pressure and temperature (Pradhan et al., 2018b). Briquettes are typically cylindrical and range in size from 75 to 300 mm in diameter and length, respectively. They can be utilized in medium to large industrial thermal facilities and are larger than pellets (Dinesha et al., 2019). The majority of pellets have a diameter of 6 to 8 mm and a maximum length of 40 mm. They're common in small appliances like domestic cookers and gasifiers (Pradhan et al., 2018b). Pellet serves as the key research object in this work due to its extensive applications. Biomass enhancement technologies of pelletizing and torrefaction was where this research work was anchored.

A by-product of the production of corn grain called corn stover, which is made up of the stalk, leaves, sheaths, husks, shanks, cobs, tassels, lower ears, and silks, is one of the raw materials this research investigated on pelletization. Islam et al. (2021) indicates that corn stover (CS) has a significant potential to add to the portfolio of alternative energy sources. However, a significant amount of agricultural waste such as corn stover is burnt or left unprocessed in the field thus requiring proper feedstock handling and preprocessing so that it becomes an abundant source of bioenergy.

According to Stasiak et al. (2017), the quality of solid biomass fuels could be improved by combining various types of biomass. This study investigated and optimized the fuel pellet quality produced by blending corn stover and eucalyptus sawdust in different mixing ratios. Linear low-density polyethylene (LLDPE) was used as a binder in varying ratios. Further enhancement of fuel pellet properties was done by torrefaction of the blended pellet. To enhance solid biomass fuel, the feedstock was thermally

treated at a low temperature of 200°C to 300°C in the absence or with little oxygen. This process is known as torrefaction (Adeleke et al., 2021). Physico-mechanical and combustion properties of corn stover-eucalyptus sawdust blended pellets was evaluated using various characterization techniques to explore process variables and additives' effects. Some of the process conditions of interest were blending ratio, binder ratio and torrefaction temperature. Taguchi design of experiments was employed to optimize the process. Minitab 18 software was used to design the experiments and analyze the outcomes of the performed experiments.

1.3 Problem Statement

There have not been many studies done to investigate different forms of agricultural biomass for pellet production, with wood wastes acting as an additive raw material in these studies. In the production of pellets, however, less research has been done on the combustion characteristics of biomass/biomass blends. Furthermore, it is impossible to generalize from published data due to the broad variety of raw materials used in the manufacturing of pellets and briquettes, as well as the different biomass densification procedures, and each case requires comprehensive research (Gil et al., 2010).

Corn stover being an agro-residue has low energy density compared to eucalyptus sawdust which is a woody residue because of the difference in lignin composition. LLDPE is a type of municipal solid waste (MSW) having binding properties and a high calorific value of 45MJ/kg (Samal et al., 2021) compared to corn stover's 15.9-16.8 MJ/kg (Jungmeier, 2017) and eucalyptus sawdust's 19.44MJ/kg (Fernandes et al., 2021). In order to improve corn stovers' calorific value, it has to be blended with other biomass having a higher calorific value like eucalyptus sawdust as a way of designing this fuel (Rebbling et al., 2020). There is scanty information in the published literature about blending corn stover and eucalyptus sawdust and using LLDPE as a

binder despite numerous research on pelleting of agro-residues. In Picchio (2020a) review, it is essential to consider how different biomass feedstocks, mixed biomass with non-biodegradable wastes like polyethylene, post-treatment techniques, and the interactions between process factors affect the quality of the fuel pellets. In summary, there is scarcity of knowledge on the impact of LLDPE binder on the qualities of blended pellets.

1.4 Objectives

1.4.1 Main objective

To undertake performance optimization of blended biomass pellets from corn stover and eucalyptus sawdust using linear low-density polyethylene as a binder.

1.4.2 Specific objectives

- 1. To perform physical and chemical characterization of corn stover and eucalyptus sawdust as raw materials for fabrication of blended pellet.
- 2. To design and fabricate a single pellet press heated mould and pellet durability tester.
- 3. To fabricate and torrefy blended pellets from corn stover and eucalyptus sawdust using LLDPE as a binder.
- 4. To characterize the physical, mechanical and thermochemical properties of blended torrefied pellets.
- 5. To optimize the pelleting process variables in terms of corn stover to eucalyptus sawdust ratio, the ratio of LLDPE binder and the torrefaction temperature.

1.5 Research Justification

Corn stover is an agro-residue that is abundantly available in maize-producing areas in Kenya (Zabed et al., 2023). Despite the fact that it is sometimes used as livestock

feed, a larger percentage of it is left in the field and burnt during land preparation. Furthermore, corn stover as livestock feed has very low nutritive value. Low-income households use also corn stover as fuel but has very high emissions and low energy value since it burns at a very high rate. In Kenya, the estimated amount of corn stover has not been explicitly defined. However, in United States of America, 108million tons of con stover are produced annually and are available for bioenergy production (Ebadian et al., 2017). This estimates generally demonstrate the significance of corn stover for bioenergy production. Eucalyptus sawdust are sawmill wastes which again are underutilized. They are sometimes used as fuel using sawdust stoves in lowincome households. Again, the emissions from utilizing sawdust as fuel are high. Although a precise numerical estimate for eucalyptus sawdust in Kenya is not easily accessible, it is evident that the quantity is significant and consistently produced because of the country's vast eucalyptus plantations and the structure of the sawmilling sector. The substantial amount of sawdust produced is further highlighted by the several recent felling operations for export (Cheboiwo et al., 2018; Ototo & Vlosky, 2018). Finally, LLDPE is a non-biodegradable MSW which when left unutilized in a proper manner is injurious to the environment (Dey et al., 2020). Kosore et al. (2022), Mugo Ephantus et al. (2015) and Odhiambo et al. (2014) have demonstrated the significance of plastic wastes in municipal solid wastes in Kenya. Mugo Ephantus et al. (2015) indicated that LLDPE accounted to 10% of these plastic wastes.

In this regard, the utilization of these three materials to produce quality pellet fuel leads to energy sustainability and improvement of the environment. It will also lead to satisfaction of pellets high demand since the use of improved cookstoves is utilized in all the levels of the energy ladder. Large scale power facilities also utilize pellets in

their operations (Pradhan et al., 2018b). In essence the pellets to be produced will benefit domestic and industrial consumers.

1.6 Scope and Limitations

This project focused on the study of: corn stover to eucalyptus ratio, LLDPE ratio and torrefaction temperature optimal levels to produce a quality pellet using Single pellet press. A L25 Taguchi design of experiments was employed using Minitab 18 software. The quality of the pellet produced was evaluated against European guidelines EN 14961-6 pellets for non-woody biomass pellets or pellet mixtures from different biomasses. Pellet qualities to be investigated and compared to standards are physical-mechanical properties, combustion and emissions properties.

This research will restrict itself to use of corn stover, eucalyptus sawdust and LLDPE as research materials.

This research project did not entail determination of hydrophobicity and Torgas analysis since it does not add any value to the research objectives. Study of the effect of machine parameters like pressure and die dimensions and temperature was also not to be considered.

1.7 Significance of the Study

With its implications on the environmental, economic, and energy sectors, this study on the production of blended pellets from corn stover and eucalyptus sawdust, using linear low-density polyethylene (LLDPE) as a binder, is anticipated to improve energy security, promote rural economic development, and help manage waste in a sustainable manner.

There are several environmental issues associated with the growing production of forestry waste (eucalyptus sawdust) and agricultural residues (corn stover), such as land

contamination, greenhouse gas emissions from open combustion, and the inefficient utilization of valuable biomass resources. This research offers a viable method for converting these abundant wastes into a more valuable, densified biofuel. By removing these materials from conventional disposal techniques, the research immediately supports carbon neutrality, emission control, and waste reduction.

The present reliance on traditional fossil fuels to generate energy is vulnerable to declining reserves and price instability. The creation of affordable, alternative biofuels, such as blended pellets, provides a feasible economic remedy. In order to save energy costs, turn waste into value, and create jobs and revenue, this study attempts to show that making these pellets is economically viable.

Reliable and sustainable energy sources are becoming more and more in demand. Compared to raw biomass, blended biomass pellets provide a homogeneous, high-density fuel with better combustion properties. It is expected that using LLDPE as a binder will improve the pellets' physical characteristics, including its hardness, calorific value, density, and durability, increasing their competitiveness. The results of this study will be essential for enhancing fuel quality, broadening the energy mix, encouraging the circular economy, and guiding investment and policy.

1.8 Outline of the thesis

In the first chapter, the research is contextualized within the larger field of biomass pelletization and its importance. The foundation of this research was biomass pellet improvement technologies, including torrefaction, mixing, and the use of binders." This section additionally presents the problem statement, objectives, justification, scope, and limitations of the research.

In the second chapter, the research conducted by other writers on biomass as a raw material for pellet production, pellet production methods, and pellet characteristics was the main focus. Additionally, the Taguchi method of analysis and experiment design was described.

Chapter three presents an in-depth description of the methods that will be employed to accomplish the objectives of this research.

Chapter four presents the results of the experiments carried out, their analysis and discussions.

Chapter five presents the conclusions and recommendations drawn from the analyzed results.

CHAPTER TWO: LITERATURE REVIEW

2.1 Introduction

This chapter focused on the research work that other authors have done on biomass as raw material for the production of pellets, pellet production techniques and pellet attributes. The design of experiments and analysis using Taguchi method was also outlined.

2.2 Biomass

Biomass includes all organic material in the biosphere, be it of plant or animal nature, and also those derived from natural or artificial conversion (Koondhar et al., 2021; Perea-Moreno et al., 2019). Rozzi et al. (2020) and Antar et al. (2021) also described biomass as non-fossil organic material with inbuilt carbon dioxide (CO₂) that has the ability to help mitigate greenhouse gas emissions. It is a renewable energy resource because the Carbon dioxide released during its combustion and utilization processes does not result in an increase in atmospheric carbon dioxide because it is of biogenic source. This insinuates that in order to grow and carry out their metabolic activities, plants utilize CO₂ that is released into the atmosphere as a result of the breakdown of other plants. The major biomasses include sewage, algae, agriculture and forestry wastes (such as shavings, sawdust, and other waste products from the wood-processing industries), animal residues (from livestock farms), and aquatic plants (illustrated in Figure 2.1). Municipal solid waste (MSW) and wastes streams from human-caused processes are also included in the biomass categorization, particularly if they cannot be utilized in further processes (Tursi, 2019). Corn stover is classified under the agricultural residues category, while eucalyptus sawdust falls under forestry and industrial residues. In fact, corn stover has been categorized by Johnson (2019) as

advanced feedstock for biofuel production and readily available as reported by Khanna & Paulson (2016).



Figure 2.1. The most important biomass resources (Tursi, 2019)

According to Global Bioenergy Statistics (2018), vast quantities of biomass are present on our globe in various ecosystems, including forests and oceans. It estimates that the world's total biomass reserves for land and water are roughly 1.8 trillion tons and 4 billion tons, correspondingly. The theoretical energy output capacity of all biomasses worldwide is 33,000 EJ, which is more than 80 times the yearly energy consumption of the entire planet. The properties of biomasses that determine its suitability for energy production are determined through characterization.

2.2.1 Characterization of biomass

Suitability of biomass for conversion to different biofuels is determined by assessing its properties through characterization (Cheng et al., 2016). Some useful biomass characterization methodologies include scanning electron microscopy (SEM), atomic force microscopy (AFM), Fourier transform infrared spectroscopy (FT-IR), X-ray diffraction (XRD) and transmission electron microscopy (TEM), depending on the

desired biofuel application. SEM when used in conjuction with Energy Dispersive X-ray Spectroscopy (EDS/EDX) offers extremely valuable micro- and nanoscale insights into the elemental composition and physical structure of biomass fuels, which are critical for thorough biomass characterisation and maximizing its use in energy production.FT-IR, XRD and TEM when combined, they provide vital information about the basic characteristics of biomass, assisting engineers and researchers in comprehending how it behaves as a fuel and improving conversion techniques. In order to get proper understanding of biomass and the process of its conversion to biofuel, it is recommended that characterization is done before and after the treatment process (Biotechnological Applications of Biomass, 2020).

Lignocellulosic biomass (LCB) is a common name used to refer to biomass (Cheng et al., 2016), is made up of various proportions of major chemical compounds including cellulose, hemicellulose and lignin, constitute a large part of the chemical components in biomass residues as illustrated in Figure 2.2. Additionally, the minor compounds include: extractives, water, proteins and inorganic elements such as potassium, calcium, aluminum, sodium and silicon, among others. These chemical structures are different from each other resulting in different chemical properties (Tursi, 2019) and, thus, establish the properties of the whole biomass.

Proximate analysis of biomass and its ultimate analysis are the main expressions of biomass characterization when biomass is used for biofuel production applicable in thermochemical processes (Anukam & Berghel, 2021). Thus, higher heating value (HHV) should be considered in characterization.



Figure 2.2: Lignocellulosic biomass structure (Tursi, 2019)

2.2.1.1 Proximate analysis

A summary of the biomass's moisture, ash, volatile matter, and fixed carbon (FC) levels describe the proximate analysis of biomass (Adeleke et al., 2021). These properties have a significant effect on combustion of biomass feedstocks (Sivabalan et al., 2021), as well as production of solid biofuels through densification (Adeleke et al., 2021). As pertains combustion, moisture content determines the amount of heat energy required for ignition of fuel, whereas, slagging and fouling phenomena in boilers are a result of ash melting temperature and elements of ash. The ability of biomass feedstock to bond together to produce solid biofuels is greatly affected by its moisture content. It acts as a binder during densification when used in its optimum level. Lower and higher moisture levels lead to challenges in adhesion of biomass particles hence difficulty in densification (Garcia-Maraver, 2015a). According to Liu et al. (2022) the amount of moisture in biomass feedstocks can be adjusted to optimum level by the addition of water as determined by equation 2.1. Volatile matter and fixed carbon determine the higher heating values for both combustion and densification processes.

$$m_{add} = m_{ini} \frac{K_2 - K_1}{1 - K_2}$$
 Equation 2. 1

Where, m_{add} is the mass of ultrapure water added, m_{ini} is the initial mass of raw material, K_1 is the initial moisture content (%) in biomass and K_2 is the targeted desired optimum moisture content (%) of the biomass.

Proximate analysis essentially provides the biomass's overall composition (Ajimotokan et al., 2019; Velusamy et al., 2022). Liu et al. (2020), Mostafa et al. (2019a), Valdés et al. (2018) and Bhavsar et al. (2018) summarized other significance of proximate analysis in pellet production as follows;

- The moisture and ash content of various biomass feedstocks can vary greatly, which can have a big impact on pelletization. While high ash concentration might reduce pellet combustion efficiency, high moisture content can result in low-quality pellets and higher drying energy consumption. These features can be found by proximate analysis, and the pelletization process parameters can then be optimized accordingly.
- The calorific value and combustion properties of biomass pellets can be understood through the application of proximate analysis. Manufacturers can guarantee constant quality control and satisfy particular specifications or needs for various uses, such as power generation, industrial operations, or home heating, by understanding the approximate composition of pellets.
- In order to enhance pellet quality and energy efficiency, choosing biomass blends or additives is made easier with an understanding of the proximate composition. For example, mixing biomass with high and low moisture contents can assist in achieving optimum moisture levels for pelletization while avoiding the need for unnecessary drying energy.
- > The evaluation of biomass pellets' effects on the environment also involves proximate analysis. When using pellets, lower ash content and higher calorific

value suggest cleaner combustion and less emissions, which promote environmental sustainability.

2.2.1.2 Ultimate analysis

The goal of ultimate biomass analysis is to evaluate the percentage of elemental ingredients, such as carbon (C), hydrogen (H), nitrogen (N), sulfur (S), oxygen (O), and other elements, that are present in biomass. Understanding these components makes it easier to calculate the volume and make-up of combustion gases and also the amount (theoretical) of air needed for complete combustion. The heating value of biomasses is usually determined by various methods depending on this analysis (Dash et al., 2015). The atomic ratio classification—which comprises hydrogen, oxygen, and carbon—helps determine the fuel's heating value. For instance, there is a strong correlation between the oxygen-to-carbon (O/C) ratio and the biomass higher heating value (Dash et al., 2015). Gummert et al. (2019) also concluded that biomass having elevated nitrogen (N) and sulfur (S) composition results in generation of harmful gases like nitrogen oxides (NOx) and sulphur oxides (SOx) during combustion, which are the major causes of acid rain and particulate matter emissions (PM).

2.2.1.3 Higher Heating Value (HHV).

Sivabalan et al. (2021) defined higher heating value as the total amount of energy produced by a unit of mass of fuel when completely combusted. The generated heating value is influenced by the chemical fuel elements.

Biomasses are unique in that they possess different chemical compositions and other characteristics. These lead to grouping of biomasses according to similarities in their characteristics. In the study on compositional analysis of biomass for production of renewable biofuels and chemicals, Williams et al. (2017) analyzed the chemical

composition of woody and herbaceous biomass, municipal solid wastes and agricultural wastes and found that specific properties were within specific ranges for their respective biomass types as illustrated in Table 2.1. Biomass characteristics considered in this classification are proximate and ultimate analysis as well as structural carbohydrates. These types of biomasses inform the best method of utilization of biomass as biofuels.

2.2.1.4 Prediction of biomass properties using proximate and ultimate analysis

Proximate and ultimate analysis, as well as higher heating values of biomasses, are important thermochemical properties which are usually determined experimentally using various equipment. The challenges with experimental determination of these properties, as reported by Xing et al. (2019), is that it is time-consuming, expensive, scarcity of equipment and prone to experimental errors. Another essential biomass property is the structural carbohydrates such as cellulose, hemicellulose and lignin. Nimmanterdwong et al. (2021) noted that tedious laboratory analytical procedures employing expensive equipment such as High-performance liquid chromatography (HPLC) and the use of strong acids which raise concerns in terms of safety and accuracy are used in analysis of these structural carbohydrates. One outstanding solution that has been developed to eliminate the above highlighted challenges is the development of models from correlations among various biomass prediction properties (Nimmanterdwong et al., 2021). Datasets of proximate and ultimate analysis from various biomasses are used to predict other properties like HHV, cellulose, hemicellulose, lignin and either proximate analysis to estimate ultimate analysis or vice versa. The Artificial Intelligence (AI) method of Machine Learning (ML)-based prediction models is often used to predict complex nonlinear regression tasks (Moayedi et al., 2019). Artificial neural network (ANN), logistic regression (LR), random forest (RF), support vector machine (SVM), genetic algorithm (GA), particle swarm

optimization (PSO) and multi-linear regression (MLR) are examples of the commonly used ML algorithms (Ceylan & Sungur, 2020; Park et al., 2023).

Table 2.1: Biomass compositions for woody, herbaceous, and waste materials; average (standard deviation) number of samples (Williams et al., 2017)

Feedstock composition	Woody	Herbaceous	Wastes				
Proximate analysis							
Volatiles (%)	84.0 (2.1) ¹⁹³	79.1 (5.8) ²⁸⁴	76.7 (5.5) ²¹				
Ash (%)	$1.3 (0.9)^{193}$	$5.5(3.2)^{284}$	$6.6(6.7)^{21}$				
Fixed carbon (%)	14.7 (1.6) ¹⁹³	$15.4 (4.0)^{284}$	$14.8 (5.0)^{21}$				
Ultimate analysis							
Hydrogen (%)	$6.0(0.1)^{192}$	$5.8 (0.3)^{276}$	$5.9(0.4)^{21}$				
Carbon (%)	50.7 (4.71) ¹⁹²	47.4 (1.9) ²⁷⁶	46.0 (4.0) ²¹				
Nitrogen (%)	$0.32(0.01)^{192}$	$0.75 (0.49)^{276}$	$1.3 (1.6)^{21}$				
Oxygen (%)	$41.9(1.4)^{134}$	$41.0 (2.4)^{107}$	38.3 (4.2) ⁷				
Sulfur (%)	$0.03 (0.01)^{135}$	$0.10 (0.32)^{107}$	$0.15 (0.16)^7$				
Structural carbohydrates							
Cellulose (%)	51.2 (8.7) ²⁴¹	$32.1 (4.5)^{2425}$	28.4 (13.2) ²⁷				
Hemicellulose (%)	$21.0(8.7)^{241}$	$18.6 (3.4)^{2425}$	$16.4 (5.5)^{27}$				
Lignin (%)	$26.1 (5.3)^{241}$	$16.3 (3.3)^{2425}$	$12.5 (2.7)^{15}$				

Some of the studies that have applied prediction models to estimate biomass properties include Park et al. (2023) estimated higher heating value using proximate or ultimate analysis. Krishnan et al. (2019) also used proximate analysis to estimated higher heating value of biomass. Park et al. (2023) developed a model to estimate the amounts of cellulose, hemicellulose and lignin from proximate and ultimate analysis. Ceylan & Sungur (2020) estimated ultimate analysis from proximate analysis. In all these studies, the conclusion is that the errors of estimation were minimal and, therefore, the models can be used for future use.

These models for predicting biomass properties have different performance capabilities. In the research done by Ghugare et al. (2017), it was found that nonlinear models developed from Artificial Neural Network (ANN), Genetic Programming (GP-extension of GA) and Support Vector Creation (SVC) to predict the quantities of Carbon, Hydrogen and Oxygen in biomass from their proximate analyses outshined

their linear counterparts. In general, Random Forrest (RF) model accurately predicted biomass properties compared to others (Dubey & Guruviah, 2022; Wang et al., 2022; Xing, Luo, Wang, & Fan, 2019).

The above-highlighted characteristics of biomasses lead to grouping of biomass into different types as discussed below.

2.3 Biomass classification

Biomass can be classified using various criteria. The most widely accepted criteria are categorization based on origin (Demirbas et al., 2017; Nunes et al., 2020) resulting in biomass types, such as wood and woody biomasses, herbaceous biomasses, aquatic biomasses, animal and human waste biomasses and mixtures of biomasses. In addition, Islas et al. (2018) included municipal solid waste as another type of biomass which encompasses wastes of cardboard, paper, plastic, textile, glass, wood and food. According to Tursi (2019), trees, shrubs and their residues are forms of wood and woody biomass. Herbaceous biomass has non-woody stems and are generally classified to agricultural residues and energy crops. Algal biomass forms aquatic biomass, while manure from animals and human excreta are examples of animal and human wastes. Finally, feedstocks containing the different types of biomasses are categorized as biomass mixtures. Figure 2.3 illustrates biomass types and their selected examples.

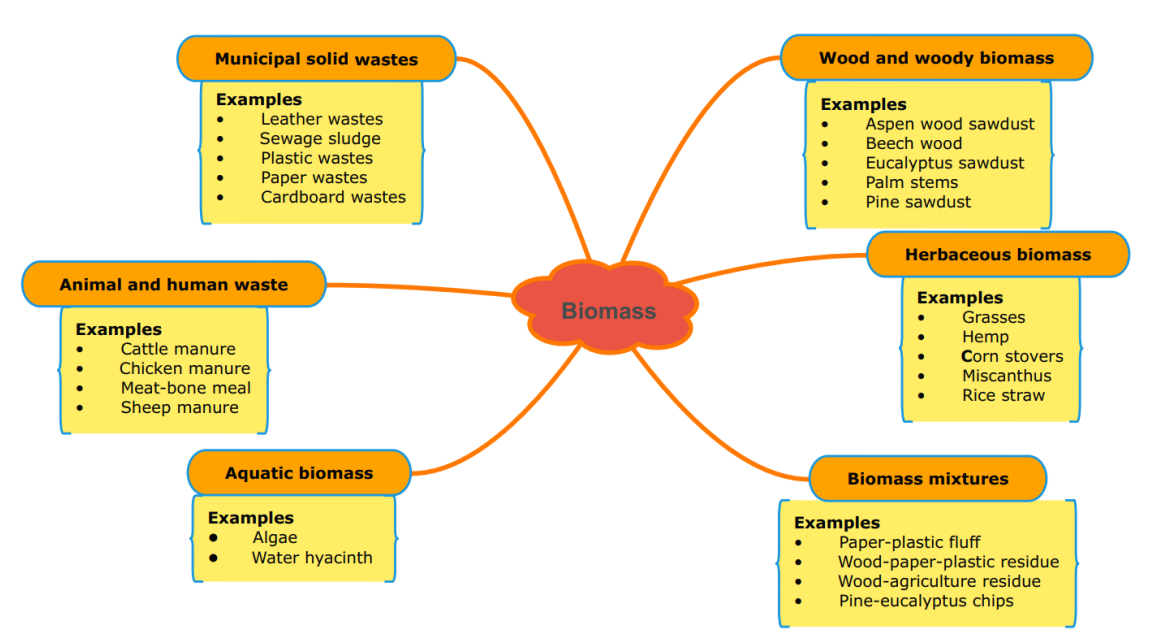


Figure 2.3: Biomass types

2.4 Biomass as feedstock for biofuel production

Solid, liquid or gaseous fuels derived directly or indirectly from biomasses is referred to as 'biofuel' (Sánchez et al., 2018) and according to Ruan et al. (2019) it is applicable in production of heat, energy, power and light. In essence, chemical, physical, thermochemical and biochemical technologies are used to manufacture biofuels (Ruan et al., 2019). Ruan et al. (2019) realized in the study on biofuels that one type of biomass feedstock can be used in production of different varieties of biofuels using different techniques, hence, the diversity and the robustness of production of biofuels from biomass. He et al. (2018) and Sitek et al. (2021) discovered that compared to raw biomass fuels, biomass solid fuels emit very little particles and have a higher energy density. Furthermore, regular shape and dimensions allow for convenient handling, compact storage, and reliable feeding in large-scale applications.

Solid biomass accounts for 86% (Figure 1.2b) of the supply of domestic biomass fuels (Global Bioenergy Statistics World Bioenergy Association, 2022) which are mainly derived from wood and woody biomass, herbaceous biomass and municipal solid wastes. There are numerous types of wood and woody biomass that is used for solid

biofuels. Pellets, wood shavings, woodfuel, sawdust (Kiang, 2018; Sharma et al., 2019) and commercial forestry (hog fuel) as well as other wood residues (Tumuluru & Fillerup, 2020) are typical examples of solid biofuels derived from the category of wood and woody biomasses. Agricultural wastes, such as corn stover, miscanthus, and switch grass among others are herbaceous biomasses that have distinct chemical properties from those of woody biomass (Popa, 2018). Thus, herbaceous biomass contains more ash but less lignin and carbon, whilst woody biomass contains more lignin and carbon but less ash. According to Kiang (2018), pellets from wood are known to possess superior qualities such as ultimate and proximate analysis, as well as higher heating value than herbaceous biomass.

2.4.1 Corn stover and Eucalyptus sawdust

Corn stover biomass materials fall under herbaceous category as stated in the Table 2.1. The stalk, leaves, sheaths, husks, shanks, cobs, tassels, lower ears, and silks are all parts of corn stover, a by-product of the production of maize grain. According to RicharddLSmith & Xiao-FeiiTian Editors (2019) the dry matter of the entire corn plant, the components of the corn stover yield are roughly distributed as follows: 22% are the stalk, 10.6% are the leaves, 5.3% are the sheaths, 4.3% are the husks, 1.5% are the shanks, 7.5% are the cobs, and 0.5% are the lower ears and 0.2% are the silks. Mowing, raking, and baling are methods used in collection of corn stovers with efficiencies of about 70%. Djatkov et al. (2018) noted that in the production of fuel pellets, herbaceous biomass can be used instead of wood, therefore, corn stover has great potential in the production of biomass fuel pellets.

Eucalyptus sawdust falls under the category of wood and woody biomasses and are residues of processing wood to timber in sawmill and furniture workshops.

According to J. A. et al. (2019) both eucalyptus sawdust and corn stover show promise as biomass feedstocks for the manufacturing of pellet fuel, providing fossil fuel substitutes with sustainable energy. They do, however, have unique qualities and processing and pellet quality issues.

In general, eucalyptus sawdust which is a woody biomass has a lower ash percentage and a higher heating value, which makes it a more straightforward alternative to conventional wood pellets (Cui et al., 2021). Corn stover whic is a herbaciuos biomass has the advantage of being widely available as an agricultural waste and having the possibility for energy-efficient high-moisture pelleting, despite having a somewhat lower energy density and more ash.

According to (Cui et al., 2021) and it is interesting to note that combining eucalyptus sawdust and corn stover can work in concert. According to studies, by combining the advantages of both materials, blending can enhance the qualities of corn stover pellets, such as raising their higher heating value and lowering their ash content. Copelletization can maximize the use of various biomass supplies and improve pellet quality overall.

2.4.2 Compositions of corn stover and eucalyptus sawdust

The amount of structural carbohydrates in corn stover and eucalyptus sawdust is illustrated in Table 2.2 below.

Table 2.2. Corn stover and Eucalyptus sawdust composition (RicharddLSmith & Xiao-FeiiTian Editors, 2019)

Lignocellulosic residue	Cellulose (%)	Hemicellulose (%)	Lignin (%)
Corn stover	36.9	21.3	12.5
Eucalyptus sawdust	43.3	31.8	24.7

2.4.3 Energy from biomass

Out of all the renewable energy sources, biomass contributes the most, with over 55% of its energy traditionally utilized for cooking and heating in underdeveloped nations (Chan et al., 2019). According to Mladenović et al. (2018) the largest source of clean energy worldwide is biomass. Wang et al.(2020) revealed that the best strategies to convert biomass to useful energy include direct combustion to produce heat and eventually electricity and conversion of biomass to solid, liquid and gaseous forms to supply heat, power and transport fuel.

Knapczyk et al. (2019) defined solid biofuels as processed and unprocessed biomass. The two forms of fuels are natural fuels (as obtained) and synthetic fuels (after mechanical and chemical treatment). For the production of solid biofuels, raw materials such as wood, stem plants, peat, sewage sludge, and cereal grains are employed. These raw materials may be used as a component of the manufacturing process or as fuel.

Direct use of biomass to heat and cook causes air pollution and has a negative influence on living creatures and the environment. To solve this issue, agricultural waste or residues can be converted into solid biomass fuels using biomass conversion methods like briquetting and pelleting. The primary biomass wastes used to create briquettes or pellets include agricultural waste, food waste, and fuel crops in addition to wood and its byproducts through densification processes (Vaish et al., 2022).

2.5 Densification of biomass residues

Adeleke et al. (2021) described densification as the process of compacting biomass into uniformly sized solid particles, such as pellets and briquettes using mechanical force. Agricultural solid biomass wastes and other biomass residues are widely spread and are only available during certain seasons of the year, posing storage and handling

challenges. Managing, transporting, storing, and combusting low-density biomass leftovers is complex. Briquettes/pellets are the perfect solid biomass fuel for utilizing raw agricultural residue. According to Adeleke et al. (2021) the benefits of densification are:

- > Increased biomass volumetric net calorific content.
- The resulting product is simple to handle, transport, and store.
- > Fuel production is of high standard and consistent size.
- > Feedstocks adhere to conversion methodologies that have been pre-planned and provide system specifications.

One of the most popular densification techniques is pelletization. Pelletization processes are as discussed in sections 2.6 and 2.7.

2.6 The pelletization process

Pre-treatment of the raw materials, pelletization, and post-treatment are the three major phases in the pelletization process. As a result, following the feedstock preparation step, the pelletization procedure is carried out as shown in Figure 2.4 (Younis et al., 2018).

FEEDSTOCK STORAGE		
REMOVAL OF UNDESIRABLE IMPURITIES		
-		
SIZE REDUCTION		
•		
MATERIAL TRANSPORTATION		
•		
BIOMASS DRYING		
•		
MIXING AND CONDITIONING		
•		
PELLETIZATION		
•		
COOLING AND SCREENING		
•		
STORAGE		

Figure 2.4. Stages of the pelletization process (Younis et al., 2018).

Extra attention should be given to feedstock storage during the raw material pretreatment process because it is essential to maintain the purity of the biomass raw

material by storing it in a dry environment with the proper feedstock storage. Furthermore, it is critical to remove any undesired contaminants. The raw material should be screened first, then ground. It must next go through a magnetic separation procedure to remove any metal particles or stones from the biomass bulk. To avoid major damage to the mechanical equipment, it is critical to remove such contaminants. After impurities are removed, the feedstock is crushed to a uniform size of 6 mm diameter to avoid clogging the pellet mill's perforations. Additionally, pellets with a greater density and greater strength during pelletization would be produced by using small raw material feed particles with a large surface area. Furthermore, a narrow raw material particle size distribution facilitates the drying phase's moisture optimization procedure (Younis et al., 2018).

Screw conveyors can then be used to move the raw materials after it has been reduced in size or by a cyclone separator. To produce pellets of the best quality, the raw material's moisture level must be kept between 10% and 20%. Raw feedstock with high moisture content leads to low energy efficiency and excessive hydrocarbon and particle emissions, hence drying solid biofuels is important. Mixing is not required for all feedstocks. However, mixers can be employed to achieve a constant and homogeneous material blend following size reduction and drying, if necessary. Furthermore, the addition of appropriate binder elements is critical for improving the final product's qualities. Pelletization takes place in pellet mills (Younis et al., 2018).

The pellets produced at the end of the pelletization process must be cooled before leaving the manufacturing facility to ensure their strength and durability. When pellets are removed from the extruder, they are typically air-cooled to speed up the solidification of the lignin, which strengthens the pellets. Pellets are screened after cooling to remove any fine particles or dust. Fine material that is left over is returned

to the pelletizing process. The final step in pelletization is screening, following which the pellets are ready for packaging (Younis et al., 2018).

2.7 Pellet production and important pellet properties as well as their process parameters

Loosely packed, prepared biomass are compacted to uniformly sized biomass particles called pellets by process of densification (Adeleke et al., 2021), through the technologies described by (Vaish et al., 2022) which include: extrusion, hydraulic piston presses, screw presses, piston type presses, roller presses, and pellet presses (ring and flat die). The resultant pellet will be of high calorific value, consistent size, easy to handle, transport and store (Adeleke et al., 2021). Generally, the bulk densities of herbaceous biomasses are between 80-150kg/m³, while that of woody biomasses are between 150-200kg/m³ which are considered to be low (Japhet et al., 2019). On densification through pelleting, these densities are improved to 600-800kg/m³ (Garcia-Maraver, 2015a). Some of the most widely used pelleting technologies are described below.

2.7.1 Pellet mills

Pellet mills, also referred to as pellet presses or extruders, are machines that use high pressure to force biomass feedstock through the die's holes, causing friction and the temperature of raw materials to rise and reshaping it into pellets (Garcia-Maraver, 2015a). Depending on the shape of the die, pellet mills can be classified as either flat or round. In flat die pellet mills, the feedstock is placed on top of a die that has holes in it. When the die starts to rotate, the raw material is squeezed and forced through the openings of the die, whereupon the pellets are eventually cut. Such mills are used to produce pellets on a small- to medium-scale (Garcia-Maraver, 2015a). In contrast, round die pellet mills have round holes that are positioned vertically along the die. The

raw material is placed in the die's center and distributed evenly throughout the process. The material is then squeezed through the perforations by the rollers, and the pellets are chopped by the die's outside blades. Figure 2.5 illustrates the two described types of pellet mills.

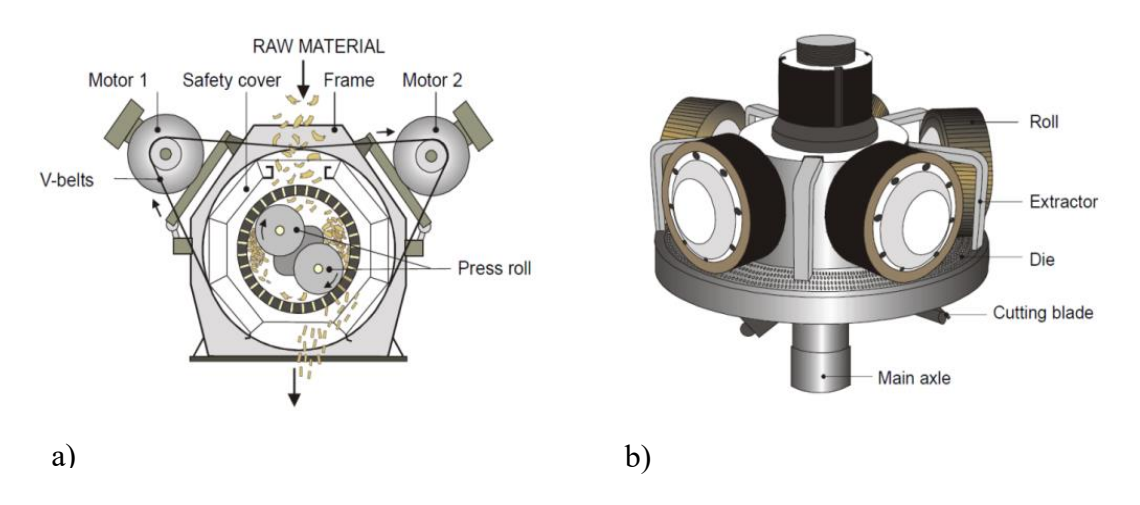


Figure 2.5. Typical pellet mill designs a) ring die and b) flat die (Garcia-Maraver, 2015b)

2.7.2 Single pellet presses (SPP)

Single pellet press (SPP) is a bench scale pelletizing machine consisting of a cylindrical die manufactured from hardened steel (Puig-Arnavat et al., 2016), having diameters ranging from 3 to 25 mm (Japhet et al., 2019) and equipped with heaters, thermal insulations, a hydraulic press, a tightly fitting piston as well as thermocouple integrated with control system for die temperature control. The biomass feedstock is compressed by pressing it against a stationery backstop using hydraulic press. It is usually difficult to control temperature resulting from friction in pellet mills making it hard to study specific quality parameters of the pellets (Mostafa et al., 2019b). To overcome this challenge, single pellet presses are useful (Hosseinizand et al., 2018; Huang et al., 2017a; Stasiak et al., 2017). Figure 2.6 illustrates single pelleting press unit consisting of a plunger and a cylindrical die with other accessories that is used to prepare biomass pellets.

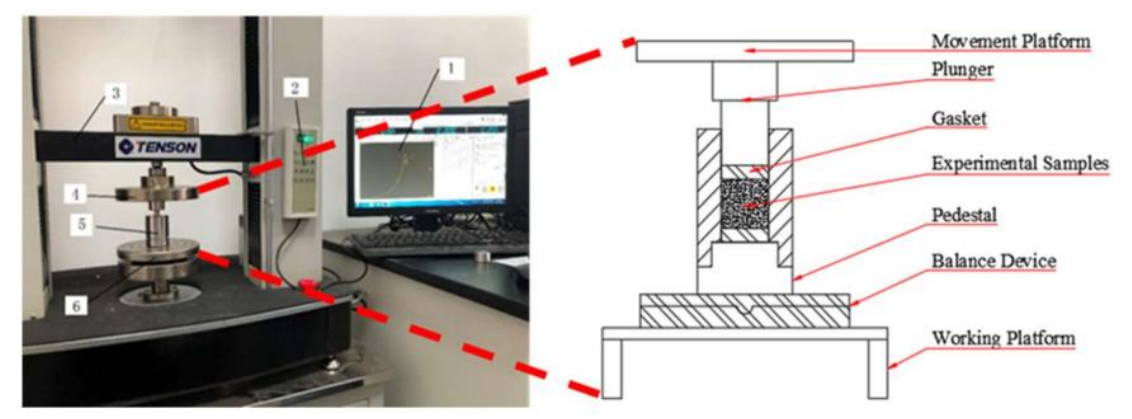


Figure 2.6.Schematic illustration of pelleting using a single piston (Liu et al., 2022). 1; Computer, 2; Control bar, 3 and 4; Movement platform, 5; Pelleting unit, 6; Balance device.

2.7.2.1 Design principles of single pellet presses

Frequently employed in research and development, single pellet presses are designed to produce individual biomass pellets in a controlled environment. This makes it possible to precisely investigate the qualities of the final pellets as well as the pelletization process. Single pellet presses place control, adaptability, and reproducibility first for experimental uses, in contrast to vast commercial pellet mills that concentrate on high throughput (ZYLAB Instruments, 2024).

According to Nielsen et al. (2020), Sun et al. (2023) and Holm et al. (2011) the main guidelines for designing single pellet presses that produce biomass fuel are discussed below:

> Controlling process parameters precisely:

O Pressure/Compaction Force: This is crucial. The press needs to be able to exert a force on the biomass that is both precisely controlled and quantifiable. This frequently entails screw-driven or hydraulic systems equipped with force sensors (load cells).

- o **Temperature:** Pelletization of biomass is a thermomechanical procedure. To activate natural binders (such lignin) and promote compaction, the die and/or the biomass itself must be heated to a regulated temperature. Design components consist of:
 - Heated dies: PID-controlled integrated heating components, such as cartridge heaters.
 - Temperature sensors: Near the compaction zone, thermocouples are placed in the die.
- Compression Time, or Dwell Time: For the biomass to properly
 consolidate, the length of time it is compressed is essential. This time
 should be precisely controlled by the press mechanism.
- The size of the feedstock particles: The biomass's particle size must be consistent with the die opening size and the compaction method. One popular preparation for biomass is pre-grinding.

Design of Die and Punch:

Selection of Materials: High temperatures, pressures, and abrasive forces are applied to the die and punch (or roller). High-strength, wearresistant materials (such as tool steel, hardened steel, or specialty alloys) must be used to make them.

Dimensions of Die:

- Diameter: determines the diameter of the pellet, usually by simulating the diameters of regular industrial pellets.
- Ratio of Length to Diameter (L/D): This ratio is an important statistic to research and is crucial for pellet quality. The die length, also known as the effective length of the die channel,

affects the pellet us durability, density, and pressure build-up. Higher friction and greater energy input are associated with longer channels.

- Taper/Relief: To lessen friction and make pellet ejection easier, some dies have a small taper or relief at the exit.
- Surface Quality: The die channel's smooth, polished surfaces enhance pellet quality and lower friction.

➤ Monitoring and Data Acquisition:

- o Load Cells: To precisely measure the applied compaction force.
- Sensors of temperature: Should monitor the biomass and die temperatures throughout the process.

> Feeding and Ejecting Materials:

- Controlled Feeding: The amount of biomass injected into the die for single pellet presses must be exact and constant for every pellet. This frequently calls for a tiny, controlled volumetric feeder or hand feeding.
- Pellet Ejection: The pellet needs to be smoothly expelled from the die after compression. This can be accomplished by using a punch to push it out or by using a specially made release mechanism. Ejection done correctly minimizes congestion and guards against pellet damage.

2.7.3 Process variables for pelletization

Process variables, including moisture content, particle size, binders, and other machine settings, such as: pressure gap, die diameter, channel length, die speed, and so on, have the most impact on pelletization (Pradhan et al., 2018a).

2.7.3.1 Moisture content

According to Matúš et al. (2015), densified biomass's moisture content is one of the limiting factors affecting the solid biofuel's quality. It also affects the production process as well as the material's calorific value, mechanical strength, density, and dimensional stability.

The physical forces which bind the particles together determine the densified product's strength and durability. Five main types of binding forces between the individual particles in densified products have been identified as: mechanical interlocking bonds, adhesion and cohesion forces, interfacial forces, capillary pressure, solid bridges, attraction forces between solid particles, and mechanical interlocking bonds (Kaliyan & Vance Morey, 2009). Water increases the area of contact between particles, which contributes to the development of Van der Waals forces. Water serves as a lubricant as well as a binding agent. When biomass is extruded, pelleted, or briquetted, moisture from the biomass helps with processes including fibre solubilization, protein degradation, and starch gelatinization (Tumuluru et al., 2010).

Zamorano et al. (2011) also noticed that a product's net higher heating value and the efficiency of combustion are both influenced by the moisture content of the product. High-moisture pellets lose dry matter, while being stored and transported, and they decompose quickly (Graham et al., 2017). Through a review of several research papers, Pradhan et al. (2018a) found out that 10% moisture concentration is ideal for pelletization in a single pellet press, and that pellet density decreases as moisture content rises. Some other research has provided different optimum moisture concentrations for pelletization. They include Abdel et al. (2023) who found out that the optimum moisture content for pelleting was 8%, with moisture ranges of 10-15% as reported by (Abdoli et al., 2022; Hu et al., 2015; Tumuluru, 2019a) and 7.8-15% as

reported by (Križan et al., 2014; Styks et al., 2020). Anukam et al. (2021) also suggest that addition of 7-10% water to dried biomass increases the quality of the pellet. According to a review on the influence of biomass moisture content on pellet properties done by Ungureanu et al. (2018), the optimum moisture content was found to be 10%. The review also reported that moisture content of less than 5% led to pellets which have low strength, break easily and generate a lot of dust when being transported while high moisture content above 15% damages pellets during storage. Hence, the conclusion that moisture content is among the key factors influencing pellet quality.

2.7.3.2 Particle size

Pelletization pressure is influenced by biomass particle size. Most experimental cases studied on single pellet presses established that a reduction in particle size resulted in an increase of pellet density, while pelletizing using ring die or flat die machines has insignificant effect on pellet density (Pradhan et al., 2018a). Zepeda-Cepeda et al. (2021) described particle size as a physical property of feedstock that occasionally restricts the quality of densified biofuels. In the study on the effect of sawdust particle size on the physical, mechanical, and energetic properties of pinus durangensis briquettes, Zepeda-Cepeda et al. (2021) found out that the smaller the particle size of feedstock the higher the physico-mechanical and higher heating values of densified feedstocks. These results agreed with those studies done by (Kers et al., 2010; Ndindeng et al., 2015; Nurek et al., 2020).

The effect of particle size on biomass densification qualities has been the focus of several investigations (Filbakk et al., 2011; Kaliyan & Vance Morey, 2009; Serrano et al., 2011; Stelte et al., 2011). According to Stelte et al. (2011), an increase in surface area of contact between the biomass particles and the channel wall causes the friction in the press channel of a pellet mill to increase as the particle size decreases. In terms

of pellet quality, Kaliyan & Vance Morey (2009) discovered that pellet density increases with decreasing particle size for corn stover grinds. Similar findings were reported by Mani et al. (2006), who demonstrated that, in the case of pellets manufactured from barley straw, corn stover, and switch grass, but not wheat straw, particle size greatly influences the density. In contrast, Serrano et al. (2011) reported that smaller particles led to less dense pellets. The utilization of an industrial pellet mill rather than single pellet press units on a laboratory scale explained their divergence from other investigations.

According to Stelte et al. (2011), the ideal particle size is determined by the densification process; in general, briquetting operations can handle larger particles than pelletizing processes. Regarding pellet quality, a wide range of particle sizes is generally preferable.

2.7.3.3 Feedstock composition

In lignocellulosic biomasses, cellulose has a semi-crystalline structure and is resistant to hydrolysis, but hemicellulose has a random, amorphous structure with little strength and is easily hydrolyzed. The adhesive substances produced by hemicellulose hydrolysis are assumed to be the cause of natural bonding (Tumuluru et al., 2011). Moreover, lignin aids in the creation of solid bridges when temperatures are high and is important in biomass pelletization. Tumuluru (2014) showed that solid bridges are primarily responsible for particle bonding in scanning electron microscopy (SEM) images. At the right temperatures and moisture content, natural binders like lignin, proteins, and starch create solid bridges. Furthermore, low molecular weight hydrocarbons, such as oils, waxes, and other extractives, reduce wall friction and subsequently the pelletization pressure because their concentration on the pellet surface rises when the temperature is raised. According to Castellano et al. (2015), in addition

to creating a weak boundary layer that keeps particles from adhering tightly to one another, extractives also have a lubricating effect that reduces friction within die channels during pelletization process. The glass transition of lignin, followed by flow and hardening, results in pellets of greater quality. At high temperatures, lignin is expected to soften and act as a binding agent. Because lignin serves as a binder, biomass with a higher lignin content produces more durable pellets.

2.7.3.4 Machine-specific parameters

In attempting to explain machine-specific parameters, the term "pellet quality" usually refers to the features and attributes of the pellets produced by pelletizing machine. Pellet quality can be greatly impacted by a number of machine-specific factors. These parameters change based on the type of pelletizing machinery, such as feed pellet mills, biomass pellet mills, and other pelletizing machinery. According to Pradhan et al. (2018a), some of the important machine-specific variables and their effect on pellet quality are as highlighted below:

- ➤ Die Thickness and Hole Diameter: The density and durability of the pellets are influenced by the die thickness and hole diameter in pelletizing machinery such as pellet mills. Denser pellets could be produced by thicker dies, and pellet size is influenced by hole diameter.
- ➤ Die Compression Ratio: Pellet density and hardness are influenced by the compression ratio, which is calculated as the effective length of the die divided by its diameter. Denser pellets are typically the outcome of higher compression ratios.
- ➤ Die Material and Quality: Pellet smoothness, durability, and wear resistance can all be impacted by the type of die and material that was used. Longer die life

- and improved pellet quality are two benefits of using high-grade dies constructed from high-quality materials.
- ➤ Roller Speed and Distance: Pellet density and quality are determined by the distance between the rollers and the speed at which the material is compressed by the rollers. Pellets that are well-compacted may come from optimum settings of roller speed and distance.
- Moisture Content and Temperature: The raw material's moisture content and the pelletization process's temperature have an impact on the material's binding qualities. To achieve high pellet cohesiveness, control over these parameters is essential.
- ➤ Feed Rate: The rate at which raw materials are fed into the pelletizing machine impacts residence time and compression. Proper feed rates help achieve uniform pellet quality.
- ➤ Conditioning: In some processes, raw materials may undergo conditioning before pelletization. Conditioning can involve the addition of steam or other additives to improve the binding properties of the material and enhance pellet quality.
- ➤ Pellet Mill Type: Pellets can be produced with a variety of qualities using several types of pellet mills, such as ring die or flat die pellet mills. Ring die pellet mills are widely employed in commercial, high-capacity production.
- ➤ Die Speed and Drive Power: The speed at which the die rotates and the power of the drive system influence the efficiency and output of the pelletizing machine. Optimal settings ensure consistent pellet quality.

Screen Size: A screen is used in some pellet mills to regulate the final pellet size. Pellet homogeneity may be impacted by the screen size.

It's essential to note that the interplay of these parameters is complex and optimizing them for specific materials and production goals is crucial to achieving the desired pellet quality. Adjustments to these machine-specific parameters should be made based on the type of raw material, desired pellet characteristics, and the specific requirements of the application. Regular maintenance of the pelletizing equipment is also important to ensure consistent performance and high-quality pellet production (Gageanu et al., 2021; Lavergne et al., 2021; Styks et al., 2020).

2.7.4 Fundamental pellet qualities (physico-mechanical properties of pellets)

2.7.4.1 Durability

Alakangas (2011) defined Mechanical durability (also known as abrasion resistance) as the ability of handled densified biofuels to maintain their original form. It is measured by the ability of densified fuels to withstand shock or friction. Because the pellet is prone to mechanical wear, it generates dust or fine particles when being transported and stored. The pellets' ability to generate dust throughout its handling, transit, and storage will be revealed by the resistance test. Consumers are inconvenienced by dust emissions, which also endangers their health. Furthermore, dust and small particles may clog boiler feeding systems, which leads to uneven combustion processes. Lastly, dust can cause fire and explosive hazards during handling, storage, and transportation (Vinterbäck, 2004).

Pellets from various types of biomasses have different durability indexes resulting from their different compositions. Blending these biomasses to produce pellets has unique effects on pellet durability depending on the chosen blends as demonstrated by (Rajput et al., 2020), in the study on methods to improve the fuel properties of pellets. The author found out that addition of sawdust which is woody biomass to groundnut shells and leaf litter wastes which are herbaceous biomass increased pellet durability. This was attributed to higher lignin content in sawdust than in both groundnut shells and leaf litter wastes. There was reduction of pellet durability when groundnut shells were added to sawdust. Torrefaction after pelletization is an important process that affects the durability index of the pellets. Sarker et al. (2022) showed that the durability index of the pellets is decreased when pellets are torrefied while the calorific value is increased.

2.7.4.2 Hardness

Hardness determines the maximum crushing stress (or compressive or crushing resistance) that a pellet may withstand before breaking or cracking (Kaliyan & Vance Morey, 2009). Tensile strength is correlated with the adhesion forces between particles at all points of contact in an agglomeration. A compressive resistance test replicates compressive stress caused by pellet crushing in a screw conveyor, and also the weight of upper pellets on lower pellets when they are stored in bins or silos (Garcia-Maraver, 2015c).

The study on the effects of post-pellet torrefaction on pellet strength and fuel characteristics by Haykiri-Acma & Yaman (2022), revealed that the pellet strength decreases in this process compared to raw pellets. The same phenomenon was also observed by Sarker et al. (2022). Concerning pellet hardness, Rajput et al. (2020), observed that pellets produced from pure woody biomass have higher hardness than others. Therefore, woody biomass can be used as an additive to improve the hardness of pellets from other types of biomasses. The loss of strength and durability of pellets after torrefaction is attributed to degradation of hemicellulose and cellulose (Wang et al., 2020).

2.7.4.3 Bulk density

The bulk density of pellets is a measurement used for stockpiling of wood fuels because spaces between the woody particles may be greater or smaller depending on the size and form of the pellets. Non-densified biomass is bulky, making long-distance transport challenging and necessitating storage space. Furthermore, because the fuel is fed by volume rather than weight, bulk density can have a significant impact on combustion efficiency (EN15103, 2009).

Some of the factors that affect bulk density include torrefaction after pelletization. The bulk density generally decreases on pelletization of pellets (Manouchehrinejad & Mani, 2018; Siyal et al., 2021). In the study of improvement of agro-pellet quality through blending, Park et al. (2020) observed that the bulk densities are generally higher for blended pellets than single strand pellets.

2.7.4.4 Particle density

According to Sarker et al (2023)., particle density is the mass-to-volume ratio of a single pellet. Its value is affected by the particle size, compression strength, protein content, and moisture content. This characteristic affects the bulk density and, consequently, the characteristics of combustion of the pellets such as heat conductivity, burning rate and degasification rate. Stasiak et al. (2017) found out that the particle density of pellets produced from blends of pine sawdust and straws was higher than when produced from pure biomasses, hence, the importance of blending in pellet production. A similar observation was made by (Serrano et al., 2011). According to Siyal et al. (2021), torrefaction adversely affects pellet particle density. It can be concluded therefore, that, blending different biomasses improves pellet particle density while torrefaction decreases it.

2.7.4.5 Size of the pellets

An important parameter in the size of the pellets is the length/diameter ratio which affects the moisture uptake of pellets in humid environments and is of great importance in feeding to the combustion chambers (Hartley & Wood, 2008).

According to Mostafa et al. (2019b), there has been an increase in biomass pellet demand, which led to an increase in the price of woody biomass and, hence, its scarcity because of exploitation for pellet production. Therefore, to curb this challenge, non-woody, herbaceous and other biomasses (Figure 2.3) have received greater attention and research for pellet production. However, pellets produced from biomasses other than woody biomass possess poor qualities (Picchio et al., 2020b). Due to the dwindling woody biomass quantities, resulting from deforestation and the many utilities of wood, other biomasses have emerged to have a greater potential in the production of biofuels. Herbaceous biomasses are the most abundant and underutilized biomasses. To use these biomasses to produce quality pellets, quality enhancement methods have to be incorporated to elevate their properties to acceptable international standards.

2.8 Binders/Additives

According to Adeleke et al. (2021) binders promote cohesiveness and aid in the production of stable, long-lasting pellets and briquettes. Additionally, they enhance fuel abrasion resistance and lessen wear on production equipment. Binders must be present in a specific quantity in the fuel, and this quantity is influenced by a host of other factors. According to EU regulations, binder additives that enhance fuel quality, reduce emissions, or increase burning efficiency must constitute not more than 2% of the total mass of the biomass pellets (Agu et al., 2018). Tumuluru et al. (2011) indicated that binders may be used in biomass pellets for bioenergy, but they must be identified as a

component of the pellet composition. According to Tumuluru et al. (2011) binders include the following:

- i. Lignosulphonates (waofin)
- ii. Lignin-derived sulphonates salts in pulp mill liquors
- iii. Bentonites/colloidal clay (made up of montmorillonite)
- iv. Amylum (starch)
- v. Protein in low lignin content biomass
- vi. Thermoplastics

2.9 Torrefaction

Torrefaction is a thermochemical conversion and pretreatment process used to produce solid biofuels, liquids that can condense, and gases that cannot condense from waste biomass. It minimizes the need for drying by releasing the moisture and volatile matter from biomass. Torrefaction additionally improves storage time and lowers transportation costs by drying out biomass. Torrefied biomass is the solid byproduct of torrefaction that is dehydrated and carbonized. To manufacture solid fuel pellets of excellent quality and minimal emissions for use in commercial, industrial, and residential applications, torrefied biomass is widely utilized (Sarker et al., 2021).

According to Sarker et al. (2021), torrefaction entails heating the biomass for at least an hour at atmospheric pressure in the absence of oxygen, at temperatures between 200 and 300 °C. With incomplete removal of volatile matter caused by torrefaction, which lowers the amount of oxygen and hydrogen in biomass while raising the carbon content, biomass's energy density is improved.

The torrefaction process of biomass feedstocks/pellets takes place in five distinct temperature-time stages as presented by Chen et al., 2021 and van der Stelt et al., 2011

and illustrated in Figure 2.7. The brief description of these temperature-time stages is presented as follows:

Stage 1-Initial heating: The biomass is first heated up until it reaches the point of drying. The temperature rises during this phase, and at its conclusion, moisture begins to evaporate.

Stage 2-Pre-drying: During the drying stage, the temperature remains constant at 100°C until the biomass reaches a certain critical moisture content and the free water in it evaporates at a constant rate. When the moisture content reaches the critical point, the rate of water evaporation begins to slow down.

Stage 3-Post-drying and intermediate heating: The biomass is heated to 200°C at this point. Water which was physically bonded is extracted, while the biomass particles' internal barrier to mass and heat transmission is retained. By the end of this stage, the biomass has essentially no water content. Due to the evaporation of light organic molecules, some mass loss is to be expected during this phase.

Stage 4-Torrefaction: The real process starts at this stage. When the temperature reaches 200 degrees Celsius, the torrefaction process begins, and it ends when the temperature is lowered back to 200 degrees Celsius. The highest constant temperature is known as the torrefaction temperature. This is the stage when the majority of the biomass's mass loss happens.

Stages 5-Solids cooling: The product that has been torrefied is cooled down to a temperature that is below 200 degrees Celsius, and then to room temperature. During this time, there is no mass loss, although there may be vaporization of some adsorbed reaction products.

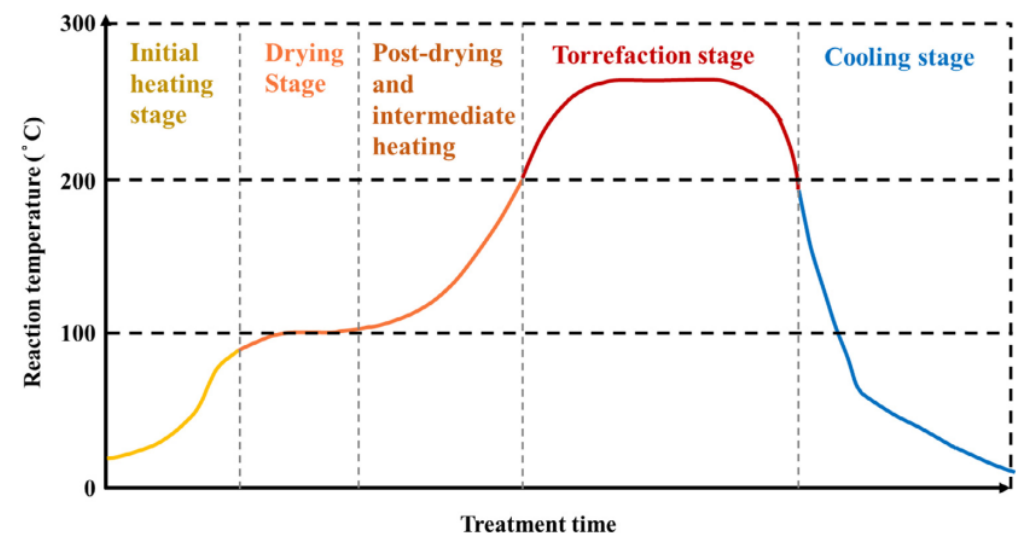


Figure 2.7 A schematic diagram showing the stages of torrefaction (Chen et al., 2021)

2.9.1 Classification of torrefaction processes

The process of torrefaction aims to improve biomass and provide higher-quality solid fuels. To achieve this objective, biomass can be torrefied using any of the three types of biomass torrefaction processes.

i. Dry torrefaction

In the process of dry torrefaction, biomass can be burned at temperatures typically between 200°C and 300°C in dry, non-oxidative (inert) or oxidative conditions. Chen & Kuo (2010) and Thanapal et al. (2014) used Nitrogen and carbon dioxide respectively as carrier gases in non-oxidative torrefaction; the former is most frequently used to sweep biomass materials after thermal pretreatment. Considering oxidative torrefaction, efforts have been undertaken to pretreat biomass utilizing carrier gases such as air (Chen et al., 2013), flue gas (Mei et al., 2015), and other gases with varying amounts of oxygen (Wang et al., 2013). Oxidative torrefaction has a faster reaction rate than non-oxidative torrefaction because of the presence of oxygen and the exothermic reactions that occur during thermal degradation (Chen et al., 2013).

ii. Wet torrefaction

At temperatures between 180 and 260°C, water and diluted acid solutions are used to upgrade biomass during wet torrefaction. The term "hydrochar" refers to the solid that is created when biomass is pretreated in wet media, such as water and diluted acid, as an alternative to improving it in dry media. It has been addressed that no substantial reaction of biomass happens in liquid water when the temperature is below 180°C for biomass torrefied in hot compressed water or hydrothermal media (Lynam et al., 2011). As a result, wet torrefaction is often carried out at a temperature of 180°C to 260°C for a reaction duration of 5 to 240 minutes (Chen et al., 2013; Thanapal et al., 2014). The qualities of water, such as its dielectric constant, ion products, density, viscosity, and diffusivity, would all drastically change as its temperature rose (Bach & Skreiberg, 2016). These modifications favor the breakdown of biomass in the liquid or aqueous phase.

iii. Steam torrefaction

In addition to dry and wet torrefactions, steam torrefaction is a method of torrefaction in which biomass is torrefied by a high-temperature and high-pressure steam explosion (Balat et al., 2008). The procedure, which is typically carried out at temperatures between 200 and 260°C with a holding period of five to ten minutes, involves introducing high-pressure and high-temperature steam into a sealed chamber containing lignocellulosic feedstock. After that, the pressure is quickly released, which results in a small loss of feedstock as well as steam that swells the lignocellulosic matrix and separates individual fibers (Mabee et al., 2007). During the steam explosion, low molecular weight volatiles in biomass are eliminated, boosting the product's calorific value and carbon content while lowering its bulk density, equilibrium moisture content (EMC), and mean particle size (Lam et al., 2012, 2013).

Recent research on steam torrefaction has mostly focused on the properties of the solid products that are left behind after the process, to produce pellets (Lam et al., 2013). In addition, compared to dry torrefaction, steam torrefaction offers the advantage of raising the calorific value, carbon content, and hydrophobicity at substantially lower temperatures and shorter treatment times. Additionally, compared to untreated pellets, steam explosion-derived pellets have greater mechanical strength and flexibility (Lam et al., 2011). However, the process of making pellets from steam torrefaction requires more energy than that of making pellets from untreated biomass, and it also requires more energy to force the pellets out of the die (Tooyserkani et al., 2012).

2.9.2 Process variables for torrefaction

Torrefaction performance is affected by several factors.

i. Temperature

According to (Chen & Kuo, 2011), the temperature at which torrefaction takes place is the most important operating parameter. Since torrefaction occurs at temperatures ranging from 200 to 300 degrees Celsius, it is well known that the operating temperature significantly affects the results of the torrefaction process. Hemicelluloses and cellulose have respective thermal decomposition temperatures of 220-315 degrees Celsius and 315-400 degrees Celsius. Djurdjevic & Papuga (2023), classified torrefaction into three distinct types based on the operating temperature range: light torrefaction (200–235 °C), mild torrefaction (235–270 °C), and severe torrefaction (275–300 °C). Moisture and light (or low molecular weight) volatiles are liberated from biomass during light torrefaction. Out of hemicelluloses, cellulose, and lignin, hemicelluloses are the most active constituents in biomass. During light torrefaction, hemicelluloses undergo some degree of thermal degradation while cellulose and lignin are barely or very slightly impacted. As a result, biomass experiences a minimal rise in its energy density or

calorific value after light torrefaction, and its weight loss is not significant. Hemicelluloses decompose and release volatiles more easily when biomass undergoes mild torrefaction. Hemicelluloses are significantly reduced, and cellulose is also partially consumed. Hemicelluloses are nearly entirely depleted and cellulose is greatly thermally decomposed in cases of severe torrefaction.

ii. Residence time

Torrefaction often lasts anything from a few minutes to several hours. Torrefaction increases the final solid fuel's or biochar's calorific value, while a longer period increases the biomass's carbon content and heating value (Chen et al., 2017). An outline of the standard temperature and residence time ranges, with a focus on how reaction temperature and residence time affect biomass qualities shows that torrefaction temperature has a greater effect than treatment duration (Chen et al., 2017).

iii. Particle size

One of the key factors in biomass torrefaction is particle size. Since biomass has a low heat conductivity, the pyrolysis mechanism of biomass will be influenced by the temperature gradient across the particle. Generally speaking, smaller particles can enhance the generation of bio-oil by inhibiting the development of char by promoting heat and mass transmission to maintain a relatively consistent temperature within them during pyrolysis (Bates & Ghoniem, 2014).

iv. Carrier gas and its flowrate:

Usually, a Nitrogen environment is used for the torrefaction process. Studies on the impact of flow rate, also known as superficial velocity, on torrefaction have been conducted. The outcomes showed that the carrier gas's superficial velocity had no

bearing on the torrefaction performance under internal conditions (Barskov et al., 2019).

v. Catalyst

Research has demonstrated that the presence of inorganic metals in biomass may act as catalysts in the thermochemical processes of the biomass, affecting the production of char, the distribution of products from pyrolysis, gasification, and combustion (Barskov et al., 2019). Potential catalysts for the thermochemical conversion of biomass include alkali and alkaline earth metals. The effects of inorganic metals on biomass torrefaction have been studied recently by several researchers. Relevant experimental findings indicated that during torrefaction, either potassium or sodium exhibited catalytic activity in the decomposition of biomass. The mass loss of woody biomass increased with rising potassium content, according to research on the effects of potassium on torrefaction performance using a thermogravimetric analyzer (Shoulaifar et al., 2016).

vi. Performance Index

The performance of torrefaction is strongly related to the severity of torrefaction (TS), that is primarily determined by temperature and duration of torrefaction. In order to assess torrefaction performance, a variety of indices have recently been developed, including the upgrading energy index (UEI), severity factor (SF), weight loss (WL), torrefaction severity factor (TSF), energy-mass co-benefit index (EMCI), and torrefaction severity index (TSI). Since higher WL is a function of temperature or torrefaction length, WL is the most commonly used index to represent TS. WL is typically calculated using a dry basis (Chen et al., 2015).

2.10 Combustion analyses of pellets

2.10.1 Combustion characteristics

2.10.1.1 Ultimate and proximate analyses and higher heating values (HHV)

Ultimate and proximate analyses as well as HHV are among the combustion characteristics considered in evaluation of pellet properties and they have been elaborated in section 2.2.1.

2.10.1.2 Combustion emissions

Combustion of biomass pellets results in heat energy and different emissions. Perez-Jimenez (2015) provided a comprehensive classification and conditions of production of various gaseous emissions from combustion biomass pellets. The two major classes are gaseous emissions from complete and incomplete combustion. Examples of emissions emanating from incomplete combustion which included CO, PAHs, NH₃, CH₄, total organic compounds (TOCs) and polychlorinated dioxins & furans. On the other hand, emissions from complete combustion included CO₂, SO₂, NO_x and hydrogen chloride. Additionally, HC and O₂ are also present in varied quantities in flue gases (He et al., 2018). These emissions are harmful to the environment, humans and combustion equipment (Kažimírová & Opáth, 2016).

Quantity of emissions from different biomass feedstocks vary since their compositions are unique. In the case of pelleting and briquetting, the type and amount of binder used also play an important role in emissions produced. Carroll & Finnan (2013) analyzed carbon monoxide (CO), sulphur dioxide (SO₂) and nitrogen oxides (NOx) emissions from different biomasses and found out that those from woody biomass met the emissions standards (EU regulations), while those of straws which are basically herbaceous biomass exceeded the set limits. In the study on combustion of waste plastics, lignite and biomass mixture pellets, Duranay (2019) found that the rate of

combustion and efficiency increased with the increase in plastic ratio. Also, CO₂ emissions increased with the increase in plastic ratio. Measures to reduce emissions have to be incorporated into the combustion process of biomass fuels prone to emissions like feedstocks from herbaceous biomasses and fuel feedstocks with plastic binders. Kida et al. (2023) stated that air pollution from burning plastics, whether in controlled incineration plants or in uncontrolled open burning, has serious negative effects on the environment and human health. The vast array of chemical additives included in plastics, which are produced from fossil fuels, all contribute to the various and frequently dangerous pollutants that are emitted when the plastics decompose thermally.

The type of plastic, the temperature, the amount of oxygen present, and the presence of other materials all have a significant impact on the range of emissions that result from the plastic's combustion. According to (Tomsej et al., 2018), (Kida et al., 2023) and Valavanidis et al. (2008) some of the main types of emissions are as follows:

> GHGs, or greenhouse gases:

- CO₂ (carbon dioxide): It is one of the main byproducts of complete combustion that causes climate change. Due to their carbon base, plastics emit carbon dioxide at every stage of their lifecycle, from manufacturing to combustion.
- Nitrous oxide (N₂O) and methane (CH₄): These are additional powerful greenhouse gases, albeit usually in smaller amounts than CO₂.

> Particulate Matter (PM):

Black carbon (BC) and PM2.5: Soot (black carbon) and other fine
 particulate matter are major emissions, particularly from incomplete

combustion (e.g., open burning). These particles have the ability to enter the lungs deeply.

Organic Carbon (OC): It is another particulate matter component.

VOCs, or volatile organic compounds:

 Benzene, toluene, xylene, formaldehyde, and acetone are among the many organic compounds that are emitted. A large number of VOCs are harmful or cause ground-level ozone to develop.

> PAHs, or polycyclic aromatic hydrocarbons:

These are dangerous organic substances, some of which, like benzo(a)pyrene, are known to cause cancer. They are created when organic components burn incompletely.

Halogenated Compounds:

- O Dioxins and Furans (PCDD/Fs): These are extremely harmful and long-lasting organic pollutants that are mostly produced by the burning of polymers that include chlorine, such as polyvinyl chloride, or PVC, particularly when combustion circumstances are not ideal. A plastic may ignite with other materials even if it does not contain chlorine.
- o **Hydrogen Chloride (HCl):** Released by the PVC combustion.
- Polychlorinated Biphenyls (PCBs): Substances with the potential to cause cancer.

Heavy Metals:

O Heavy metals (such as lead, cadmium, mercury, chromium, antimony, and arsenic) that are added to plastics may be discharged into the atmosphere or accumulated in the ash.

> Other Toxic Gases:

 It is also possible to release hydrogen sulfide (H₂S), sulfur dioxide (SO₂), and nitrogen oxides (NOx).

Standard procedures are used to determine the various combustion characteristics of biomasses. These methods are enlisted in Table 2.3.

Table 2.3. The standard methods for analyses of biomass fuels (Suman et al., 2021)

Property	Standard methods	
Proximate analysis		
Ash	ASTM D1102 (873 K),	
Moisture	ASTM E871	
Volatile matter	ASTM E 872, ASTM E 897	
Fixed carbon	By difference	
Ultimate analysis		
Carbon, hydrogen	ASTM E 777	
Nitrogen	ASTM E 778	
Sulphur	ASTM E 775	
Oxygen	By difference	
Heating value (gross calorific value)	ASTM D 2015, E 711	
Ash elemental	ASTM D3682, ASTM D2795, ASTM D4278	

2.11 Methods of Biomass Pellet Quality Enhancement

2.11.1 Use of woody biomass as an additive

Gilvari et al. (2019) tied pellet quality to the type of biomass resource. The shortcomings of herbaceous biomass regarding the physical property (lower density), chemical makeup (higher ash, lower carbon, and lower lignin), and fuel property (lower heating value) could be resolved by blending with woody biomass (Picchio et al., 2020b; Tumuluru & Fillerup, 2020). In the study on co-pelletization, Cui et al. (2021) concluded that addition of woody biomass to straw (herbaceous biomass), to produce pellets, improved significantly pellet qualities. For instance, according to Tumuluru et al. (2012), it significantly enhances proximate and ultimate composition whilst also reducing the ash content of pellets. The study also reports that the addition of woody

biomass enhances the densification properties of herbaceous biomass because of its higher lignin content which is the primary binder in pelleting/briquetting.

In the review on biomass pelleting process, Dujmović et al. (2022) reported that addition of woody biomass on agricultural biomass produced pellets with enhanced physico-mechanical properties and this was affirmed by pellets from cornstalk blended with fir. Contrary, addition of herbaceous biomass to woody biomass as studied by Lehmann et al. (2012) has a negative effect on the durability of densified biomass and it revealed that the density of the pellet reduces.

Table 2.4 presents the observations of the effect on pellet properties caused by blending herbaceous biomass with woody biomass.

Table 2.4 Research on effect of addition of woody biomass to herbaceous biomass for pelleting

Sr No.	Feedstock blend	S	Observation	References
	Herbaceous biomass	Woody biomass		
1	Switch grass	Pine	Increased bulk density and durability.	(Tumuluru, 2019b)
2	Rice straw	Sawdust	Increased unit density and shatter index. Higher heating value increased by 6-7.2%.	(Rahaman & Salam, 2017)
3	Barley straw	Pine sawdust	Pellet durability increased by 3%.	(Serrano et al., 2011)
4	Miscanthus	Pine sawdust	Improved thermal properties. Decreased ash content.	(Mohammadi & Anukam, 2023)
5	Rapeseed straw and wheat straw	Pine sawdust	Pellets strength and higher heating value decreased with an increase in straws ratio. Pellet density decreased with an increase in straws ratio. The increased straw proportion increased the ash content of the pellets.	(Stasiak et al., 2017)
6	Miscanthus and switch grass	Pine sawdust	Pellet met industrial quality with switchgrass and miscanthus blends of less than 30%.	(García, Gil, Rubiera, et al., 2019)
7	Reed canary grass, timothy hay and switchgrass	Spruce and pine sawdust	Improved overall pellet quality. Lowers pelleting energy requirement.	(Harun et al., 2018)

2.11.2 Use of plastic additives

According to Anukam et al. (2021), all biomasses can be pelleted, but not all can produce high-quality pellets. As a result, additives are utilized to enhance pelletization. Lignosulfonates, spent sulfite liquor, starch, kraft lignin, waste vegetable oils, and citrus peels are additives discussed by Anukam et al. (2021). Other additives include plastics (Auprakul et al., 2014a). Emadi et al. (2017) stated that linear low-density polyethylene (LLDPE) and low-density polyethylene (LDPE) are the most abundant types of plastics which can be easily derived from municipal solid wastes (MSW) and have favorable fuel and adhesion properties. Thus, according to Emadi et al. (2017), the use of LLDPE as additives results in pellets with high density, strength, higher heating value, and decreased ash content. High-density polyethylene (HPDE) is also extractable from MSW (Agu et al., 2021). HDPE, according to Agu et al. (2021), significantly increases higher heating values of pellets produced from torrefied and non-torrefied wheat and barley straws. It also increases pellet strength and durability of pellets as well as pellet particle density. Although the pellet particle density was seen to improve, it was not to the extent when LLDPE was used as a binder. Ash content and moisture adsorption of biomass pellets are greatly reduced when HDPE is used as a binder (Agu et al., 2018). Generally, plastic binders enhance bulk densities, mechanical strength and higher heating values as depicted by research presented in Table 2.5.

2.11.3 Use of TAP (Torrefaction After Pelletization)

Torrefaction is one method for improving the properties of solid biomass which has gained popularity. It is a mild thermochemical treatment used on biomass at ambient pressure in low-oxygen environment (Mukherjee et al., 2022; Nunes et al., 2014; Tumuluru et al., 2021) at temperature ranges of 200-300°C and residence time of 30-180 minutes (Fisher et al., 2012; García et al., 2019; Shang et al., 2012). The results of

torrefaction in this kind of environment are the decomposition of hemicellulose partially to volatile matter and the removal of all the moisture in biomass while lignin content and cellulose are unaffected (García et al., 2019).

Table 2.5 Research on effect of plastic additives biomass pelleting

Sr No	Feedstock blends	Observation	References
1	Torrefied wheat and barley straws and LLDPE	Increased higher heating value. Increased mechanical strength. Decreased ash content.	(Emadi et al., 2017)
2	Corn stover and mixed plastic wastes	Carbon, hydrogen and higher heating value increased with increase in plastic content. Durability, bulk density, particle density and ash content decreased with increase in plastic content.	` =
3	Refuse derived fuel with 20% plastic	Increased higher heating value. Improved mechanical strength.	(Rezaei et al., 2020)
4	Pinus radiata sawdust, LLDPE and polypropylene (PP)	Increased durability. Greatly improved hydrophobicity. Improves HHV moderately to highly.	(Song et al., 2021)
5	Sawdust, date palm trunk and plastic wastes	•	(Garrido et al., 2017)
6	Torrefied wheat, barley straws and HDPE	Pellet density and tensile strength was improved. HHV increased. Hydrophobicity improved. Ash content decreased.	(Agu et al., 2021)

The most important process conditions for optimum energy yield in torrefaction from past researchers are torrefaction temperature, time and the size of biomass particles (Adeleke et al., 2021; Akanni et al., 2019). Chen et al. (2021) further narrowed down the conditions to temperature and residence time, while Akanni et al. (2019) again further narrowed down to only torrefaction temperature, stating that the effect of residence time reduces after one hour of torrefaction. Thus, further pointing out that as torrefaction temperature rises the mass and energy yields decrease leading to increase in energy density.

Torrefaction can be employed as a pre-treatment method of biomasses before pelletization commonly referred as TOP (Torrefaction before Pelletization) process or as a post-treatment after pelletization referred to commonly as TAP (Torrefaction After Pelletization) process (Azargohar et al., 2018; Manouchehrinejad & Mani, 2018). The discussion of some research on torrefaction after pelletization (TAP) processes are as follows: Manouchehrinejad & Mani (2018) studied the effect of torrefaction of wood pellets produced from mixed sawmill wastes of soft and hardwoods at temperatures of between 230°C and 290°C. The observation was that the shape of the pellets was retained, the mass and energy yields decreased with increasing torrefaction temperature. Higher heating values increased by 26%, as well as its hydrophobicity, while pellet particle and bulk densities, moisture, durability and hardness decreased. Wang et al. (2020) found out that the torrefied pellets maintained their integrity while mass yield decreased with temperature increase, higher heating values and hydrophobicity increase. The mechanical properties of torrefied pellets generally decreased with increasing torrefaction temperature. In their studies, Ghiasi et al. (2014), Shang et al. (2012), and Kumar et al. (2017) concluded that post-pelletization torrefaction resulted in improved higher heating value, energy density and hydrophobicity, while particle and bulk densities, mass and energy yields, as well as the mechanical properties of pellets, reduced with torrefaction. They also observed that the structural integrity of the pellets is maintained.

2.11.4 Optimization as quality enhancement method

According to Mostafa et al. (2021a), the conditions of pelletization influence biomass pellet qualities. Thus, the exact effect of pellet production process parameters to give the best physico-mechanical and combustion properties of pellets have to be determined. Data from optimization studies can then be used for subsequent production

of quality pellets, hence, a quality enhancement method.

Liu et al. (2023) described process optimization as a condition in which several factors interdependently affect the outcomes in order to obtain a specific quality required. Optimization studies can be multi-parameter, multi-response, single response, single factor or a mix of them and analysis done using different statistical tools (Thapa et al., 2018a).

Pellet qualities are maximum at optimum conditions of production (Cui et al., 2021). Pellet durability, hardness, bulk density and higher heating values are qualities used to determine the optimal process parameters in pellet production (Thapa & Engelken, 2020). These are desirable pellet qualities and, therefore, have to be maximized, so that it gives the best combination of process parameters. At the same time, undesirable pellet qualities like emissions have to be minimized. Said et al. (2015) observed that pellet quality is dependent on feedstock composition and controllable process factors. An example of controllable factors is moisture content, in which if it is high decreases the durability, higher heating values and shelf life of pellets, while increased binder concentration improves its durability (Akbar et al., 2021).

Various process parameters considered in optimization have been studied in literature and they include; feedstock material, moisture content, blending ratio, particle size, binders (Thapa & Engelken, 2020), and die pressure (Huang et al., 2017b; Mostafa et al., 2021a). It also includes torrefaction temperature and residence time (Akanni et al., 2019), in the case of torrefaction after pelletization studies. The shortcomings brought about by feedstock variability in terms of physical and chemical properties can be resolved by blending different biomass feedstocks (Edmunds et al., 2018; Ray et al., 2017). Tumuluru (2019b), studied the effect of blending feedstock material from pine

and switchgrass on the pellet durability and bulk density. The resultant pellet attained a maximum durability index greater than 95% and bulk density of 550 Kg/m³. In optimization study done by Thapa & Engelken (2020) using Taguchi-grey relational analysis, blending ratio, particle size, feedstock material and blending ratio were found to have significantly impacted on pellets physico-chemical characteristics. Park et al. (2021), in the study of performance optimization of fuel pellets, found out that the optimal ratio of pepper stem to coffee waste was 8:2 and the optimal torrefaction temperature was 250°C. In the study, performance indicators used in the study were moisture content, bulk density, durability, ash content, fine particles and gross calorific value. Zhang et al. (2020), researched on optimization of pellets produced from hydrothermally pretreated wheat straw using response surface methodology. The parameters studied included wheat straw feedstock particle size, hydrothermal pressure and temperature, mold pressure, moisture content, compression speed and pressure holding time. Optimum pelletization conditions were as presented in Appendix 1. Conspicuously, in all the above studies, none of them analyzed emissions. Again, only one of the studies went ahead to include torrefaction after pelletization. Appendix 1 presents biomass pelleting optimization studies carried out by different researchers and their outcomes on pellet quality.

2.12 Pellet quality standards

According to Garcia-Maraver (2015a), by-products from the combustion of pellets and their effects on combustion equipment like pellet stoves and boilers, are some of the important customer concerns other than pellets' energy content. It is also important to appreciate the fact that biomass fuel pellets from different biomass feedstocks produced from different processes are unique. In order to ensure the best quality pellets are produced, quality control and standardization have been introduced in many countries

(Japhet et al., 2019; Mostafa et al., 2021b). These standards have ranges of different properties of pellets that define the acceptable quality of pellets (Mostafa et al., 2021a). Biomass pellet standards and their general requirements have been produced for different types of biomasses and even their mixtures (Mostafa et al., 2019b). For instance, Table 2.6 illustrates the European guidelines EN 14961-6 pellets for non-woody biomass pellets or pellet mixtures from different biomasses. Pellets from non-woody biomass are categorized as A class, while those from mixtures of different biomasses are B class pellets (Garcia-Maraver, 2015a). Pellet quality parameters are compared to these standard specifications so as to evaluate the overall quality of the pellet produced. According to Garcia-Maraver (2015a), some of the European Pellet quality standards and certifications include:

- Austrian standard: ÖNORM M 7135 (Compressed wood or compressed bark in natural state, pellets and briquettes. Requirements and test specifications: 2003).
- 2. Swedish standards: SS 187120 (Biofuels and peat, fuel pellets. Classification (Swedish Standards Institution): 1998).
- 3. German standards: DIN 51731 (Testing of solid fuels, compressed untreated wood. Requirements and testing (Deutsches Institut für Normung): 1996).
- 4. Italian standard: CTI-R04/05 (Recommendation: solid biofuels. Pellet characterization for energetic purposes: 2004).
- 5. French recommendation: ITEBE (Not an official standard but a set of quality controls developed. 2009).
- 6. European standard committee EN14961-1 (Solid biofuels. Fuel specification and classes. Part 1: general requirements: 2010).

Table 2.6: European normative guidelines for pellets produced from herbaceous and fruit biomass and blends and mixtures (Garcia-Maraver, 2015a)

Pellet property	Units	Straw	Miscanthus	Reed canary grass	
Diameter and	Mm	D06-10: D±1; 3	.15≤L≤40	gruss	
length, D and L		D12-25: D±1; 3			
Moisture, M	% as received	M10≤10	M12≤12		
Ash, A	% dry basis	A6.0≤6	A4.0≤4	A8.0≤8	
		A6.0+>6		A8.0+>8	
Mechanical	% as	DU97.5≥97.5	DU96.5≥96.5		
durability, DU	received				
Fines	% as received	F1.0≤1.0			
Additives	% dry basis	Type and Quant			
Lower heating value as received, Q	MJ/kg	Minimum value	Q14.5≥14.5		
Bulk density, BD	kg/m³ % as received	BD600≥600	BD580≥580	BD550≥550	
Nitrogen, N	% dry basis	N0.7≤0.7	N0.5≤0.5	N2.0≤2.0	
Sulphur, S	% dry basis	S0.10≤0.10	S0.05 \le 0.05	S0.20≤0.20	
Chlorine, Cl	% dry basis	C10.1≤0.10	Cl0.1≤0.10 Cl0.8≤0.8		

2.13 Literature review matrix: Summary and gaps

This section provides a summary of literature reviews and their research gaps as well as the conceptual framework Figure 2.8 to place the pellet to be researched in a broader context of different pelleting concepts. Literature review matrix is presented in Appendix 2.

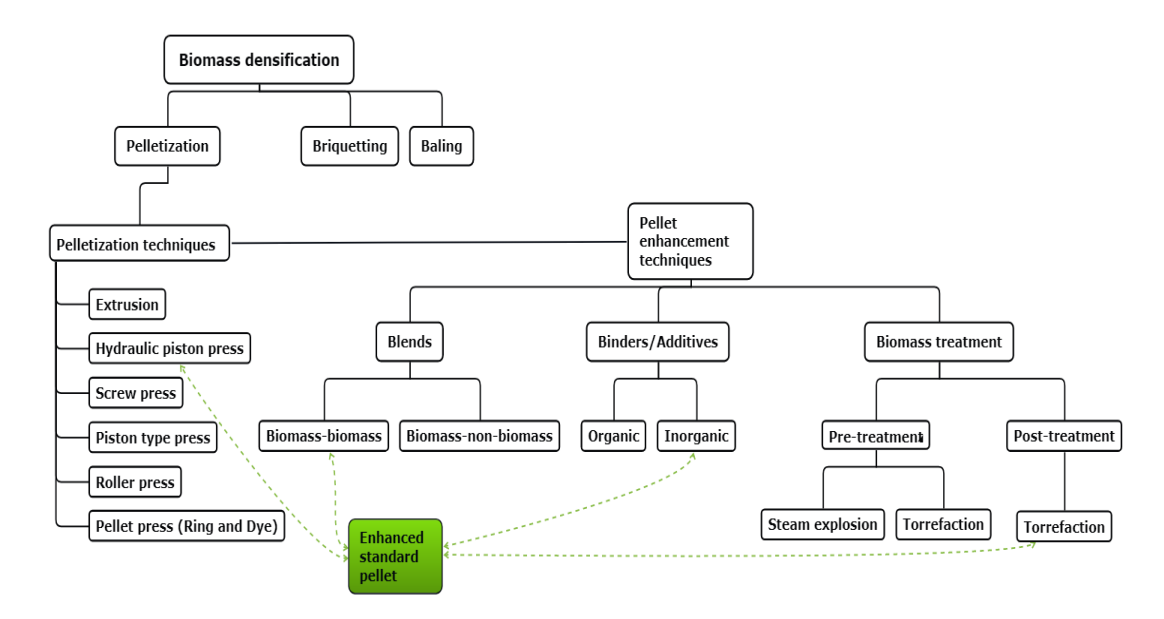


Figure 2. 8: Conceptual framework

2.14 Design of experiments

Design of experiments (DOE) is the process of defining and investigating each potential outcome of an experiment involving multiple factors (Butler, 1992). It is an offline method of quality control used to ensure that products and processes operate at their optimum performance (Krishniah et al., 2012). DOE entails designing of experiments, conducting of experiments and analyzing data. Experimental designs can be classified into traditional methods such as Completely Randomized Design, Randomized Complete Block Design, Latin Square Design, full factorial designs, response surface methods, etc. and Taguchi methods, which include, orthogonal array (OA), robust designs, multi-level factor designs and multi-response optimization.

2.14.1 Taguchi method

The discipline of quality engineering benefited greatly from the work of Japanese scientist Dr. Genichi Taguchi. According to his quality philosophy, a product's quality should be designed into it rather than only inspected into it. In other words, inspection, a postmortem activity, is not how quality is achieved. His second guiding principle is that minimizing the variance from the desired value is a good way to achieve quality.

Additionally, the performance of that product ought to be impervious to uncontrollable (noise-related) elements. He promoted measuring the price of quality in relation to variance from the norm. According to Krishnaiah & Shahabudeen (2012) the Taguchi Techniques include;

- ➤ Off-line Quality Assurance techniques.
- Ensures Quality of Design of Processes and Products.
- Robust Design method.
- Makes use of Orthogonal Arrays for designing experiments.

2.14.2 Steps in Taguchi Experimentation

The following are steps related to the Taguchi-based experiments (Krishniah et al., 2012):

- 1. State the problem.
- 2. Determine the objective.
- 3. Determine the response and its measurement.
- 4. Identify factors influencing the performance characteristic.
- 5. Separate the factors into control and noise factors.
- 6. Determine the number of levels and their values for all factors.
- 7. Identify control factors that may interact.
- 8. Select the Orthogonal Array.
- 9. Assign factors and interactions to the columns of OA.
- 10. Conduct the experiment.
- 11. Analyze the data.
- 12. Interpret the results.
- 13. Select the optimal levels of the significant factors.

- 14. Predict the expected results.
- 15. Run a confirmation experiment.

2.14.3 Design of experiments using Orthogonal Arrays (OA)

Taguchi proposes adopting a factorial design that is highly fractional with unique orthogonal arrays for organizing trials, with factors serving as the column headings and treatment combinations as the rows (Freddi & Salmon, 2019).

Arrays with orthogonal column vectors are referred to as orthogonal arrays. They have the property that the scalar product of each pair of vectors is zero. This indicates that a vector cannot be projected onto another. Therefore, each vector is linearly independent and conveys information once only. Each treatment provides a distinct piece of information in Taguchi arrays L, in which the factor levels are permuted to produce uncorrelated responses (Freddi & Salmon, 2019).

2.14.3.1 Nomenclature of arrays in OA approach

Equation 2.2 below shows how to determine the number of experimental runs given the variables synonymous to the number of columns and their levels.

 $L_a(b^c)$ Equation 2.2

Where,

L=Latin square

a=Number of rows

b=Number of levels

c=Number of columns (factors)

Degrees of freedom associated with the OA = a - 1.

2.14.3.2 Assignment of factors and interactions

When all the primary factors need to be examined, the factors can be placed in any order in any column of the OA. When studying primary factors and some interactions, we must adhere to a particular procedure. To make it easier to assign the orthogonal array columns' factors and interactions, Taguchi has created the following two tools (Krishniah et al., 2012):

- i. Interaction Tables and
- ii. Linear Graphs

All possible interactions between columns (factors) are contained in the interaction table while Linear Graph (LG) provides interaction data represented graphically.

2.14.4 Data analysis from Taguchi experiments

Data from experiments with Taguchi/Orthogonal Arrays (OA) can be analyzed using both the response graph method and the Analysis of Variance (ANOVA). ANOVA approach takes into consideration variation from all sources, including errors. ANOVA and percent contribution suggest that choosing the best condition may not be beneficial if the error sum of squares is high in comparison to the experiment's control factors. ANOVA is necessary also for statistically confirming the data. The response graph approach is relatively simple to comprehend and use. There is no statistical expertise needed for this procedure. This approach might be adequate for practical or industrial purposes (Krishniah et al., 2012). In the case where there is need for optimization in which there are many responses, Taguchi multi-response optimization is done as explained in section 2.14.4.3.

2.14.4.1 Regression analysis

A functional relationship (model or equation) between response or dependent variables and predictor, explanatory or independent variables can be found using the regression analysis methodology. Regression analysis is referred to as univariate regression when it deals with a single response variable and as multivariate regression when it deals with two or more response variables.

Fitting a linear equation to the data is the method used in linear regression analysis to try and predict the relationship between variables. There are two commonly used types of Linear regression; simple and multiple linear regression (Fumo & Rafe Biswas, 2015). Multiple linear regression is most commonly used and it allows use of varied predictors and it is generalized by the following equation;

$$Y = \beta_0 + \beta_1 X_1 + \beta_2 X_2 + \dots + \beta_n X_n + \varepsilon$$

Where;

Y is the response variable, $X_1, X_2...X_n$ are the design variables and the *n*th number of variables, $\beta_0, \beta_1, \beta_2...\beta_n$ are regression coefficients and ϵ is the error due to the discrepancy between the actual and the predicted responses.

2.14.4.2 Model adequacy checking

According to Montgomery et al. (2016), it is always important to (a) check that the fitted model accurately represents the underlying system and (b) make sure that none of the assumptions of least squares regression are broken. If the model does not provide a good enough fit, pursuing the exploration and optimization of a fitted linear regression will probably result in unsatisfactory or inaccurate outcomes. There are a number of methods for evaluating the validity of the fitted model model. Some of these methods include;

- Residual analysis-in which a normal probability plot of the residuals is constructed to verify the normality assumption. The normality assumption is achieved if the residuals approximately lie around a straight line (Borkowski, 2010).
- Scaling residuals- standardized and studentized residuals are examples of scaling residuals and they are important in optimization studies. These standardized residuals are helpful in identifying outliers because they have a mean of zero and a variance of roughly one unit. Any observation with a standardized residual outside of this range may be uncommon in relation to its observed response. The majority of the standardized residuals should fall within the interval -3 ≤di ≤ 3 (di is the residual). These outliers need to be closely investigated since they could indicate anything from a straightforward data recording error to a more serious issue, such an area of the regressor variable space where the fitted model is an inadequate representation of the actual response values (Borkowski, 2010).
- Influence Diagnostics-The fitted regression model is sometimes disproportionately impacted by a small subset of the data. In other words, estimations of parameters or forecasts may rely more on the significant subset than on the bulk of the data. The goal is to identify these influential points and evaluate how they affect the model (Borkowski, 2010).
- Testing for Lack of Fit- Regression model fitting in optimization typically involves using data from a designed experiment. Getting two or more observations (replicates) on the response at the identical settings for the independent or regressor variables is often useful. Once this is accomplished, a

formal test on the regression model to check lack of fit is conducted (Borkowski, 2010).

2.14.4.3 Taguchi multi-response optimization

Multi-response optimization cannot be done directly using the Taguchi method. Nevertheless, Taguchi designs can be used to gather the observed data for each response, and many researchers have devised various methods for statistical analysis. The usual method for solving these challenges is to integrate the multiple responses into a single statistic (response), and then to determine the optimal levels. Among these methods is Grey relational analysis (Krishniah et al., 2012; Thapa & Engelken, 2020). These two authors outlined the technique of multi-response optimization in the following five steps:

Step 1: Computation of signal-to-noise ratio(S/N). Signal-to-noise, sometimes known as S/N, is a statistical performance metric used by Taguchi. Equation (2.3) is used to determine S/N for a "bigger the better" (desirable responses) and equation (2.4) "smaller the better" (undesirable responses) characteristic (Krishniah et al., 2012).

$$S/N ratio(\eta) = -10log_{10}\left(\frac{1}{n}\right)\sum_{i=1}^{n}\frac{1}{Y_{ij}^{2}}$$
..... Equation 2.3

$$S/N ratio(\eta) = -10log_{10}\left(\frac{1}{n}\right)\sum_{i=1}^{n}Y_{ij}^{2}$$
..... Equation 2.4 where,

 Y_{ij} = Observed response value (i = 1, 2..., n; j = 1, 2,....k)

n = number of replications.

Step 2: Normalizing *Yij* as *Zij*. After the determination of the S/N ratio, Y_{ij} is Normalized (transformation carried out on a single input to scale and spread the data into an appropriate range for subsequent analysis) using the following equations (Krishniah et al., 2012).

$$Z_{ij} = \frac{Y_{ij} - min(Y_{ij}, i=1,2,...,n)}{max(Y_{ij}, i=1,2,...,n) - min(Y_{ij}, i=1,2,...,n)}.$$
Equation 2.5

(for S/N ratio with the "larger the better")

$$Z_{ij} = \frac{\max(Y_{ij}, i=1,2,...,n) - Y_{ij}}{\max(Y_{ij}, i=1,2,...,n) - \min(Y_{ij}, i=1,2,...,n)}.$$
Equation 2.6

(for S/N ratio with the "smaller the better")

Where,

 Z_{ij} =jth dependent variable/response normalized value for ith experiment/trial

Step 3: Compute the Grey relational coefficient (GC). Grey relational co-efficient (GC) is then calculated as follows (Krishniah et al., 2012);

$$GC_{ij} = \frac{\Delta_{min} + \lambda \Delta_{max}}{\Delta_{ij} + \lambda \Delta_{max}} \begin{cases} i = 1, 2, \dots n - experiments \\ j = 1, 2, \dots, m - responses \end{cases} \dots$$
Equation 2.7

Where,

 GC_{ij} = grey relational coefficient for the *i*th experiment/trial and *j*th dependent variable/ response.

 Δ = absolute difference between Y oj and Yij which is a deviation from the target value and can be treated as a quality loss.

 Y_{oj} = optimum performance value or the ideal normalized value of jth response

 Y_{ij} =the *i*th normalized value of the *j*th response/dependent variable

 Δ_{min} =minimum value of Δ

 Δ_{max} =maximum value of Δ

 λ is the distinguishing coefficient which is defined in the range $0 \le \lambda \le 1$

Step 4: Compute grey relational grade (*Gi*). Calculated as (Krishniah et al., 2012); $G_i = \frac{1}{m} \sum GC_{ij}$ Equation 2.8 where *m* is the number of responses.

Step 5: Optimization. Use the response graph method or ANOVA and select optimal levels for the factors based on the maximum average Gi value.

CHAPTER THREE: METHODOLOGY

3.1 Introduction

This chapter provides detailed description of the methods to be used to achieve the goals of this research.

3.2 Materials

This research focused on utilizing agricultural and forestry wastes, so the two typical samples that were used in this study were a woody biomass waste (eucalyptus sawdust) representing forestry waste and a non-woody biomass waste (corn stover) representing agricultural waste as well as LLDPE which was used as a binder.

Corn stover was sourced from farms in Uasin Gishu county while eucalyptus sawdust was sourced from sawmills and wood workshops in Uasin Gishu county. The source of LLDPE raw material was Pyramid East Africa Limited, Eldoret. LLDPE acquired was a Q2018 series which is used in production of hygiene packaging such as freezer film, bread bags, shoppers and lamination film. Its melting point is 121°C and softening point is 100°C which are good properties for binding. Approximately 20kg of corn stover, 20kg of eucalyptus sawdust and 5kg of LLDPE were acquired. These raw materials are as presented in Plate 3.1.

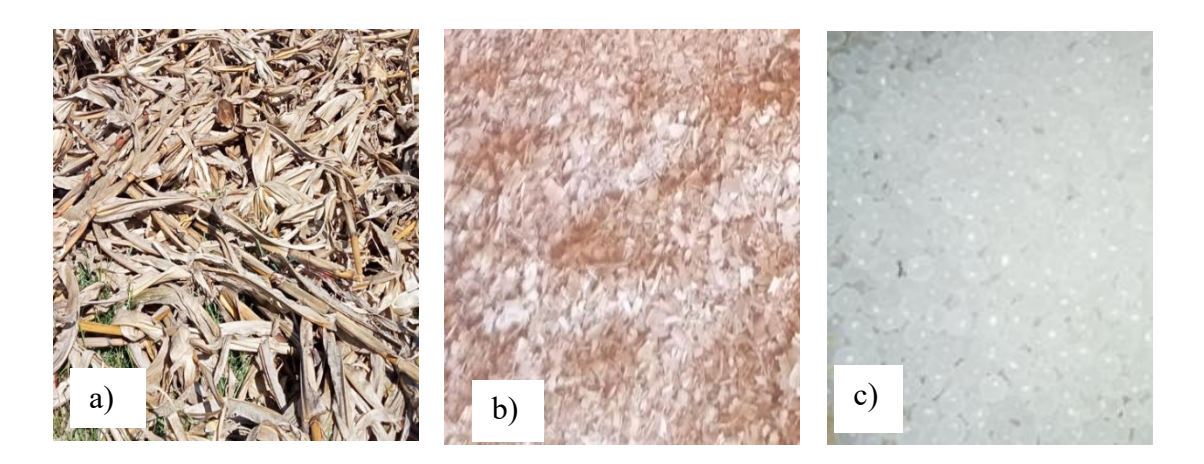


Plate 3.1: a) Corn stover b) Eucalyptus sawdust c) LLDPE pellets

3.3 Preparation of corn stover and eucalyptus sawdust

3.3.1 Removal of undesirable impurities

The first step in preparation of biomass feedstock was to make sure that they are free of undesirable impurities. Before grinding, the raw materials were screened to remove foreign objects such as stones or metal particles. According to (Garcia-Maraver, 2015b), it is undesirable if these materials are present in the finished product, even in trace amounts. They can also seriously damage the mechanical equipment of compaction.

3.3.2 Size reduction of the raw materials

An electric hammer mill with 1mm screen size in Chemical and process engineering laboratory in Moi university was used to grind the raw materials. Plate 3.2 shows the ground raw materials.



Plate 3.2: Ground raw materials

3.3.3 Drying

Ground raw materials were then oven dried at 105°C to moisture content of 8-14% which is a suitable range for pelleting according to Styks et al. (2020) and Križan et al. (2014).

3.5 Determination of specific objectives of research

The standard procedures employed for the purpose of accomplishing the particular goals of this study are covered in this section.

3.5.1 Perform characterization of corn stover and eucalyptus sawdust

This research goal was achieved by determination of feedstock properties. To determine these properties, experiments were carried out in terms of proximate analysis, ultimate analysis and higher heating values.

3.5.1.1 Proximate analysis

Proximate analysis is the determination of moisture content, volatile matter, fixed carbon and ash of the feedstocks and it was determined by the procedures described below. Before all analysis was done, the feedstock was sampled by use of the cone and quarter method as illustrated in Figure 3.1 below and Appendix 3. This involved heaping the prepared feedstock to form a cone and then the tip of the cone is flattened. It was then subdivided into four equal quarters and the quarters diagonal to each other were taken as a sample while the rest was discarded. This procedure was repeated until the sample was small enough to be used for analysis and at this stage it will be a true representative sample for the whole feedstock considered.

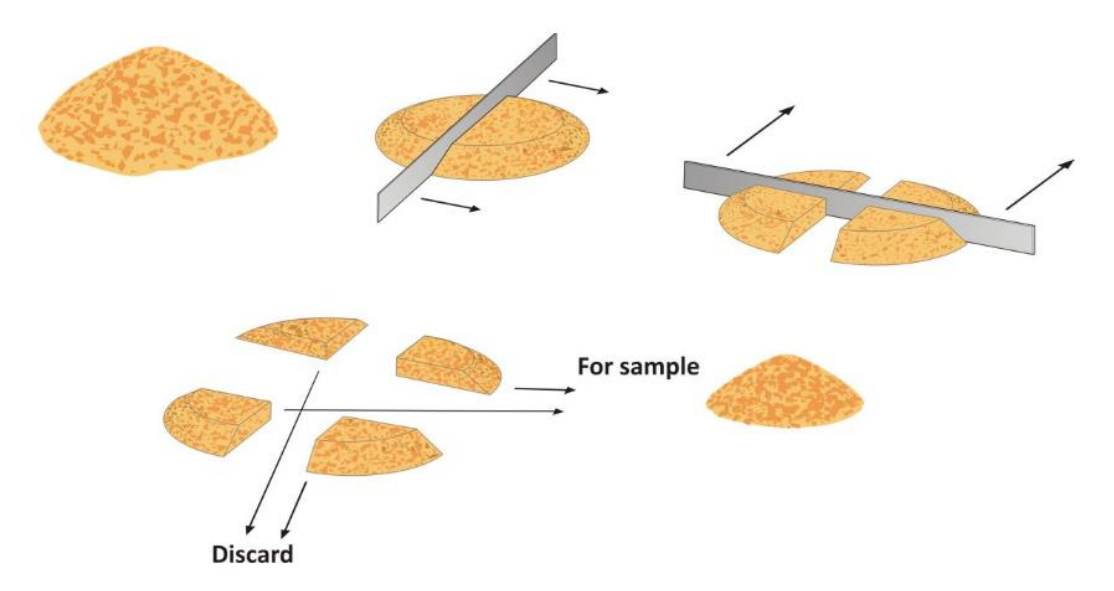


Figure 3.1 Coning and quartering method of sampling (Alakangas, 2015.)

i) Moisture content

Amount of moisture content in raw materials was determined by ASTM E871. By ASTM E871 procedure, a crucible was dried in the oven for 30 minutes at $103\pm1^{\circ}$ C, then allowed to cool to ambient temperature. Crucible weight was recorded as, Wc, to the nearest 0.02 g. 50g of sample was placed on the crucible and its weight were recorded to the nearest 0.01g as initial weight, Wi.

The crucible and sample were then placed in an oven at 103±1°C for 16h. The crucible and the sample were then removed from the oven and cooled in a desiccator and weighed to the nearest 0.01g.

The crucible and sample were then placed in the oven at 103±1°C for 2h until weight change was less than 0.2% and this weight was recorded as the final weight, Wf.

Moisture content was then calculated as shown in Equation 3.1 (International, 2006);

%moisture =
$$\frac{w_i - w_f}{w_i - w_c} \times 100\%$$
.....Equation 3.1 Where,

 w_c -crucible weight

 w_i -initial weight

 w_f -final weight

ii) Ash content

Ash content was determined by ASTM D1102 (873 K). The description of the procedure of ash content determination was as presented below.

The crucible was heated in the oven at 600°C, cooled in a desiccator and weighed to the nearest 0.1mg. A sample weighing 2g was placed in a crucible and weighed then placed in an oven for drying at 100 to 105°C for 1h. The crucible and sample were removed and cooled in a desiccator. The procedure was repeated until the weight change was

within 0.1mg. This weight was recorded (crucible plus specimen minus weight of crucible) as the oven-dry weight of the sample.

The crucible and sample were then placed in a muffle furnace and ignited until all carbon was eliminated. Gradual heating was used to a final temperature of 600°C. The crucible and sample were removed from the furnace, cooled in a desiccator and weighed. Heating was repeated for 30-minute periods until weight change was less than 0.1mg.

Ash content was then calculated using Equation 3.2;

$$\% ash = \frac{w_1}{w_2} \times 100\%$$
 Equation 3.2

Where,

 w_1 -weight of ash

 w_2 -weight of oven-dry sample

iii) Volatile content

Volatile content was determined by ASTM E 872. The crucible was weighed to the nearest 0.01g and recorded as crucible weight, Wc. Approximately 1 g of sample was placed in the crucible and covered. The crucible, cover, and sample were weighed to the nearest 0.01 g, and recorded as initial weight, Wi.

The covered crucible with the sample was placed on platinum or nickel-chromium wire supports and inserted directly into the furnace chamber, which was maintained at a temperature of 950 ± 20°C and lowered immediately to the 950°C zone. After heating for a total of exactly 7 min, the crucible was removed from the furnace without disturbing the cover and allowed to cool in a desiccator. The covered crucible with sample was weighed as soon as it cooled to the nearest 0.1 mg and recorded as the final weight, Wf.

Volatile content was then calculated using Equation 3.3;

weight loss,
$$\% = \frac{w_i - w_f}{w_i - w_c} \times 100\% = A$$
.... Equation 3.3

where:

Wc -weight of crucible and cover, g,

Wi -initial weight, g, and

Wf- final weight, g.

Volatile matter in analysis sample, % = A - B

where:

A =weight loss %, and

B = moisture, %, as determined using Method ASTM E 871.

iv) Fixed carbon

Fixed carbon was determined by difference as follows;

Fixed carbon=100%- (ash+ volatile contents) % (Bajo & Acda, 2017).

3.5.1.2 Ultimate analysis

Elemental analysis to ascertain the proportions of the elements Carbon, Hydrogen, Nitrogen, Sulphur and Oxygen was done by The Kenya ECO-prenuers Ltd-Nairobi. ASTM D5373-02 standard procedures were used in determination of Carbon, Hydrogen, Nitrogen and Sulphur (Mansor et al., 2018), while the biomass samples' oxygen concentration was determined by difference according to Equation 3.4 (Onochie et al., 2017).

$$\%O_2 = 100 - (C + H + N + S + \%Ash)$$
 (Onochie et al., 2017)..... Equation 3.4

3.5.2 Design and Fabrication of Single Piston Pellet Press (SPP) heated mould

A single pellet piston press (SPP) with a heating system was fabricated according to the description in (Lu et al., 2014; Stasiak et al., 2017) and selected dimensions adapted from (Auprakul et al., 2014b). The SPP was produced from stainless steel using a lathe machine. The major parts of the heated cylindrical mould include the cylindrical die, plunger/piston, backstop and heating coils as illustrated in Figure 3.2. Also incorporated in the complete setup of the heated mould were the temperature controller, 30A AC contactor, type K thermocouple for temperature sensing and glass fibre insulation.

Figure 3.3 shows the orthographic views of the dimensioned die, piston and backstop. Figure 3.4 shows the circuit diagram of heating and controlling the temperature of the die. The power supply for heating was 240V. The temperature controller regulates the temperature of the die by sensing and measuring the temperature using the thermocouple. Upon reaching the desired set temperature, which was displayed on the screen, the feed was sent to the AC contactor which then opened the circuit to stop further heating. On the other hand, when the temperature falls below the set point, the AC contactor closes the circuit to start heating again after receiving feedback from the temperature controller.

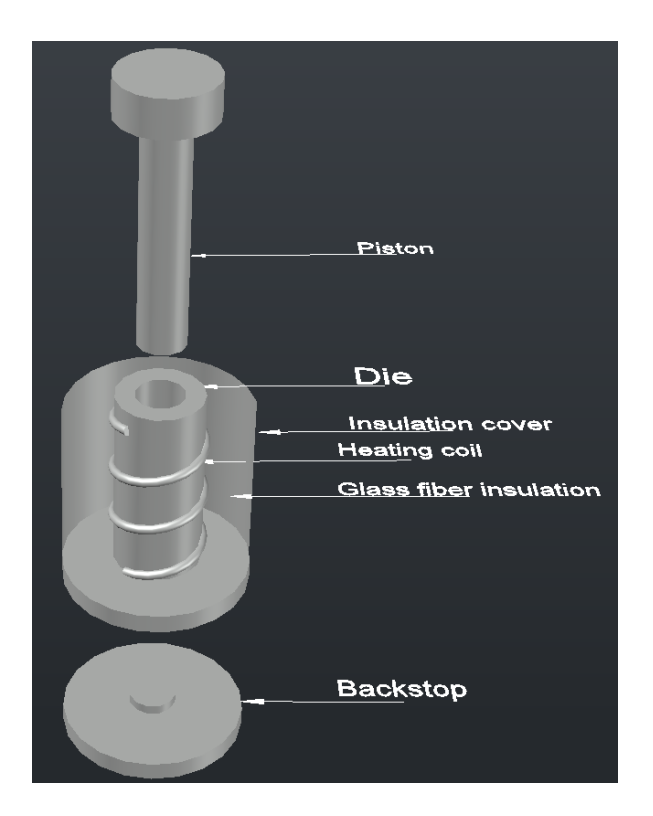


Figure 3.2: 3-Dimensional CAD drafting of single pellet press (SPP) heated mould

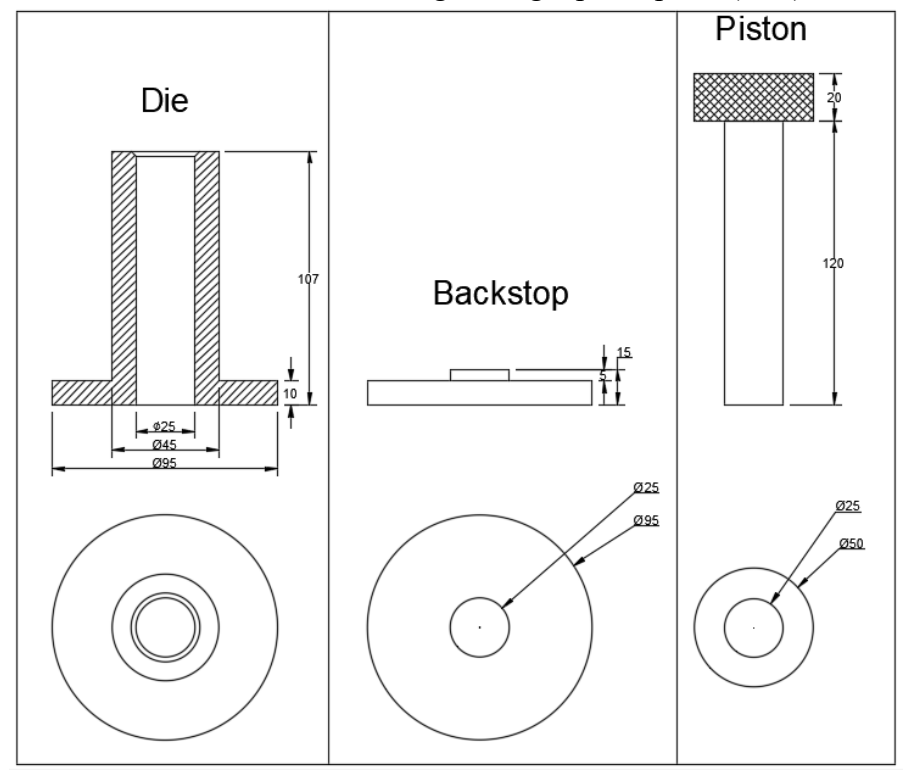


Figure 3.3: Orthographic views with dimensions of the die, piston and backstop

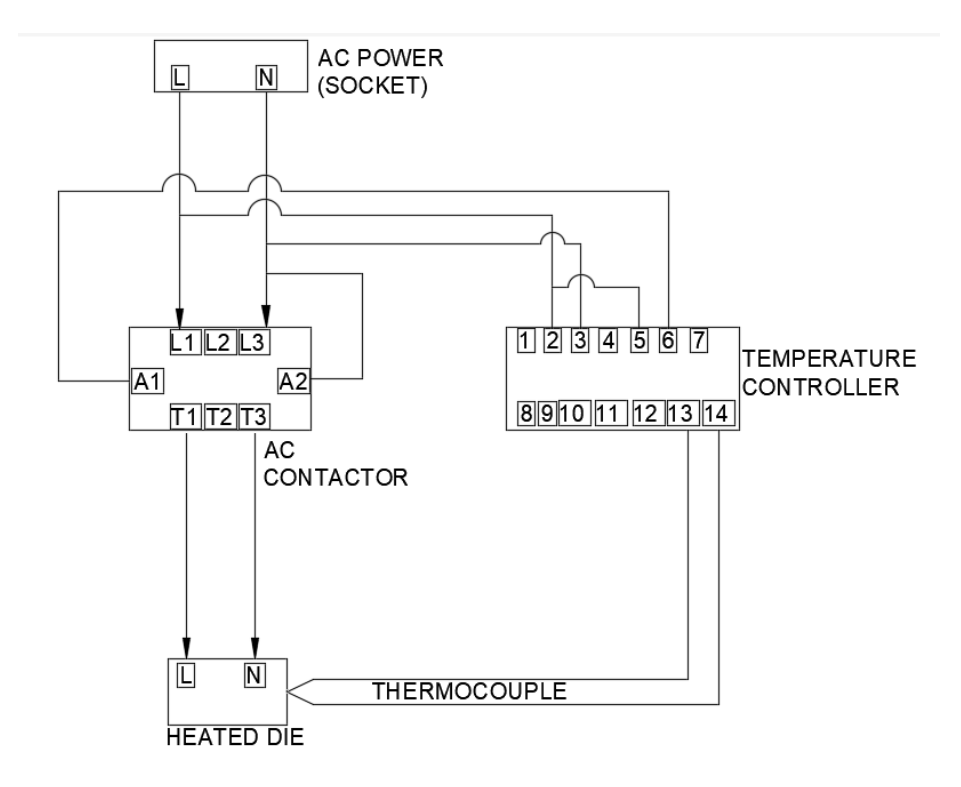


Figure 3.4: Circuit diagram of temperature control of the heated die 3.5.3 Design and Fabrication of durability tester

Pellet durability tester chamber was fabricated according to the dimensions provided in ISO 17831-1 (Solid Biofuels-Determination of Mechanical Durability of Pellets and Briquettes-Part 1:(E) copyright protected document, 2015), as illustrated in Figure 3.5. The pellet durability tester was made out of a drive mechanism and a dust-tight enclosure with an interior baffle to mix the pellets. The interior of the box must be smooth, and any protrusion, like rivets and screws, must be well-rounded. Any side can have a door installed.

Details of the box, including interior dimensions were as follows:

Material: stainless steel sheet metal (1.5 ± 0.1) mm thick

Width (300 ± 3) mm

Height (300 ± 3) mm

Breadth (125 ± 1.3) mm

Specification of baffle and dimensions were as follows:

Material: stainless steel sheet metal (1.5 ± 0.1) mm thick

Length: (230 ± 2.3) mm

Width: $(50 \pm 1.0) \text{ mm}$

Attached to one of the box's 300 mm by 300 mm diagonal sides was the baffle. The baffle was firmly attached to the rear of the box and extended (50 ± 1.0) mm into it (Figure 3.5). The baffle's edges must be rounded rather than sharp to prevent any cutting impact. To prevent vibrations, the electric motor driving the box must have the capacity to rotate at a steady speed of (50 ± 2) revolutions per minute or use appropriate pulleys or gears. Variable frequency drive (VFD) was fitted to the motor to control its speed to the desired revolutions per minute.

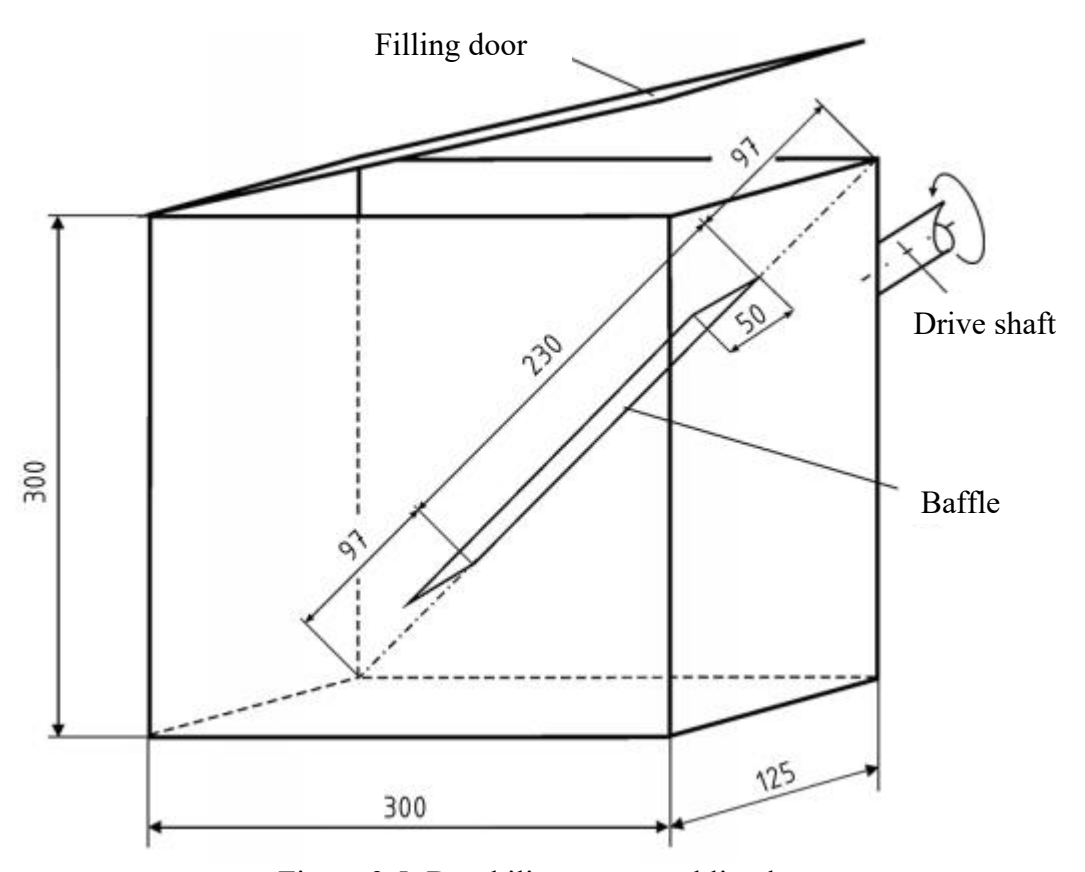


Figure 3.5: Durability tester tumbling box

3.5.4 Fabrication and torrefaction of blended pellets from corn stover and eucalyptus sawdust using LLDPE as a binder

This research goal was achieved by the production of pellets in a fabricated heated mould using different mixtures of feedstock as determined by the experimental design. The mould was heated to a temperature of 150°C and maintained there throughout the pelletization process according to Emadi et al. (2017). This temperature will enable LLDPE to melt and enhance the binding of biomass particles together.

3.5.4.1 Experimental design

The design parameters under study in this research were three, i.e., corn stover to eucalyptus sawdust ratio, linear low-density polyethylene (LLDPE) binder and torrefaction temperature. The levels of each design parameter were five. The values of the ranges of design variables were adapted from Park et al. (2021), Tumuluru (2019b) and Tumuluru & Fillerup (2020) for mixing ratios and torrefaction while for the ratios of LLDPE it was adapted from Garrido et al. (2017) and Emadi et al. (2017).

These parameters and their corresponding levels were tabulated in Table 3.1.

Table 3.1 Design parameters and their levels

Corn stover: Eucalyptus sawdust (wt: wt) (X1)	LLDPE (%) (X2)	Torrefaction temperature (°C) (X3)	Level
9:1	2	210	1
8:2	4	230	2
7:3	6	250	3
6:4	8	270	4
5:5 (1:1)	10	290	5

X1- Corn stover: Eucalyptus sawdust (wt: wt)

X2- Linear low-density polyethylene ratio (%)

X3- Torrefaction temperature (⁰C)

The number of experimental runs was given by Taguchi Array L25(5³) which was equal to 25 and was tabulated as shown in Table 3.2.

3.5.4.2 Compaction of raw materials to pellets

Based on Stasiak et al. (2017), raw materials prepared were compacted into a 25mm diameter cylindrical die with a height of 107mm as shown in Figure 3.6. On a steel table, a cylindrical die was positioned and filled with loosely prepared feedstock. The piston driven by a 15-ton press in the automotive laboratory was used to compact the raw materials into pellets. The compressed pellets were then extracted from the cylinder using the same piston after the back stop has been removed.

Table 3.2 Taguchi parameter experimental design (Krishniah et al., 2012)

RUN		PROCES		RESPONSES (MEAN VALUES)			UES)			
NO.	X1	X2	X3	Y1	Y2	Y3	Y4	Y5	Y6	Y7
1	1	1	1	*	*	*	*	*	*	*
2	1	2	2	*	*	*	*	*	*	*
3	1	3	3	*	*	*	*	*	*	*
4	1	4	4	*	*	*	*	*	*	*
5	1	5	5	*	*	*	*	*	*	*
6	2	1	2	*	*	*	*	*	*	*
7	2	2	3	*	*	*	*	*	*	*
8	2	3	4	*	*	*	*	*	*	*
9	2	4	5	*	*	*	*	*	*	*
10	2	5	1	*	*	*	*	*	*	*
11	3	1	3	*	*	*	*	*	*	*
12	3	2	4	*	*	*	*	*	*	*
13	3	3	5	*	*	*	*	*	*	*
14	3	4	1	*	*	*	*	*	*	*
15	3	5	2	*	*	*	*	*	*	*
16	4	1	4	*	*	*	*	*	*	*
17	4	2	5	*	*	*	*	*	*	*
18	4	3	1	*	*	*	*	*	*	*
19	4	4	2	*	*	*	*	*	*	*
20	4	5	3	*	*	*	*	*	*	*
21	5	1	5	*	*	*	*	*	*	*
22	5	2	1	*	*	*	*	*	*	*
23	5	3	2	*	*	*	*	*	*	*
24	5	4	3	*	*	*	*	*	*	*
25	5	5	4	*	*	*	*	*	*	*

Definition of parameters and responses

X1-Corn stover: Eucalyptus sawdust (wt: wt)

- X2- Linear low density polyethylene ratio (%)
- X3- Torrefaction temperature (⁰C)
- Y1- Pellet particle density (kg/m³)
- Y2- Bulk density of pellets (kg/m³)
- Y3- Pellet durability index (%)
- Y4- Pellet hardness (kg)
- Y5- Mass yield of pellets (%)
- Y6- Higher heating value (MJ/kg)
- Y7- Carbon dioxide emissions (%VOL)

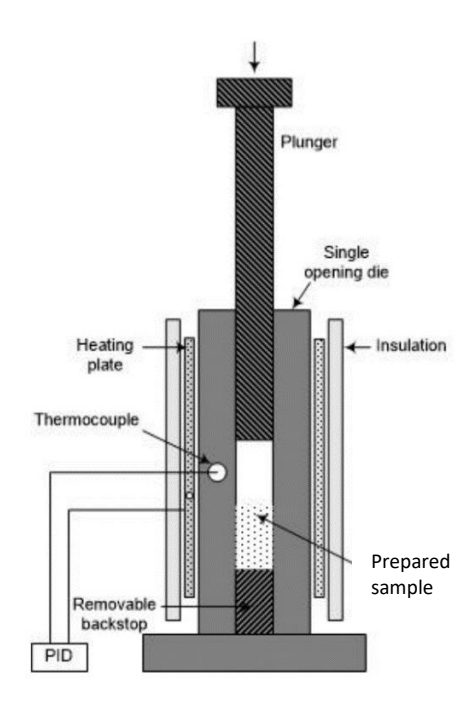


Figure 3.6 Schematic diagram of a single die pellet press (Bajo & Acda, 2017)

3.5.4.3. Torrefaction of the blended pellet

Torrefaction of pellets produced was done by using a modified tube furnace in the automotive laboratory to mimick torrefaction equipment. To determine the effect of torrefaction on the produced biomass pellets, mass yield (MY) was determined. This concept was based on mass reduction after torrefaction. The mass yield was evaluated as shown in Equation 3.5 (Rudolfsson et al., 2017). According to Rudolfsson et al.

(2017) and Kota et al. (2022) in order to achieve torrefaction, the steps followed were as follows:

- Weighed raw blended biomass pellets (M_{raw}) were packed in the tube of the modified torrefaction equipment and nitrogen gas purged through at 0.8bar to expel air within it.
- ➤ Heating of the furnace to the desired set torrefaction temperature was started.

 Heating was maintained at this temperature for one hour. Heating was then stopped and the torrefied pellets left to cool still under the inert environment.

 After cooling nitrogen gas purging was stopped.
- \triangleright The weight of the blended torrefied pellets ($M_{torrefied}$) were then taken and mass yield evaluated.

Mass Yield
$$MY = \frac{M_{torrefied}}{M_{raw}} \times 100\%$$
.....Equation 3.5 Where, $M_{torrefied}$ - mass of torrefied biomass and M_{raw} -mass of raw biomass

Modification of tube furnace to torrefaction equipment

Siyal et al. (2021) described the process of torrefaction as a thermal pre-treatment of biomass by heating at a temperature of 200 to 300°C in oxygen deficient environment. Therefore, in modification of the tube furnace, inertness of the combustion chamber was achieved by purging nitrogen gas through it at approximately 0.8bar adjusted using the nitrogen gas regulator. The modified torrefaction equipment is illustrated in Plate 3.3 below.



Plate 3.3: Modified tube furnace to torrefaction equipment

3.5.5 Characterization of physical, mechanical and thermochemical properties of blended torrefied pellets

3.5.5.1 Physical properties

i) Pellet size-in most cases, pellet diameter is determined by the die hole for standard commercial pellets (Romuli et al., 2021). In this case pellet diameter was determined by the use of a vernier caliper since there could be a change of dimensions on the release of compaction pressure. A vernier caliper was used to estimate the length of the pellets, L_P (mm). This process was executed as it is presented in Plate 3.4.



Plate 3.4: Measuring pellet dimensions

ii) Bulk density- In order to determine the bulk density, pellets were filled in a 1L container to approximately 20cm above the top edge. The container was then dropped three times onto a firm, level surface made of wood. Any pellets that remain above the container's top will be removed with a flat object and weighed. There were three repetitions of this procedure. Next, the bulk density was computed using the following equation, with the result rounded to the nearest decimal (Park et al., 2021). Plate 3.5 illustrates the packing of torrefied biomass pellets for purposes of determination of bulk density while Equation 3.6 was used to determine the bulk density of the blended torrefied pellets.



Plate 3.5: Determination of bulk density

iii) Pellet particle density

Determination of particle densities of pellets was done by stereometric methods (Rabier et al., 2006). Zafari & Kianmehr (2012) and Carrillo et al. (2016) provided a detailed description of evaluation of pellet particle density by stereometric methods. Measurements of a single regularly formed particle's dimensions such as the diameter, length, width, and height, are made using length-measuring devices like calipers, gauges and rules in stereometric procedures (Plate 3.4). The next step was to calculate the volume of the closest regular geometric shape like cylinders, cuboids and cubes to estimate the sample's volume.

In stereometric measurements on pellets, the mass of one pellet sample was determined to the closest 0.0001 g accuracy. The size (pellet diameter and length) measurements were taken with 0.1 mm accuracy. The pellet's shape was assumed to be cylindrical for computation.

The pellet particle density for each trial was computed according to the Equation 3.7 and Equation 3.8 below;

Where,

 ρ_{PD} -Pellet particle density

m- Mass of the pellet

v- Volume of the pellet

$$V = \frac{\pi D^2}{4} L.$$
 Equation 3.8

Where,

V- Volume of the pellet

D- Diameter of the pellet

L- Length of the pellet

Π- A constant

3.5.5.2 Mechanical properties

i) **Durability** – The durability of the pellets was done in a fabricated durability tester. The principle of operation of the durability tester was that tests were done in a specified spinning test chamber, where pellets collide with one another and the walls of the chamber to subject a test sample to regulated shocks. During testing, the durability tester was filled with 500±50 g of pellets, and tests were carried out at a rate of 50± 2rev/min for 60 seconds according to research done by (Kantová et al., 2022; Larsson & Samuelsson, 2017). The pellets were then manually sieved through a 3.15 mm mesh sieve, and the weight of the pellets still in the sieve weighed twice. Durability was then computed using the Equation 3.9. This test was done in accordance to ISO 17831-1 (Park et al., 2021).

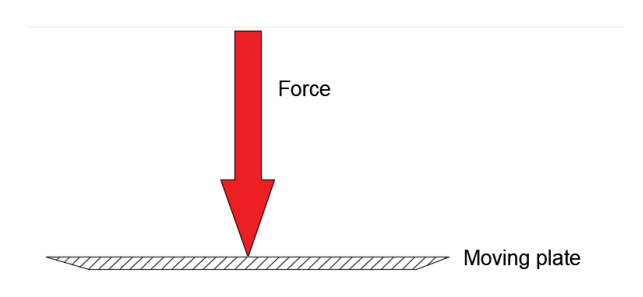
$$DU = \frac{m_a}{m_b} \times 100 \dots Equation 3.9$$
 Where,

DU-durability (%), m_a -pellet weight post-sieving after durability test (g) and m_b -pellet

weight before sieving before the durability test (g).

ii) Hardness -Determination of pellet's hardness was done according to the procedure outlined by (Kaliyan & Vance Morey, 2009) where the diametrical compression test was used in a universal testing machine. According to Santana et al. (2010) and Thapa & Engelken (2020), evidence points out that the diametral compressive strength is a more significant measure of pellet hardness. The pellet was sandwiched between two parallel, flat platens, with the surfaces of their faces larger than the pellet's projected area as illustrated in Figure 3.7. Up until the test specimen breaks/fails, a steadily increasing load is applied. The compressive strength, which is expressed as force or stress, was obtained by reading the load at fracture. Hardness testing in the universal

testing machine at Rivatex East Africa Limited is illustrated in Plate 3. 6. The hardness of the pellets obtained was recorded in triplicate for every experimental run.



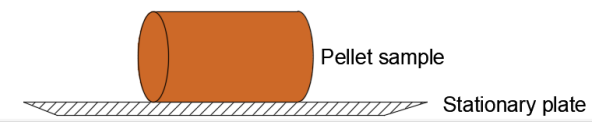


Figure 3.7: Biomass pellet orientation during compressive strength testing. Adapted from (Obi et al., 2022)



Plate 3. 6: Hardness testing in universal testing machine

3.5.5.3 Combustion properties

1. Calorific value (HHV)

The calorific value of the pellet was determined using an automated bomb calorimeter in the materials laboratory in the Mechanical Engineering Department at Moi University. This was done by loading a predetermined mass of the sample on the bomb calorimeter's crucible carried by the oxygen bomb head and installing nichrome fuse wire as illustrated in Appendix 4. The oxygen bomb head loaded with the sample was put in the oxygen bomb and fastened tightly. The oxygen charger was then used to charge oxygen into the bomb at a pressure of 2.8-3.0MPa and held there for approximately 15 seconds as illustrated in Appendix 3. Finally, the sample-loaded oxygen bomb was placed in the bucket as illustrated in Appendix 3 and the bucket closed. Analysis of the sample was then started by running the testing software in the computer which records and gives the calorific value of the sample displayed on the screen after analysis.

2. Emissions testing

Carbon dioxide concentrations emitted from the combustion of blended pellets for all experimental runs were determined by a portable multi-gas detector sourced from the Chemical and Process Engineering laboratory. For more accurate results testing of emissions was done on optimized pellets in a Laboratory Emissions Monitoring System (LEMS) in KIRDI. ISO 19867-1: 2018 standard method was used to determined the emissions using LEMS apparatus. This method estimates emissions by gravimetric method and the specific emissions that can be measured by LEMS are carbon monoxide (CO), carbon dioxide (CO₂) and particulate matter (PM_{2.5}). The experimental set-up of determination of emissions using LEMS at KIRDI was illustrated in appendix 21 and appendix 22. The rating of the optimized pellets in terms of emissions was also provided

by ISO 19867-1: 2018 tiers and these were then compared with that of Kenyan standard (KEBS Standard- KS 1814:19) to determine whether it is acceptable or not. Tier three and above is acceptable according to KEBS Standard.

3.5.6 Optimization of pelleting process variables

In order to determine the optimal conditions of pelleting, i.e, cornstover: eucalyptus sawdust ratio, LLDPE ratio and torrefaction temperature, the responses of different conditions were input into a Minitab 18 software in Taguchi design of experiments as shown in Table 3.2. Taguchi method cannot optimize multiple responses as explained in section 2.12.4.1. Therefore, Grey relational analysis (GRA) statistical analysis was used to transform data in Table 3.5 to grey relational grade which can now be optimized as a single response. Response graphs, three-way ANOVA, Pareto analysis, contour and response surface plots was then used to test the significance of corn stover: eucalyptus sawdust ratio, %LLDPE, torrefaction temperature as well as the optimum blended pellet properties. The analysis of the interactions was also determined.

3.5.6.1 The Pellet quality check against International Standard

The pellet with optimal parameters was then produced and its overall physicomechanical and combustion characteristics were determined so as to compare it with international standards of pellets.

Table 3.3 illustrates the European guidelines EN 14961-6 pellets for non-woody biomass pellets or pellet mixtures from different biomasses. Pellets from non-woody biomass are categorized as A class while those from mixtures of different biomasses are B class pellets. Pellet quality parameters were compared to these standard specifications so as to evaluate the overall quality of the pellet produced (Garcia-Maraver, 2015b). This particular standard is appropriate for use in this research since it

accommodates varied types of feedstocks, unlike other standards which are specific to certain types of feedstocks.

Table 3.3. European normative guidelines for pellets produced from herbaceous and fruit biomass and blends and mixtures(Garcia-Maraver, 2015b)

	Units	A	В
Diameter and	mm	D06-10: D ± 1	$; 3.15 \le L \le 40$
length, D and L		D12-25: D \pm 1	$; 3.15 \le L \le 50$
Moisture, M	% as received	$M12 \le 12$	$M15 \le 15$
Ash, A	% dry basis	$A5.0 \le 5$	$A10 \le 10$
Mechanical durability, DU	% as received	DU97.5 ≥ 97.5	DU96.5 ≥ 96.5
Fines	% as received	$F2.0 \le 2.0$	$F3.0 \le 3.0$
Additives	% dry basis	Type and	l quantity
Lower heating value as received, Q	MJ/kg	$Q14.1 \ge 14.1$	$Q13.2 \ge 13.2$
Bulk density, BD	kg/m ³ as received	BD600	$0 \ge 600$
Nitrogen, N	% dry basis	$N1.5 \le 1.5$	$N2.0 \le 2.0$
Sulphur, S	% dry basis	S0.20	≤ 0.20
Chlorine, Cl	% dry basis	$C10.20 \le 0.20$	$C10.30 \le 0.30$

3.7 Presentation of the results

3.7.1 Compositional analysis of feedstock

The results from the evaluation of proximate and ultimate analysis of corn stover and eucalyptus sawdust were as recorded as shown in Table 3.4.

Table 3.4 Proximate and ultimate analysis of corn stover and eucalyptus sawdust feedstock.

Biomass sample	Corn stover		Eucalyptus	sawdust
	Mean	STDEV	Mean	STDEV
Proximate analysis (%wt)				
Moisture content	*	*	*	*
Volatile matter	*	*	*	*
Fixed carbon	*	*	*	*
Ash	*	*	*	*
Ultimate analysis (%wt)				
Carbon	*	*	*	*
Hydrogen	*	*	*	*
Nitrogen	*	*	*	*
Sulphur	*	*	*	*
Oxygen	*	*	*	*
HHV (MJ/kg)	*	*	*	*

3.7.2 Pellet characteristics

3.7.2.1 Physico-mechanical and Combustion characteristics

All experiments were done in triplicate and were recorded as shown in Table 3.5.

Table 3.5 Physico-mechanical and combustion characteristics of produced pellets

RUN		OCESS METEI	RS		RESPO	ONSES	(MEA	N VALUE	ES)	
NO.	X1	X2	X3	Y1	Y2	Y3	Y4	Y5	Y6	Y7
1	1	1	1	*	*	*	*	*	*	*
2	1	2	2	*	*	*	*	*	*	*
3	1	3	3	*	*	*	*	*	*	*
4	1	4	4	*	*	*	*	*	*	*
5	1	5	5	*	*	*	*	*	*	*
6	2	1	2	*	*	*	*	*	*	*
7	2	2	3	*	*	*	*	*	*	*
8	2	3	4	*	*	*	*	*	*	*
9	2	4	5	*	*	*	*	*	*	*
10	2	5	1	*	*	*	*	*	*	*
11	3	1	3	*	*	*	*	*	*	*
12	3	2	4	*	*	*	*	*	*	*
13	3	3	5	*	*	*	*	*	*	*
14	3	4	1	*	*	*	*	*	*	*
15	3	5	2	*	*	*	*	*	*	*
16	4	1	4	*	*	*	*	*	*	*
17	4	2	5	*	*	*	*	*	*	*
18	4	3	1	*	*	*	*	*	*	*
19	4	4	2	*	*	*	*	*	*	*
20	4	5	3	*	*	*	*	*	*	*
21	5	1	5	*	*	*	*	*	*	*
22	5	2	1	*	*	*	*	*	*	*
23	5	3	2	*	*	*	*	*	*	*
24	5	4	3	*	*	*	*	*	*	*
25	5	5	4	*	*	*	*	*	*	*

CHAPTER FOUR: RESULTS, ANALYSIS AND DISCUSSION

4.1 Introduction

This chapter presents the results of the experiments carried out, their analysis and discussions.

4.2 Proximate and Ultimate analysis of Cornstover and Eucalyptus sawdust

4.2.1 Proximate analysis

1. Moisture content

Amount of moisture content in raw materials was determined by ASTM E871. Computations were done according to the Equation 3.1.

Table 4.1 and Table 4.2 indicate the analysis of moisture content of corn stover and eucalyptus sawdust respectively. It was found that the moisture contents were 5.9164% and 3.7027% for corn stover and eucalyptus sawdust respectively. These figures were generally very low for pelletization of both feedstocks using single pellet press. According to Pradhan et al. (2018b) the recommended moisture content for use in single pellet press is 10%. Therefore, to be able to use the feedstocks for pelletization, ultrapure water was added to the feedstocks according to equation 2.1 to elevate the moisture content of the feedstocks to 10%. Again, this optimum pelleting moisture content is varied as presented in different texts in published literature. For instance, Frodeson et al. (2019) stated that the optimum moisture content is between 6-12% and Kwapong (2023) stated that the moisture content range is between 10-15%.

Table 4.1 Corn stover moisture content analysis

Replica	w_c	w_i	W_f	%moisture
1	9.2081	11.3422	11.2418	4.7046
2	9.3813	11.3846	11.2760	7.1282
Mean				5.9164
STDEV				1.7137

Table 4.2 Eucalyptus sawdust moisture content analysis

Replica	W_{c}	w_i	W_f	%moisture
1	34.5858	36.8122	36.7256	3.8897
2	6.4945	8.5795	8.5062	3.5156
Mean				3.7027
STDEV				0.2645

2. Ash content

Ash content was determined by ASTM D1102 (873 K) and calculated using the Equation 4.1.

%ash =
$$\frac{w_1}{w_2} \times 100\%$$
.....Equation 4.1

Where,

 w_1 -weight of ash

 w_2 -weight of oven-dry sample

Table 4.3 presents the ash content for corn stover obtained from this research as 5.2112% while Table 4.4 presents ash content analysis of eucalyptus sawdust as 3.2209%. These figures and their trends agree with those presented by Williams et al. (2017). The trends were also similar in that the ash content of corn stover (herbaceous biomass) were higher than those of eucalyptus sawdust (woody biomass). The selection and blending of materials for production of biofuels with optimal qualities can be guided by understanding of the ash content of various biomass feedstocks. For instance, feedstocks with lower ash content are often preferred to mitigate the negative impacts associated with high ash content. Although the recommended range of ash content for solid biofuel production is not explicitly stated in published literature, Li et al. (2017), Zhai et al. (2021) and Williams et al. (2016) reported that the ash content for woody biomass is about 0.5-3% and for herbaceous and agricultural residues is about 5-15%.

 $w_1 = w_f - w_c$ %ash Replica W_{c} w_i W_f W_2 $= w_i - w_c$ 27.4152 29.4152 27.5580 0.0996 5.0899 1.9568 18.5082 20.1435 5.3324 18.5954 0.0872 1.6353 Mean 5.2112 **STDEV** 0.1715

Table 4.3 Corn stover ash content analysis

Table 4.4 Eucalyptus sawdust ash content analysis

Replica	$W_{\mathcal{C}}$	w_i	w_f	$w_1 = w_f - w_c$	w_2	%ash
					$= w_i - w_c$	
1	17.0924	18.9564	17.1429	0.0505	1.8640	2.7092
2	20.1507	21.4688	20.1999	0.0492	1.3181	3.7326
Mean						3.2209
STDEV						0.7237

3. Volatile content

Volatile content was determined by ASTM E 872 and using the equation presented below for computation.

Wi -initial weight, g, and

Wf- final weight, g.

Volatile matter in analysis sample, % = A - B

where: A = weight loss %, and

B = moisture, %, as determined using Method ASTM E 871.

Volatile matter for corn stover obtained from this research was 74.662% while for eucalyptus sawdust was 84.6649% as presented in Table 4.5 and Table 4.6 respectively. The data and patterns show that these figures align with what Williams et al. (2017) presented. The trends were also similar in that the volatile content of corn stover (herbaceous biomass) were lower than that of eucalyptus sawdust (woody biomass). Silva et al. (2021) in the research on whether volatile matter changes with the standard

used, found out that volatile matter ranges between 65-85% for lignocellulosic biomass. Tu et al. (2022) further found out that volatile matter for woody biomass is usually higher than that of herbaceous biomass. The results of this study shows that they are in agreement with those presented by Tu et al. (2022) and Silva et al. (2021).

Table 4.5 Corn stover volatile content analysis

Replica	W_{C}	w_i	W_f	Α	В	Volatile matter, %
1	27.4572	29.5809	27.9107	78.6458	5.9164	72.7294
2	18.5082	20.1435	18.7942	82.5109	5.9164	76.5945
Mean						74.6620
STDEV	STDEV					2.7330

Table 4.6 Eucalyptus sawdust volatile content analysis

Replica	W_{c}	w_i	w_f	Α	В	Volatile matter, %
1	17.0924	18.9564	17.3046	88.6159	3.7027	84.9132
2	20.1507	21.4688	20.3073	88.1193	3.7027	84.4166
Mean						84.6649
STDEV						0.3511

4. Fixed carbon

Fixed carbon was determined by difference as follows;

Fixed carbon (FC)=100%- (ash+ volatile contents) % (Bajo & Acda, 2017).

Cornstover

Eucalyptus sawdust

This investigation determined the fixed carbon content as 20.1268% for corn stover and 12.1142% for eucalyptus sawdust, respectively. These numbers align with the facts and trends that Williams et al. (2017) reported. Another similarity across the patterns was the higher fixed carbon content of corn stover (herbaceous biomass) compared to eucalyptus sawdust (woody biomass).

96

5. Higher Heating Value (HHV)

Bomb calorimeter was used to determine HHV.

Cornstover

HHV=17.384MJ/Kg

Eucalyptus sawdust

HHV=17.926MJ/Kg

According to Teh et al. (2022), higher heating values of biomasses is in the range of 15.33 MJ/kg and 19.71 MJ/kg. The results of this research show that the higher heating values of corn stover and eucalyptus sawdust are within the given range. Further, it can also be seen that the higher heating value of eucalyptus sawdust is higher than that of corn stover. This is in line with studies that have shown that woody biomass generally has higher calorific values than herbaceous biomass due to lower ash content (Kim et al., 2019; Malaťák & Passian, 2011).

4.2.2 Ultimate analysis of corn stover and eucalyptus sawdust at ECO prenuers

ltd-Nairobi

The ultimate analysis quantified the elements in corn stover and eucalyptus sawdust samples and their results were presented in Table 4.7 and Table 4.8 respectively. Corn stovers' elemental analysis was carbon (39.5433%), oxygen (53.3167%), hydrogen (5.6967%), nitrogen (1.3767%), and sulphur (0.0667%), while eucalyptus sawdust's was carbon (47.16%), oxygen (47.7633%), hydrogen (4.9667%), nitrogen (0.0797%), and sulphur (0.0303%). According to Mostazur Rahman et al. (2022), ultimate analysis assists in determining the heat of biomass combustion as well as the volume and makeup of the combustion gases. In addition, it assisted in determining the heat of biomass combustion as well as the volume and makeup of the combustion gases. In the ultimate analysis, the main components of the elemental compositions are carbon, oxygen, and

hydrogen. Typically, carbon is found in partially oxidized state, which highlights biomass's lower heating value when compared to coal. The heating value of biomasses is significantly influenced by the hydrogen content. The oxygen needed for the combustion reaction is partially met by the organically bound oxygen in biomass that is released during thermal breakdown; the remaining oxygen is supplied by air injection. However, the evolution of harmful emissions is primarily attributed to sulphur and nitrogen emissions like nitrogen oxides (NOx) and sulphur oxides (SOx) during combustion, which are the major causes of acid rain and particulate matter emissions (PM). The elemental compositions of corn stover and eucalyptus sawdust in this research were found to be in between the ranges presented by Williams et al. (2017). There were slight variabilities in nitrogen and oxygen contents of corn stover in which they were higher than those presented in literature. It is possible that the high nitrogen concentration in the soil, where the corn stover was harvested contributed to the excessive nitrogen contents, while the excessive oxygen could arise from some of the reasons presented by Williams et al. (2016) for biomass composition variability such as: feedstock types, methods for component analysis, harvesting practices, storage conditions, and preprocessing methods, among other factors.

Table 4.7 Ultimate analysis of Corn stover

Corn stove	Corn stover										
Replica	С	Н	N	S	O (by difference)						
1	38.33	5.84	1.37	0.07	54.39						
2	40.87	5.65	1.38	0.07	52.03						
3	39.43	5.6	1.38	0.06	53.53						
Mean	39.5433	5.6967	1.3767	0.0667	53.3167						
STDEV	1.2738	0.1266	0.0058	0.0058	1.1944						

Table 4.8 Ultimate analysis of Eucalyptus sawdust

Eucalyptu	Eucalyptus sawdust									
Replica	С	Н	N	S	O (by difference)					
1	47.29	4.8	0.08	0.03	47.8					
2	46.87	5.2	0.078	0.031	47.821					
3	47.32	4.9	0.081	0.03	47.669					
Mean	47.16	4.9667	0.0797	0.0303	47.7633					
STDEV	0.2516	0.2082	0.0015	0.0006	0.0824					

Table 4.9 presents the summary of results of proximate, ultimate and higher heating values of corn stover and eucalyptus sawdust. Significant heterogeneity exists within particular feedstock categories, even though a high degree of variability is anticipated within broad categories like lignocellulosic biomass and municipal solid waste (Williams et al., 2017). According to Williams et al. (2016), a wide range of factors, such as: feedstock varieties, component analysis methodologies, environmental variables, harvesting techniques, storage conditions, and preprocessing techniques, contribute to biomass variability. While some of these characteristics can be managed by standardization procedures, others may be more challenging to manage. Since environmental factors are influenced by daily and seasonal temperature swings, changes in local soil conditions (e.g. sand, clay, nutrient content, rock and pH), and fluctuations in the amount and timing of water supplies, it is especially difficult to manage how these factors affect the composition of biomass.

Table 4.9 Summary of Proximate, Ultimate and Higher heating values.

Ca No	Duomontry	Corn stove	er	Eucalyptus sa	awdust
Sr. No.	Property	wt%	STDEV	wt%	STDEV
Proximate	e analysis				
1	Moisture	5.9164	1.7137	3.7027	0.2645
2	Volatile matter	74.662	2.733	84.6649	0.3511
3	Fixed carbon	20.1268		12.1142	
4	Ash	5.2112	0.1715	3.2209	0.7237
Ultimate	analysis				
5	С	39.5433	1.2738	47.16	0.2516
6	Н	5.6967	0.1266	4.9667	0.2082
7	N	1.3767	0.0058	0.0797	0.0015
8	S	0.0667	0.0058	0.0303	0.0006
9	0	53.3167	1.1944	47.7633	0.0824
10	HHV (MJ/Kg)	17.384	0.123	17.926	0.0933

4.3 Fabrication of single pellet press and durability tester

4.3.1 Fabrication of single pellet press

Figure 4.1 illustrates the die, plunger and the backstop, while Figure 4.2 and Figure 4.3 illustrates a complete assembly of the heated mould in its working position using a 15tonne press in automotive laboratory.

Biomass and LLDPE feedstock were ground using electric mill in chemical engineering laboratory of Moi University. Pellets produced using the fabricated SPP were illustrated in Figure 4.4. In conclusion, the fabricated heated mould can produce well densified pellets as illustrate in Figure 4.4.

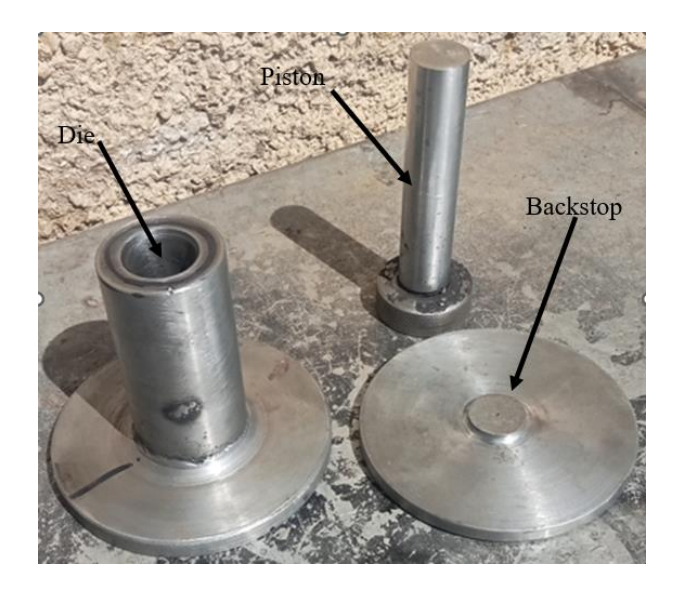


Figure 4.1: Fabricated die, piston and backstop

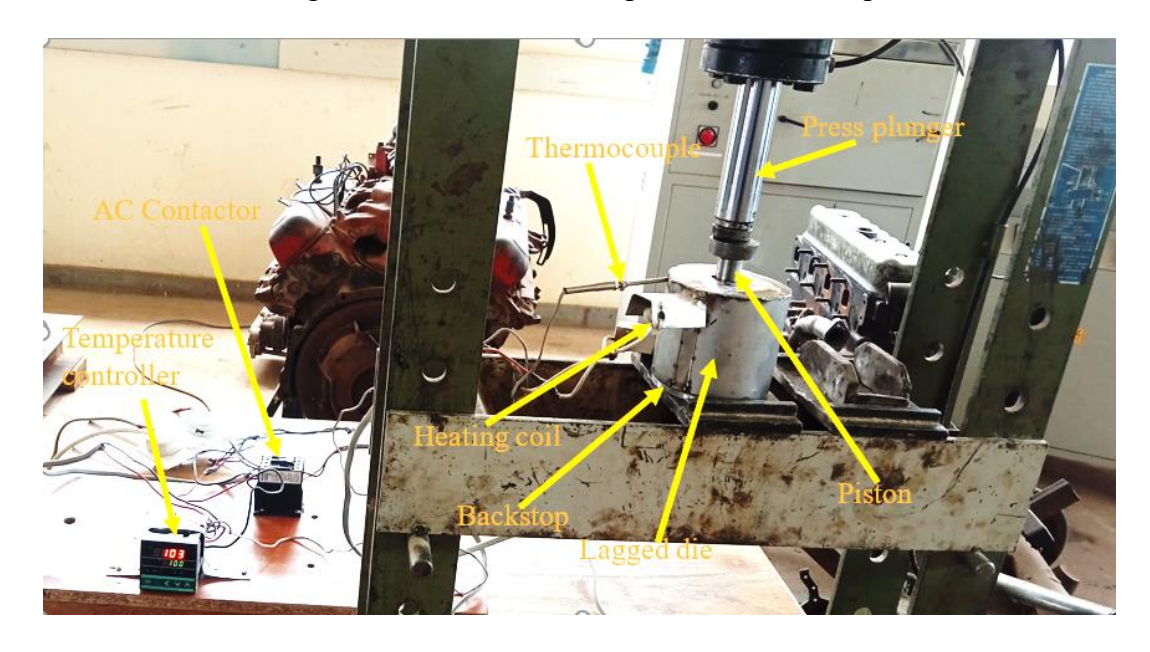


Figure 4.2: Picture of SPP and all its accessories in their working position



Figure 4.3: Hydraulic press and heated mould in operation



Figure 4.4: Pellets produced in the fabricated die

4.3.2 Fabrication of durability tester

A complete assembly of the fabricated durability tester was as illustrated in Figure 4.5. In order to have the motor automatically run at predetermined number of revolutions per minute, the potentiometer was also incorporated.

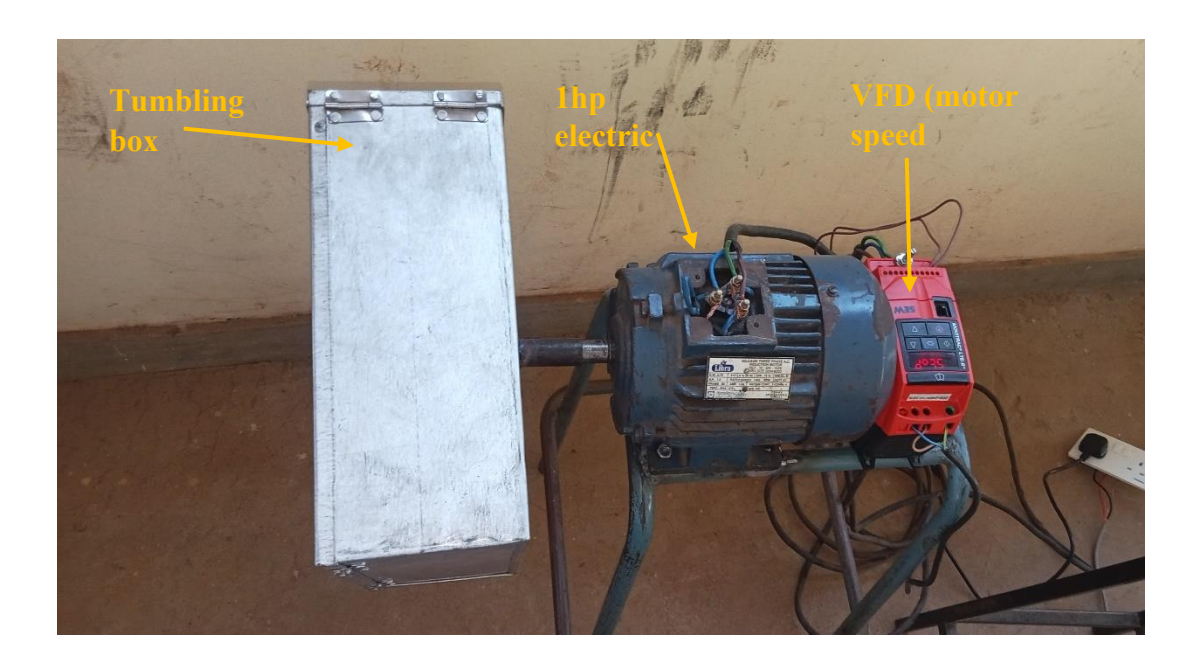


Figure 4.5: Fabricated pellet durability tester

4.4 Fabrication and torrefaction of blended pellets

Fabrication and torrefaction of the blended biomass pellets was successfully done and the products are as illustrated in Figure 4.6.



Figure 4.6: Fabricated and torrefied blended biomass pellets

4.5 Characterization of blended torrefied pellets

In this section, the physico-mechanical and thermochemical properties of fabricated blended pellets were presented and analyzed.

4.5.1 Physical properties

The blended pellets' particle density, as well as the bulk density, were some of the physical properties considered and analyzed in this section.

4.5.1.1 Pellet particle density

Appendix 5 (a) presents the trials and mean values of pellet particle density that were obtained during experimentation. Three trials of each run were carried out. Therefore, from the standard deviations' column, it can be seen that none of the runs had a standard deviation more than two. This indicates that the variations in the results obtained were insignificant.

According to Sarker et al. (2023), particle density is mass-to-volume ratio of a single pellet. Its value is affected by the particle size, compression strength, protein content, and moisture content. This characteristic affects the bulk density and, consequently, the characteristics of combustion of the pellets such as heat conductivity, burning rate and degasification rate. The mean pellet particle density of corn stover-eucalyptus sawdust blended pellet was found to be 917.9036 kg/m³ in a range of 825.7330 kg/m³ to 995.1530 kg/m³ (Appendix 5a). Comparing these results to those from published literature, it was seen that their values are slightly lower than those of non-torrefied pellets.

Pellet density of non-torrefied pellets is between 1250 kg/m³ and 1350 kg/m³, while that of torrefied pellets is between 1000 kg/m³ and 1170 kg/m³ as presented in a study carried out by Lim et al. (2017). This was almost similar to the results presented by

Rudolfsson et al. (2015), in the parametric study of process optimization of combined biomass torrefaction and pelletization for fuel pellet production, in which the pellet particle density was found to be between 1000 kg/m³ and 1200 kg/m³. Tumuluru et al.(2010) stated that under the recommended pelletization conditions and proper feedstock preparation, the pellet particle density of non-torrefied pellets is about 1200kg/m^3 .

According to Siyal et al. (2021), torrefaction adversely affects pellet particle density, where it decreased to 630 kg/m³ from 1100 kg/m³. In addition to the studies done by Cao et al. (2015), Manouchehrinejad & Mani (2018), Onyenwoke et al. (2023) and Li et al. (2012), this reduction in pellet particle density was attributed to several reasons some of which include;

- Loss of volatile matter Water, hemicellulose, and volatile organic chemicals found in the biomass are driven out by torrefaction. The loss of volatile components causes the material's mass decrease, which lowers the pellet density.
- ➤ The biomass undergoes structural changes as a result of the thermal treatment during torrefaction. Components of lignin, hemicellulose, and cellulose go through processes like condensation reactions and depolymerization. These modifications may lead to a more porous structure and a decrease in the material's density.
- Mass loss The total mass of the torrefied biomass reduces as volatile components are driven out and some biomass components begin to break down.

 The resultant pellets have a decreased density due to this mass reduction without a matching volume reduction.

➤ Depending on the torrefaction conditions and the handling/storage of torrefied biomass, moisture content can vary. Less dense pellets are often witnessed after torrefaction since moisture is eliminated.

a) Analysis of results for pellet particle density optimization

Signal-to-noise (S/ N) ratios were used to evaluate the optimum process parameters conditions for single pellet quality characteristic using Taguchi method. The higher the S/N ratio the minimum the effect of noise factors. The S/N ratios for different quality characteristics were calculated using Equation 2.3 and Equation 2.4. Taguchi method used the larger the better criteria for desirable pellet properties and the smaller the better criteria for undesirable properties.

The response table for signal-to-noise ratio and means was presented in Appendix 5 (b) and Appendix 5 (c) respectively, while the response graphs for the main effects plot for signal-to-noise ratio and means for pellet particle density were presented in Figure 4.7. The optimal level setting for parameters that lead to higher pellet particle density was depicted in Figure 4.7 (a) for the main effect plots for S/N ratios, where it showed that optimal parameter level settings for higher pellet particle density, were X1₁X2₁X3₅.

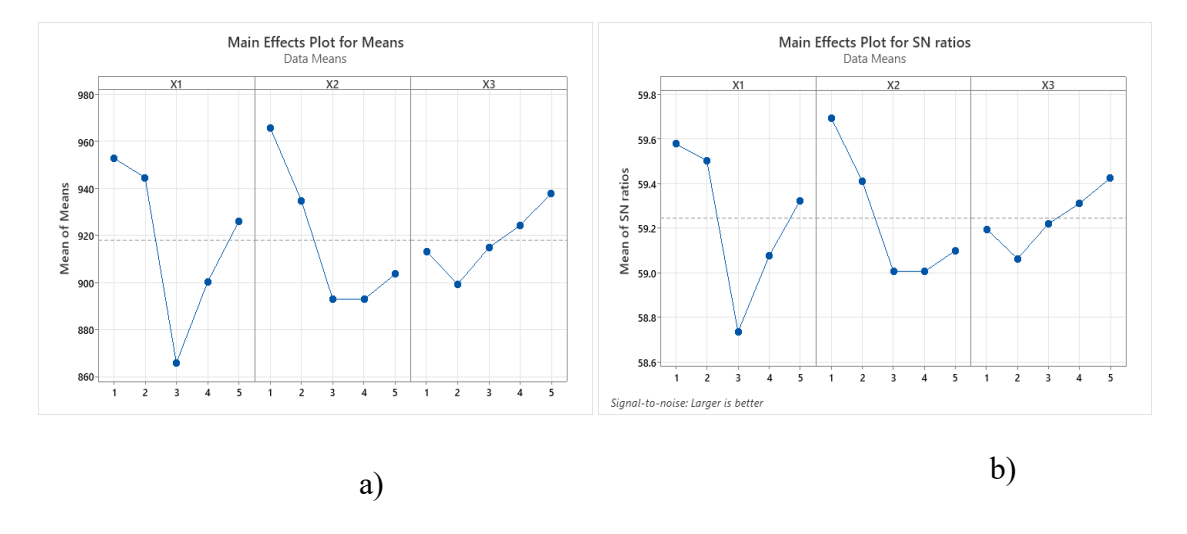


Figure 4.7 Response graph for main effects plot for, a) means and b) SN ratios for pellet particle density

The ANOVA table (Table 4.10) was employed to determine the significant design parameters for pellet particle density. A Pareto chart (Figure 4.8) illustrates the statistical significance of the parameters influencing the pellet particle density.

The two most significant design parameters for the optimum pellet particle density quality features (Figure 4.8) were linear low density polyethylene ratio and corn stover to eucalyptus sawdust ratio; torrefaction temperature had the least impact.

Table 4.10 Analysis of Variance of pellet particle density

Source	DF	Adj SS	Adj MS	F-Value	P-Value
Regression	3	21260	7087	4.23	0.017
X1	1	4781	4781	2.86	0.106
X2	1	13728	13728	8.20	0.009
X3	1	2752	2752	1.64	0.214
Error	21	35145	1674		
Total	24	56405			

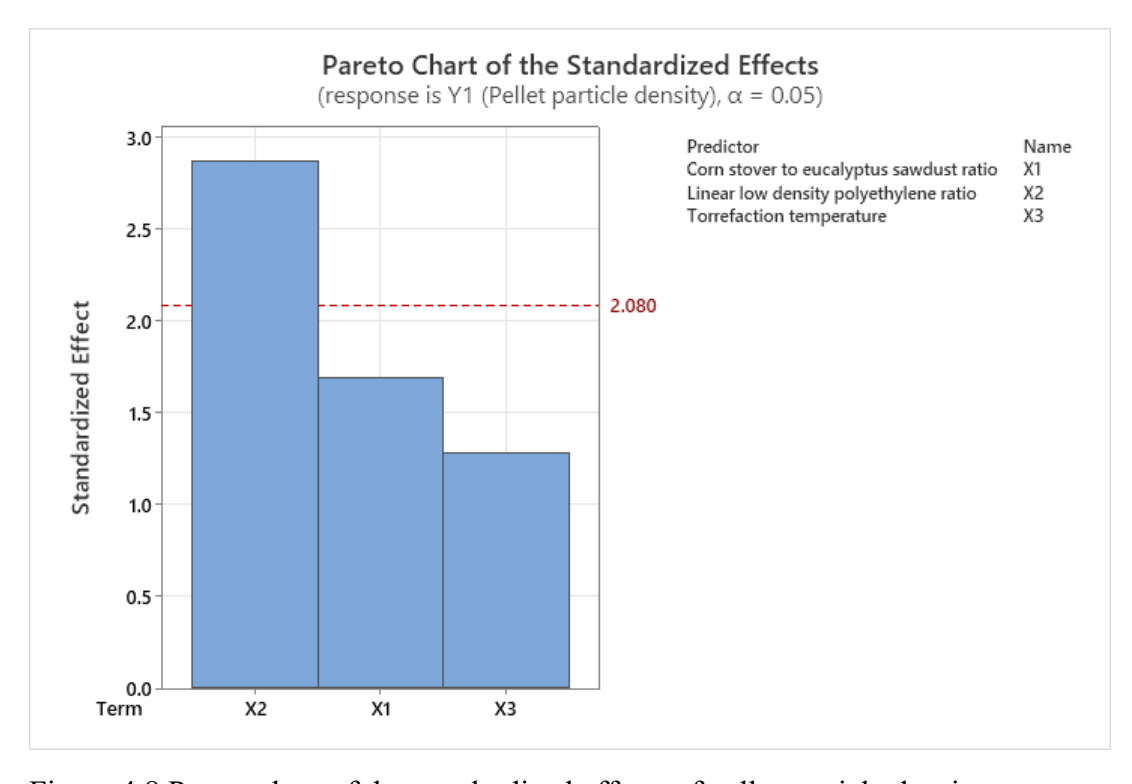


Figure 4.8 Pareto chart of the standardized effects of pellet particle density

b) Multivariable linear regression model

Minitab 18 software was used in this research to carry out statistical multivariable linear regression which involved the determination of a relationship between dependent and independent variables. The relationship between pellet particle density and the input parameters (corn stover to eucalyptus sawdust ratio, linear low-density polyethylene and torrefaction temperature) was as presented in Equation 4.4 below with model summary statistics as presented in Table 4.11. Figure 4.9 shows plot of the standardized residuals. It can be observed that the plots were around the straight line hence providing a good fit for the multivariable linear regression model derived (Equation 4.4). The fact that the residuals fall between -3 and 3 further supports the adequacy of the fitted model. The pellet particle density was shown to be mostly contributed by linear low-density polyethylene, corn stover to eucalyptus sawdust, and torrefaction temperature, in that order, according to the results of the linear regression model. In addition to the analysis provided by the pellet particle density response tables, see Appendix 5 (b) and Appendix 5 (c) respectively for means and signal-to-noise ratios, indicated an exact similarity in their findings.

Based on the multivariable linear regression model and the optimum levels for determination of pellet particle density obtained from the response graph (Figure 4.7), the optimum pellet particle density was 1020.4900Kg/m³.

Regression Equation

Table 4.11 Model Summary statistics for pellet particle density

S	R-sq	R-sq(adj)	R-sq(pred)
40.9095	37.69%	28.79%	6.51%

c) Analysis of contour and surface plots for pellet particle density

Contour plot analysis was performed using the statistical modeling software program Minitab 18.0. By displaying the contours and the response surface plots of the predicted response variables, the analysis was aimed to investigate the relationship between the response variable and the two independent variables (parameters) while holding one variable at a constant level (preferably the central level).

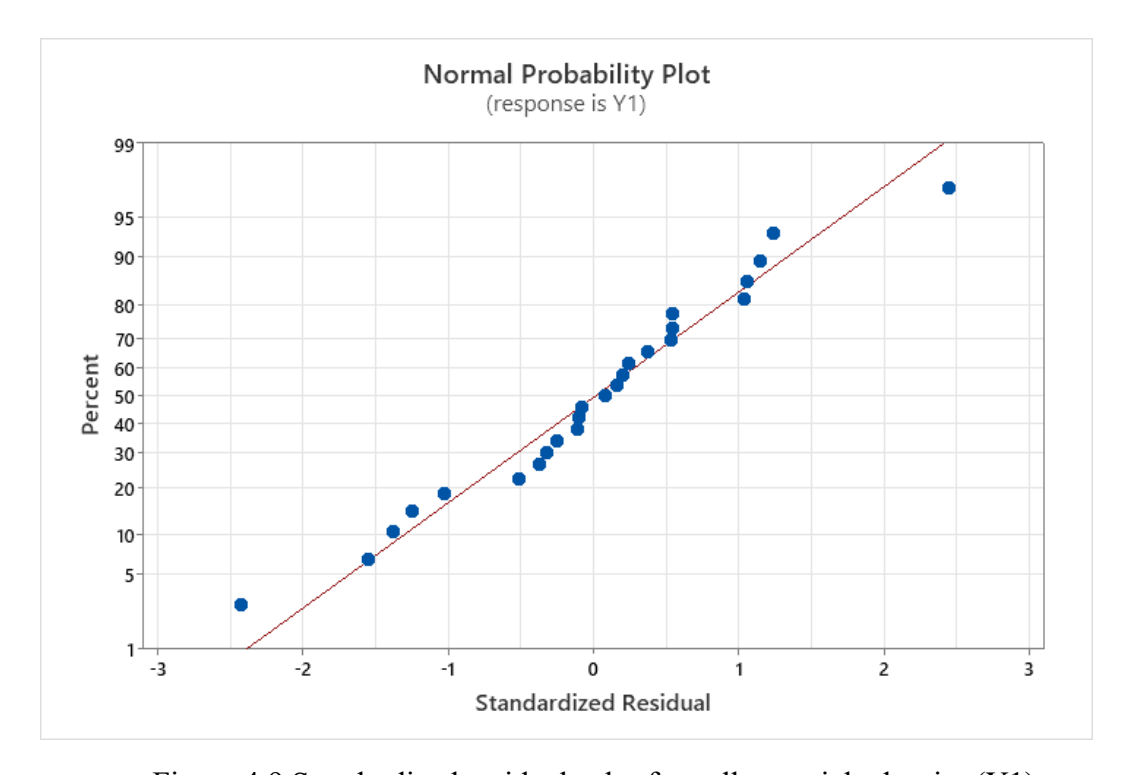


Figure 4.9 Standardized residuals plot for pellet particle density (Y1)

Figure 4.10 and Figure 4.11 illustrate the contour plots and response surface plots respectively explaining the relationship between process parameters of fabrication of blended pellets and the pellet particle density of the fabricated pellet. Process parameters not considered for all the cases were held at the median level which was 3 in this case.

It can be seen from Figure 4.10 (a) and Figure 4.11 (a) that to obtain a high pellet particle density, blended pellets should be fabricated using a corn stover to eucalyptus sawdust ratio of 9:1 and 2% linear low-density polyethylene. From Figure 4.10 (b) and

Figure 4.11 (b) it was found that high pellet particle density was achieved by fabricating blended pellets using a corn stover to eucalyptus sawdust ratio of 9:1 and a torrefaction temperature of 290°C. In Figure 4.10 (c) and Figure 4.11 (c), it was observed that the high values of the blended pellets' particle density were obtained by fabrication of the blended pellet using 10% linear low density polyethylene binder and a torrefaction temperature of 210°C. It can also be seen from the contour plots that the optimized blended pellet attained a pellet particle density of greater than 960Kg/m³ depicted by the dark green regions.

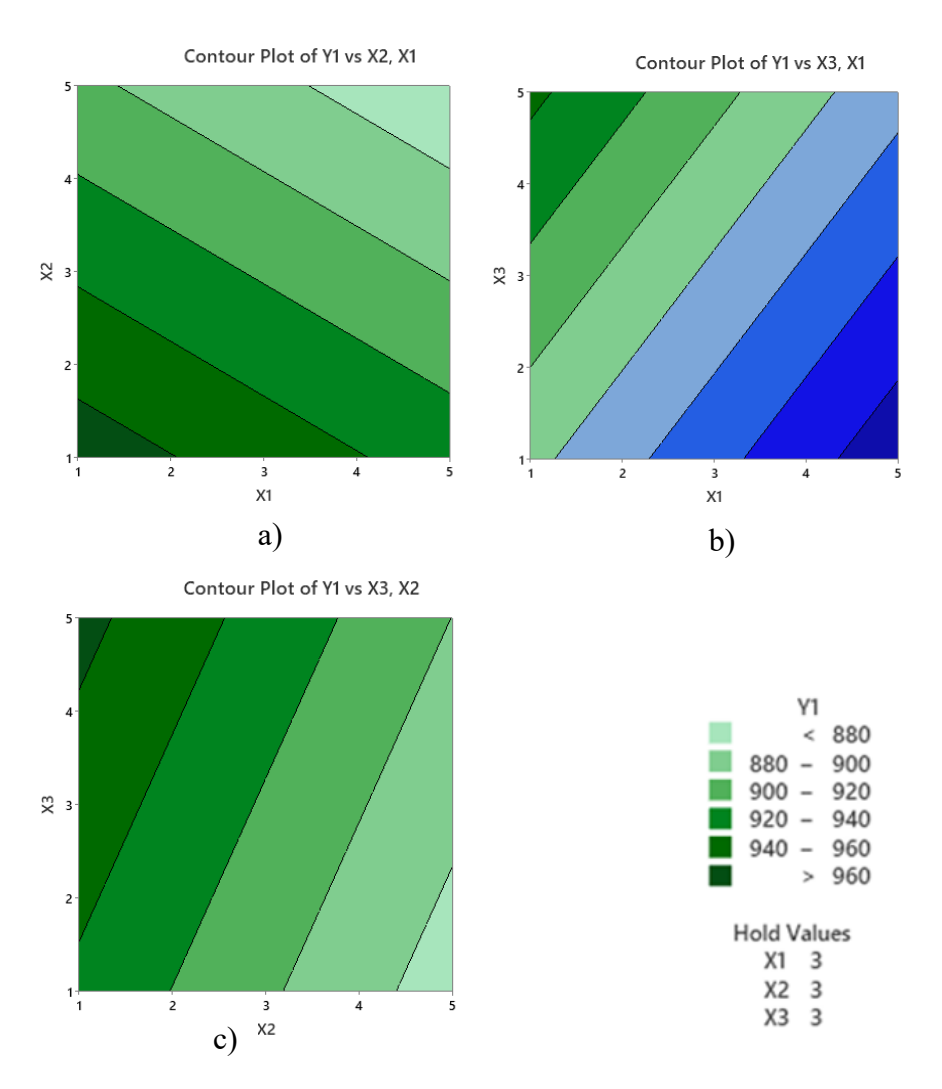
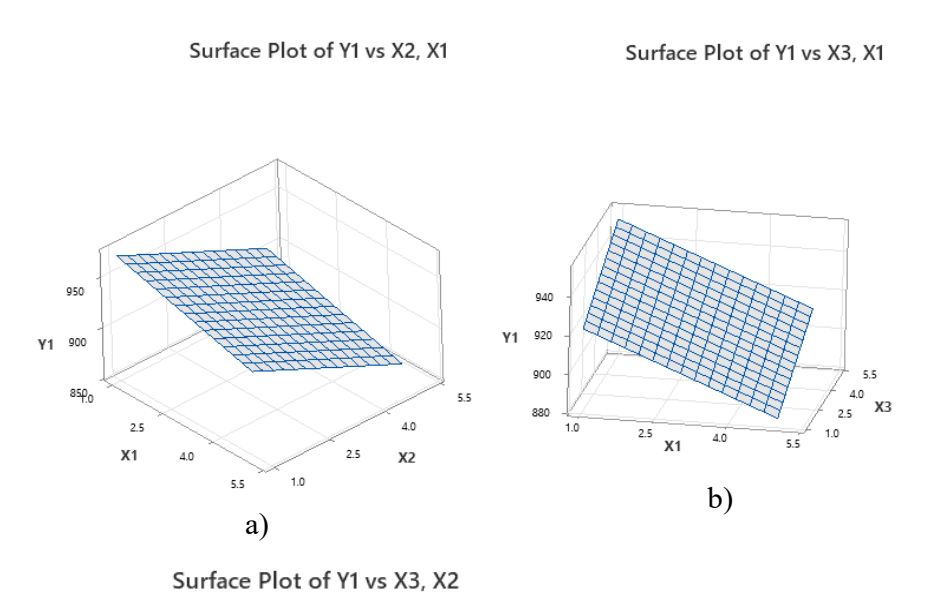


Figure 4.10 Contour plots for pellet particle density (Y1): a) corn stover to eucalyptus sawdust ratio (X1) vs linear low-density polyethylene (X2), b) corn stover to eucalyptus sawdust ratio (X1) vs torrefaction temperature (X3), c) linear low density polyethylene (X2) vs torrefaction temperature (X3).



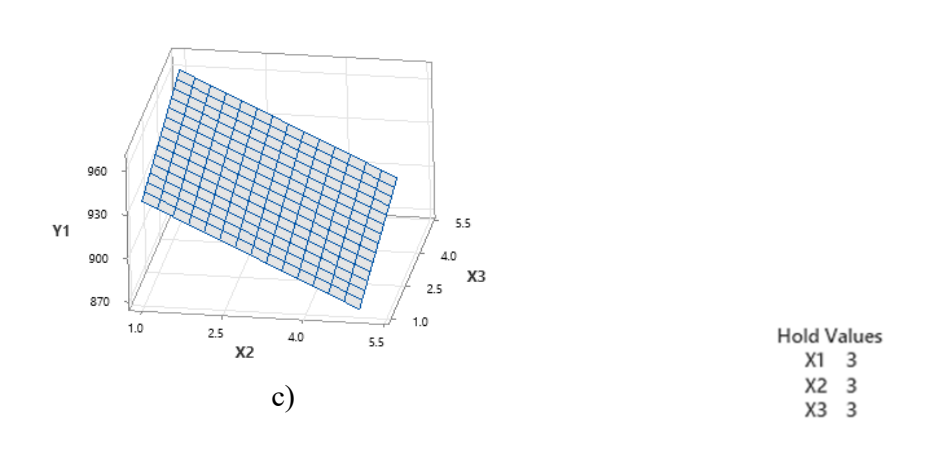


Figure 4.11 Response surface plots for pellet particle density (Y1): a) corn stover to eucalyptus sawdust ratio (X1) vs linear low-density polyethylene (X2), b) corn stover to eucalyptus sawdust ratio (X1) vs torrefaction temperature (X3), c) linear low density polyethylene (X2) vs torrefaction temperature (X3).

d) Analysis of interactions of pellet particle density

The pellet particle density interaction plot is shown in Figure 4.12 below. This plot illustrates the interaction between the linear low density polyethylene percent ratio and the corn stover to eucalyptus sawdust ratio. The highest pellet particle density was found at a ratio of 2% for LLDPE and 1:1 for corn stover to eucalyptus sawdust ratio. The torrefaction temperature and corn stover to eucalyptus sawdust ratio interact as well; at 290°C, the pellet particle density is greatest at a corn stover to eucalyptus

sawdust ratio of 1:1. Additionally, there was an interaction between the linear low density polyethylene ratio and the torrefaction temperature that maximized the pellet particle density at 2% LLDPE and 290°C.

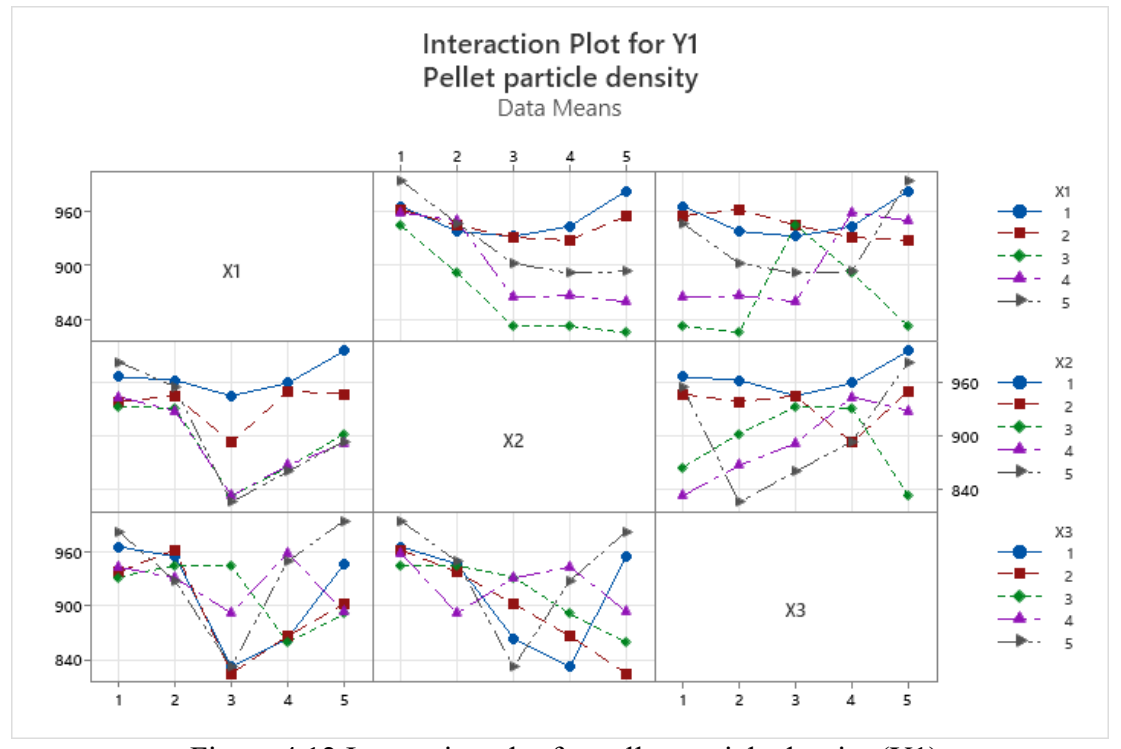


Figure 4.12 Interaction plot for pellet particle density (Y1)

4.5.1.2 Bulk density

Appendix 6 (a) presents the results of bulk density of the torrefied blended pellets. The mean bulk density of the torrefied blended pellets was 576.9904 kg/m³ with the maximum value being 661.6172 kg/m³ and the minimum value being 477.3099 kg/m³. Physically the shape of the pellets didn't change after torrefaction but the colour turned brownish to dark depending on the temperature of torrefaction.

The mean pellet bulk density obtained was lower compared to the raw pellet bulk densities reported in some other works of literature. According to Garcia-Maraver (2015b) the bulk densities of densified biomasses is generally between 600-800kg/m³. Tumuluru (2019b) studied the effect of blending feedstock material from pine and switchgrass on the pellet durability and bulk density. The resultant pellet maximum bulk

density attained was 550 Kg/m³. It can be seen that this figure is lower than the results of this study.

Some of the factors that lead to decreased bulk density, as observed in this study, include torrefaction after pelletization. The bulk density generally decreases on torrefaction of pellets (Manouchehrinejad & Mani, 2018; Siyal et al., 2021). The primary component of biomass materials, hemicellulose, is broken down during torrefaction due to depolymerization, demethoxylation, bond cleavage, and condensation processes, which also removes moisture and some volatile compounds (Wang et al., 2020), leading to mass loss and thus the reason for low bulk density since the structural integrity of the pellet is maintained. Other reasons for decreased pellet bulk density in torrefaction after pelletization according to Prapakarn et al. (2018) and Lee et al. (2016) are:

- ➤ Due to the release of volatiles and moisture during torrefaction, some biomass materials may undergo swelling and thermal expansion. Because the pellets take up more space on expansion and swelling for the same mass, this expansion may result in a decreased bulk density.
- ➤ Increased porosity is one of the structural alterations that might result from the thermal treatment of the biomass material during torrefaction. The pellets' overall density is decreased by the pores that form within them, even if their dimensions remain the same.
- A biomass's total density is influenced by lignin and extractive chemicals.

 Torrefaction causes these molecules to undergo changes chemically and become volatile, which results in the loss of material that would otherwise contribute to the bulk density of the pellet.

Torrefaction causes a loss of mass in the biomass material as volatile chemicals are pushed out. Reduction in bulk density is the outcome of this mass loss without a matching decrease in pellet volume.

Manouchehrinejad & Mani (2018) studied the effect of torrefaction of wood pellets produced from mixed sawmill wastes of soft and hardwoods at temperatures of between 230°C and 290°C. The observation was that the shape of the pellets was retained, while pellet particle and bulk densities decreased. Wang et al. (2020) found out that the torrefied pellets maintained their integrity, while the mechanical properties of torrefied pellets generally decreased with increasing torrefaction temperature. In their studies, Ghiasi et al. (2014), Shang et al. (2012) and Kumar et al. (2017) concluded that post-pelletization torrefaction resulted in decreased bulk densities. They also observed that the structural integrity of the pellets is maintained. The observations of results of bulk densities in literature agree with the results of this research.

a) Analysis of results for pellet bulk density optimization

Using the Taguchi approach, the optimal process parameter conditions for a pellet bulk density were evaluated using signal-to-noise (S/N) ratios. Since pellet bulk density is a desirable attribute when high, the larger the better criteria of analysis were used.

The response table for signal-to-noise ratio and means for the main effects for pellet bulk density were presented in Appendix 6 (b) and Appendix 6 (c) respectively. The optimal level setting for parameters that leads to higher pellet bulk density was depicted in Figure 4.13. The main effect plots for S/N ratios (Figure 4.13) showed that optimal parameter level settings for higher pellet bulk density, were X1₅X2₁X3₃.

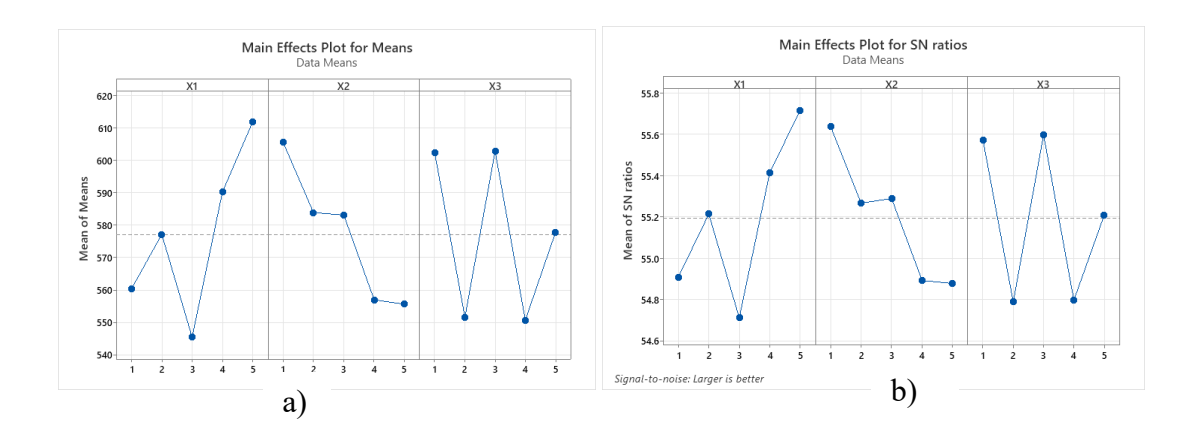


Figure 4.13 Response graph for main effects plot for, a) means and b) SN ratios for pellet bulk density

The ANOVA table (Table 4.12) was employed to determine the significant design parameters for pellet bulk density. A Pareto chart (Figure 4.14) illustrates statistical significance of the parameters influencing the pellet bulk density. Almost all the design variables had significant effect on bulk density. The two most significant design parameters for the optimum pellet bulk density quality features (Figure 4.14) were linear low density polyethylene ratio and corn stover to eucalyptus sawdust ratio; torrefaction temperature had the least impact.

Table 4.12 Analysis of Variance of pellet bulk density

Source	DF	Adj SS	Adj MS	F-Value	P-Value
Regression	3	16011	5337	2.98	0.054
X1	1	6753	6753	3.77	0.066
X2	1	8014	8014	4.48	0.046
X3	1	1243	1243	0.70	0.414
Error	21	37567	1789		
Total	24	53578			

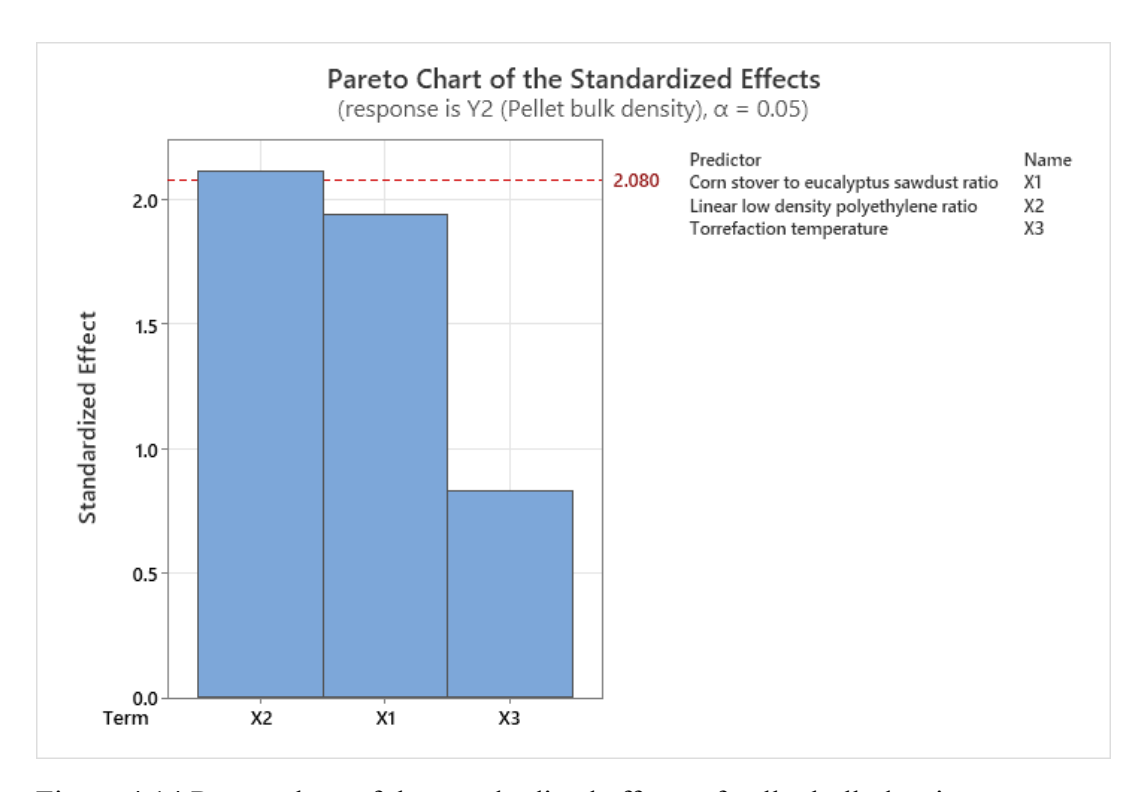


Figure 4.14 Pareto chart of the standardized effects of pellet bulk density

b) Multivariable linear regression model

The relationship between pellet bulk density and the input parameters (corn stover to eucalyptus sawdust ratio, linear low-density polyethylene and torrefaction temperature) was as presented in Equation 4.5 below with model summary statistics as presented in Table 4.13. Figure 4.15 shows the standardized residuals plot. It can be observed that the plots were around the straight line hence providing a good fit for the multivariable linear regression model for the bulk density of the pellets. From the linear regression model, it was observed that corn stover: eucalyptus sawdust contributed more to the pellet bulk density followed by torrefaction temperature and linear low-density polyethylene respectively. This was in tandem with the analysis provided from the bulk density response tables for signal to noise ratios and means in Appendix 6 (b) and Appendix 6 (c) respectively. The fitted model's adequacy was further supported by the residuals' range of -3 to 3. The pellet bulk density response tables' analysis for the

means and signal to noise ratios presented in appendices, found that their outcomes were exactly the same.

The response graph (Figure 4.13) provided the optimal levels for determining pellet bulk density, and these levels, along with the multivariable linear regression model, indicated that the optimal pellet bulk density was 666.1560 kg/m³.

Regression Equation

Table 4.13 Model Summary statistics of pellet bulk density

S	R-sq	R-sq(adj)	R-sq(pred)
42.2956	29.88%	19.87%	0.00%

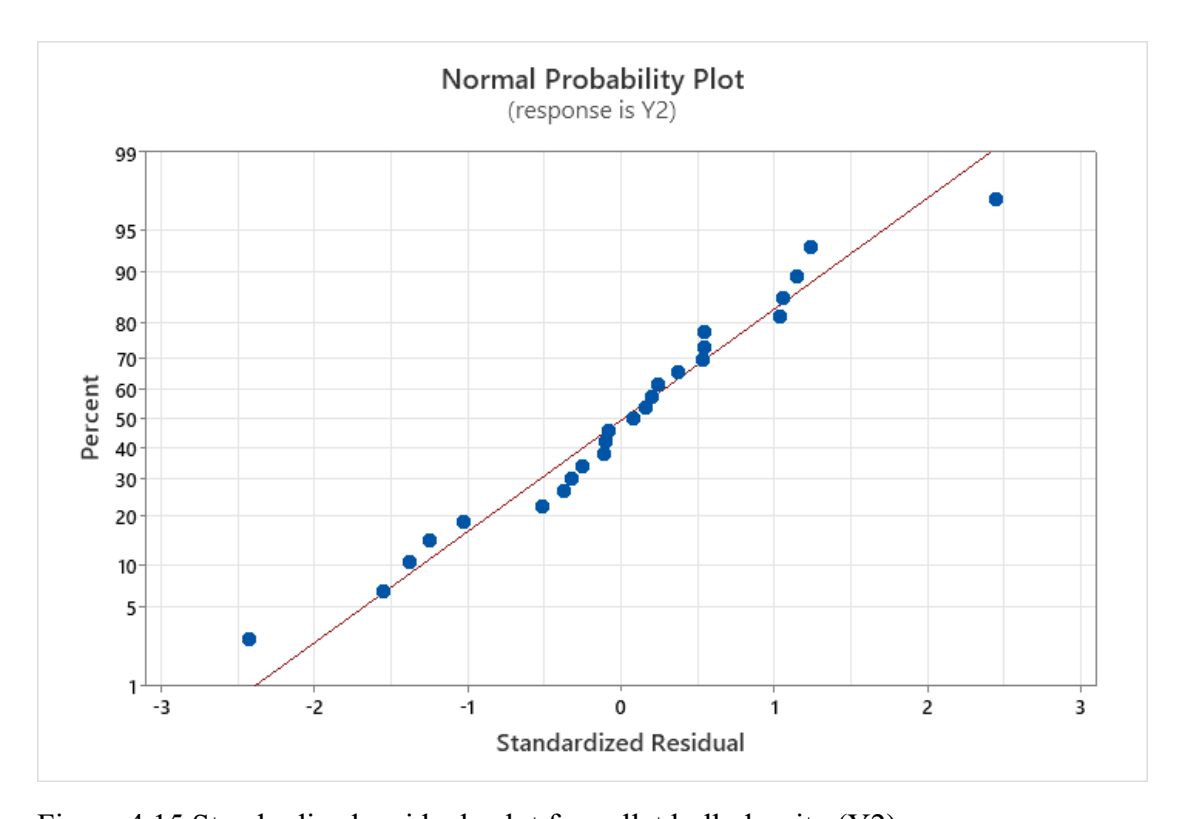


Figure 4.15 Standardized residuals plot for pellet bulk density (Y2)

c) Analysis of contour and surface plots for pellet bulk density

Figure 4.16 and Figure 4.17 show the contour plots and response surface plots, respectively, that explain the relationship between the blended pellet fabrication process

parameters and the pellet bulk density of the final product. In this situation, the median level of the process parameters—which were not taken into account for all cases—was 3.

Figure 4.16 (a) and Figure 4.17 (a) indicate that in order to get a high pellet bulk density, blended pellets should be produced with 2% linear low-density polyethylene and a corn stover to eucalyptus sawdust ratio of 1:1. Based on Figure 4.16 (b) and Figure 4.17 (b), it was discovered that fabricating blended pellets with a corn stover to eucalyptus sawdust ratio of 1:1 and a torrefaction temperature of 210°C would result in high pellet bulk density. It was noted in Figure 4.16 (c) and Figure 4.17 (c) that the high bulk density values of the blended pellets were achieved by the use of a 2% linear low density polyethylene binder and a 210°C torrefaction temperature during the blended pellet's production. The contour plots also show that the optimized blended pellet achieved high pellet bulk density of more than 620 kg/m³, as indicated by the dark green regions.

d) Analysis of interactions of pellet bulk density

The interaction plot for pellet bulk density was presented in Figure 4.18. The plot indicates that there was an interaction between the percent ratio of linear low-density polyethylene and the ratio of corn stover to eucalyptus sawdust. The maximum pellet bulk density was seen at a ratio of 4% for LLDPE and 1:1 for corn stover to eucalyptus sawdust ratio. Similarly, the torrefaction temperature and the corn stover to eucalyptus sawdust ratio interact, with a value of 1:1 for corn stover to eucalyptus sawdust ratio at 210°C torrefaction temperature maximizing the pellet bulk density. There was also an interaction between the ratio of linear low-density polyethylene and torrefaction temperature maximizing pellet bulk density at 4% LLDPE and a torrefaction temperature of 210°C.

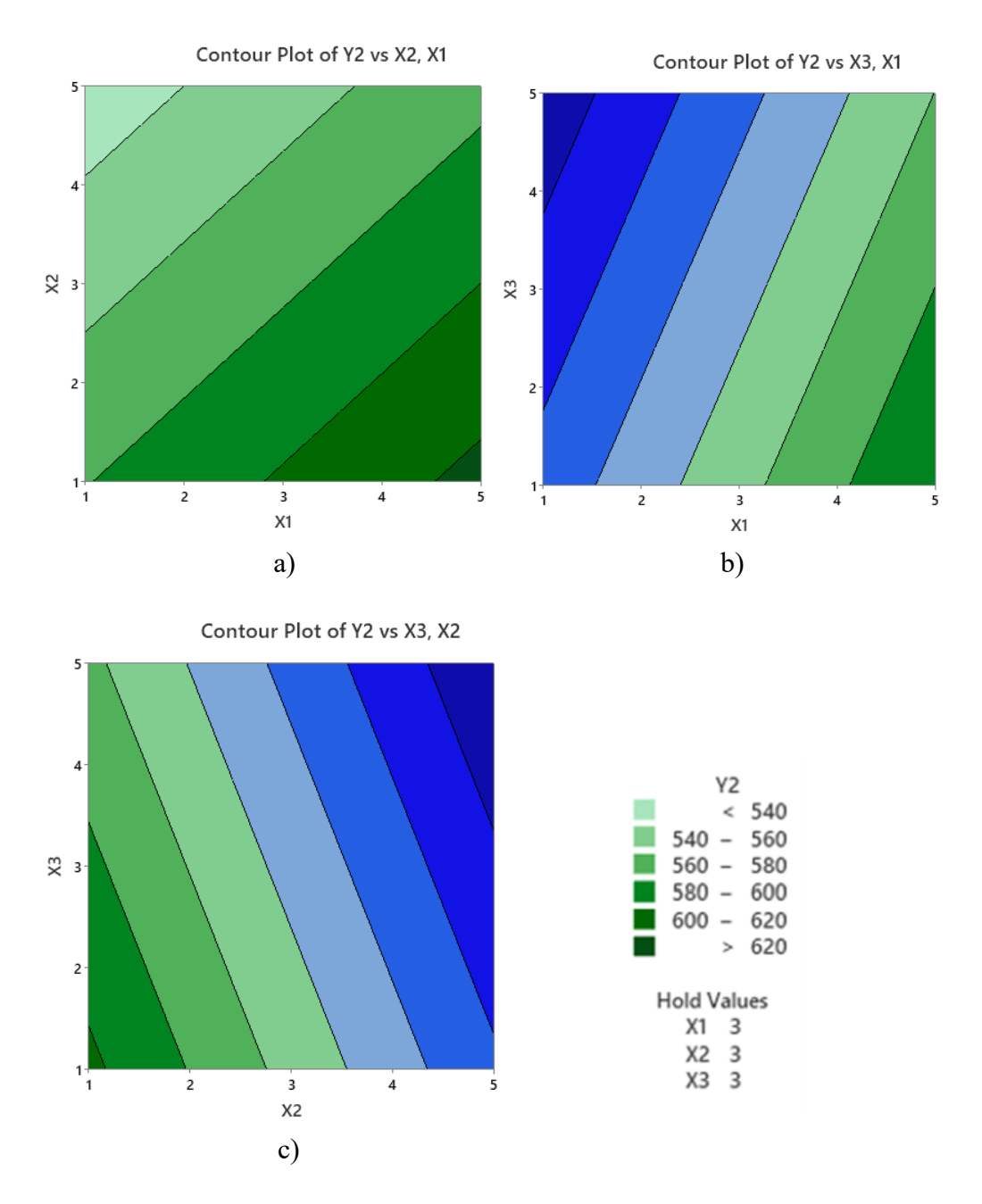


Figure 4.16 Contour plots for pellet bulk density (Y2): a) corn stover to eucalyptus sawdust ratio (X1) vs linear low density polyethylene (X2), b) corn stover to eucalyptus sawdust ratio (X1) vs torrefaction temperature (X3), c) linear low density polyethylene (X2) vs torrefaction temperature (X3).

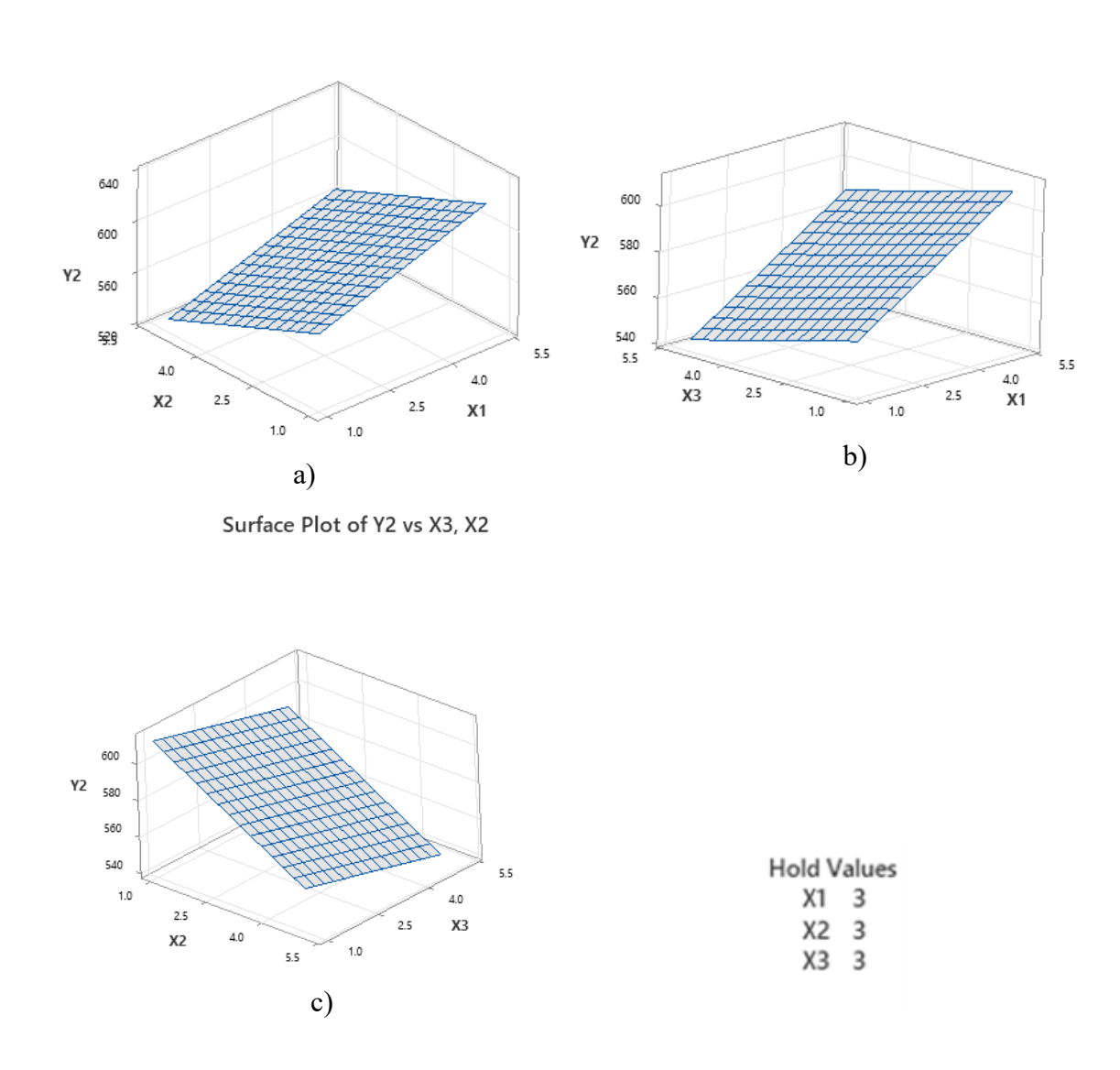


Figure 4.17 Response surface plots for pellet bulk density (Y2): a) corn stover to eucalyptus sawdust ratio (X1) vs linear low density polyethylene (X2), b) corn stover to eucalyptus sawdust ratio (X1) vs torrefaction temperature (X3), c) linear low density polyethylene (X2) vs torrefaction temperature (X3).

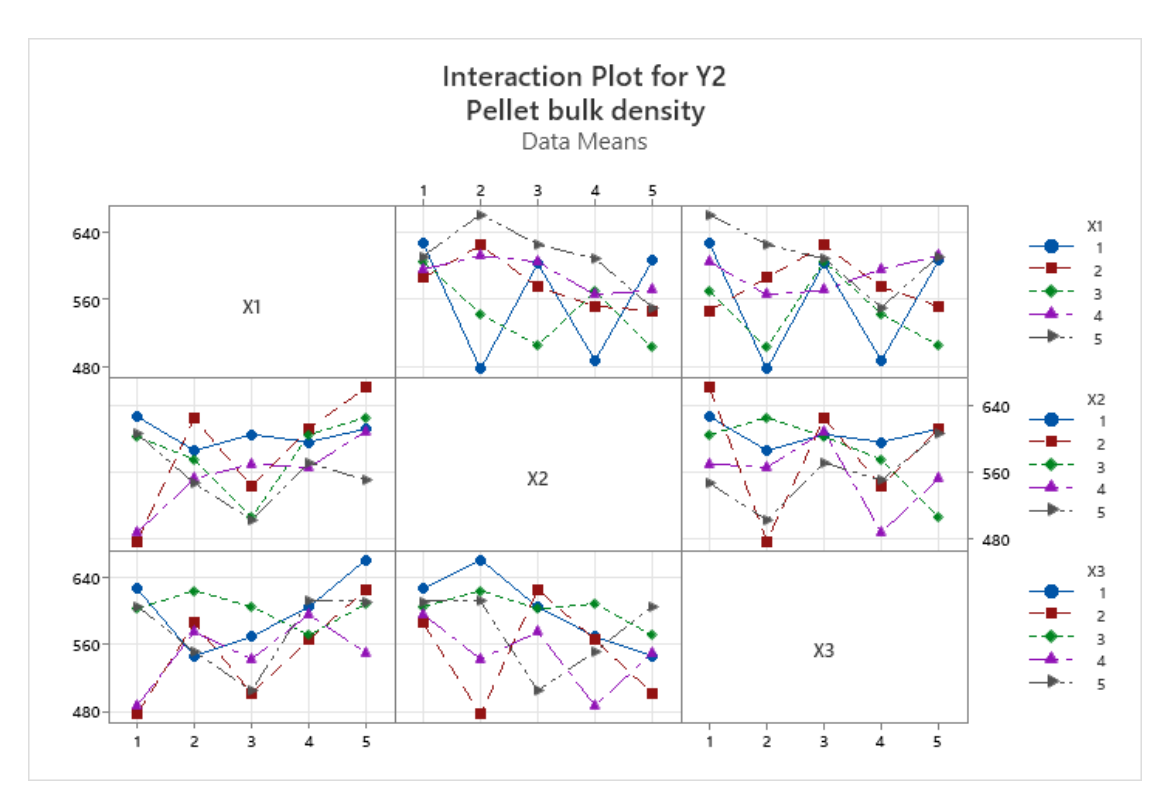


Figure 4.18 Interaction plots for pellet bulk density (Y2)

4.5.2 Mechanical properties

4.5.2.1 Pellet durability index

Pellet durability index (PDI) results were presented in Appendix 7 (a). The mean PDI for the blended pellets was 96.6532%, while the maximum and minimum PDI respectively were 98.2377% and 88.5926% respectively.

Comparing these results with the standards, i.e. European normative guidelines for pellets produced from herbaceous and fruit biomass and blends and mixtures, the minimum pellet durability index of non-torrefied pellets is 96.5%. This makes the PDI of the blended pellet in this research to be within the required standard despite the fact that it is torrefied pellets. The PDI of the pellets is just on the lower limit of the standard. This could mean that torrefaction affected the value of PDI slightly.

Most researches in literature concluded that torrefaction of pellets leads to decreased PDI, while the shape of the pellets is maintained. These include researches done by

Manouchehrinejad & Mani (2018), Wang et al. (2020), Ghiasi et al. (2014), Shang et al. (2012) and Kumar et al. (2017). Since the PDI of the torrefied pellets in this research is high i.e., above the lower limit of non-torrefied pellets, then the appropriate explanation for this observation was attributed to both eucalyptus sawdust which has a binding effect and the linear low density polyethylene binder. Other reasons that lead to reduced pellet durability index as explained by Azargohar et al. (2019), Dyjakon et al. (2021), Sarker et al. (2021), Siyal et al. (2020) and Whittaker & Shield (2017) include:

- ➤ Increased brittleness Due to the loss of hemicellulose and other organic components, torrefaction can cause biomass materials to become more brittle.

 The enhanced brittleness of the pellets may contribute to a decreased PDI since they become more susceptible to breaking during handling and transportation.
- ➤ Changes in material composition During torrefaction, the chemical composition of biomass changes, resulting in a decrease in volatile matter and oxygen content. The strength of the pellets created during pelletization may vary as a result of these modifications to the binding characteristics of the biomass particles.
- ➤ Increased susceptibility to fracture Because of the heat treatment process, torrefaction can cause internal stresses in biomass particles. Lower durability may result from the pellets' increased susceptibility to fracturing under mechanical loads as a result of these internal stresses.
- ➤ Decreased moisture content In general, torrefaction lowers the moisture content of biomass, which may have an impact on the interparticle bonding and pelletization process. Lower PDI and weaker pellet structures can result from uneven distribution or inadequate moisture content.

a) Analysis of results for pellet durability index optimization

Pellet durability index is a desirable property of pellets when it is high. Therefore, the larger the better criterion was used to optimize the design parameters. Signal to noise (S/N) ratios were used to identify the optimal process parameter conditions for a pellet durability index using the Taguchi method.

The response table for signal to noise ratio and means for the main effects for pellet durability index were presented in Appendix 7 (b) and Appendix 7 (c) respectively. The optimal level setting for parameters that leads to higher pellet durability index was depicted in Figure 4.19. The main effect plots for S/N ratios (Figure 4.19) showed that optimal parameter level settings for higher pellet durability index, were X1₅X2₄X3₁.

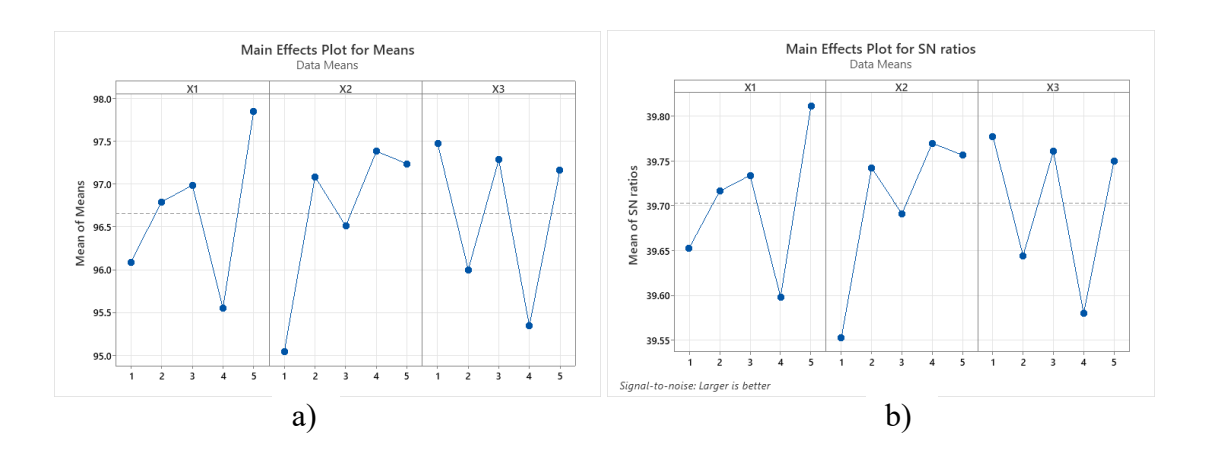


Figure 4.19 Response graph for main effects plot for, a) means and b) SN ratios for pellet durability index

Using the ANOVA table (Table 4.14), the significant design parameters for the pellet durability index were determined. The statistical significance of the factors affecting the pellet durability index is shown by a Pareto chart (Figure 4.20). The significance of design parameters for the optimum pellet durability index in descending order (Figure 4.20) were: linear low-density polyethylene, corn stover to eucalyptus sawdust ratio and torrefaction temperature. This was similar to the ranking of parameters as depicted from response graphs.

J		1	J		
Source	DF	Adj SS	Adj MS	F-Value	P-Value
Regression	3	14.3437	4.7812	1.25	0.316
X1	1	2.5836	2.5836	0.68	0.420
X2	1	10.9436	10.9436	2.87	0.105
X3	1	0.8165	0.8165	0.21	0.649
Error	21	80.1852	3.8183		
Total	24	94.5289			

Table 4.14 Analysis of Variance of pellet durability index

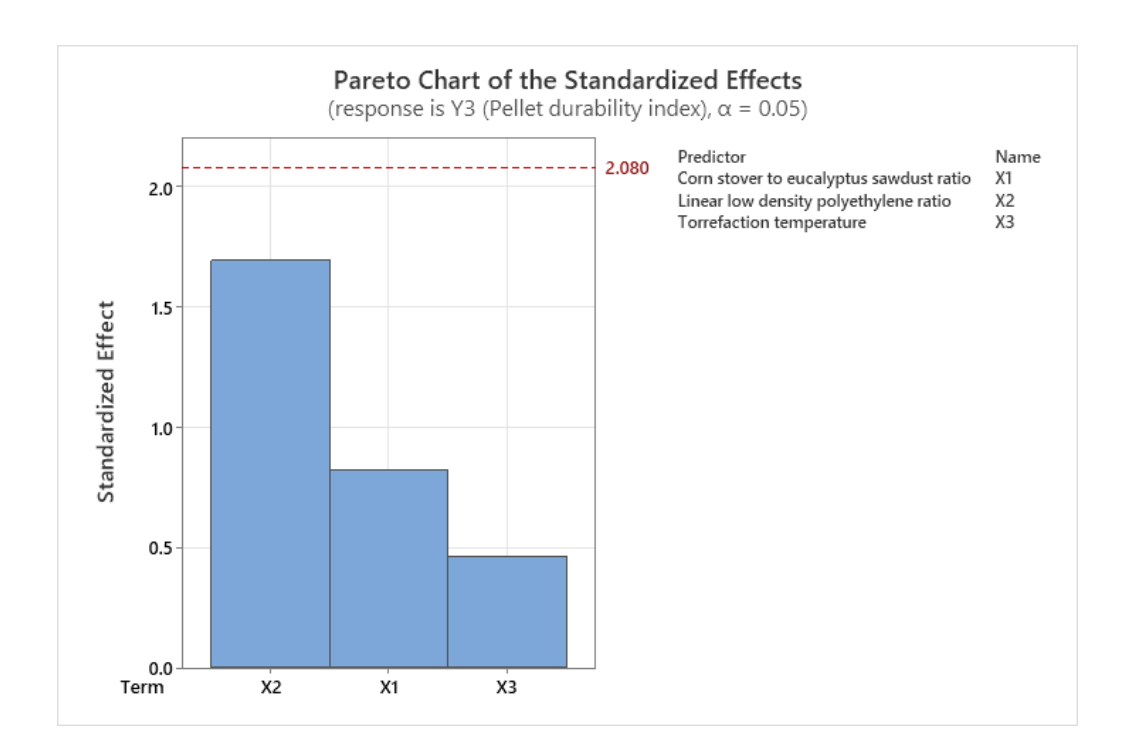


Figure 4.20 Pareto chart of the standardized effects of pellet durability index (Y3)

b) Multivariable linear regression model for pellet durability index

The following Equation 4.6 establishes a link between the pellet durability index and the input parameters: linear low-density polyethylene, torrefaction temperature, and corn stover to eucalyptus sawdust ratio. The model summary statistics are presented in Table 4.15. The standardized residuals plot is presented in Figure 4.21. As can be seen, the plots were centered around the straight line, which gave the multivariable linear regression model for the pellets' durability index an excellent match. Furthermore, the residuals are within the range of -3 and 3 which further confirms the adequacy of the fitted model. The results of the linear regression model showed that the most significant

factors influencing the pellet durability index were linear low-density polyethylene, followed by corn stover to eucalyptus sawdust ratio and torrefaction temperature, in that order. This was in addition to the analysis that was supplied by the pellet durability index response tables for the above means and signal-to-noise ratios.

Regression Equation

Table 4.15 Model Summary statistics for pellet durability index

S	R-sq	R-sq(adj)	R-sq(pred)
1.95406	15.17%	3.06%	0.00%

c) Analysis of contour and surface plots for pellet particle density

The contour plots and response surface plots, respectively, in Figure 4.22 and Figure 4.23 illustrate the relationship between the final product's pellet durability index and the parameters of the blended pellet fabrication process. The median level of the process parameters in this instance, which were not considered in every case, was 3.

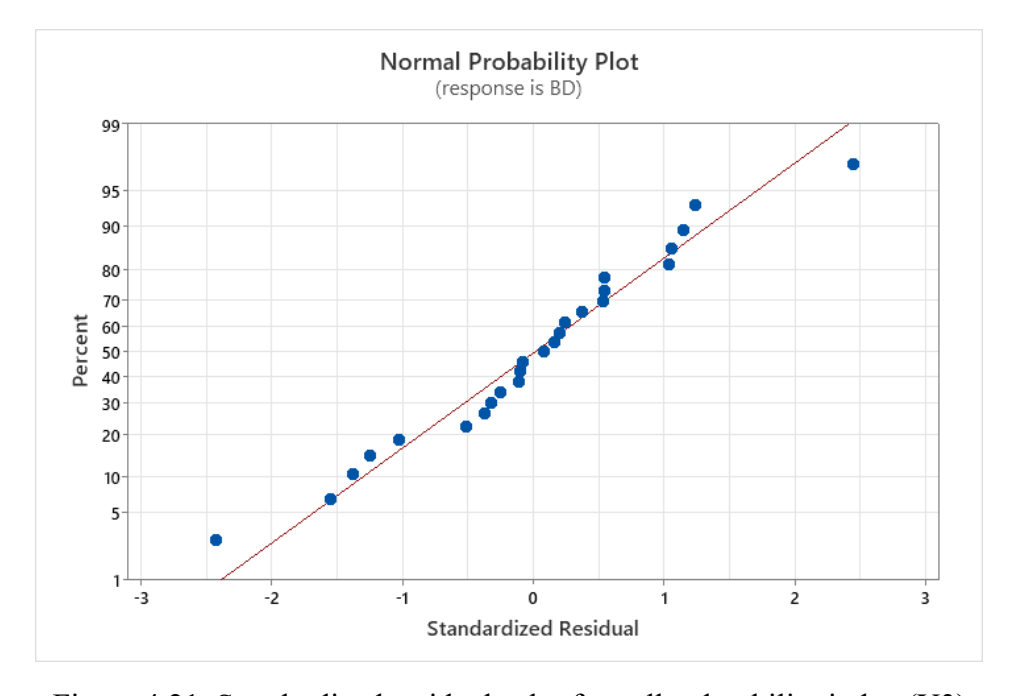


Figure 4.21 Standardized residuals plot for pellet durability index (Y3)

Based on the results shown in Figure 4.22 (a) and Figure 4.23 (a), blended pellets with a ratio of 1:1 of corn stover to eucalyptus sawdust and 10% linear low-density polyethylene are recommended for one to achieve a high pellet durability index. It was found, based on Figure 4.22 (b) and Figure 4.23 (b), that producing blended pellets at a 1:1 ratio of corn stover to eucalyptus sawdust and a 210°C torrefaction temperature would produce a high pellet durability index. The high pellet durability index values of the blended pellets were attained by using a 2% linear low density polyethylene binder and a 210°C torrefaction temperature during the blended pellet's production, as shown in Figure 4.22 (c) and Figure 4.23 (c). The contour plots also show that the optimized blended pellet achieved high pellet durability index of more than 98%, as indicated by the dark green regions.

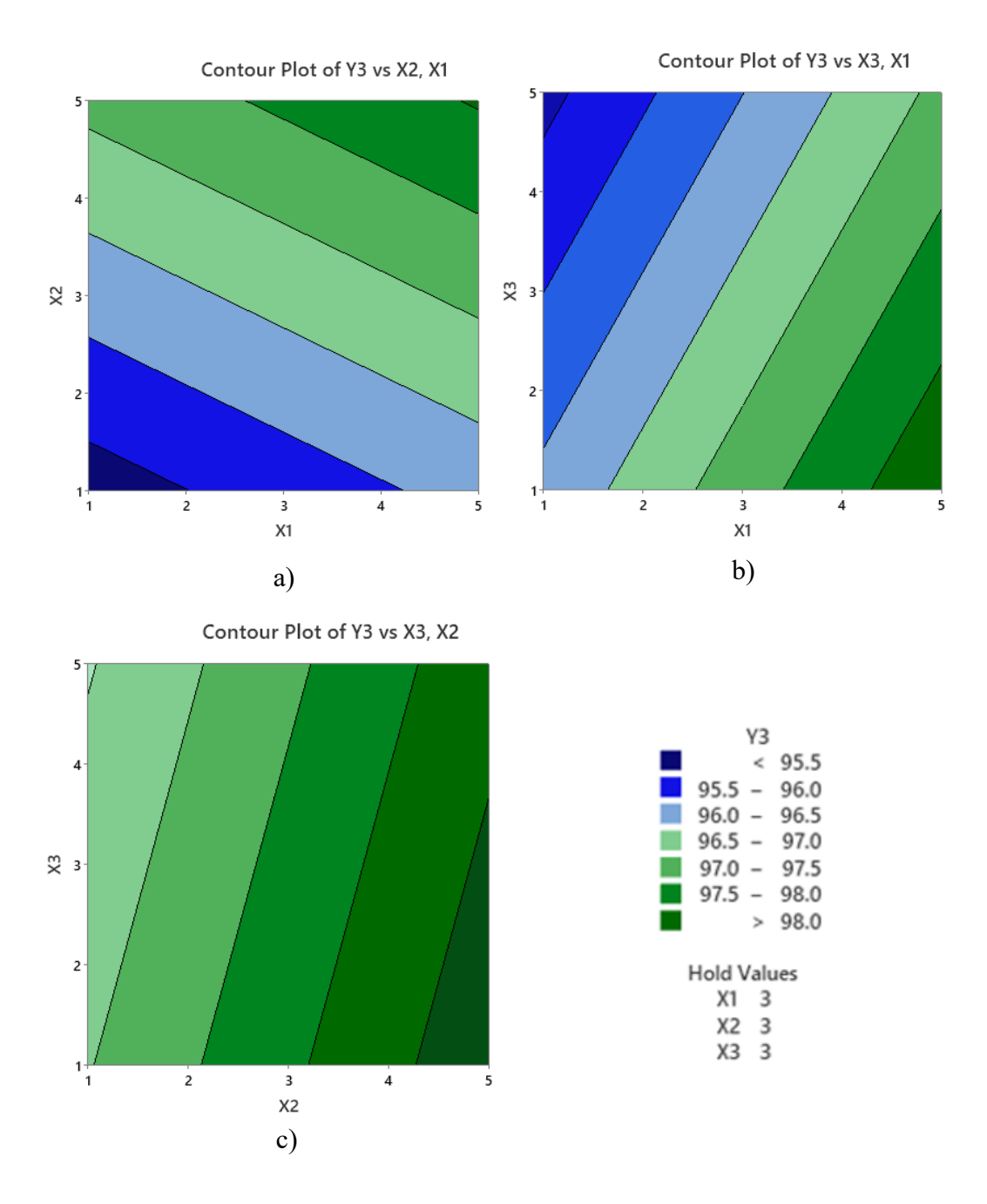
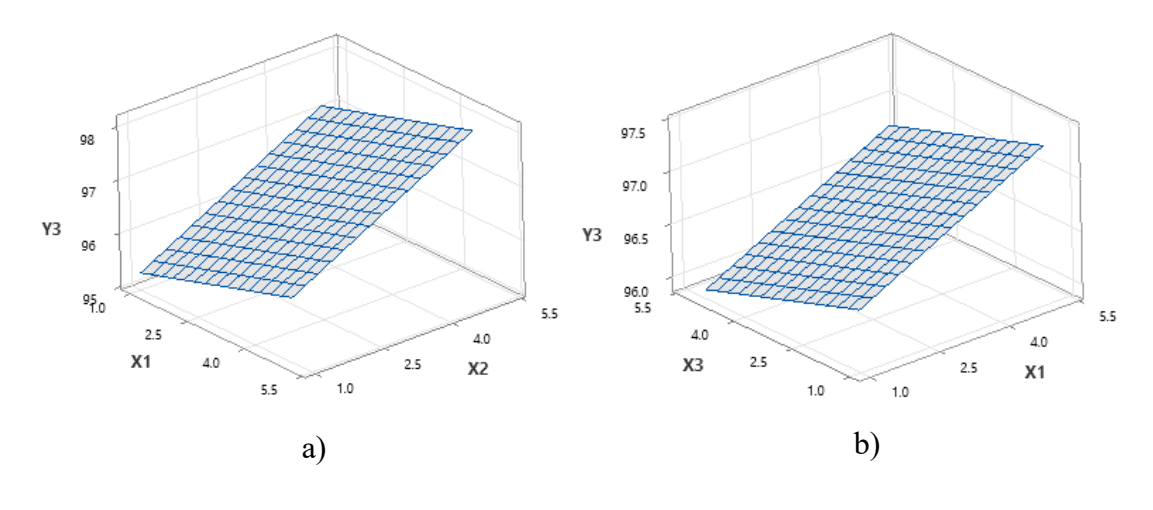


Figure 4.22 Contour plots for pellet durability index (Y3): a) corn stover to eucalyptus sawdust ratio (X1) vs linear low-density polyethylene (X2), b) corn stover to eucalyptus sawdust ratio (X1) vs torrefaction temperature (X3), c) linear low density polyethylene (X2) vs torrefaction temperature (X3).



Surface Plot of Y3 vs X3, X2

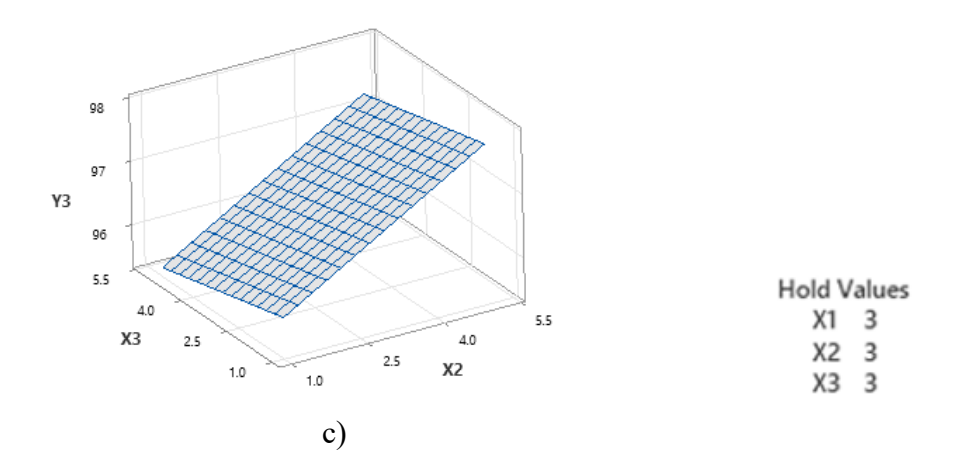


Figure 4.23 Response surface plots for pellet durability index (Y3): a) corn stover to eucalyptus sawdust ratio (X1) vs linear low-density polyethylene (X2), b) corn stover to eucalyptus sawdust ratio (X1) vs torrefaction temperature (X3), c) linear low density polyethylene (X2) vs torrefaction temperature (X3).

d) Analysis of interactions of pellet durability index

Figure 4.24 below shows the interaction pattern for the pellet durability index. The plot shows that the ratio of corn stover to eucalyptus sawdust and the percent ratio of linear low-density polyethylene interacted. For LLDPE and corn stover to eucalyptus sawdust ratio, the greatest pellet durability index was observed at a ratio of 4% and 1:1,

respectively. The torrefaction temperature and the corn stover to eucalyptus sawdust ratio also interact, with the pellet durability index being maximized at a corn stover to eucalyptus sawdust ratio of 1:1 at 210°C torrefaction temperature. Additionally, at 4% LLDPE and a torrefaction temperature of 210°C, there was an interaction between the linear low density polyethylene ratio and the torrefaction temperature that maximized the pellet durability index.

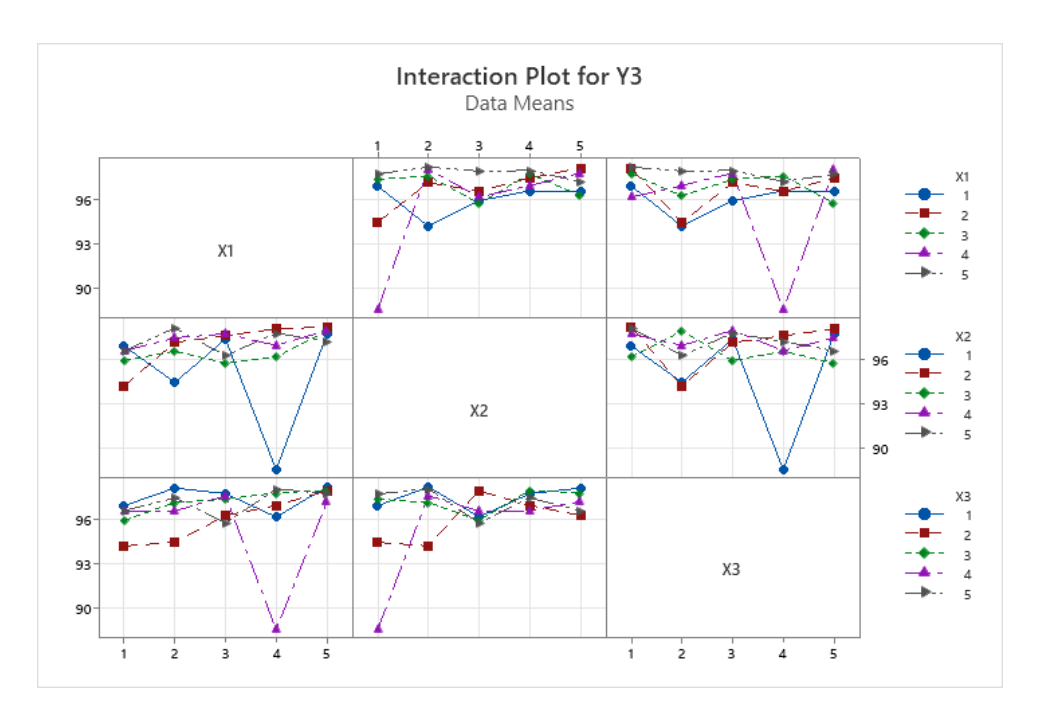


Figure 4.24 Interaction plot for pellet durability index

4.5.2.2 Pellet Hardness

The strength of the biomass pellets, which indicates the amount of force required to fracture or damage (i.e., crush) a pellet, is another crucial characteristic (Rudolfsson et al., 2017) and it is evaluated in terms of hardness with units of force (N) or force per unit area (N/m²). Appendix 8 (a) presents the results of hardness testing of torrefied pellets considered in this research that were produced from corn stover and eucalyptus sawdust using LLDPE as a binder. It can be observed that the mean hardness of pellets was 699.7060N with the maximum value being 996.2601N and the minimum hardness observed was 541.8128N.

The mean hardness of the pellets observed was way smaller than that of the control pellet which was 1296N. Therefore, it means there was approximately a 46% drop in the hardness of the pellets. The trends in literature indicate that there is always a reduction in pellet strength after torrefaction. According to Rudolfsson et al. (2017), the physical forces that hold the particles together are primarily responsible for the pellet's strength and durability. After torrefaction treatment, one of the primary reasons for the loss of strength in biomass pellets was proposed to be the degradation of hemicellulose and cellulose polymers. According to Pellet Fuels Institute Standard Specifications (2012), these polymers break down, weakening, and rupturing secondary links between hemicellulose and cellulose as well as cleaving covalent linkages between hemicellulose and lignin. The embedded cell fibrils are disrupted and their ability to share the load in the lignin-hemicellulose matrix is reduced (Filbakk et al., 2011). Additionally, when the wood polymers break down, the pellets release water and volatiles. As a result, there are fewer interactions and binding forces between the particles in the pellet as more voids grow inside and between them (Moriana et al., 2015). Pellet strength decreases due to a combination of particle bonding deterioration and wood polymer decomposition (Wang et al., 2020). The loss of lignin and other naturally occurring binders found in biomass can occur during the torrefaction process. Weaker pellet structures may arise from the removal of binders because they are essential for maintaining the cohesiveness of biomass particles during pelletization. High temperatures during torrefaction can cause biomass particles to become more brittle and prone to fragmentation. This can result in pellets with uneven densities and reduced overall hardness (Çetinkaya et al., 2024; Haykiri-Acma & Yaman, 2022; Lima et al., 2023).

a) Analysis of results for pellet hardness optimization

Pellet hardness is a desirable property of pellets when it is high. Therefore, the larger the better criterion was used to optimize the design parameters. Signal-to-noise (S/N) ratios were used to identify the optimal process parameter conditions for a pellet hardness using the Taguchi method.

The response table for signal-to-noise ratio and means was presented in Appendix 8 (b) and Appendix 8 (c) respectively. The optimal level setting for parameters that lead to higher hardness was illustrated in Figure 4.25. The main effect plots for S/N ratios (Figure 4.25) showed that optimal parameter level settings for higher hardness, were $X1_5X2_1X3_1$.

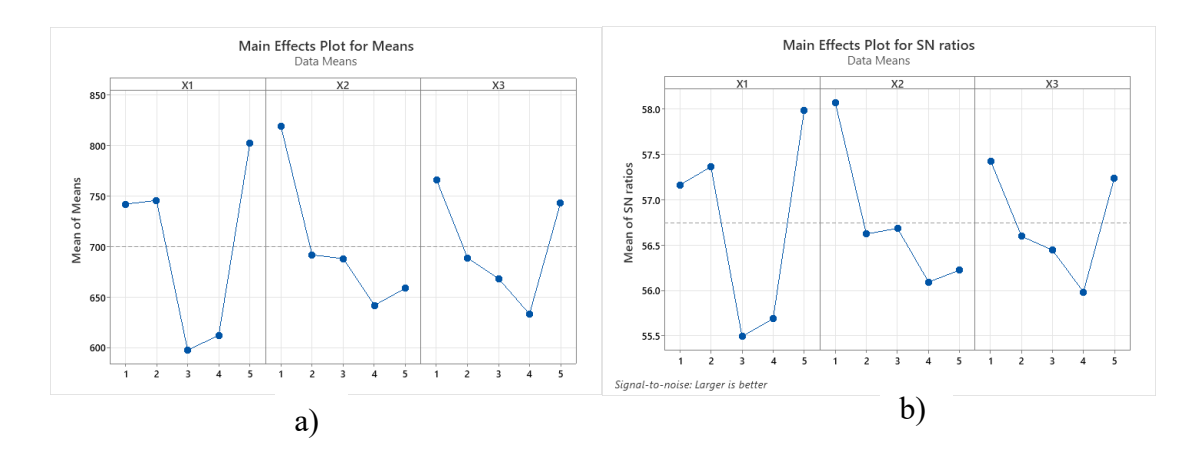


Figure 4.25 Response graph for main effects plot for, a) means and b) SN ratios for pellet hardness

ANOVA table (Table 4.16) was used to identify the significant design parameters for pellet hardness. Figure 4.26 displays a Pareto chart that illustrates the statistical significance of the parameters influencing pellet hardness. The two most significant design parameters for the optimum pellet hardness quality features (Figure 4.26) were linear low density polyethylene ratio and torrefaction temperature; corn stover to eucalyptus sawdust ratio had the least impact.

ruste 1.16 rinarysis of variance of penet naraness					
Source	DF	Adj SS	Adj MS	F-Value	P-Value
Regression	3	73446	24482.0	1.26	0.315
X1	1	90	90.1	0.00	0.946
X2	1	68179	68179.1	3.50	0.075
X3	1	5177	5176.7	0.27	0.612
Error	21	409174	19484.5		
Total	24	482620			

Table 4.16 Analysis of Variance of pellet hardness

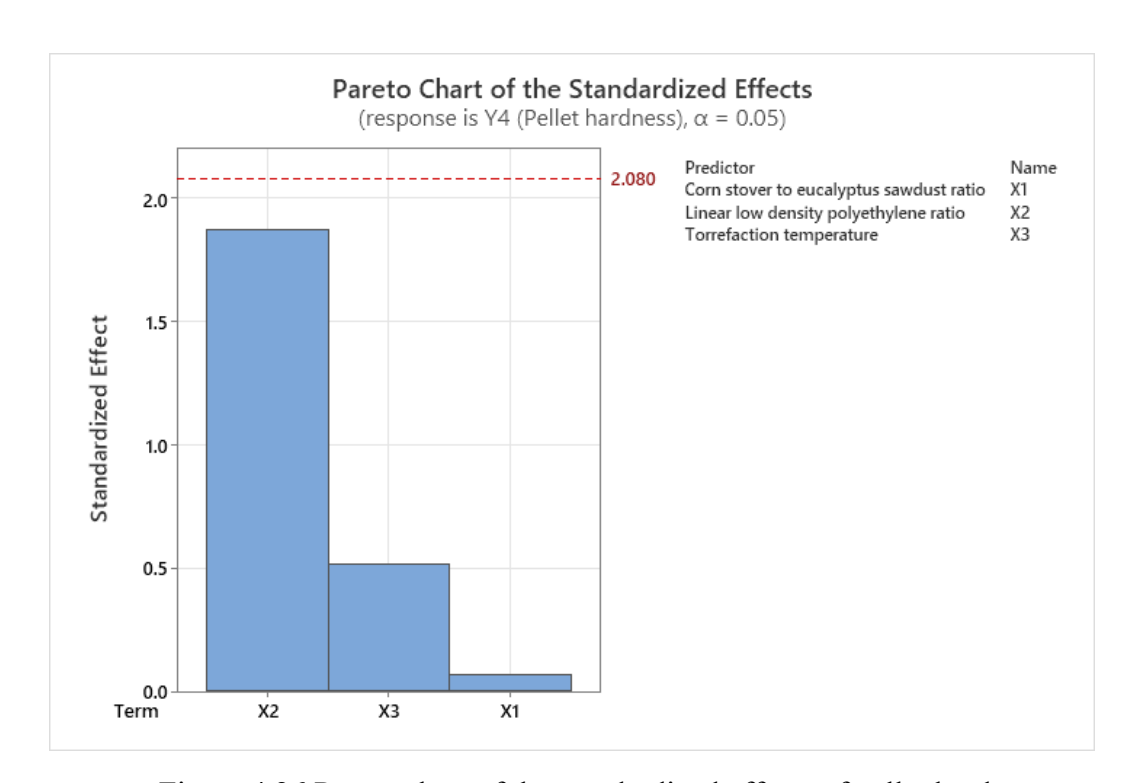


Figure 4.26 Pareto chart of the standardized effects of pellet hardness

b) Multivariable linear regression model for pellet hardness

The relationship between the input parameters; linear low-density polyethylene, torrefaction temperature, and corn stover to eucalyptus sawdust ratio and the pellet hardness was demonstrated by the Equation 4.7. The summary statistics for the model were displayed in the Table 4.17 below. Figure 4.27 illustrates the standardized residuals plot. The plots were, as can be observed, centered around the straight line, indicating a very good fit between the pellets' hardness and the multivariable linear regression model. The fact that the residuals fall between -3 and 3 further supports the suitability of the fitted model. The linear regression model's findings indicated that corn

stover: eucalyptus sawdust ratio, was the most important component contributing to pellet hardness. This was followed by torrefaction temperature and linear low-density polyethylene, in that order. In addition, the analysis provided by the pellet hardness response tables for the aforementioned means and signal-to-noise ratios, indicate a similarity with the analysis of the fitted model.

Regression Equation

Table 4.17 Model Summary statistics of pellet hardness

		•	•
S	R-sq	R-sq(adj)	R-sq(pred)
139.587	15.22%	3.11%	0.00%

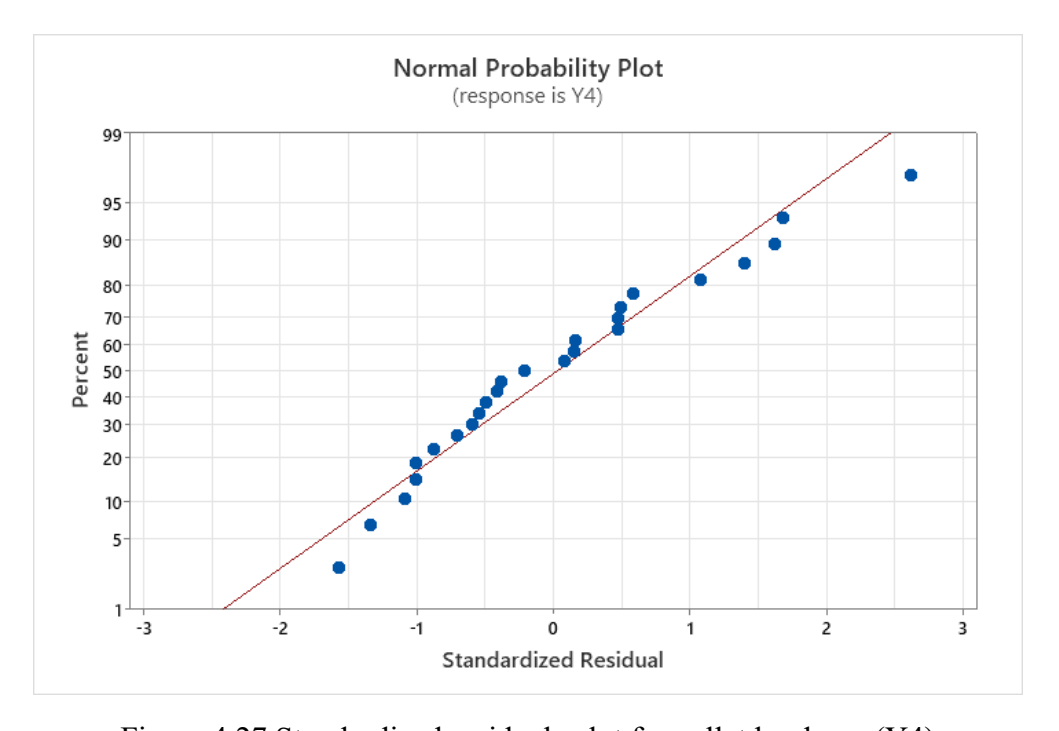


Figure 4.27 Standardized residuals plot for pellet hardness (Y4)

c) Analysis of contour and surface plots for pellet hardness

The link between the parameters of the blended pellet production process parameters and the pellet hardness was depicted by the contour plots and response surface plots, respectively, in Figure 4.28 and Figure 4.29. In these plots, the process parameters' median level, which was not taken into account in every situation, was 3.

In order to attain a high pellet hardness, blended pellets containing a 1:1 ratio of corn stover to eucalyptus sawdust and 2% linear low-density polyethylene should be considered, according to the results displayed in Figure 4.28 (a) and Figure 4.29 (a). Based on Figure 4.28 (b) and Figure 4.29 (b), it was discovered that high pellet hardness could be obtained by production of blended pellets at a 9:1 ratio of corn stover to eucalyptus sawdust and a 210°C torrefaction temperature. As seen in Figure 4.28 (c) and Figure 4.29 (c), the high pellet hardness values of the blended pellets could be achieved by using a 2% linear low density polyethylene binder and a 210°C torrefaction temperature during the blended pellet's production. The contour plots further demonstrate that, at the dark green region, the optimized blended pellet attained high pellet hardness of more than 780N.

a) Analysis of interactions of pellet hardness

Figure 4.30 below shows the pellet hardness interaction plot. The plot shows that the ratio of corn stover to eucalyptus sawdust and the percent ratio of linear low-density polyethylene interacted. For LLDPE, the maximum pellet hardness was observed at a ratio of 2%, whereas for corn stover to eucalyptus sawdust ratio, it was 9:1. In the same way, the torrefaction temperature and the corn stover to eucalyptus sawdust ratio interact, with the pellet hardness being maximized at a corn stover to eucalyptus sawdust ratio of 9:1 at 210°C torrefaction temperature. Additionally, at 2% LLDPE and a torrefaction temperature of 210°C, there was an interaction between the linear low-density polyethylene ratio and the torrefaction temperature that maximized pellet hardness.

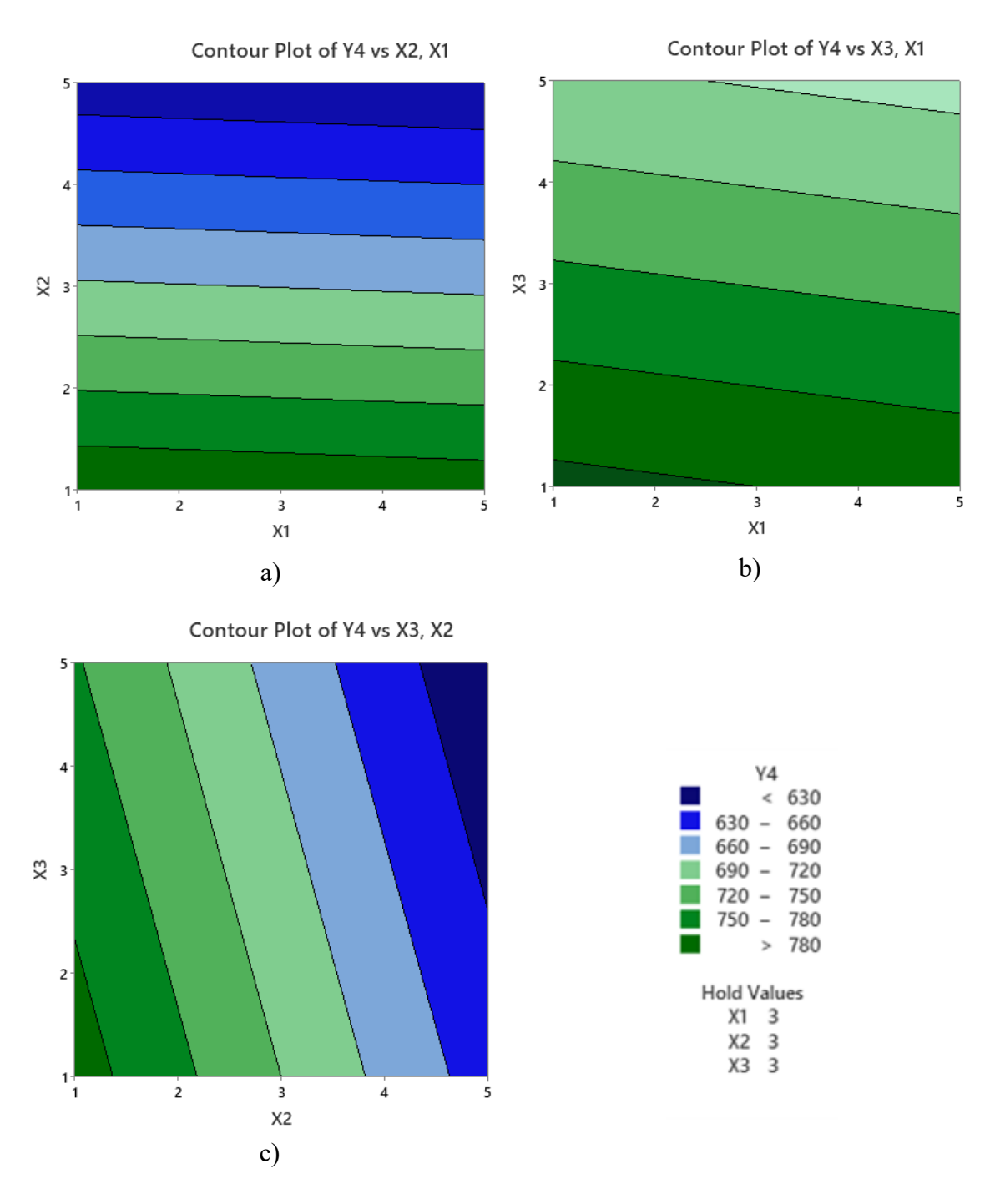
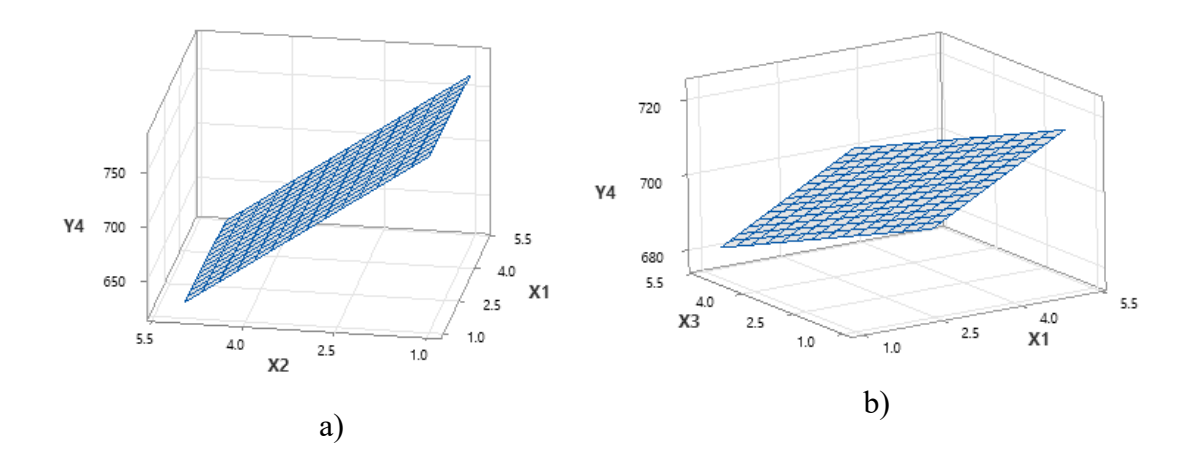


Figure 4.28 Contour plots for pellet hardness (Y4): a) corn stover to eucalyptus sawdust ratio (X1) vs linear low density polyethylene (X2), b) corn stover to eucalyptus sawdust ratio (X1) vs torrefaction temperature (X3), c) linear low-density polyethylene (X2) vs torrefaction temperature (X3).



Surface Plot of Y4 vs X3, X2

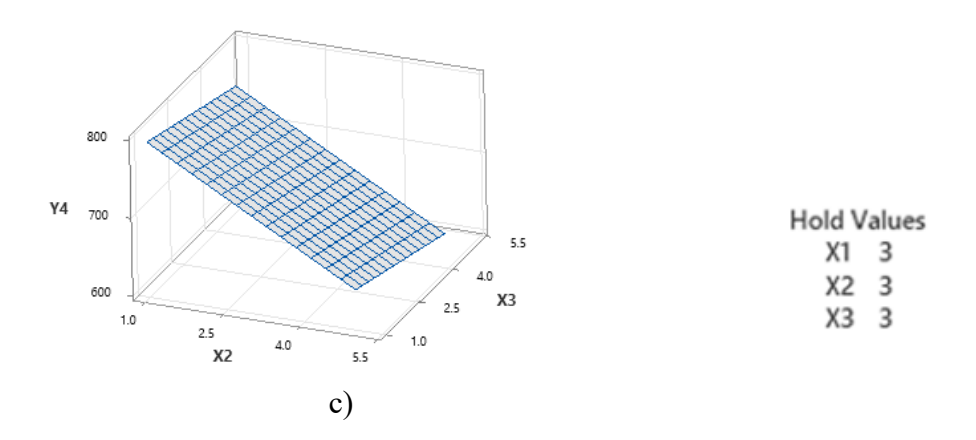


Figure 4.29 Response surface plots for pellet hardness (Y4): a) corn stover to eucalyptus sawdust ratio (X1) vs linear low density polyethylene (X2), b) corn stover to eucalyptus sawdust ratio (X1) vs torrefaction temperature (X3), c) linear low-density polyethylene (X2) vs torrefaction temperature (X3).

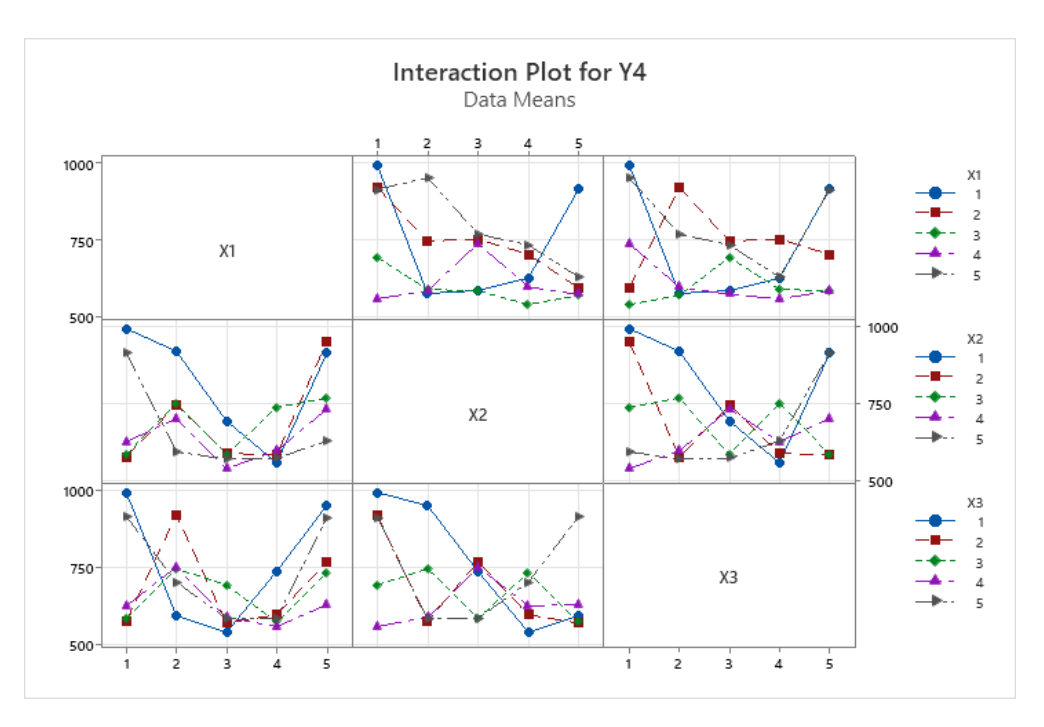


Figure 4.30 Interaction plot for pellet hardness (Y4)

4.5.3 Torrefaction yields

4.5.3.1 Mass yields

Wang et al. (2020) defined torrefaction as the process of thermally treating biomass to a specific holding or residence duration at 200–300°C in an inert or oxygen-depleted environment. The primary component of biomass materials, hemicellulose, is broken down during torrefaction due to depolymerization, demethoxylation, bond breakage, and condensation processes, which also remove moisture as well as some volatile matter. The net effect is mass loss. During the biomass torrefaction process, hemicellulose degradation is the main cause of the mass loss. Therefore, a measure of the extend of torrefaction is by mass loss and it is expressed as the ratio of the resultant mass after torrefaction to the initial mass before torrefaction. Some of the other reasons that lead to variations in mass yield as reported by Medic et al. (2012), Chen et al. (2017), Chen et al. (2015), Hu et al. (2018) and Yu et al. (2019) are as follows:

> The elimination of moisture from the biomass during torrefaction is one of the main causes of the lower mass yield. The moisture content of the biomass

- evaporates when it heats up, causing its mass to decrease. This mass loss results in a reduced mass yield even though it can increase the energy content of the biomass that is still left.
- Volatile organic compounds (VOCs) and other light components in the biomass are liberated as gases during the torrefaction process. Water vapour, organic acids, aldehydes, ketones, and terpenes are a few examples of these volatile compounds. The mass yield decreases overall as a result of the volatile components being lost during heating.
- ➤ Carbonation and char formation Char can arise from the partial carbonization of biomass materials at higher temperatures within the torrefaction range. This carbon-rich waste is a part of the initial biomass that is transformed into a more stable, carbonaceous form, which lowers the mass yield.
- Loss of ash content The amount of inorganic ash that is present in the biomass may also be removed by torrefaction, depending on the type of biomass feedstock. Usually composed of minerals and other inorganic substances, ash's reduction during torrefaction contributes to the mass yield's overall decrease.
- Incomplete torrefaction Higher mass losses can occasionally result from incomplete torrefaction processes or situations that are not optimal. Uneven heating, insufficient residence time, or incorrect temperature control are a few examples of factors that can cause biomass to be converted less effectively, resulting in greater mass losses.
- Particle size reduction Because of the heat treatment, biomass pellets may experience physical changes during torrefaction, such as fragmentation and shrinking. A perceived decrease in mass yield may also result from these modifications to particle size and structure, particularly when comparing the

mass of the original pellet with the mass of the torrefied product in the final stage.

From the experiment that was carried out in this research, the average mass yield was found to be 64.3365% in a range of 41.6183% and 98.0867% (Appendix 9 (a)). Most of the work done by researchers on post-pellet torrefaction reported varied outcomes of mass yields. This was strongly attributed to varied pellet composition and the methodology of torrefaction.

Some of the research that analyzed the mass loss are as follows. Three wood pellets were torrefied between 270 and 450°C in a fixed bed reactor by Peng et al. (2015), and found out that the mass yield was 70%. Shang et al. (2012) examined the characteristics of Scot pine pellets that had been torrefied between 230 and 270 degrees Celsius and reported that the mass yield was 58.1%. Ren et al. (2012) reported a mass yield of between 52.61–83.15% for microwave-assisted torrefied Douglas fir pellets.

Comparing the results obtained from torrefaction of blended corn stover and eucalyptus sawdust and those from published literature, it was seen that the mass yield was within the range with most of them.

a) Analysis of results for mass yield optimization

Signal-to-noise (S/ N) ratios were used to evaluate the optimum process parameters conditions for single pellet quality characteristics using Taguchi method. The higher the S/N ratio the minimum the effect of noise factors. The S/N ratios for different quality characteristics were calculated using Equation 2.3 and Equation 2.4. Taguchi method used the larger the better criteria for desirable pellet properties and the smaller the better criteria for undesirable properties.

The response table for signal-to-noise ratio and means for the main effects were presented in Appendix 9 (b) and Appendix 9 (c). The optimal level setting for parameters that lead to higher mass yield was depicted in Figure 4.31. The main effect plots for S/N ratios (Figure 4.31) showed that optimal parameter level settings for mass yield, were X1₂X2₃X3₂.

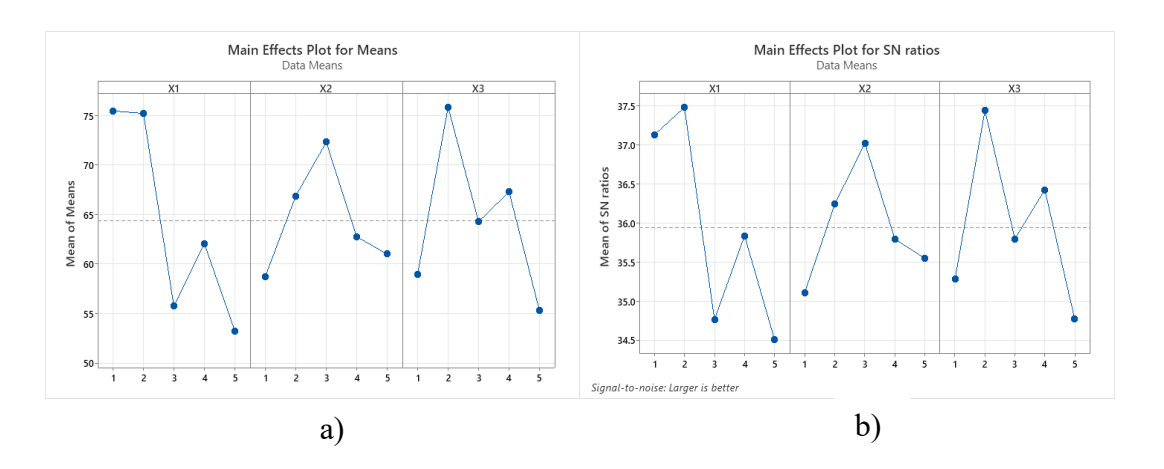


Figure 4.31 Response graph for main effects plot for, a) means and b) SN ratios for pellet mass yield

To determine the significant design parameters for pellet mass yield, an ANOVA table (Table 4.18) was developed. A Pareto chart showing the statistical significance of the factors affecting pellet mass yield is shown in Figure 4.32. The two most significant design parameters for the optimum pellet mass yield quality features (Figure 4.32) were corn stover to eucalyptus sawdust ratio and torrefaction temperature; linear low density polyethylene ratio had the least impact.

Table 4.18 Analysis of Variance for mass yield

•		•			
Source	DF	Adj SS	Adj MS	F-Value	P-Value
Regression	3	1785.95	595.32	3.24	0.043
X1	1	1658.60	1658.60	9.02	0.007
X2	1	0.07	0.07	0.00	0.984
X3	1	127.28	127.28	0.69	0.415
Error	21	3860.29	183.82		
Total	24	5646.25			

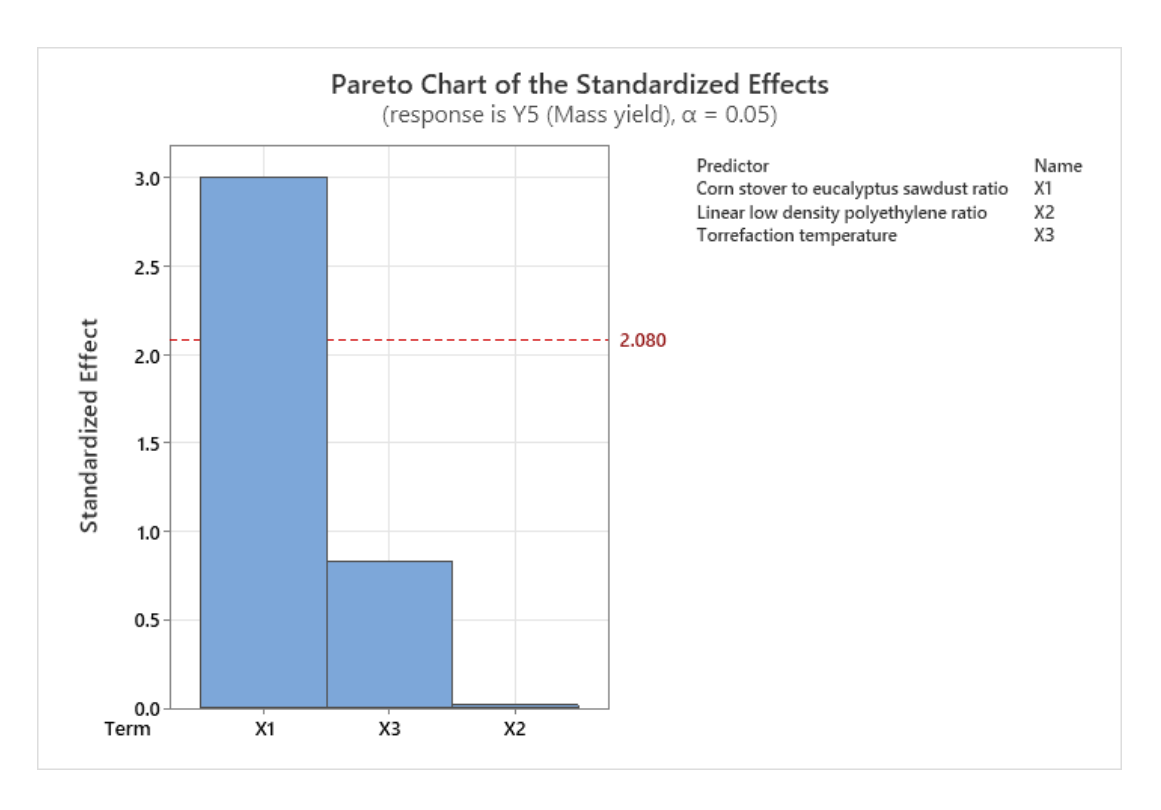


Figure 4.32 Pareto chart of the standardized effects of pellets' mass yields

b) Multivariable linear regression model for pellet mass yield

The relationship between the input parameters (corn stover to eucalyptus sawdust ratio, temperature of torrefaction, and linear low-density polyethylene) and the mass yield of pellets was demonstrated using Equation 4.8. The Table 4.19 below displays the summary statistics of the model. Figure 4.33 displays the standardized residuals plot. Plots were concentrated around the straight line, as illustrated, indicating a good fit between the mass yield value of the pellets and the multivariable linear regression model. The -3 to 3 range of the residuals provides additional support for the validity of the fitted model. The ratio of corn stover to eucalyptus sawdust was found to be the most significant factor determining pellet mass yield, according to the results of the linear regression model. Then followed the torrefaction temperature and linear low-density polyethylene, in that order. Along with the analysis provided by the pellet mass yield response tables for the previously presented means and signal to noise ratios, there was a similarity with the analysis of the fitted model.

Regression Equation

Table 4.19 Model Summary statistics for pellets mass yield

S	R-sq	R-sq(adj)	R-sq(pred)
11.5263	71.76%	43.53%	0.00%

c) Analysis of contour and surface plots for pellet mass yield

The contour plots and response surface plots in Figure 4.34 and Figure 4.35, respectively, showed the relationship between the parameters of the blended pellet production process and the pellet mass yield. The median level of the process parameters, which was not considered in every scenario, was 3 in these figures.

These results show that blended pellets with a 9:1 ratio of corn stover to eucalyptus sawdust and 10% linear low-density polyethylene should be considered in order to achieve a high pellet mass yield (Figure 4.34 (a) and Figure 4.35 (a)). Using a 9:1 ratio of corn stover to eucalyptus sawdust and a 210°C torrefaction temperature, it was shown that a high pellet mass yield could be achieved, based on Figure 4.34(b) and Figure 4.35 (b). Figure 4.34 (c) and Figure 4.35 (c) demonstrate how utilizing a 10% linear low density polyethylene binder and a 210°C torrefaction temperature during the blended pellet's fabrication could result in high pellet mass yield values. The contour plots also show that the optimized blended pellet achieved a high pellet mass yield of more than 75%, as indicated by the dark green zones.

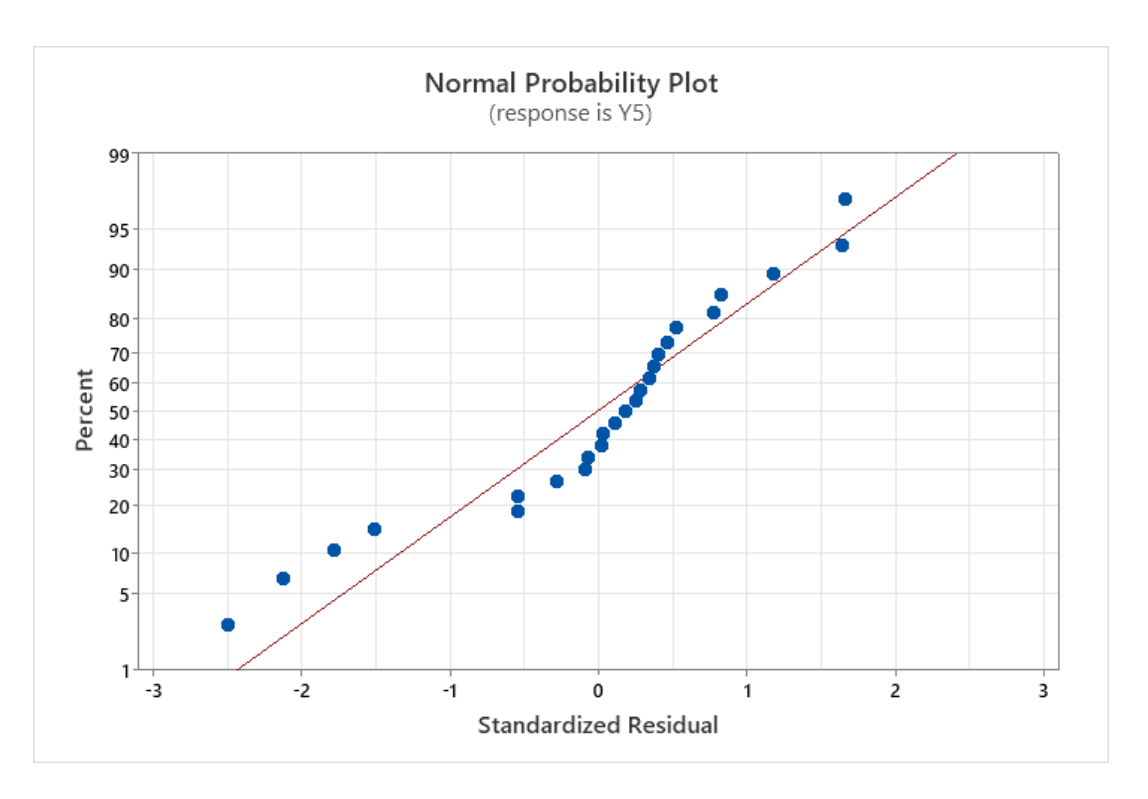


Figure 4.33 Standardized residuals plot for pellet mass yield

d) Analysis of interactions of mass yield

The pellet's mass yield interaction plot is depicted in Figure 4.36. The plot illustrates the interaction between the percent ratio of linear low-density polyethylene and the ratio of corn stover to eucalyptus sawdust. The maximum mass yield of pellets was observed at LLDPE and corn stover to eucalyptus sawdust ratio of 4% and 9:1, respectively. There was an interaction between the torrefaction temperature and the corn stover to eucalyptus sawdust ratio as well; at a torrefaction temperature of 230°C, the mass yield was maximum at a corn stover to eucalyptus sawdust ratio of 9:1. Furthermore, there was an interaction between the linear low density polyethylene ratio and the torrefaction temperature at 4% LLDPE and a 230°C torrefaction temperature that maximized the mass yield of pellets.

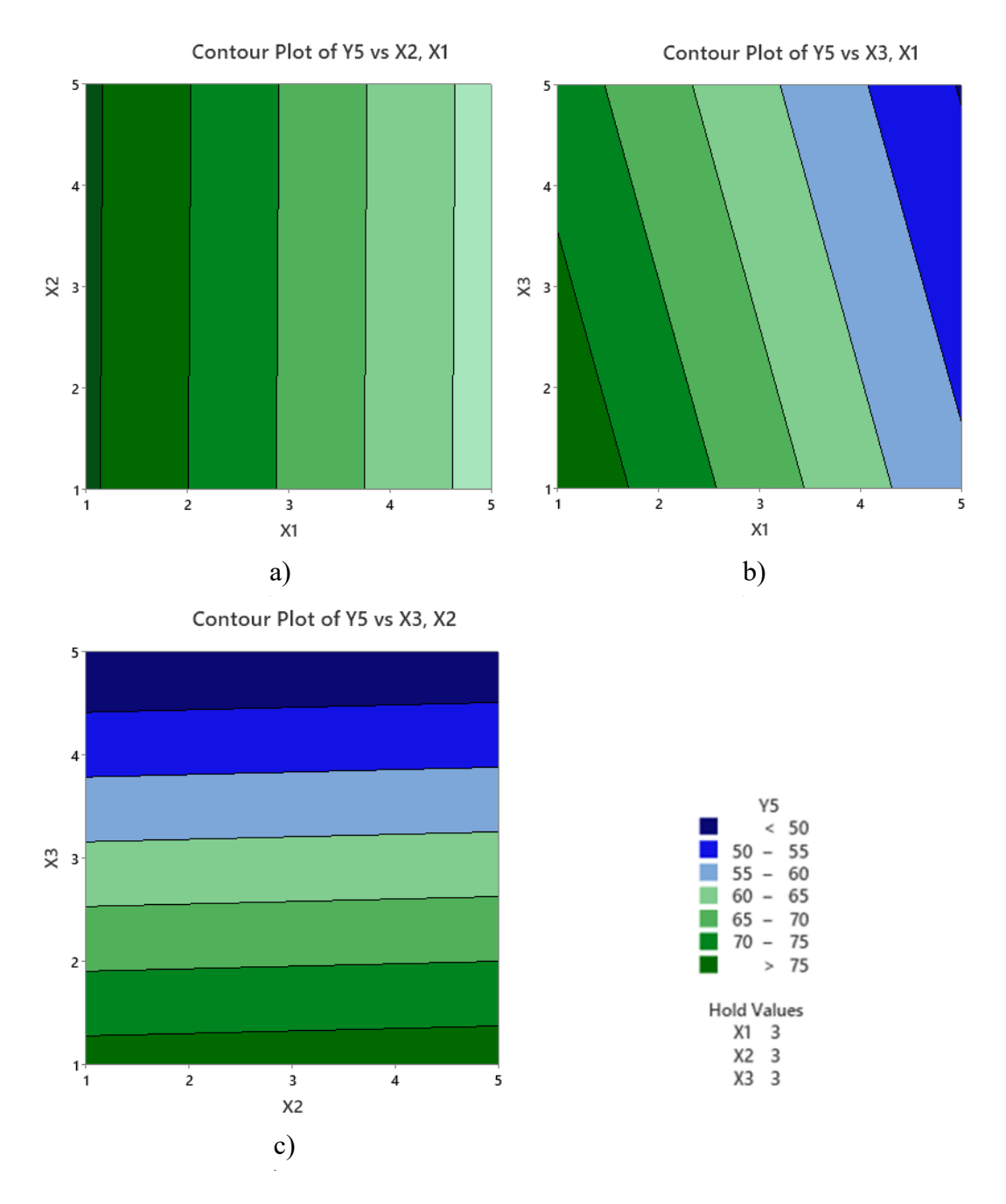
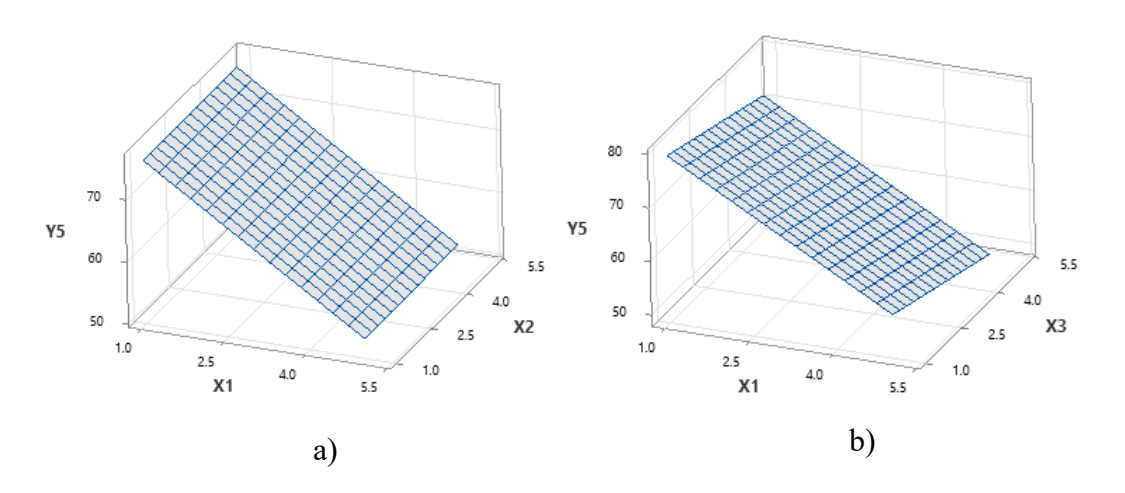


Figure 4.34 Contour plots for pellet mass yield (Y5): a) corn stover to eucalyptus sawdust ratio (X1) vs linear low-density polyethylene (X2), b) corn stover to eucalyptus sawdust ratio (X1) vs torrefaction temperature (X3), c) linear low density polyethylene (X2) vs torrefaction temperature (X3).



Surface Plot of Y5 vs X3, X2

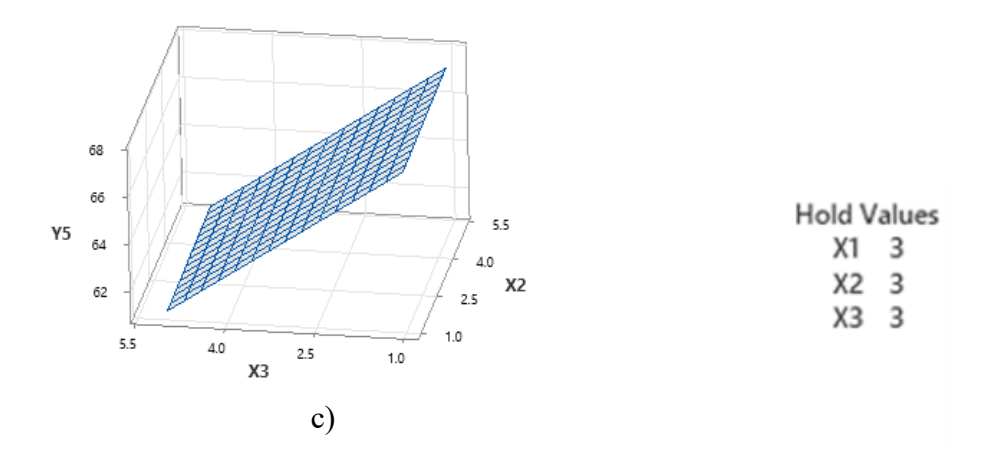


Figure 4.35 Response surface plots for pellet mass yield (Y5): a) corn stover to eucalyptus sawdust ratio (X1) vs linear low-density polyethylene (X2), b) corn stover to eucalyptus sawdust ratio (X1) vs torrefaction temperature (X3), c) linear low density polyethylene (X2) vs torrefaction temperature (X3).

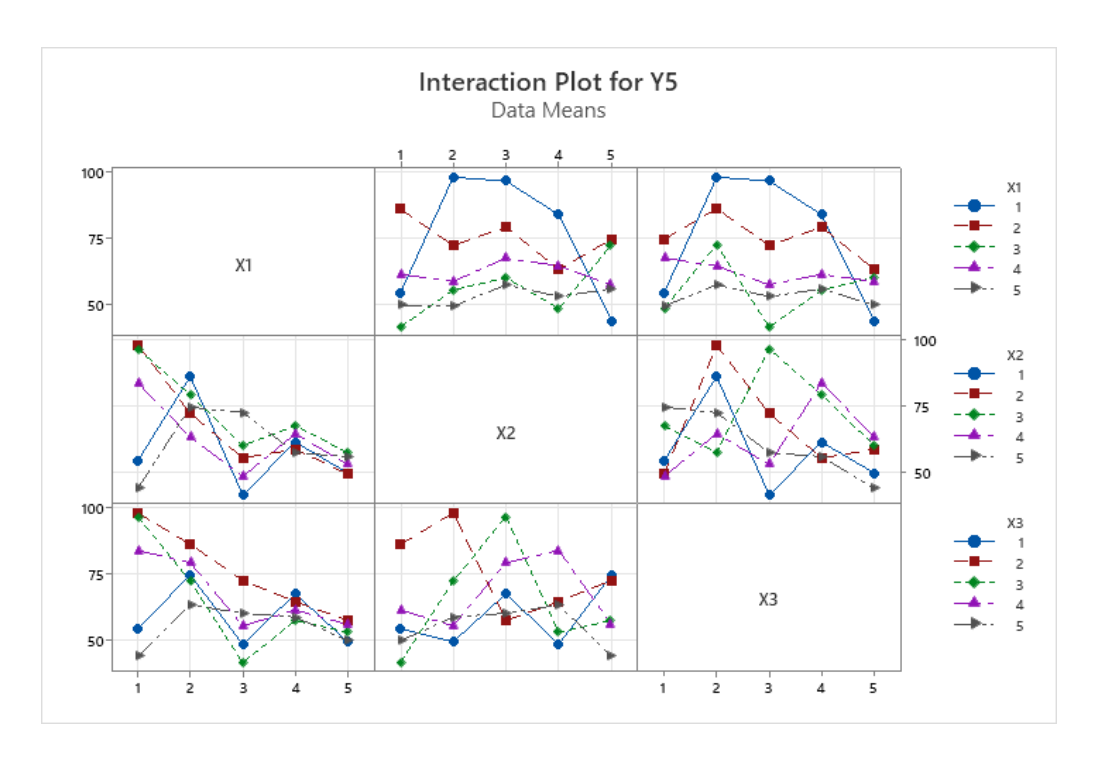


Figure 4.36 Interaction plots for pellet mass yield

4.5.4 Combustion properties

4.5.4.1 Higher heating value (HHV)

Appendix 10 (a) presents the results of HHV obtained after torrefaction of blended pellet produced from corn stover and eucalyptus sawdust using LLDPE as a binder. The mean HHV was found to be 26.7572 MJ/kg. This value was within the values of HHV obtained between 21.0767MJ/kg-31.1188MJ/kg in the given experimental runs. Considering the results obtained from characterization of corn stover and eucalyptus sawdust feedstocks, their mean HHV was 17.6550MJ/kg (raw feedstocks) and HHV obtained from torrefied pellet of 26.7572 MJ/kg, then the increase in HHV after torrefaction was 51.556%. This increase was also attributed to the LLDPE binder which has a HHV of about 41.3MJ/kg.

These results are in agreement with those from literature, which include the following: In the research on the torrefaction method as a pretreatment for corn stover and miscanthus biomass, Tumuluru et al. (2010) reported that when torrefied at 200–300°C,

the calorific value increases by roughly 20% to its initial value. According to Prasongthum et al. (2022) the HHV of the torrefied wood pellets rose by 38% over that of the original feedstock at 300 °C. Shang et al. (2012) examined the characteristics of Scot pine pellets that had been torrefied between 230 and 270 degrees Celsius and found out that the HHV rose from 18.37 to 24.34 MJ/kg. Shao et al. (2019) studied the effect of combined torrefaction and pelletization on particulate matter emissions from biomass pellet combustion and found that the heating value of the pellets increased by 8% to 28%. In general, apart from blending herbaceous biomass (corn stover) with woody biomass (eucalyptus sawdust) as well as addition of LLDPE as a blending material leading to increased heating value of pellets, torrefaction process also increases this property in several ways as discussed by (Isemin et al., 2017; Lunguleasa et al., 2019; Romyen et al., 2023) which include:

- ➤ Reduction in moisture content in that torrefaction removes moisture from biomass, reducing its moisture content significantly. As a result, the energy content per unit mass of the material increases since energy is no longer needed to vaporize the water during combustion.
- Reduction in volatile organic compounds, including hemicellulose and some lignin constituents, which are pushed out during the torrefaction process. This increases the calorific value since these compounds have a lower energy density than the carbon-rich residue that remains after torrefaction.
- Increased carbon content- When volatile molecules are driven out by the torrefaction process, a substance with a higher carbon concentration than in its original biomass form is left behind. The calorific value rises because carbon contains more energy per unit mass than other components in biomass, such as oxygen and hydrogen.

- ➤ Improved fuel characteristics- biomass undergoes changes in its chemical and physical characteristics due to torrefaction, including improved grindability, decreased hydrophilicity, and greater homogeneity. These alterations may result in increased heat transfer and combustion efficiency while burning, which would raise the effective calorific value even further.
- ➤ Reduced ash content and impurities- torrefaction can lower the biomass's ash content and mineral impurities, which might hinder combustion and lower the production of energy ultimately. Higher calorific value and improved combustion characteristics can result from a cleaner and more homogenous biomass material after torrefaction.

a) Analysis of results for higher heating value optimization

Signal-to-noise (S/ N) ratios were used to evaluate the optimum process parameters conditions for single pellet quality characteristics using Taguchi method. The higher the S/N ratio the minimum the effect of noise factors. The S/N ratios for different quality characteristics were calculated using Equation 2.3 and Equation 2.4. Taguchi method used the larger the better criteria for desirable pellet properties and the smaller the better criteria for undesirable properties.

The response table for signal-to-noise ratio and means was presented in Appendix 10 (b) and Appendix 10 (c) respectively. The optimal level setting for parameters that leads to greater higher heating value was illustrated in Figure 4.37. The main effect plots for S/N ratios (Figure 4.37) showed that optimal parameter level settings for greater higher heating value, were: X1₁X2₄X3₁.

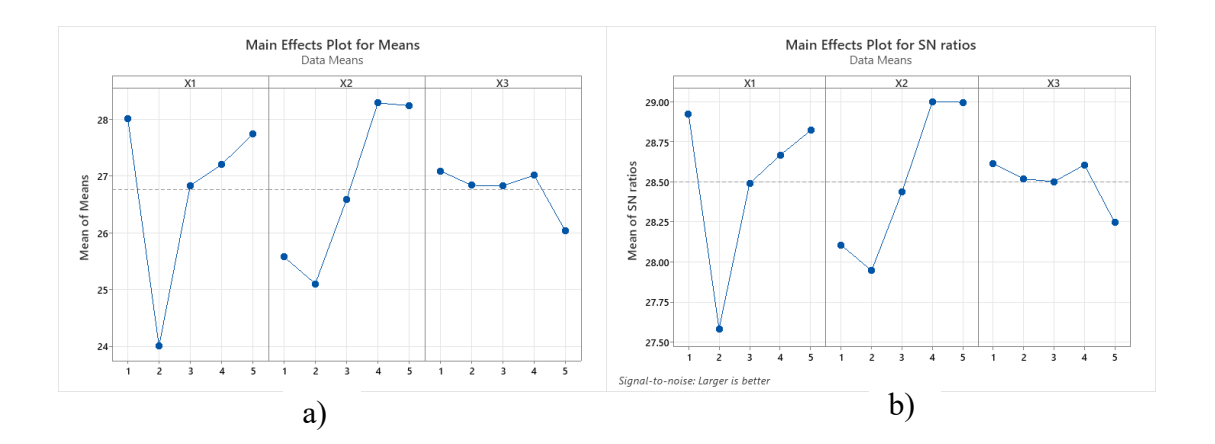


Figure 4.37 Response graph for main effects plot for, a) means and b) SN ratios for pellet higher heating values

To determine the significant design parameters for pellet higher heating value, an ANOVA table (Table 4.20) was developed. A Pareto chart showing the statistical significance of the factors affecting pellet HHV is shown in Figure 4.38. The two most significant design parameters for the optimum higher heating values quality features (Figure 4.38) were linear low-density polyethylene ratio and corn stover to eucalyptus sawdust ratio; torrefaction temperature had the least impact.

Table 4.20 Analysis of Variance pellet higher heating values

Source	DF	Adj SS	Adj MS	F-Value	P-Value
Regression	3	41.580	13.860	1.81	0.176
X1	1	3.494	3.494	0.46	0.507
X2	1	36.196	36.196	4.73	0.041
X3	1	1.890	1.890	0.25	0.625
Error	21	160.830	7.659		
Total	24	202.410			

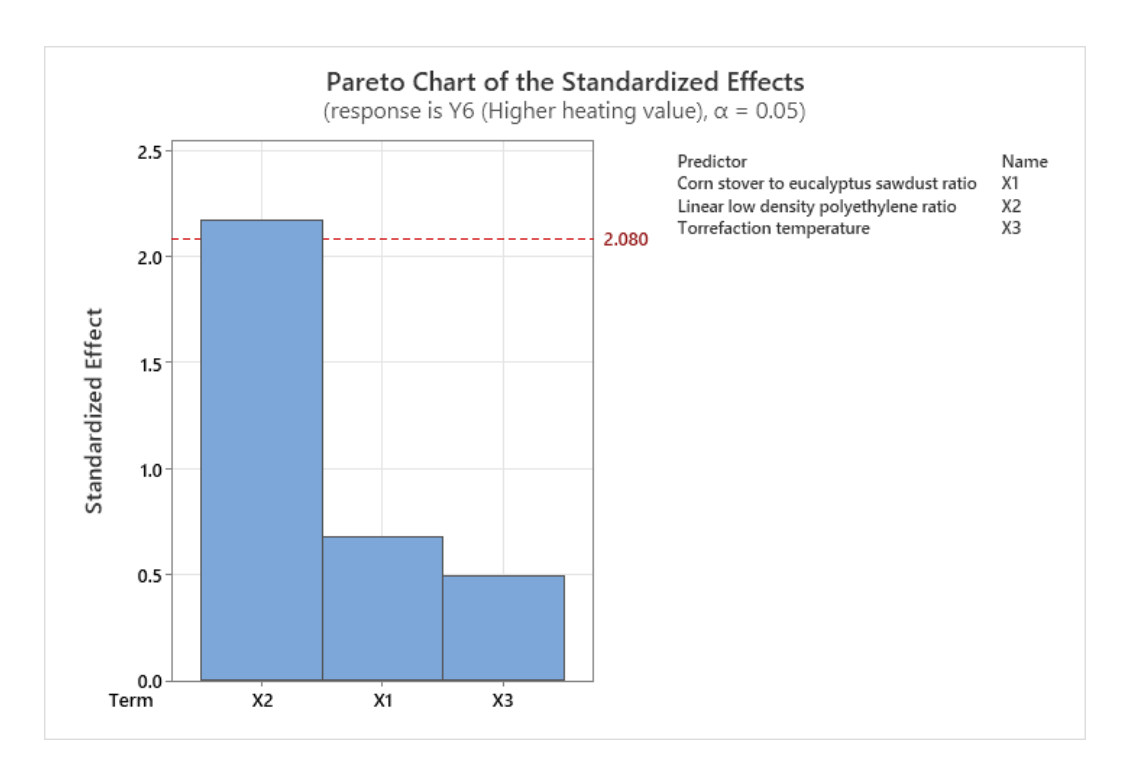


Figure 4.38 Pareto chart of the standardized effects of pellet higher heating values

b) Multivariable linear regression model for pellet higher heating value

Equation 4.9 revealed the correlation between the input parameters (corn stover to eucalyptus sawdust ratio, torrefaction temperature, and linear low-density polyethylene) and the pellet higher heating value. The model's summary statistics were shown in the Table 4.21 below. The standardized residuals plot was shown in Figure 4.39. As has been shown, the plots were oriented around the straight line, suggesting that the multivariable linear regression model and the higher heating value of the pellets have a good fit. The residuals' range of -3 to 3 adds more evidence to the fitted model's validity. The results of the linear regression model showed that the most significant factor influencing pellet higher heating value was linear low-density polyethylene. Then followed by corn stover to eucalyptus sawdust ratio and torrefaction temperature, in that sequence. There was a similarity with the analysis of the fitted model in addition to the analysis given by the pellet higher heating value response tables for the previously indicated means and signal-to-noise ratios.

Regression Equation

Table 4.21 Model Summary statistics for higher heating values

S	R-sq	R-sq(adj)	R-sq(pred)
2.76741	20.54%	9.19%	0.00%

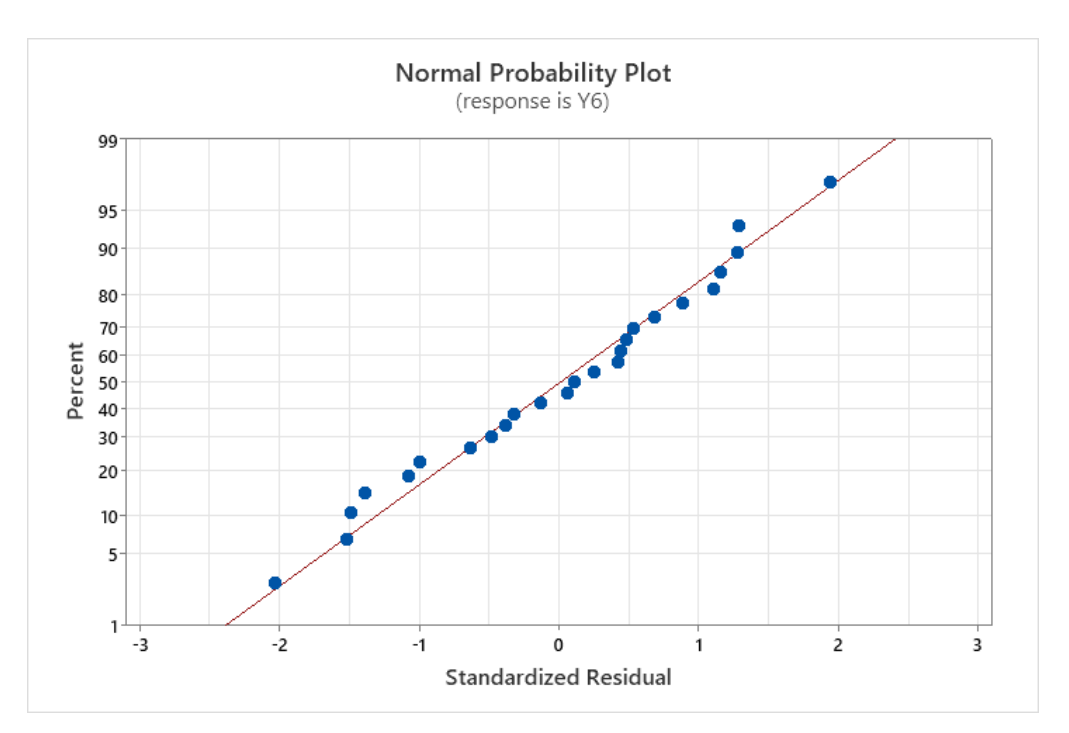


Figure 4.39 Standardized residuals plot for HHV c) Analysis of contour and surface plots for pellet higher heating value

The relationship between the parameters of the blended pellet production process and the pellet higher heating value was depicted by the contour plots and response surface plots in Figure 4.40 and Figure 4.41, respectively. These results show that the median level of the process parameters, which was not taken into account in every scenario, was 3.

These findings indicate that in order to attain a high pellet HHV, blended pellets with a 1:1 ratio of corn stover to eucalyptus sawdust and 10% linear low-density polyethylene should be taken into consideration (Figure 4.40 (a) and Figure 4.41 (a)). Based on Figure 4.40 (b) and Figure 4.41 (b), it was demonstrated that a high HHV could be

attained using a 1:1 ratio of corn stover to eucalyptus sawdust and a 210°C torrefaction temperature. High pellet HHV values could result from using a 10% linear low-density polyethylene binder and a 290°C torrefaction temperature during the blended pellet's manufacturing, as shown in Figure 4.40 (c) and Figure 4.41 (c). Also, the optimized blended pellet produced a high HHV of greater than 28MJ/kg at the dark green regions in the contour plots.

d) Analysis of the interaction of higher heating values

Figure 4.42 below shows the interaction plot of the pellet's higher heating values. The interaction plot shows how the ratio of corn stover to eucalyptus sawdust interacts with the percent ratio of linear low-density polyethylene. The maximum pellet's higher heating values were recorded at a corn stover to eucalyptus sawdust ratio of 1:1 and an LLDPE ratio of 8%, respectively. Additionally, there was an interaction between the corn stover to eucalyptus sawdust ratio and the torrefaction temperature; at a corn stover to eucalyptus sawdust ratio of 1:1, the higher heating values reached their maximum at a torrefaction temperature of 250°C. Additionally, the higher heating values of pellets were maximized by an interaction between the linear low density polyethylene ratio and the torrefaction temperature at 8% LLDPE and a 250°C torrefaction temperature respectively.

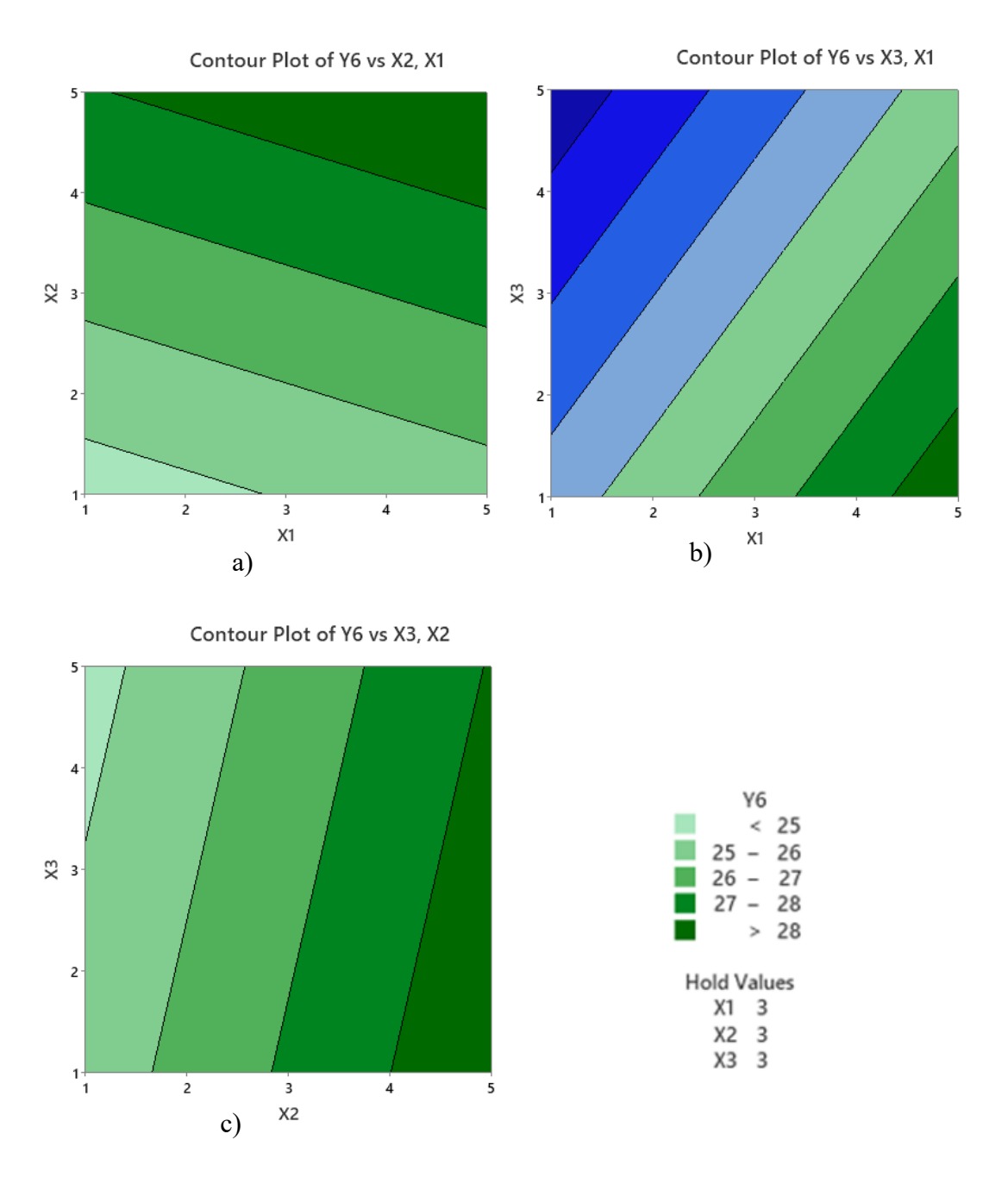
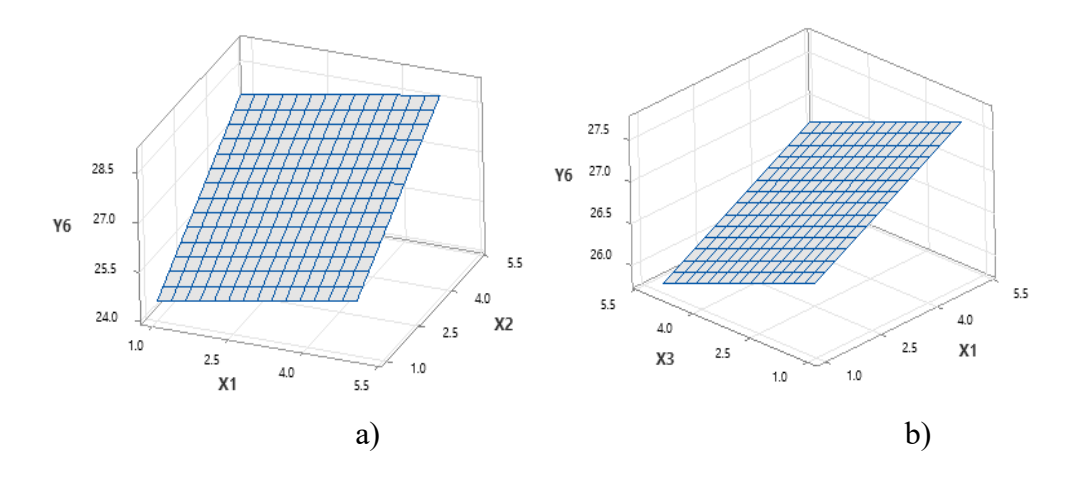


Figure 4.40 Contour plots for pellet higher heating value (Y6): a) corn stover to eucalyptus sawdust ratio (X1) vs linear low-density polyethylene (X2), b) corn stover to eucalyptus sawdust ratio (X1) vs torrefaction temperature (X3), c) linear low density polyethylene (X2) vs torrefaction temperature (X3).



Surface Plot of Y6 vs X3, X2

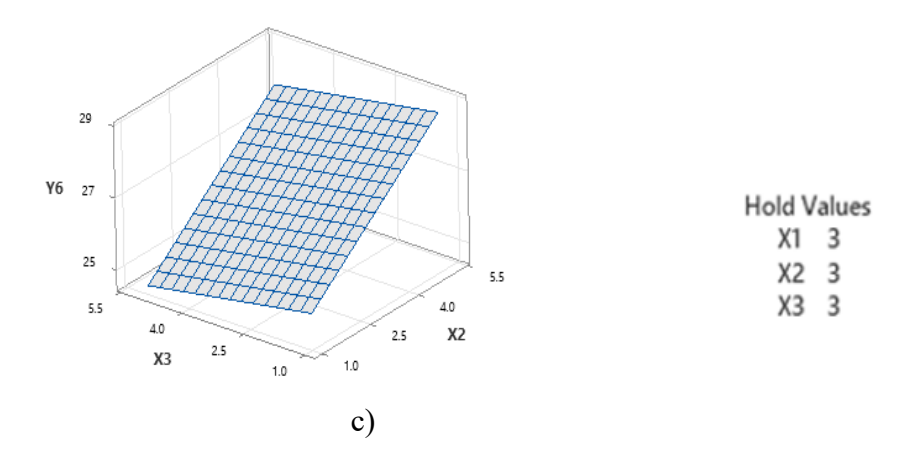


Figure 4.41 Response surface plots for pellet higher heating value (Y6): a) corn stover to eucalyptus sawdust ratio (X1) vs linear low-density polyethylene (X2), b) corn stover to eucalyptus sawdust ratio (X1) vs torrefaction temperature (X3), c) linear low density polyethylene (X2) vs torrefaction temperature (X3).

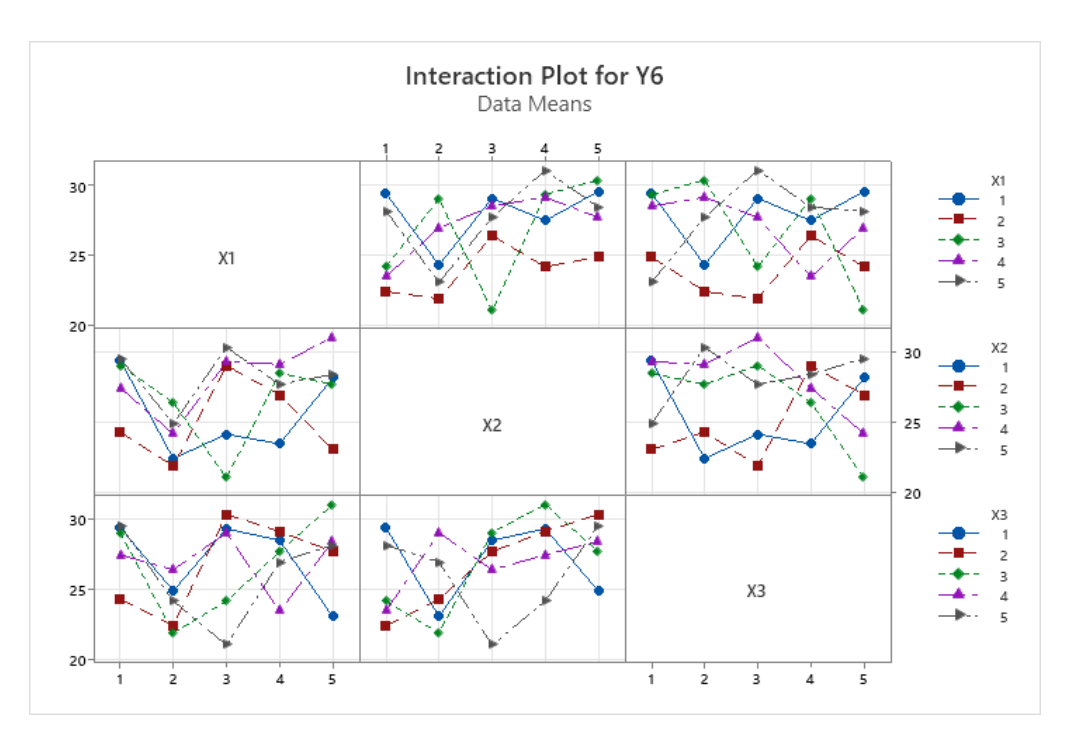


Figure 4.42 Interaction plots for HHV

4.5.5 Emissions analysis

The kind of emissions examined in this study was carbon dioxide. The results of carbon dioxide emissions are presented in Appendix 11 (a). The blended torrefied pellets had a mean CO₂ of 3.07%, with maximum and minimum CO₂ values of 6.91% and 1.15%, respectively.

Ndibe et al. (2014) concluded that the percentage of carbon dioxide emissions from the combustion of torrefied biomass pellets can vary depending on several factors such as the type of biomass feedstock, the torrefaction process, combustion efficiency, and any emissions control technologies in place. Furthermore, Choiński et al. (2023), also made a conclusion that carbon dioxide emissions are not regulated and that comparisons can simply be made with the common emission levels for wood pellets. However, generally speaking, the combustion of torrefied biomass pellets typically results in lower carbon dioxide emissions compared to traditional fossil fuels like coal or natural gas.

Shen et al. (2012) found that the emissions of carbon monoxide, organic carbon, elemental carbon, and particulate matter from the combustion of biomass pellets were significantly lower than those from raw fuels but did not provide specific data on carbon dioxide emissions. Ndibe et al. (2014) did not directly address carbon dioxide emissions from torrefied biomass pellets, focusing instead on combustion reactivity and emissions of other pollutants. Therefore, the specific percentage of carbon dioxide emissions from the combustion of torrefied biomass pellets remains unclear and may require further research. Carbon dioxide emissions from previous studies are highly varied and depend on factors highlighted by Rokni et al. (2018), Wei et al. (2012) and Ren et al. (2017) which include the following:

- The amount of energy and the chemical composition of the biomass can be affected by the degree of torrefaction, which is influenced by temperature, residence time, and environment during treatment. The quantity of volatile matter, fixed carbon, and ash content in the torrefied biomass can vary depending on the torrefaction conditions, which can impact CO₂ emissions during combustion.
- ➤ The kind of feedstock and its place of origin affect the amount of carbon in biomass. The carbon contents of various biomass sources, such as wood, agricultural residue, and energy crops, vary, and this has a direct impact on the amount of CO₂ emitted during combustion.
- Emission levels and combustion efficiency are influenced by the amount of oxygen present in torrefied biomass. When compared to untreated biomass, torrefied biomass with a reduced oxygen content can burn more completely and emit less CO₂.

- ➤ The amount of moisture in biomass influences the generation of heat and combustion efficiency. Because torrefied biomass usually has less moisture than raw biomass, it burns more efficiently and might emit less CO₂ per unit of energy produced.
- The kind of technology utilized for combustion (such as gasification, fluidized bed, or grate furnace) can affect the residence times, conditions under which CO₂ and other pollutants are released, and the final amount of emissions. Reducing CO₂ emissions can be achieved with the use of optimized combustion methods made for torrefied biomass.

a) Analysis of results for carbon dioxide emissions optimization

A high carbon dioxide emission is not a desired quality in pellets. Therefore, the smaller is better criterion was used to optimize the design parameters. Using the Taguchi approach, the optimal process parameter conditions for carbon dioxide emissions were determined by analyzing the main effects plots for means.

Appendix 11 (b) and Appendix 11 (c) provide the response table for the signal-to-noise ratio and means respectively for carbon dioxide emissions. The optimal level setting for parameters that lead to lower amounts of carbon dioxide emissions was depicted in Figure 4.43. The main effect plots for S/N ratios (Figure 4.43) showed that optimal parameter level settings for lower carbon dioxide emissions, were X1₁X2₂X3₃.

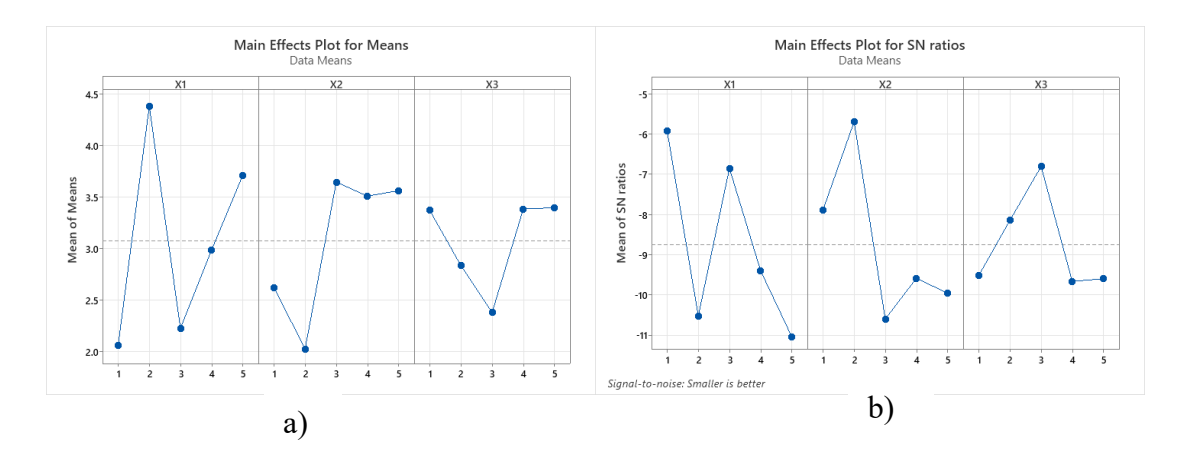


Figure 4.43 Response graph for main effects plot for, a) means and b) SN ratios for carbon dioxide emissions

The ANOVA table (Table 4.22) was employed to determine the significance of the design parameters for carbon dioxide emissions. In the Pareto chart (Figure 4.44), it can be seen that the ratio of linear low-density polyethylene, corn stover to eucalyptus sawdust ratio and the torrefaction temperature, were the design characteristics that were shown to be significant for the optimal carbon dioxide emissions, arranged in descending order.

Table 4.22 Analysis of Variance for carbon dioxide emissions

Source	DF	Adj SS	Adj MS	F-Value	P-Value
Regression	3	7.6904	2.5635	1.02	0.404
X1	1	1.8374	1.8374	0.73	0.402
X2	1	5.6717	5.6717	2.26	0.148
X3	1	0.1812	0.1812	0.07	0.791
Error	21	52.7843	2.5135		
Total	24	60.4746			

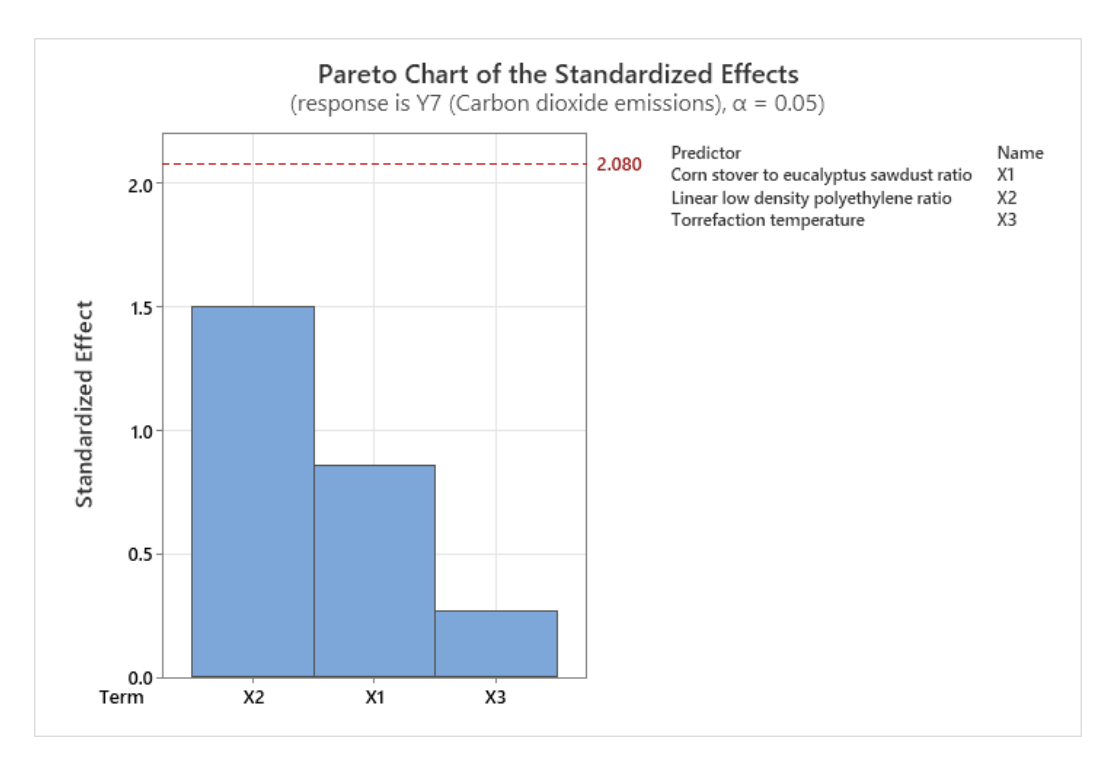


Figure 4.44 Pareto chart of the standardized effects of carbon dioxide emissions.

b) Multivariable linear regression model for carbon dioxide emissions

Equation 4.10 showed the link between the input parameters (corn stover to eucalyptus sawdust ratio), linear low-density polyethylene, and torrefaction temperature) and carbon dioxide emissions, while Table 4.23 presents it model summary statistics. The plot of the standardized residuals is shown in Figure 4.45. As can be seen, the plots were centered around the straight line, suggesting that the multivariable linear regression model and carbon dioxide emissions of the pellets fit each other quite well. The residuals' range of -3 to 3 adds more evidence to the fitted model's appropriateness. The results of the linear regression model showed that the most significant factor influencing carbon dioxide emissions from the combustion of the blended pellet was linear low-density polyethylene. Then followed by the ratio of corn stover to eucalyptus sawdust and torrefaction temperature, in that sequence. There is a similarity with the analysis of the fitted model in addition to the analysis given by the carbon dioxide

emissions from response tables for the previously indicated means and signal-to-noise ratios.

Regression Equation

Table 4.23 Model Summary statistics for carbon dioxide emissions

S	R-sq	R-sq(adj)	R-sq(pred)
1.58541	12.72%	0.25%	0.00%

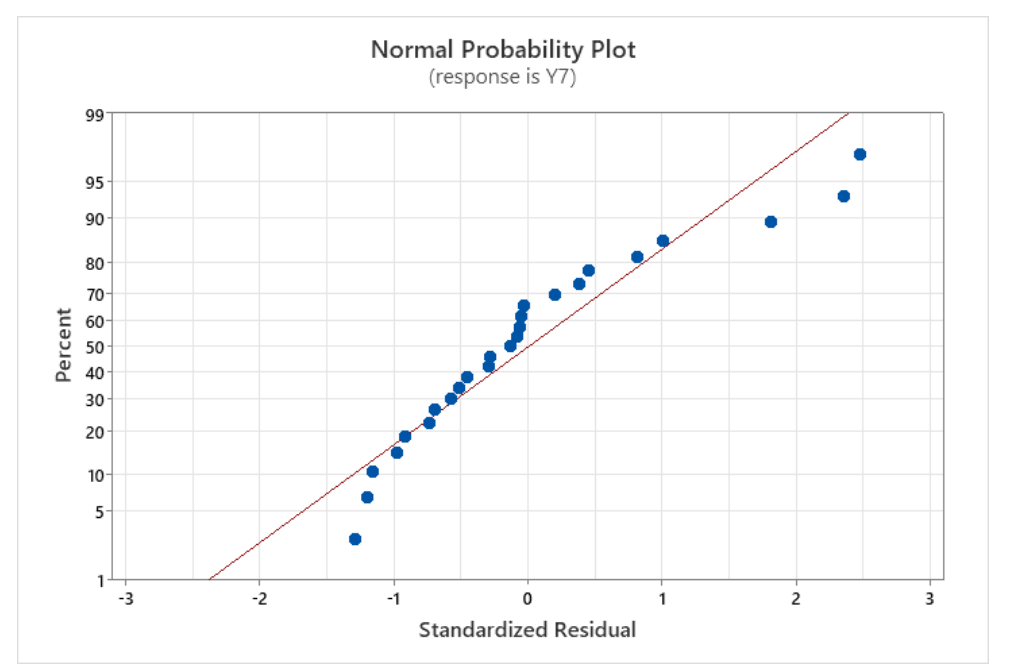


Figure 4.45 Standardized effects plot of residuals for carbon dioxide emissions

c) Analysis of contour and surface plots for carbon dioxide emissions

Figure 4.46 and Figure 4.47 show the contour plots and response surface plots, respectively, that describe the link between the carbon dioxide emissions of the fabricated pellet and the process parameters of the blended pellet production. Process parameters, which were retained at the median level in this instance was three, were not taken into account for all of the cases.

Figure 4.46 (a) and Figure 4.47 (a) demonstrate that in order to achieve minimal carbon dioxide emissions, blended pellets should be produced using 2% linear low density

polyethylene and a corn stover to eucalyptus sawdust ratio of 9:1. It was discovered from Figure 4.46 (b) and Figure 4.47 (b) that creating blended pellets with a 9:1 corn stover to eucalyptus sawdust ratio and a 210°C torrefaction temperature resulted in reduced carbon dioxide emissions. It was noted in Figure 4.46 (c) and Figure 4.47 (c) that the blended pellet's reduced carbon dioxide emissions could be achieved by using a 2% linear low density polyethylene binder and a 210°C torrefaction temperature. The contour plots, which show the light green and blue zones, also demonstrate that the optimized blended pellet achieved carbon dioxide emissions of less than 2.5 percent.

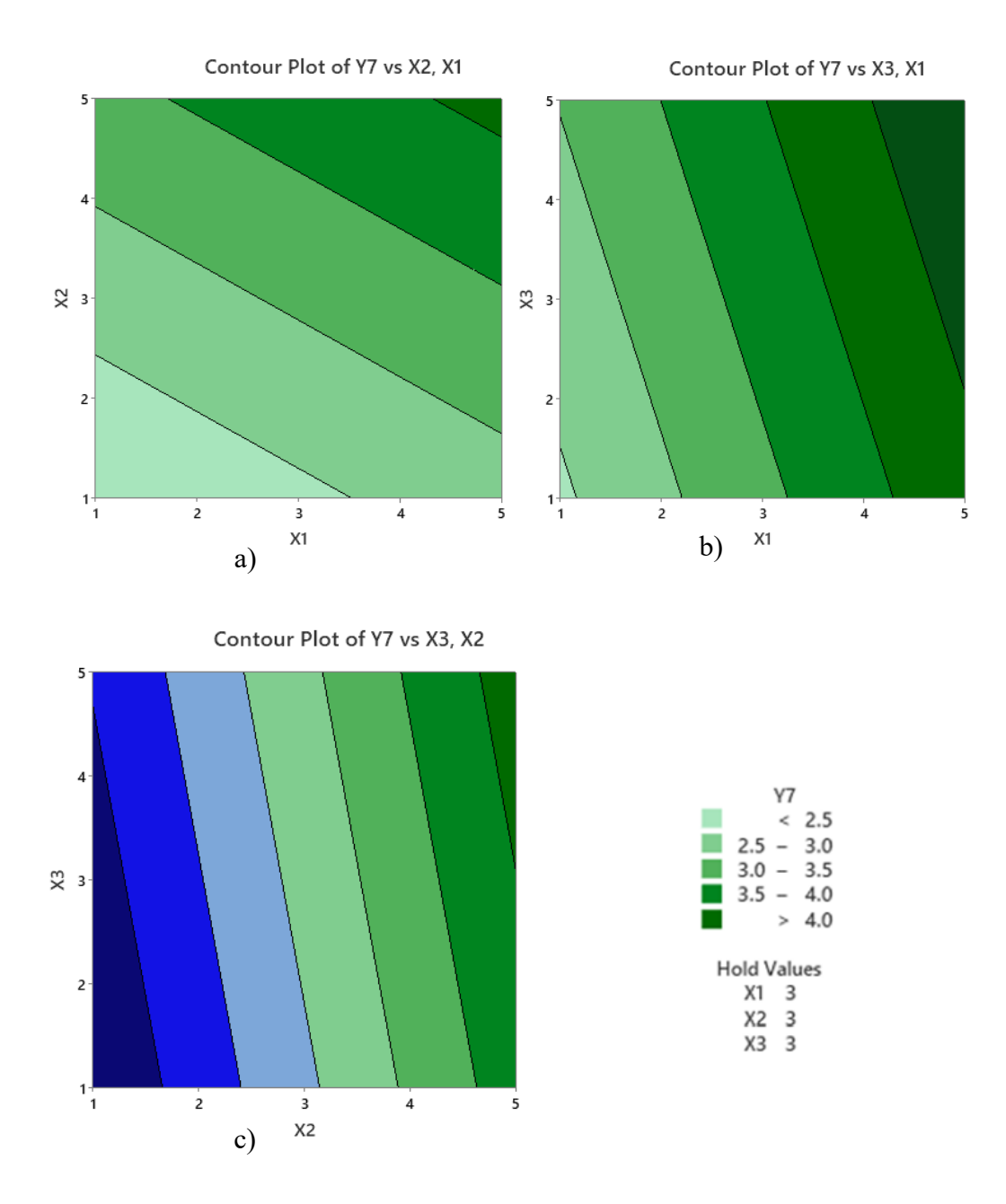
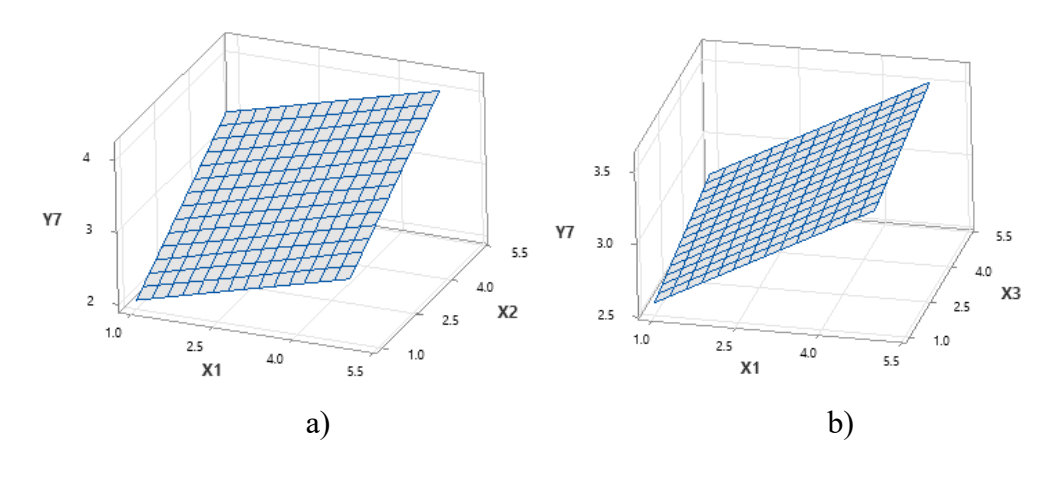


Figure 4.46 Contour plots for carbon dioxide emissions (Y7): a) corn stover to eucalyptus sawdust ratio (X1) vs linear low-density polyethylene (X2), b) corn stover to eucalyptus sawdust ratio (X1) vs torrefaction temperature (X3), c) linear low density polyethylene (X2) vs torrefaction temperature (X3).



Surface Plot of Y7 vs X3, X2

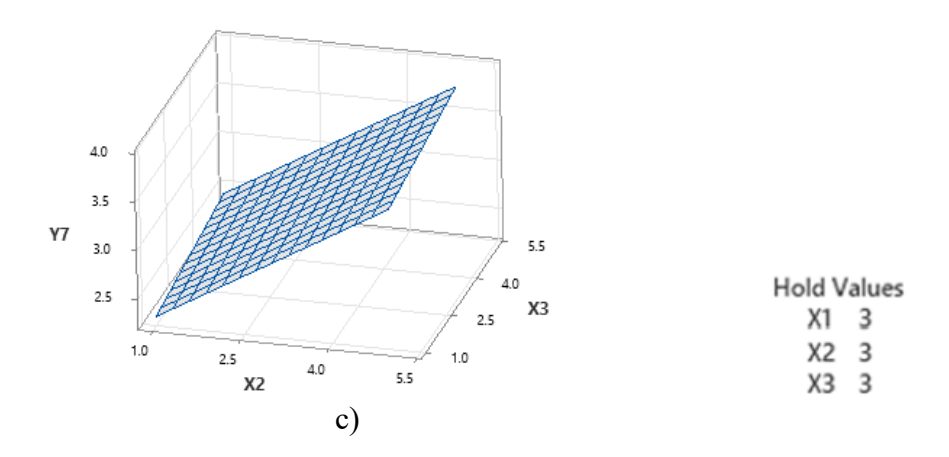


Figure 4.47 Response surface plots for carbon dioxide emissions (Y7): a) corn stover to eucalyptus sawdust ratio (X1) vs linear low-density polyethylene (X2), b) corn stover to eucalyptus sawdust ratio (X1) vs torrefaction temperature (X3), c) linear low density polyethylene (X2) vs torrefaction temperature (X3).

d) Analysis of the interaction of carbon dioxide emissions

Figure 4.48 below shows the interaction plot of the pellet's carbon dioxide emissions. The interaction plot shows how the ratio of corn stover to eucalyptus sawdust interacts with the ratio of linear low-density polyethylene. The maximum pellet's carbon dioxide

emissions were recorded at a corn stover to eucalyptus sawdust ratio of 8:2 and an LLDPE ratio of 10%, respectively. Additionally, there was an interaction between the corn stover to eucalyptus sawdust ratio and the torrefaction temperature; at a corn stover to eucalyptus sawdust ratio of 8:2, the carbon dioxide emissions reached their maximum at a torrefaction temperature of 210°C. Additionally, the carbon dioxide emissions of pellets were maximized by an interaction between the linear low-density polyethylene ratio and the torrefaction temperature at 10% LLDPE and a 210°C torrefaction temperature respectively.

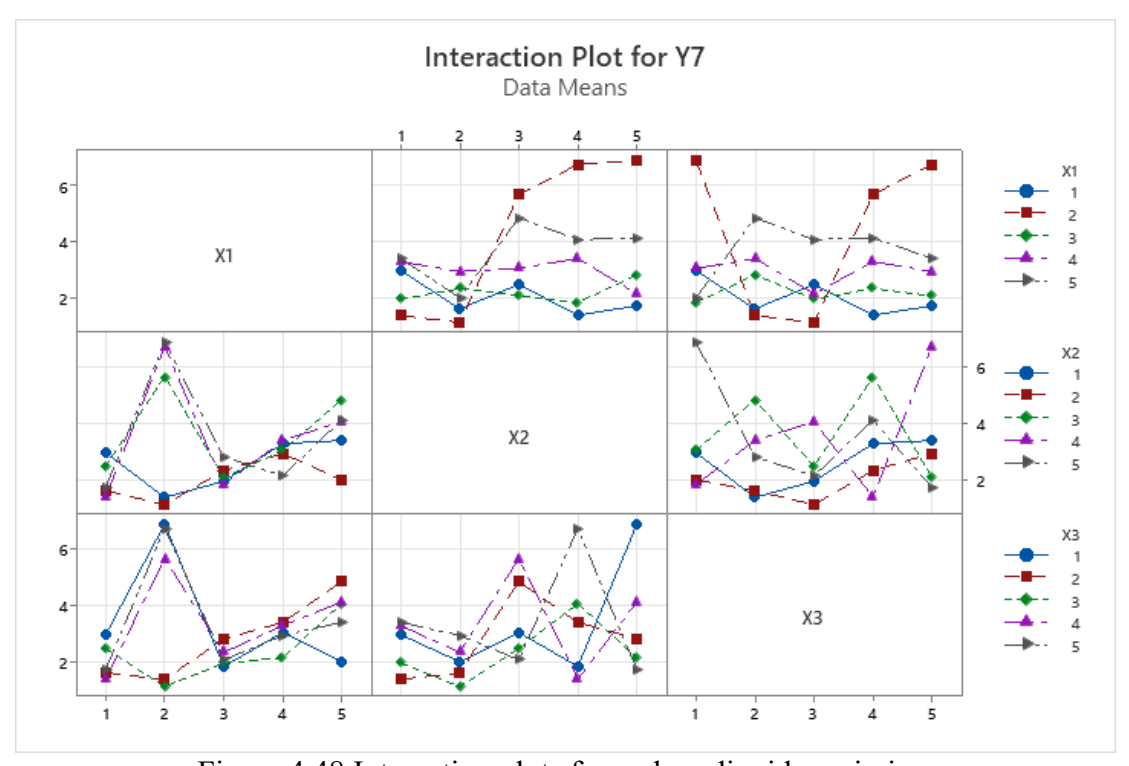


Figure 4.48 Interaction plots for carbon dioxide emissions

4.6 Taguchi multi-response optimization using grey relational analysis

Section 4.5 above dealt with the presentation, analysis and discussion of results of each of the responses (Y1, Y2, Y3, Y4, Y5, Y6 & Y7) independently. In this section, in order to get optimal parameter settings that will yield optimum output considering all the responses at once, Taguchi multi-response optimization using grey relational analysis is employed. According to Krishniah et al. (2012), interrelationships between the

various responses are resolved by the application of grey relational analysis. When the results of single response optimization are added together, a grey area is arrived at where no single parameter stands out as having the best overall quality of pellets, as shown in the ANOVA of single response optimization in section 4.5 (Mohamed et al., 2019; Thapa & Engelken, 2020; Wang et al., 2015). The procedure for execution of Taguchi multi-response optimization using grey relational analysis is outlined in section 2.14.4.3.

4.6.1 Computation of signal-to-noise ratios (S/N), Normalized data (Z_{ij}), quality loss (Δ) and grey relational coefficient (GC_{ij}) of the responses

Using grey relational analysis and the larger the better optimization technique, the multiple response optimizations for the targets were combined into a single objective response optimization problem by employing the stages of grey relational analysis (section 2.14.4.3) and presented in Appendix 19. Computation of signal-to-noise ratio (S/N), normalizing and computation of grey relational coefficients of the responses were computed using the formulas presented in section 2.14.4.3 and their results presented in Appendix 12 to Appendix 18.

4.6.2 Computation of grey relational grade (Gi)

Grey relational grade (Gi) was computed using the formulas presented in section 2.14.4.3 and results presented in Appendix 19. The computed Gi was then ranked in descending order. The experimental run No. 1 was found to have the greatest grey relational grade value and, thus, the largest S/N ratio, as shown by Appendix 18 and Figure 4.49. A greater Gi suggests that the value is approaching the optimal point. Therefore, the best parameter settings for improved multiresponse characteristics were found in Experiment 1. Stated otherwise, experimental run 1 presents the most suitable

combinations of input parameters that, in this particular case, yield the best output responses, or desired quality attributes.

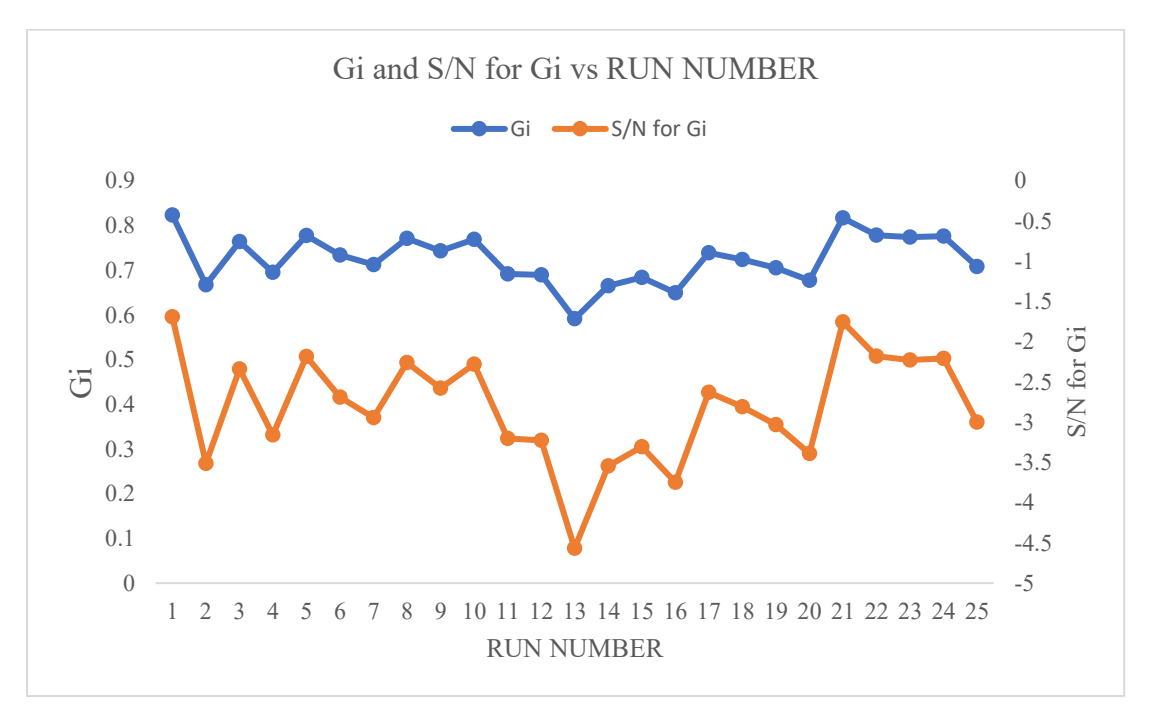


Figure 4.49 A graph of grey relational grade and its corresponding S/N ratios

4.6.3 Optimization of design parameters

The optimum parameter settings for the best-quality pellet were determined using the response graphs method. The grey relational grade was computed and presented as illustrated in Appendix 20 (a) as well as its signal-to-noise ratio. Since all the responses have been converted to a single response (Gi), response tables for signal to noise ratio and means was computed and presented in Appendix 20 (b) and Appendix 20 (c) respectively. Response graphs of the signal-to-noise ratio and means were presented in Figure 4.50. From the response tables and graphs, it was seen that the optimum parameter levels were level five for corn stover to eucalyptus sawdust ratio, level one for linear low-density polyethylene and level one for torrefaction temperature (i.e. X1₅X2₁X3₁). The ranking of the design parameters indicated that corn stover to eucalyptus ratio contributed the most to the overall pellet qualities followed by torrefaction temperature and percent linear low-density polyethylene.

Therefore, the pelletization parameter levels to produce pellets with optimum qualities were presented in Table 4.24 in terms of levels and Table 4.25 in terms of actual values.

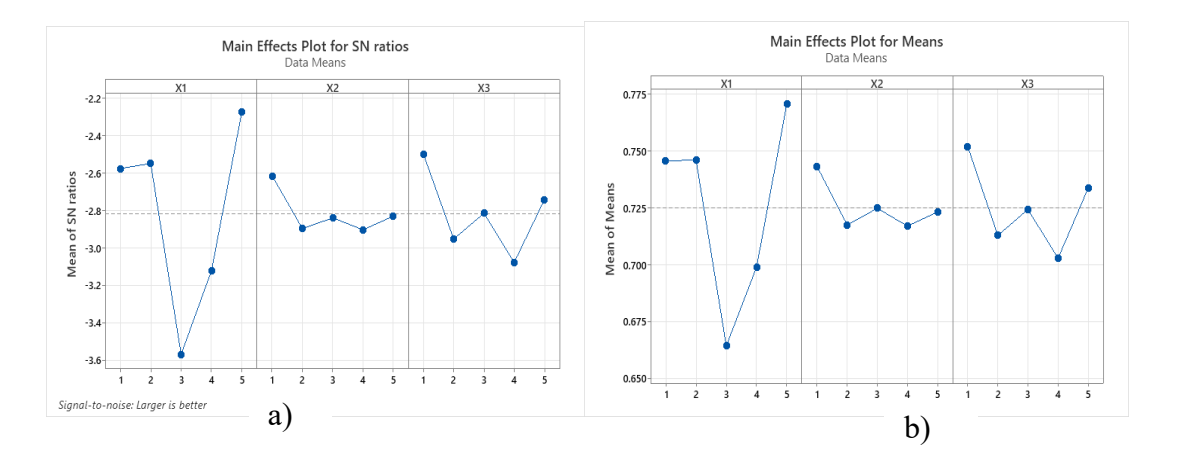


Figure 4.50 Main effects plot for (a) SN ratios and (b) means for grey relational grade (Gi)

Table 4.24 Parameters and their levels for optimum pellet production

Corn stover: Eucalyptus sawdust	LLDPE (%)	Torrefaction
(wt: wt)		temperature (⁰ C)
5	1	1

Table 4.25 Optimum actual values of parameters for pellet production

Corn stover: Eucalyptus sawdust	LLDPE (%)	Torrefaction temperature
(wt: wt)		(^{0}C)
1:1	2	210

4.6.3.1 Multivariable linear regression model for grey relational grade (Gi)

Equation 4.11 showed the link between the input parameters (corn stover to eucalyptus sawdust ratio, linear low-density polyethylene ratio, and torrefaction temperature) and the grey relational grade. The plot of the standardized residuals is shown in Figure 4.51. As can be seen, the plots were centered around the straight line, suggesting that the multivariable linear regression model and the grey relational grade of the pellets fit each other quite well. The residuals' range of -3 to 3 adds more evidence to the fitted model's appropriateness. The results of the linear regression model showed that the most significant factor influencing the grey relational grade was the torrefaction temperature.

It was then followed by linear low-density polyethylene and the ratio of corn stover to eucalyptus sawdust, in that sequence. Figure 4.52 illustrates a Pareto chart for Gi. The sequence of significance of the parameters for Gi as presented by the Pareto chart was exactly the same as that presented by the linear regression model.

Regression Equation

Gi=0.7502 + 0.00031 X1 - 0.00405 X2 - 0.00467 X3 Equation 4.10

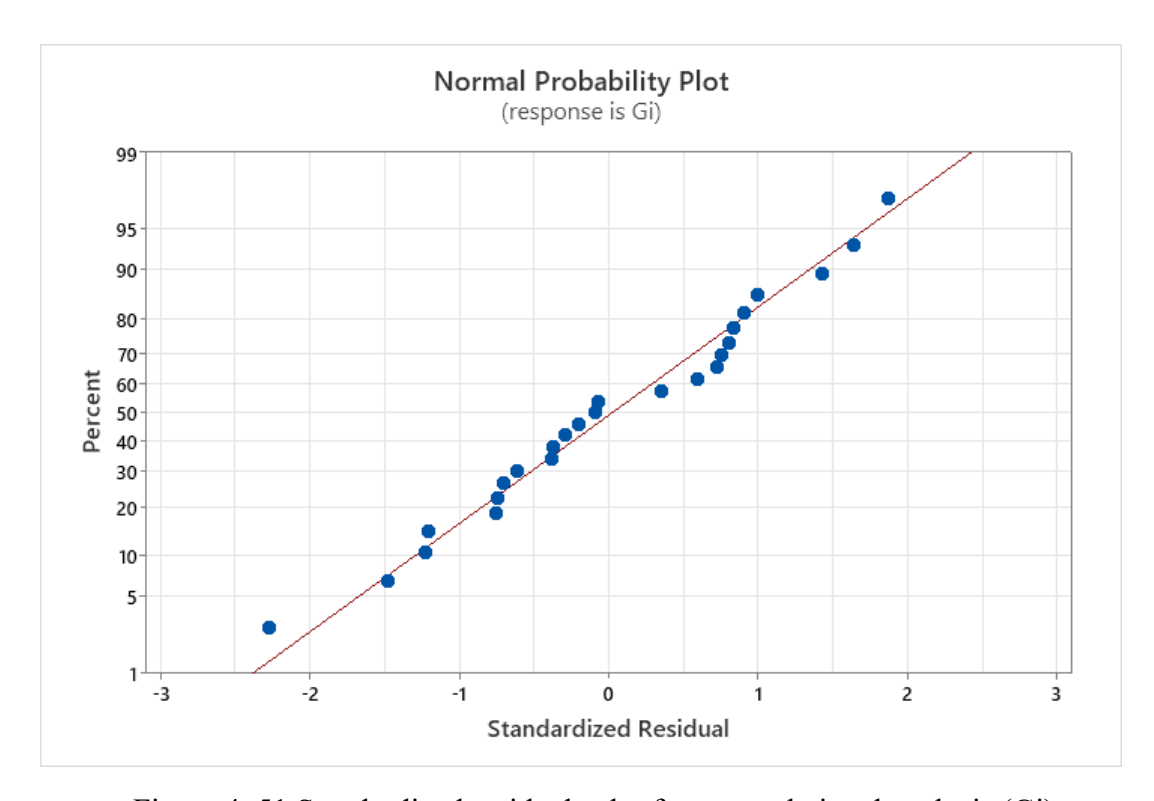


Figure 4. 51 Standardized residuals plot for grey relational analysis (Gi)

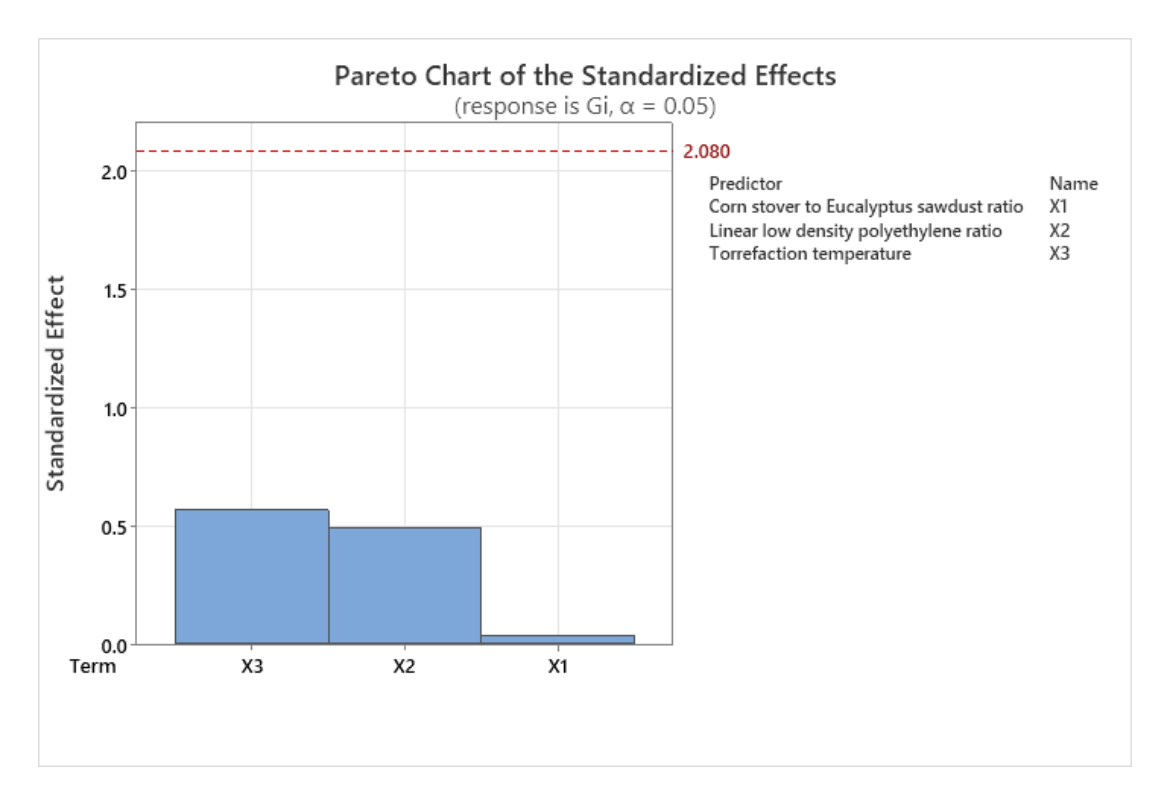


Figure 4. 52 Pareto chart of the standardized effects of grey relational grade (Gi)

4.6.3.2 Analysis of contour and surface plots for grey relational grade (Gi)

Figure 4.53 and Figure 4.54 depict the contour plots and response surface plots, respectively, that explain how the process parameters of the blended pellet production relate to the grey relational grade of the fabricated pellet. It should be noted that not every parameter is included in the process parameters, which in this case were kept at the median level of three.

Figure 4.53 (a) and Figure 4.54 (a) show that blended pellets should be produced utilizing 2% linear low-density polyethylene and a 1:1 ratio of corn stover to eucalyptus sawdust in order to get the highest possible grey relational grade. A 1:1 corn stover to eucalyptus sawdust ratio and a 210°C torrefaction temperature were found to produce blended pellets that yielded an increased grey relational grade Figure 4.53 (b) and Figure 4.54 (b). Figure 4.53 (c) and Figure 4.54 (c) showed that a 2% linear low density polyethylene binder and a 210°C torrefaction temperature would lead to an increased grey relational grade in the blended pellet. The dark green regions in the contour plots

indicate that the optimized blended pellet obtained a grey relational grade of more than 0.740.

4.6.3.3 Analysis of interactions of grey relational analysis (Gi)

The interaction plot for the grey relational grade (Gi) was shown in Figure 4.55. The interaction plot shows how the ratio of corn stover to eucalyptus sawdust interacts with the percent ratio of linear low-density polyethylene. The maximum pellet's grey relational grade was recorded at a corn stover to eucalyptus sawdust ratio of 9:1 and an LLDPE ratio of 2%, respectively. Additionally, there was an interaction between the corn stover to eucalyptus sawdust ratio and the torrefaction temperature; at a corn stover to eucalyptus sawdust ratio of 9:1, the grey relational grade reached its maximum at a torrefaction temperature of 210°C. Additionally, the grey relational grade of pellets were maximized by an interaction between the linear low density polyethylene ratio and the torrefaction temperature at 2% LLDPE and a 210°C torrefaction temperature respectively.

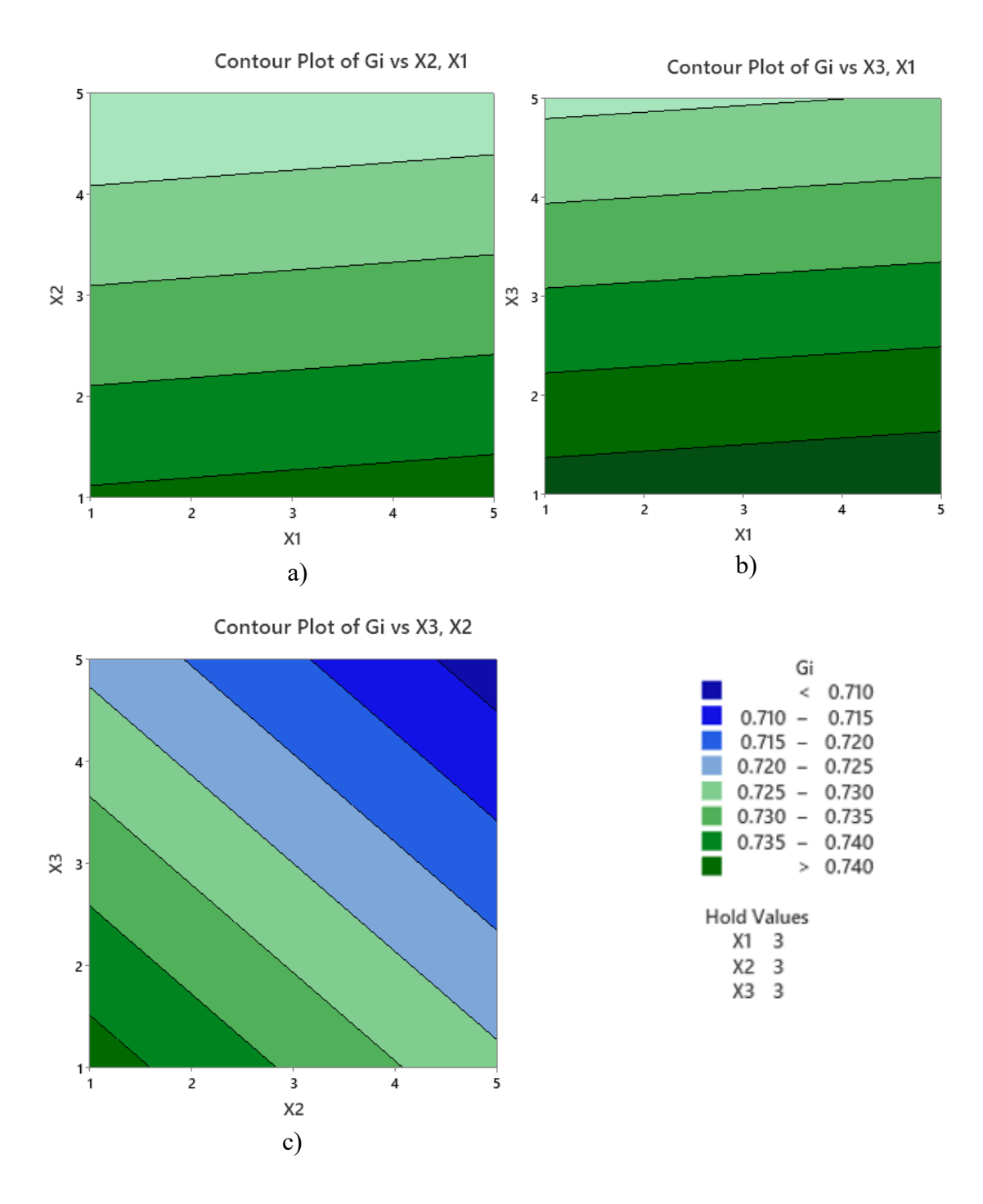


Figure 4.53 Contour plots for grey relational grade - Gi (Y5): a) corn stover to eucalyptus sawdust ratio (X1) vs linear low-density polyethylene (X2), b) corn stover to eucalyptus sawdust ratio (X1) vs torrefaction temperature (X3), c) linear low density polyethylene (X2) vs torrefaction temperature (X3).

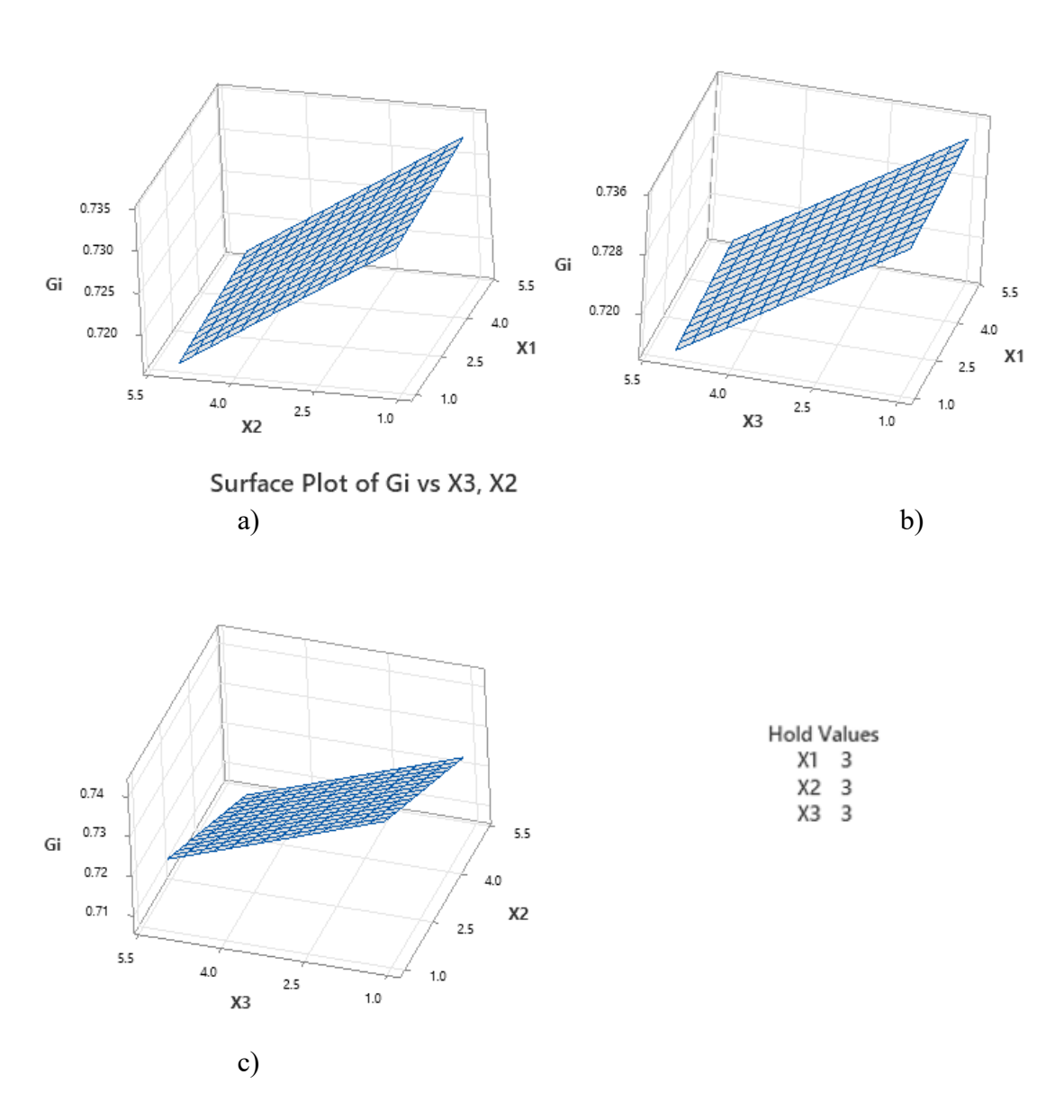


Figure 4.54 Response surface plots for grey relational grade - Gi (Y5): a) corn stover to eucalyptus sawdust ratio (X1) vs linear low-density polyethylene (X2), b) corn stover to eucalyptus sawdust ratio (X1) vs torrefaction temperature (X3), c) linear low density polyethylene (X2) vs torrefaction temperature (X3).

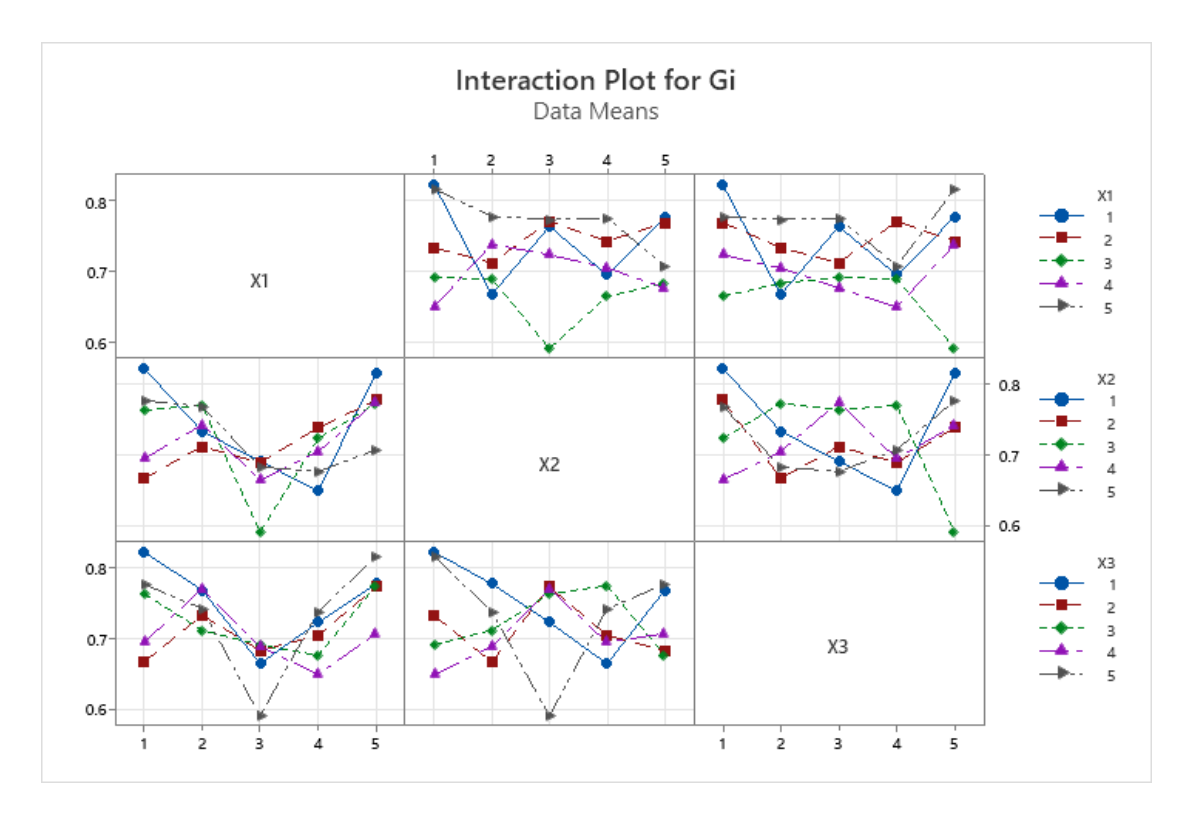


Figure 4.55 Analysis of interactions of grey relational analysis

4.7 Validation Test

Design parameter optimal levels are used to estimate optimal performance characteristics. Therefore, the last stage of the Taguchi-Grey relational analysis is to perform an experimental confirmation with the design parameters set at their optimal levels (Borkowski, 2010; Krishniah et al., 2012; Thapa et al., 2018b). Using Equation 4.12 and also Minitab software, the estimated/predicted grey relational grade was found to be 0.8155 by applying the optimal level of parameters. Given that the predicted value was close to 1, it was anticipated that the newly determined optimal parameter combination would yield the best pellets for the performance attributes under investigation. As a result, samples of pellets were fabricated by replicating the combination of optimal parameter values that were considered to yield the highest quality pellets. Subsequently, the performance characteristics of the produced pellets were analyzed.

The pellets fabricated under optimum conditions and hypothesized conditions were compared and contrasted in Table 4.26 Optimized pellets for every performance characteristic had a higher signal to noise ratio than both the predicted condition and the results of each experimental run except for carbon dioxide emissions which were lower as its performance was minimized. Based on the mean GRG, it was observed that the experimental condition X1₅X2₁X3₁ had a GRG that is much greater and is around the predicted values. Therefore, multi-response criteria showed that pellets produced under optimal conditions were of superior quality. Table 4.27 presents the evaluated properties of optimized blended pellets.

$$\gamma_e = \gamma_m + \sum_{i=1}^q (\bar{\gamma}_i - \gamma_m)$$
......Equation 4.11 where,

 γ_e = Estimated/predicted value of Gi.

 γ_m = The total mean of the grey relational grade q = Number of input parameters/factors $\bar{\gamma}_i$ = Mean grey relational grade value at the optimal level for the ith parameter Calculation of γ_e

$$\gamma_e = \gamma_m + (\bar{\gamma}_{CS:ESD} - \gamma_m) + (\bar{\gamma}_{\%LLDPE} - \gamma_m) + (\bar{\gamma}_{TT} - \gamma_m)$$

$$\gamma_e = 0.7250 + (0.7706 - 0.7250) + (0.7431 - 0.7250) + (0.7519 - 0.7250)$$

$$\gamma_e = 0.8156$$

Where,

 $\bar{\gamma}_{CS:ESD}$ =Optimal Gi for corn stover to eucalyptus sawdust ratio

 $\bar{\gamma}_{\%LLDPE}$ =Optimal Gi for the ratio of linear low-density polyethylene

 $\bar{\gamma}_{TT}$ =Optimal Gi for torrefaction temperature

Table 4.26 Confirmation experiments under optimal conditions

Responses	Initial setting	Grey relational analysis	Improvement in S/N
	(Hypothesized)	(Experimental)	ratio
Level	$X1_1X2_1X3_1$	X1 ₅ X2 ₁ X3 ₁	X15X21X31
BD (kg/m^3)	627.17 (55.9476)	633.2 (56.0308)	0.0832
PDI (%)	96.97 (39.7318)	99.07 (39.9182)	0.1864
$D (kg/m^3)$	966.20 (59.7013)	1074.75 (60.6262)	0.9249
H (N)	996.26 (59.9675)	1046.972 (60.3987)	0.4237
MY (%)	54.50 (34.7244)	64.45 (36.1818)	1.1457
HHV(MJ/kg)	29.47 (29.3815)	29.894 (29.5071)	0.1256
CO2(%VOL)	2.99 (-9.5139)	3.55 (-11.0727)	-1.5588

Table 4.27 Summary of optimized blended pellet properties

SR NO.	Pellet property	Mean	STDEV
1	Pellet particle density	1074.75	1.9273
2	Hardness	1046.972	1.5591
3	Bulk density	633.2	1.8526
4	Pellet durability index	99.07	0.5623
5	HHV	29.894	0.6799
6	Mass yield	64.45	1.4331
7	Carbon dioxide emissions	3.55	0.5133

4.7.1 Emissions test of optimized blended pellets using Laboratory Emissions Monitoring Systems (LEMS)

LEMS was able to detect and quantify CO, CO2 and PM2.5. Combustion emissions from the optimized blended pellet were: 44.3g/min for CO2, 0.40g/min for CO and 7.55mg/min for particulate matter (PM2.5). Graphical presentation of real-time combustion emissions on combustion of optimized blended pellets from LEMS over a period of 120 minutes was as shown in Figure 4.56 for CO and CO₂ emissions while for PM2.5 emissions in Figure 4.57. ISO tiers for the emissions for CO and PM_{2.5} was 3.6 and 3.7 respectively as determined from the sensor box processing software of LEMS. These tiers were above 3 and this implies that the emission levels from the combustion of the optimized pellet is within acceptable limits of KEBS Standard-KS 1814:19.

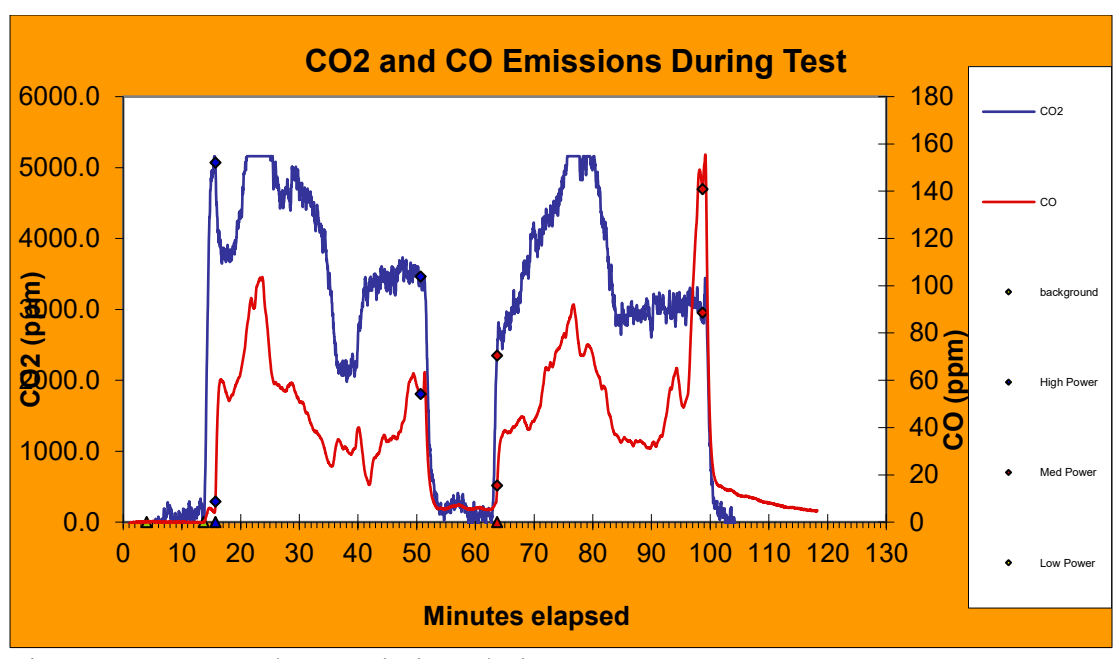


Figure 4.56: CO₂ and CO emissions during test

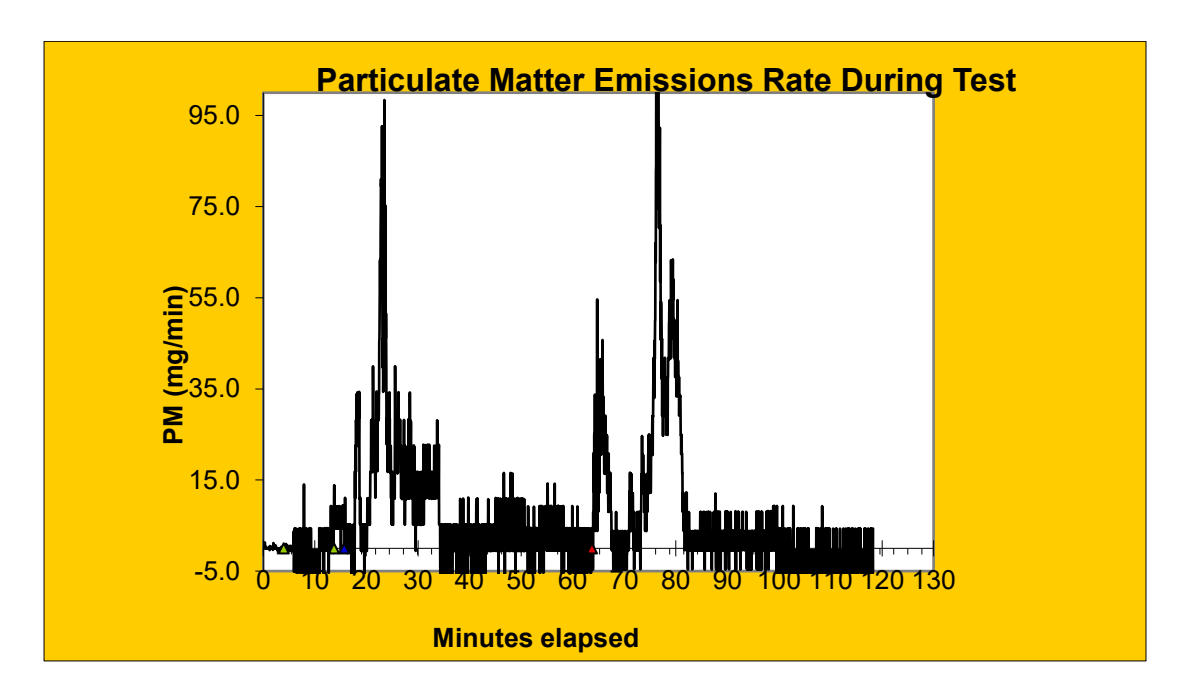


Figure 4.57: Particulate Matter (PM2.5) emissions rate during test

CHAPTER FIVE: CONCLUSIONS AND RECOMMENDATIONS

5.1 Introduction

This chapter presents the conclusions and recommendations drawn from the analyzed results.

5.2 Conclusions

This research aimed at optimizing the performance of blended biomass pellets from corn stover and eucalyptus sawdust using linear low-density polyethylene as a binder. Corn stover and eucalyptus sawdust used in this research were characterized to determine their proximate and ultimate analysis. The production of pellets to be analyzed was done using a fabricated heated mould. Evaluation of the performance properties of the fabricated blended pellets was achieved through physical, mechanical and thermochemical characterization of blended torrefied pellets. A pellet durability tester was fabricated to evaluate the pellet durability index of the blended pellets. Finally, optimization of the pelleting process variables in terms of corn stover to eucalyptus sawdust ratio, the ratio of LLDPE binder and the torrefaction temperature was done. As a result of this experimental research, the following conclusions were drawn:

Proximate analysis of biomass raw materials for biofuel production provides initial findings for the assessment of fuel quality. Conclusions drawn from the results obtained from proximate analysis of corn stover and eucalyptus sawdust are as follows:

Moisture contents of both feedstocks were way below the recommended quantities for pelleting of 10-15%. Since moisture content affects higher heating values and ability of biomass particles to bind, it can be concluded that the higher heating value of the blended pellet was not affected. On the other hand, there was difficulty in pelletization of the

biomass feedstocks due to low moisture content. To curb this challenge, ultrapure water was added to the biomass feedstocks to raise its moisture content.

- Ash is a quantitative measure of the non-combustible inorganic contaminants present in biomass. While the exact effects of ash content on heating value are unknown, it is assumed that increasing ash content lowers heating value. From ash content analysis, it can be concluded that both feedstocks analyzed are suitable for pelleting since the recommended ranges for wood residues are around 3% and below and less than 5-7% for agricultural residues.
- ➤ When biomass has a high volatile matter content, the combustion process is typically more sustainable and results in a highly reactive fuel that burns quickly during the devolatization stage. The volatile contents of both feedstocks were high and within the ranges of 70-90% for herbaceous and woody biomass as presented in published literature. Therefore, it can be concluded that the blended pellet obtained can undergo combustion process quickly and sustainably.
- Fixed carbon is the amount of carbon that is available for char combustion after all volatile materials in biomass, which serves as the primary energy source during combustion, are removed. Fixed carbons of corn stover and eucalyptus sawdust was within the ranges provided from the literature. Therefore, it can be concluded that, the resultant blended pellet will have high energy density since fixed carbon contributes significantly to the energy content of the biomass. Another conclusion tied to the fixed carbon was that the blended pellet produced

was likely to have high durability index as biomass with a higher fixed carbon content tends to produce denser pellets that are more structurally stable. Finally, since fixed carbon content influences combustion efficiency, blended pellet produced will most probably burn more efficiently, producing more heat per unit of mass.

This objective aimed at design and fabrication of a single pellet press heated mould that could be able to densify biomass feedstocks at specific temperatures to pellets. Therefore, a single pellet piston press was fabricated using locally available materials. The machine was capable of densifying loosely packed grounded feedstock to a hard solid (pellet). The various parts of the machine like the temperature controller, the thermocouple, the insulation, the AC contactor and the hydraulic press worked effectively. Thus, the fabrication of a single pellet press heated mould was successful and it led to proceeding to the next phase of research of the actual production of pellets according to the design of experiments. The fabrication of this single pellet press will also go a long way in other research projects on densification of biomasses.

Pellet durability index was determined by subjecting pellets to tumbling motion in a tumbler box and a ratio of mass of pellets before and after tumbling computed. A pellet durability tester was fabricated from locally available materials. This fabrication was able to create a tumbling motion to mimmick the situation in transportation of pellets. This was an important procedure to help in determination of pellet durability index. The various components of the pellet durability tester like the tumbling box, the variable frequency drive, the potentiometer and the three-phase motor worked as required. This was evident as the tumbling box could be rotated and maintained at the required revolutions per minute and this was displayed in the LCD screen of the variable

frequency drive. Therefore, the design and fabrication of the pellet durability tester was successful.

Fabrication of blended pellets involved densification of the loosely packed biomass feedstocks while the subsequent process of torrefaction as designed in this research involved heat treatment of pellets at low temperatures of between 200°C and 300°C in little or no oxygen for a predetermined period of time. Blended pellets from corn stover and eucalyptus sawdust using linear low-density polyethylene as a binder were successfully fabricated using the single pellet press fabricated. Torrefaction of these fabricated pellets was done also successfully in a modified tube furnace. The torrefied pellets maintained their structural integrity but their colour changed due to heat treatment under inert conditions. Therefore, it follows that the modification of the tube furnace to a torrefaction equipment was a success since no pellet underwent combustion.

The efficiency of fabrication of pellets and biomass pellet enhancement techniques considered in this research such as: blending, use binders and post pelletization torrefaction, was determined by, the evaluation of physical, mechanical and thermochemical properties of blended torrefied pellets. These properties were successfully derived using various specific criteria for properties as explained in methodology. These torrefied pellets were found to be superior because most of the properties exceeded the thresholds presented by the European normative guidelines for pellets produced from herbaceous and fruit biomass and blends and mixtures and other presented literatures.

To fabricate a blended torrefied pellet that possess optimum overall pellet qualities studied using linear low-density polyethylene as a binder, it can be concluded that one

has to fabricate the pellet using a blend ratio of 1:1 for corn stover to eucalyptus sawdust, 2% linear low density polyethylene ratio and 210°C torrefaction temperature.

It was evident from Pareto analysis of results that linear low density polyethylene binder was the most significant parameter in pellet particle density, bulk density, pellet durability index, pellet hardness and the higher heating values of pellets. Therefore, it can be concluded that linear low-density polyethylene is an important additive in biomass pellet fabrication of a pellet with superior qualities.

In summary, this research affirms that the use of eucalyptus sawdust as an additive on corn stover in pellet production, the use of LLDPE has a binder and torrefaction of pellets improves the pellet properties significantly. Therefore, this research is a gateway to production of pellets which are of high calorific value, thus leading to increase in fuel for use in households and industry for energy production. The use of LLDPE as a binder will go along way in reduction of non biodegradable wastes, hence ensuring a safe and clean environment. One limitation of this thesis is the lack of a standard or data from literature on carbon dioxide emissions from combustion of the blended torrefied pellets.

5.3 Recommendations

This research yielded important findings on the fabrication of blended pellets, evaluation of their properties and optimization of pellet fabrication process parameters. Since the optimized pellets have a high energy output and improved mechanical and physical properties that make them easy to transport to their destination of application, it is highly recommended that they should be utilized in improved pellet cookstoves and industrial boilers. However, the following research areas about pellet production

from corn stover and eucalyptus sawdust ratio, with linear low density as a binder requires more research to further improve the pellet properties:

- ➤ Characterization of feedstocks indicated that eucalyptus sawdust has higher fuel properties than corn stover. Therefore, it is recommended that higher ratios of eucalyptus sawdust be used as an additive to improve fuel properties of the blended pellet.
- Extensive performance testing, including material versatility, should be carried out on the designed and fabricated single-pellet press with a heated mold and pellet durability tester in order to assess how well it performs when various biomasses and binders are utilized.
- ➤ The validated optimized pellet indicated that there was improvement in all the tested properties except emissions tests. It is highly recommended this analysis is extended to other biomasses and binders so as to achieve produce pellets with superior qualities.

Further research

Areas that need further research from this thesis are listed below.

- A study on the effect of linear low-density polyethylene on Torgas.
- Further analysis on emissions to include other gaseous emissions like NOx and SOx as well as particulate matter from combustion of pellets bound by linear low-density polyethylene.
- Analysis of hydrophobicity of the pellets to evaluate the effect of linear low density polyethylene binder on it.
- > From the review of literature on carbon dioxide emissions from combustion of pellets, it was found that carbon dioxide from combustion of biomass pellets is

not regulated, and more so unclear in combustion of torrefied pellets. Therefore, there is need to research further on acceptable carbon dioxide emission levels from torrefied pellets.

➤ Characterization of structural carbohydrates (cellulose, hemicellulose and lignin) as well as extractives of corn stover and eucalyptus sawdust so as to determine its relation to effectiveness of LLDPE binder.

REFERENCES

- Abdel Aal, A. M. K., Ibrahim, O. H. M., Al-Farga, A., & El Saeidy, E. A. (2023). Impact of Biomass Moisture Content on the Physical Properties of Briquettes Produced from Recycled Ficus nitida Pruning Residuals. *Sustainability (Switzerland)*, 15(15). https://doi.org/10.3390/su151511762
- Abdoli, M. A., Golzary, A., Hosseini, A., & Sadeghi, P. (2022). Wood pellet as a renewable source of energy: From production to consumption. In *Springer* (Issue May 2022).
- Adeleke, A. A., Odusote, J. K., Ikubanni, P. P., Lasode, O. A., Malathi, M., & Paswan, D. (2021). Essential basics on biomass torrefaction, densification and utilization. In *International Journal of Energy Research* (Vol. 45, Issue 2, pp. 1375–1395). John Wiley and Sons Ltd. https://doi.org/10.1002/er.5884
- Adeleke, A., Odusote, J., Ikubanni, P., Lasode, O., Malathi, M., & Pasawan, D. (2021). Physical and mechanical characteristics of composite briquette from coal and pretreated wood fines. *International Journal of Coal Science and Technology*, 8(5), 1088–1098. https://doi.org/10.1007/s40789-021-00438-0
- Agu, O. S. (2018). Effect of binders on agricultural crop residues and wastes pellets . A review. *The Canadian Society for Bioengineering*, CSBE18-116, 1–9.
- Agu, O. S., Tabil, L. G., Emadi, B., & Mupondwa, E. (2018). Microwave-assisted torrefaction of biomass: Effect of biochar and recycled polymer plastic (HDPE) on the physical quality of fuel pellets. *ASABE 2018 Annual International Meeting*. https://doi.org/10.13031/aim.201801398
- Agu, O. S., Tabil, L. G., Mupondwa, E., & Emadi, B. (2021). Torrefaction and Pelleting of Wheat and Barley Straw for Biofuel and Energy Applications. *Frontiers in Energy Research*, 9. https://doi.org/10.3389/fenrg.2021.699657
- Ajimotokan, H. A., Ehindero, A. O., Ajao, K. S., Adeleke, A. A., Ikubanni, P. P., & Shuaib-Babata, Y. L. (2019). Combustion characteristics of fuel briquettes made from charcoal particles and sawdust agglomerates. *Scientific African*, 6. https://doi.org/10.1016/j.sciaf.2019.e00202
- Akanni, A. A., Kolawole, O. J., Dayanand, P., Ajani, L. O., & Madhurai, M. (2019). Influence of torrefaction on lignocellulosic woody biomass of Nigerian origin. *Journal of Chemical Technology and Metallurgy*, 54(2).
- Akbar, A., Aslam, U., Asghar, A., & Aslam, Z. (2021). Effect of binding materials on physical and fuel characteristics of bagasse based pellets. *Biomass and Bioenergy*, 150(April), 106118. https://doi.org/10.1016/j.biombioe.2021.106118
- Alakangas, E. (n.d.). *Quality guidelines of wood fuels in Finland*. https://doi.org/10.13140/RG.2.1.3290.3127
- Alakangas, E. (2011). European Standards for Fuel Specification and Classes of Solid Biofuels. *Green Energy and Technology*, 28. https://doi.org/10.1007/978-1-84996-393-0_2

- Ali, A., Liu, Y., Mao, X., Ali, Z., Ran, C., Ao, W., Fu, J., Zhou, C., Wang, L., Li, X., Liu, G., & Dai, J. (2021). Biomass and Bioenergy Co-pelletization of sewage sludge, furfural residue and corn stalk: Characteristics and quality analysis of pellets. *Biomass and Bioenergy*, 150(May), 106121. https://doi.org/10.1016/j.biombioe.2021.106121
- Alizadeh, R., Lund, P. D., & Soltanisehat, L. (2020). Outlook on biofuels in future studies: A systematic literature review. *Renewable and Sustainable Energy Reviews*, 134(August), 110326. https://doi.org/10.1016/j.rser.2020.110326
- Ambaye, T. G., Vaccari, M., Bonilla-Petriciolet, A., Prasad, S., van Hullebusch, E. D., & Rtimi, S. (2021). Emerging technologies for biofuel production: A critical review on recent progress, challenges and perspectives. *Journal of Environmental Management*, 290(May). https://doi.org/10.1016/j.jenvman.2021.112627
- Antar, M., Lyu, D., Nazari, M., Shah, A., Zhou, X., & Smith, D. L. (2021). Biomass for a sustainable bioeconomy: An overview of world biomass production and utilization. *Renewable and Sustainable Energy Reviews*, *139*(December 2020), 110691. https://doi.org/10.1016/j.rser.2020.110691
- Anukam, A., & Berghel, J. (n.d.). *Biomass Pretreatment and Characterization: A Review*. www.intechopen.com
- Anukam, A., Berghel, J., Henrikson, G., Frodeson, S., & Ståhl, M. (2021). A review of the mechanism of bonding in densified biomass pellets. *Renewable and Sustainable Energy Reviews*, 148(August 2020), 111249. https://doi.org/10.1016/j.rser.2021.111249
- Arevalo-Gallegos, A., Ahmad, Z., Asgher, M., Parra-Saldivar, R., & Iqbal, H. M. N. (2017). Lignocellulose: A sustainable material to produce value-added products with a zero waste approach—A review. In *International Journal of Biological Macromolecules* (Vol. 99). https://doi.org/10.1016/j.ijbiomac.2017.02.097
- Auprakul, U., Promwungkwa, A., Tippayawong, N., & Chaiklangmuang, S. (2014a). Densified fuels from mixed plastic wastes and corn stover. *Advanced Materials Research*, 931–932(May), 1117–1121. https://doi.org/10.4028/www.scientific.net/AMR.931-932.1117
- Auprakul, U., Promwungkwa, A., Tippayawong, N., & Chaiklangmuang, S. (2014b). Densified fuels from mixed plastic wastes and corn stover. *Advanced Materials Research*, 931–932(May), 1117–1121. https://doi.org/10.4028/www.scientific.net/AMR.931-932.1117
- Azargohar, R., Nanda, S., & Dalai, A. K. (2018). Densification of agricultural wastes and forest residues: A review on influential parameters and treatments. *Recent Advancements in Biofuels and Bioenergy Utilization*, 27–51. https://doi.org/10.1007/978-981-13-1307-3 2
- Azargohar, R., Soleimani, M., Nosran, S., Bond, T., Karunakaran, C., Dalai, A. K., & Tabil, L. G. (2019). Thermo-physical characterization of torrefied fuel pellet from co-pelletization of canola hulls and meal. *Industrial Crops and Products*, 128. https://doi.org/10.1016/j.indcrop.2018.11.042

- Bach, Q. V., & Skreiberg, O. (2016). Upgrading biomass fuels via wet torrefaction: A review and comparison with dry torrefaction. In *Renewable and Sustainable Energy Reviews* (Vol. 54). https://doi.org/10.1016/j.rser.2015.10.014
- Bajo, P. O., & Acda, M. N. (2017). Fuel pellets from a mixture of rice husk and wood particles. *BioResources*, 12(3). https://doi.org/10.15376/biores.12.3.6618-6628
- Balat, M., Balat, H., & Öz, C. (2008). Progress in bioethanol processing. In *Progress in Energy and Combustion Science* (Vol. 34, Issue 5). https://doi.org/10.1016/j.pecs.2007.11.001
- Barskov, S., Zappi, M., Buchireddy, P., Dufreche, S., Guillory, J., Gang, D., Hernandez, R., Bajpai, R., Baudier, J., Cooper, R., & Sharp, R. (2019). Torrefaction of biomass: A review of production methods for biocoal from cultured and waste lignocellulosic feedstocks. In *Renewable Energy* (Vol. 142). https://doi.org/10.1016/j.renene.2019.04.068
- Bartocci, P., Barbanera, M., Skreiberg, O., Wang, L., Bidini, G., & Fantozzi, F. (2018). Biocarbon pellet production: Optimization of pelletizing process. *Chemical Engineering Transactions*, 65. https://doi.org/10.3303/CET1865060
- Bates, R. B., & Ghoniem, A. F. (2014). Modeling kinetics-transport interactions during biomass torrefaction: The effects of temperature, particle size, and moisture content. *Fuel*, *137*. https://doi.org/10.1016/j.fuel.2014.07.047
- Bhavsar, P. A., Jagadale, M. H., Khandetod, Y. P., & Mohod, A. G. (2018). Proximate Analysis of Selected Non Woody Biomass. *International Journal of Current Microbiology and Applied Sciences*, 7(09). https://doi.org/10.20546/ijcmas.2018.709.353
- Biotechnological Applications of Biomass. (2020). In *Biotechnological Applications of Biomass*. https://doi.org/10.5772/intechopen.89320
- Borkowski, John. (2010). Response Surface Methodology: Process and Product Optimization Using Designed Experiments (3rd ed.). by Raymond H. Myers, Douglas C. Montgomery, and Christine M. Anderson-Cook. *Journal of the American Statistical Association*, 105(490).
- Butler, C. (1992). A primer on the Taguchi method. *Computer Integrated Manufacturing Systems*, 5(3). https://doi.org/10.1016/0951-5240(92)90037-d
- Cao, L., Yuan, X., Li, H., Li, C., Xiao, Z., Jiang, L., Huang, B., Xiao, Z., Chen, X., Wang, H., & Zeng, G. (2015). Complementary effects of torrefaction and copelletization: Energy consumption and characteristics of pellets. *Bioresource Technology*, 185. https://doi.org/10.1016/j.biortech.2015.02.045
- CARRILLO T, CASANOVA P, & SOLÍS K. (2016). Effect of Densification Conditions on Physical Properties of Pellets Made From Sawmill Residues. *American Journal of Engineering Research (AJER)*, 5.
- Carroll, J., & Finnan, J. (2013). Emissions and efficiencies from the combustion of agricultural feedstock pellets using a small scale tilting grate boiler. *Biosystems Engineering*, 115(1). https://doi.org/10.1016/j.biosystemseng.2013.01.009

- Castellano, J. M., Gómez, M., Fernández, M., Esteban, L. S., & Carrasco, J. E. (2015). Study on the effects of raw materials composition and pelletization conditions on the quality and properties of pellets obtained from different woody and non woody biomasses. *Fuel*, *139*. https://doi.org/10.1016/j.fuel.2014.09.033
- Çetinkaya, B., Erkent, S., Ekinci, K., Civan, M., Bilgili, M. E., & Yurdakul, S. (2024). Effect of torrefaction on fuel properties of biopellets. *Heliyon*, *10*(2). https://doi.org/10.1016/j.heliyon.2024.e23989
- Ceylan, Z., & Sungur, B. (2020). Estimation of coal elemental composition from proximate analysis using machine learning techniques. *Energy Sources, Part A: Recovery, Utilization and Environmental Effects*, 42(20), 2576–2592. https://doi.org/10.1080/15567036.2020.1790696
- Chan, Y. H., Cheah, K. W., How, B. S., Loy, A. C. M., Shahbaz, M., Singh, H. K. G., Yusuf, N. R., Shuhaili, A. F. A., Yusup, S., Ghani, W. A. W. A. K., Rambli, J., Kansha, Y., Lam, H. L., Hong, B. H., & Ngan, S. L. (2019). An overview of biomass thermochemical conversion technologies in Malaysia. *Science of the Total Environment*, 680. https://doi.org/10.1016/j.scitotenv.2019.04.211
- Cheboiwo, J. K., Mutta, D., Kiprop, J., & Gattama, S. (2018). Public Private Partnerships Opportunities for Forestry Sector Development in Kenya: Synthesis of Primary and Secondary Production Actors, and Trade. *Journal of Environment and Earth Science*, 8(1).
- Chen, C. Y., Chen, W. H., & Ilham, Z. (2021). Effects of torrefaction and water washing on the properties and combustion reactivity of various wastes. *International Journal of Energy Research*, 45(6). https://doi.org/10.1002/er.5458
- Chen, D., Zhang, H., Liu, D., & Chen, Y. (2017). Effect of Torrefaction Pretreatment on Properties of Pyrolysis Product and Energy Distribution of Corn Stalk. *Taiyangneng Xuebao/Acta Energiae Solaris Sinica*, 38(2).
- Chen, D., Zheng, Z., Fu, K., Zeng, Z., Wang, J., & Lu, M. (2015). Torrefaction of biomass stalk and its effect on the yield and quality of pyrolysis products. *Fuel*, 159. https://doi.org/10.1016/j.fuel.2015.06.078
- Chen, W. H., Hsu, H. J., Kumar, G., Budzianowski, W. M., & Ong, H. C. (2017). Predictions of biochar production and torrefaction performance from sugarcane bagasse using interpolation and regression analysis. *Bioresource Technology*, 246. https://doi.org/10.1016/j.biortech.2017.07.184
- Chen, W. H., & Kuo, P. C. (2010). A study on torrefaction of various biomass materials and its impact on lignocellulosic structure simulated by a thermogravimetry. *Energy*, 35(6). https://doi.org/10.1016/j.energy.2010.02.054
- Chen, W. H., & Kuo, P. C. (2011). Torrefaction and co-torrefaction characterization of hemicellulose, cellulose and lignin as well as torrefaction of some basic constituents in biomass. *Energy*, *36*(2). https://doi.org/10.1016/j.energy.2010.12.036
- Chen, W. H., Lin, B. J., Huang, M. Y., & Chang, J. S. (2015). Thermochemical conversion of microalgal biomass into biofuels: A review. In *Bioresource Technology* (Vol. 184). https://doi.org/10.1016/j.biortech.2014.11.050

- Chen, W. H., Lin, B. J., Lin, Y. Y., Chu, Y. S., Ubando, A. T., Show, P. L., Ong, H. C., Chang, J. S., Ho, S. H., Culaba, A. B., Pétrissans, A., & Pétrissans, M. (2021). Progress in biomass torrefaction: Principles, applications and challenges. In *Progress in Energy and Combustion Science* (Vol. 82). https://doi.org/10.1016/j.pecs.2020.100887
- Chen, W. H., Lu, K. M., Liu, S. H., Tsai, C. M., Lee, W. J., & Lin, T. C. (2013). Biomass torrefaction characteristics in inert and oxidative atmospheres at various superficial velocities. *Bioresource Technology*, 146. https://doi.org/10.1016/j.biortech.2013.07.064
- Cheng, Y.-L., Lee, C.-Y., Huang, Y.-L., Buckner, C. A., Lafrenie, R. M., Dénommée, J. A., Caswell, J. M., Want, D. A., Gan, G. G., Leong, Y. C., Bee, P. C., Chin, E., Teh, A. K. H., Picco, S., Villegas, L., Tonelli, F., Merlo, M., Rigau, J., Diaz, D., ... Mathijssen, R. H. J. (2016). We are IntechOpen, the world 's leading publisher of Open Access books Built by scientists, for scientists TOP 1 %. *Intech*, *11*(tourism), 13. https://www.intechopen.com/books/advanced-biometric-technologies/liveness-detection-in-biometrics
- Choiński, B., Szatyłowicz, E., Zgłobicka, I., & Joka Ylidiz, M. (2023). A Critical Investigation of Certificated Industrial Wood Pellet Combustion: Influence of Process Conditions on CO/CO2 Emission. *Energies*, *16*(1). https://doi.org/10.3390/en16010250
- Cui, X., Yang, J., Wang, Z., & Shi, X. (2021). Better use of bioenergy: A critical review of co-pelletizing for biofuel manufacturing. *Carbon Capture Science and Technology*, *I*(September), 100005. https://doi.org/10.1016/j.ccst.2021.100005
- Dash, M., Venkata Dasu, V., & Mohanty, K. (2015). Physico-chemical characterization of Miscanthus, Castor, and Jatropha towards biofuel production. *Journal of Renewable and Sustainable Energy*, 7(4). https://doi.org/10.1063/1.4926577
- Demirbas, A., Omar Al-Sasi, B., & Nizami, A. S. (2017). Recent volatility in the price of crude oil. In *Energy Sources, Part B: Economics, Planning and Policy* (Vol. 12, Issue 5). https://doi.org/10.1080/15567249.2016.1153751
- Dey, A. S., Bose, H., Mohapatra, B., & Sar, P. (2020). Biodegradation of Unpretreated Low-Density Polyethylene (LDPE) by Stenotrophomonas sp. and Achromobacter sp., Isolated From Waste Dumpsite and Drilling Fluid. *Frontiers in Microbiology*, 11. https://doi.org/10.3389/fmicb.2020.603210
- Dinesha, P., Kumar, S., & Rosen, M. A. (2019). Biomass Briquettes as an Alternative Fuel: A Comprehensive Review. *Energy Technology*, 7(5), 1–8. https://doi.org/10.1002/ente.201801011
- Djatkov, D., Martinov, M., & Kaltschmitt, M. (2018). Influencing parameters on mechanical–physical properties of pellet fuel made from corn harvest residues. *Biomass and Bioenergy*, 119(October), 418–428. https://doi.org/10.1016/j.biombioe.2018.10.009
- Djurdjevic, M., & Papuga, S. (2023). Torrefaction: Process Parameters and Reactor Design. *Periodica Polytechnica Chemical Engineering*, 67(3). https://doi.org/10.3311/PPch.22081

- Dubey, R., & Guruviah, V. (2022). Machine learning approach for categorical biomass higher heating value prediction based on proximate analysis. *Energy Sources, Part A: Recovery, Utilization and Environmental Effects*, 44(2). https://doi.org/10.1080/15567036.2022.2065386
- Dujmović, M., Šafran, B., Jug, M., Radmanović, K., & Antonović, A. (2022). Biomass Pelletizing Process: A Review. *Drvna Industrija*, 73(1), 99–106. https://doi.org/10.5552/drvind.2022.2139
- Duranay, N. D. (2019). CO2 emission from combustion of lignite, waste plastics and biomass mixture pellets. *Chemical Industry and Chemical Engineering Quarterly*, 25(3). https://doi.org/10.2298/CICEQ180921002D
- Dyjakon, A., Noszczyk, T., & Mostek, A. (2021). Mechanical durability and grindability of pellets after torrefaction process. *Energies*, 14(20). https://doi.org/10.3390/en14206772
- Ebadian, M., Sokhansanj, S., & Webb, E. (2017). Estimating the required logistical resources to support the development of a sustainable corn stover bioeconomy in the USA. *Biofuels, Bioproducts and Biorefining*, 11(1). https://doi.org/10.1002/bbb.1736
- Edmunds, C. W., Molina, E. A. R., André, N., Hamilton, C., Park, S., Fasina, O., Adhikari, S., Kelley, S. S., Tumuluru, J. S., Rials, T. G., & Labbé, N. (2018). Blended feedstocks for thermochemical conversion: Biomass characterization and bio-oil production from switchgrass-pine residues blends. *Frontiers in Energy Research*, 6(AUG). https://doi.org/10.3389/fenrg.2018.00079
- Emadi, B., Iroba, K. L., & Tabil, L. G. (2017). Effect of polymer plastic binder on mechanical, storage and combustion characteristics of torrefied and pelletized herbaceous biomass. *Applied Energy*, 198, 312–319. https://doi.org/10.1016/j.apenergy.2016.12.027
- Emadi, B., Tabil, L. G., Li, X., & Mupondwa, E. (n.d.). The Canadian Society for Bioengineering La Société Canadienne de Génie Agroalimentaire et de Bioingénierie Techno-economic feasibility of using recycled polymer plastic in torrefied and pelletized herbaceous biomass.
- EN15103. (2009). Solid Biofuels-Determination of Bulk Density. In *Landtechnik* (Vol. 60, Issue 3).
- Fernandes, F., Matos, S., Gaspar, D., Silva, L., Paulo, I., Vieira, S., Pinto, P. C. R., Bordado, J., & dos Santos, R. G. (2021). Boosting the higher heating value of Eucalyptus globulus via thermochemical liquefaction. *Sustainability* (Switzerland), 13(7). https://doi.org/10.3390/su13073717
- Filbakk, T., Jirjis, R., Nurmi, J., & Høibø, O. (2011). The effect of bark content on quality parameters of Scots pine (Pinus sylvestris L.) pellets. *Biomass and Bioenergy*, 35(8). https://doi.org/10.1016/j.biombioe.2010.09.011
- Fisher, E. M., Dupont, C., Darvell, L. I., Commandré, J. M., Saddawi, A., Jones, J. M., Grateau, M., Nocquet, T., & Salvador, S. (2012). Combustion and gasification characteristics of chars from raw and torrefied biomass. *Bioresource Technology*, 119, 157–165. https://doi.org/10.1016/j.biortech.2012.05.109

- Freddi, A., & Salmon, M. (2019). Design Principles and Methodologies. In *Design Principles and Methodologies*.
- Frodeson, S., Henriksson, G., & Berghel, J. (2019). Effects of moisture content during densification of biomass pellets, focusing on polysaccharide substances. *Biomass and Bioenergy*, 122. https://doi.org/10.1016/j.biombioe.2019.01.048
- Frodeson, S., & Tumuluru, J. S. (2023). Blending and Densification: Significance and Quality. In *Densification Impact on Raw, Chemically and Thermally Pretreated Biomass: Physical Properties and Biofuels Production*. https://doi.org/10.1142/9781800613799 0004
- Fumo, N., & Rafe Biswas, M. A. (2015). Regression analysis for prediction of residential energy consumption. In *Renewable and Sustainable Energy Reviews* (Vol. 47). https://doi.org/10.1016/j.rser.2015.03.035
- Gageanu, I., Cujbescu, D., Persu, C., Tudor, P., Cardei, P., Matache, M., Vladut, V., Biris, S., Voicea, I., & Ungureanu, N. (2021). Influence of input and control parameters on the process of pelleting powdered biomass. *Energies*, *14*(14). https://doi.org/10.3390/en14144104
- Gao, W., Tabil, L. G., Dumonceaux, T., Espinel Ríos, S., & Zhao, R. (2017). Optimization of biological pretreatment to enhance the quality of wheat straw pellets. *Biomass and Bioenergy*, 97. https://doi.org/10.1016/j.biombioe.2016.12.012
- García, R., Gil, M. V., González-Vázquez, M. P., Rubiera, F., & Pevida, C. (2019). Biomass Pelletization: Contribution to Renewable Power Generation Scenarios. 269–294. https://doi.org/10.1007/978-981-13-3768-0 9
- García, R., Gil, M. V., Rubiera, F., & Pevida, C. (2019). Pelletization of wood and alternative residual biomass blends for producing industrial quality pellets. *Fuel*, 251(January), 739–753. https://doi.org/10.1016/j.fuel.2019.03.141
- Garcia-Maraver, A. (2015a). *Biomass Pelletization Process* (pp. 53–66). https://doi.org/10.2495/978-1-84566-062-8/004
- Garcia-Maraver, A. (2015b). *Biomass Pelletization Process* (pp. 53–66). https://doi.org/10.2495/978-1-84566-062-8/004
- Garcia-Maraver, A. (2015c). *Factors Affecting Pellet Quality*. 85, 21–35. https://doi.org/10.2495/978-1-84566-062-8/002
- Garrido, M. A., Conesa, J. A., & Garcia, M. D. (2017). Characterization and production of fuel briquettes made from biomass and plastic wastes. *Energies*, 10(7). https://doi.org/10.3390/en10070850
- Ghiasi, B., Kumar, L., Furubayashi, T., Lim, C. J., Bi, X., Kim, C. S., & Sokhansanj, S. (2014). Densified biocoal from woodchips: Is it better to do torrefaction before or after densification? *Applied Energy*, 134. https://doi.org/10.1016/j.apenergy.2014.07.076
- Ghugare, S. B., Tiwary, S., & Tambe, S. S. (2017). Computational intelligence based models for prediction of elemental composition of solid biomass fuels from proximate analysis. *International Journal of System Assurance Engineering and Management*, 8. https://doi.org/10.1007/s13198-014-0324-4

- Gilvari, H., de Jong, W., & Schott, D. L. (2019). Quality parameters relevant for densification of bio-materials: Measuring methods and affecting factors A review. *Biomass and Bioenergy*, *120*(March 2018), 117–134. https://doi.org/10.1016/j.biombioe.2018.11.013
- Global Bioenergy Statistics. (2018). WBA Global Bioenergy Statistics 2018. World Bioenergy Association.
- GLOBAL BIOENERGY STATISTICS 2022 World Bioenergy Association. (2022).
- Graham, S., Eastwick, C., Snape, C., & Quick, W. (2017). Mechanical degradation of biomass wood pellets during long term stockpile storage. *Fuel Processing Technology*, 160. https://doi.org/10.1016/j.fuproc.2017.02.017
- Gummert, M., Van Hung, N., Chivenge, P., & Douthwaite, B. (2019). Sustainable Rice Straw Management. In *Sustainable Rice Straw Management*. https://doi.org/10.1007/978-3-030-32373-8
- Haq, I. U., Qaisar, K., Nawaz, A., Akram, F., Mukhtar, H., Zohu, X., Xu, Y., Mumtaz, M. W., Rashid, U., Ghani, W. A. W. A. K., & Choong, T. S. Y. (2021). Advances in valorization of lignocellulosic biomass towards energy generation. *Catalysts*, 11(3), 1–26. https://doi.org/10.3390/catal11030309
- Hartley, I. D., & Wood, L. J. (2008). Hygroscopic properties of densified softwood pellets. *Biomass and Bioenergy*, 32(1). https://doi.org/10.1016/j.biombioe.2007.06.009
- Harun, N. Y., Parvez, A. M., & Afzal, M. T. (2018). Process and energy analysis of pelleting agricultural and woody biomass blends. *Sustainability (Switzerland)*, 10(6). https://doi.org/10.3390/su10061770
- Haykiri-Acma, H., & Yaman, S. (2022). Effects of torrefaction after pelleting (TAP) process on strength and fuel characteristics of binderless bio-pellets. *Biomass Conversion and Biorefinery*. https://doi.org/10.1007/s13399-022-02599-7
- He, C., Tang, C., Li, C., Yuan, J., Tran, K. Q., Bach, Q. V., Qiu, R., & Yang, Y. (2018). Wet torrefaction of biomass for high quality solid fuel production: A review. *Renewable and Sustainable Energy Reviews*, 91(March 2018), 259–271. https://doi.org/10.1016/j.rser.2018.03.097
- Henriksen, U. B., Holm, J. K., Simonsen, P., Berg, M., Posselt, D., Nikolaisen, L., Plackett, D., & Møller, J. D. (2008). Fundamental Understanding of Pelletization. June.
- Holm, J. K., Stelte, W., Posselt, D., Ahrenfeldt, J., & Henriksen, U. B. (2011). Optimization of a multiparameter model for biomass pelletization to investigate temperature dependence and to facilitate fast testing of pelletization behavior. *Energy and Fuels*, 25(8), 3706–3711. https://doi.org/10.1021/ef2005628
- Hosseinizand, H., Sokhansanj, S., & Lim, C. J. (2018). Co-pelletization of microalgae Chlorella vulgaris and pine sawdust to produce solid fuels. *Fuel Processing Technology*, 177. https://doi.org/10.1016/j.fuproc.2018.04.015
- Hu, Q., Shao, J., Yang, H., Yao, D., Wang, X., & Chen, H. (2015). Effects of binders on the properties of bio-char pellets. *Applied Energy*, 157. https://doi.org/10.1016/j.apenergy.2015.05.019

- Hu, Q., Yang, H., Xu, H., Wu, Z., Lim, C. J., Bi, X. T., & Chen, H. (2018). Thermal behavior and reaction kinetics analysis of pyrolysis and subsequent in-situ gasification of torrefied biomass pellets. *Energy Conversion and Management*, 161. https://doi.org/10.1016/j.enconman.2018.02.003
- Huang, Y., Finell, M., Larsson, S., Wang, X., Zhang, J., Wei, R., & Liu, L. (2017a). Biofuel pellets made at low moisture content Influence of water in the binding mechanism of densified biomass. *Biomass and Bioenergy*, 98. https://doi.org/10.1016/j.biombioe.2017.01.002
- Huang, Y., Finell, M., Larsson, S., Wang, X., Zhang, J., Wei, R., & Liu, L. (2017b). Biofuel pellets made at low moisture content Influence of water in the binding mechanism of densified biomass. *Biomass and Bioenergy*, 98, 8–14. https://doi.org/10.1016/j.biombioe.2017.01.002
- Isemin, R., Mikhalev, A., Klimov, D., Grammelis, P., Margaritis, N., Kourkoumpas, D. S., & Zaichenko, V. (2017). Torrefaction and combustion of pellets made of a mixture of coal sludge and straw. *Fuel*, *210*. https://doi.org/10.1016/j.fuel.2017.09.032
- Islam, M. T., Saha, N., Hernandez, S., Klinger, J., & Reza, M. T. (2021). Integration of air classification and hydrothermal carbonization to enhance energy recovery of corn stover. *Energies*, 14(5). https://doi.org/10.3390/en14051397
- Islas, J., Manzini, F., Masera, O., & Vargas, V. (2018). Solid biomass to heat and power. In *The Role of Bioenergy in the Emerging Bioeconomy: Resources, Technologies, Sustainability and Policy*. Elsevier Inc. https://doi.org/10.1016/B978-0-12-813056-8.00004-2
- J. A., J., A., T., & E. E., K. (2019). A Review of Pellet Production from Biomass Residues as Domestic Fuel. *International Journal of Environment, Agriculture and Biotechnology*, 4(3), 835–842. https://doi.org/10.22161/ijeab/4.3.34
- Johnson, J. M. F. (2019). A "soil lorax" perspective on corn stover for advanced biofuels. *Agronomy Journal*, *111*(1). https://doi.org/10.2134/agronj2018.02.0093
- Jungmeier, G. (2017). The Biorefinery Fact Sheet. *The International Journal of Life Cycle Assessment*, 23(1).
- Kaliyan, N., & Vance Morey, R. (2009). Factors affecting strength and durability of densified biomass products. In *Biomass and Bioenergy* (Vol. 33, Issue 3). https://doi.org/10.1016/j.biombioe.2008.08.005
- Kantová, N. Č., Belány, P., Holubčík, M., & Čaja, A. (2022). Energy Consumption Depending on the Durability of Pellets Formed from Sawdust with an Admixture of FFP2 Masks. *Energies*, 15(13). https://doi.org/10.3390/en15134813
- Kažimírová, V., & Opáth, R. (2016). Biomass combustion emissions. *Research in Agricultural Engineering*, 62, S61–S65. https://doi.org/10.17221/69/2015-RAE
- Kers, J., Kulu, P., Aruniit, A., Laurmaa, V., Križan, P., Šooš, L., & Kask, Ü. (2010). Determination of physical, mechanical and burning characteristics of polymeric waste material briquettes. *Estonian Journal of Engineering*, *16*(4). https://doi.org/10.3176/eng.2010.4.06

- Khanna, M., & Paulson, N. (2016). To Harvest Stover or Not: Is it Worth it? *Farmdoc Daily*, 6(32).
- Khazraie Shoulaifar, T., Demartini, N., Karlström, O., & Hupa, M. (2016). Impact of organically bonded potassium on torrefaction: Part 1. Experimental. *Fuel*, *165*. https://doi.org/10.1016/j.fuel.2015.06.024
- Kiang, Y. H. (2018). Fuel Property Estimation and Combustion Process Characterization: Conventional Fuels, Biomass, Biocarbon, Waste Fuels, Refuse Derived Fuel, and Other Alternative Fuels. In Fuel Property Estimation and Combustion Process Characterization: Conventional Fuels, Biomass, Biocarbon, Waste Fuels, Refuse Derived Fuel, and Other Alternative Fuels.
- Kida, M., Ziembowicz, S., & Koszelnik, P. (2023). Influence of microplastic decomposition conditions on the emission of substances harmful to the environment. *Desalination and Water Treatment*, 288. https://doi.org/10.5004/dwt.2023.29373
- Kim, G. M., Lee, D. G., & Jeon, C. H. (2019). Fundamental characteristics and kinetic analysis of lignocellulosic woody and herbaceous biomass fuels. *Energies*, 12(6). https://doi.org/10.3390/en12061008
- Knapczyk, A., Francik, S., Fraczek, J., & Slipek, Z. (2019). Analysis of research trends in production of solid biofuels. *Engineering for Rural Development*, 18, 1503–1509. https://doi.org/10.22616/ERDev2019.18.N415
- Koondhar, M. A., Tan, Z., Alam, G. M., Khan, Z. A., Wang, L., & Kong, R. (2021). Bioenergy consumption, carbon emissions, and agricultural bioeconomic growth: A systematic approach to carbon neutrality in China. *Journal of Environmental Management*, 296. https://doi.org/10.1016/j.jenvman.2021.113242
- Kosore, C. M., Ojwang, L., Maghanga, J., Kamau, J., Shilla, D., Everaert, G., Khan, F. R., & Shashoua, Y. (2022). Microplastics in Kenya's marine nearshore surface waters: Current status. *Marine Pollution Bulletin*, 179. https://doi.org/10.1016/j.marpolbul.2022.113710
- Kota, K. B., Shenbagaraj, S., Sharma, P. K., Sharma, A. K., Ghodke, P. K., & Chen, W. H. (2022). Biomass torrefaction: An overview of process and technology assessment based on global readiness level. *Fuel*, *324*. https://doi.org/10.1016/j.fuel.2022.124663
- Krishnan, R., Hauchhum, L., Gupta, R., & Pattanayak, S. (2019). Prediction of Equations for Higher Heating Values of Biomass Using Proximate and Ultimate Analysis. 2nd International Conference on Energy, Power and Environment: Towards Smart Technology, ICEPE 2018, June. https://doi.org/10.1109/EPETSG.2018.8658984
- Krishniah, K., Shahabudeen, P., Krishnaiah, K., & Shahabudeen, P. (2012). Applied design of experiments and Taguchi methods. In *e-Book EEE*.

- Križan, P., Svátek, M., Matúš, M., Beniak, J., & Lisý, M. (2014). Determination of compacting pressure and pressing temperature impact on biomass briquettes density and their mutual interactions. *International Multidisciplinary Scientific GeoConference Surveying Geology and Mining Ecology Management, SGEM*, 1(4). https://doi.org/10.5593/sgem2014/b41/s17.018
- Kumar, L., Koukoulas, A. A., Mani, S., & Satyavolu, J. (2017). Integrating torrefaction in the wood pellet industry: A critical review. In *Energy and Fuels* (Vol. 31, Issue 1). https://doi.org/10.1021/acs.energyfuels.6b02803
- Kwapong, N. A. (2023). Biomass Pelletisation: Influence of biomass characteristics on pellet quality.
- Lam, P. S., Lam, P. Y., Sokhansanj, S., Bi, X. T., & Lim, C. J. (2013). Mechanical and compositional characteristics of steam-treated Douglas fir (Pseudotsuga menziesii L.) during pelletization. *Biomass and Bioenergy*, 56. https://doi.org/10.1016/j.biombioe.2013.05.001
- Lam, P. S., Sokhansanj, S., Bi, X., Lim, C. J., & Melin, S. (2011). Energy input and quality of pellets made from steam-exploded douglas fir (Pseudotsuga menziesii). *Energy and Fuels*, 25(4). https://doi.org/10.1021/ef101683s
- Lam, P. S., Sokhansanj, S., Bi, X. T., Lim, C. J., & Larsson, S. H. (2012). Drying characteristics and equilibrium moisture content of steam-treated Douglas fir (Pseudotsuga menziesii L.). *Bioresource Technology*, 116. https://doi.org/10.1016/j.biortech.2012.03.093
- Larsson, S. H., & Samuelsson, R. (2017). Prediction of ISO 17831-1:2015 mechanical biofuel pellet durability from single pellet characterization. *Fuel Processing Technology*, 163. https://doi.org/10.1016/j.fuproc.2017.04.004
- Lavergne, S., Larsson, S. H., Da Silva Perez, D., Marchand, M., Campargue, M., & Dupont, C. (2021). Effect of process parameters and biomass composition on flat-die pellet production from underexploited forest and agricultural biomass. *Fuel*, *302*. https://doi.org/10.1016/j.fuel.2021.121076
- Lee, J. Y., Kim, C. H., Sung, Y. J., Nam, H. G., Park, H. H., Kwon, S., Park, D. H., Joo, S. Y., Yim, H. T., Lee, M. S., & Kim, S. Bin. (2016). Study of oil palm biomass resources (part 5) Torrefaction of pellets made from oil palm biomass. *Palpu Chongi Gisul/Journal of Korea Technical Association of the Pulp and Paper Industry*, 48(2). https://doi.org/10.7584/ktappi.2016.48.2.034
- Lehmann, B., Schröder, H. W., Wollenberg, R., & Repke, J. U. (2012). Effect of miscanthus addition and different grinding processes on the quality of wood pellets. *Biomass and Bioenergy*, 44, 150–159. https://doi.org/10.1016/j.biombioe.2012.05.009
- Li, H., Liu, X., Legros, R., Bi, X. T., Jim Lim, C., & Sokhansanj, S. (2012). Pelletization of torrefied sawdust and properties of torrefied pellets. *Applied Energy*, 93. https://doi.org/10.1016/j.apenergy.2012.01.002

- Li, W., Dang, Q., Brown, R. C., Laird, D., & Wright, M. M. (2017). The impacts of biomass properties on pyrolysis yields, economic and environmental performance of the pyrolysis-bioenergy-biochar platform to carbon negative energy.

 Bioresource Technology, 241.** https://doi.org/10.1016/j.biortech.2017.06.049
- Li, Y. H., Lin, H. T., Xiao, K. L., & Lasek, J. (2018). Combustion behavior of coal pellets blended with Miscanthus biochar. *Energy*, *163*, 180–190. https://doi.org/10.1016/j.energy.2018.08.117
- Lim, C., Sokhansanj, S., Mani, S., & Berruti, F. (2017). Engineering Conferences International ECI Digital Archives Biochar: Production, Characterization and Applications Proceedings Physical properties of charred pellets after two months of storage Recommended Citation "Physical properties of charred pellets after two months of storage" in "Biochar: Production, Characterization and. In *Symposium Series*. http://dc.engconfintl.org/biochar/53
- Lima, L. V. L., de Castro, V. R., Surdi, P. G., Zanuncio, A. J. V., Zanuncio, J. C., Carneiro, A. de C. O., Gominho, J., & Araújo, S. de O. (2023). Properties of Pinus sp. Pellets Prepared after In-line Pre-compaction with Torrefaction. *BioResources*, 18(2). https://doi.org/10.15376/biores.18.2.3440-3451
- Liu, D., Teng, D., Zhu, Y., Wang, X., & Wang, H. (2023). Optimization of Process Parameters for Pellet Production from Corn Stalk Rinds Using Box–Behnken Design. *Energies*, 16(12), 4796. https://doi.org/10.3390/en16124796
- Liu, J., Jiang, X., Yuan, Y., Chen, H., Zhang, W., Cai, H., & Gao, F. (2022). Densification of Yak Manure Biofuel Pellets and Evaluation of Parameters: Effects on Properties. *Energies*, 15(5), 1–14. https://doi.org/10.3390/en15051621
- Liu, X., Feng, X., Huang, L., & He, Y. (2020). Rapid determination of wood and rice husk pellets proximate analysis and heating value. *Energies*, 13(14), 1–12. https://doi.org/10.3390/en13143741
- Lu, D., Tabil, L. G., Wang, D., Wang, G., & Emami, S. (2014). Experimental trials to make wheat straw pellets with wood residue and binders. *Biomass and Bioenergy*, 69. https://doi.org/10.1016/j.biombioe.2014.07.029
- Lunguleasa, A., Ayrilmis, N., Spirchez, C., & Croitoru, C. (2019). Increasing the calorific properties of sawdust waste from pellets by torrefaction. *BioResources*, 14(4). https://doi.org/10.15376/biores.14.4.7821-7839
- Lynam, J. G., Coronella, C. J., Yan, W., Reza, M. T., & Vasquez, V. R. (2011). Acetic acid and lithium chloride effects on hydrothermal carbonization of lignocellulosic biomass. *Bioresource Technology*, 102(10). https://doi.org/10.1016/j.biortech.2011.02.035
- Ma, J., Feng, S., Shen, X., Zhang, Z., Wang, Z., Kong, W., Yuan, P., Shen, B., & Mu, L. (2021). Integration of the pelletization and combustion of biodried products derived from municipal organic wastes: The influences of compression temperature and pressure. *Energy*, 219. https://doi.org/10.1016/j.energy.2020.119614

- Mabee, W. E., Gregg, D. J., Arato, C., Berlin, A., Bura, R., Gilkes, N., Mirochnik, O., Pan, X., Pye, E. K., & Saddler, J. N. (2007). Updates on Softwood-to-Ethanol Process Development. In *Twenty-Seventh Symposium on Biotechnology for Fuels and Chemicals*. https://doi.org/10.1007/978-1-59745-268-7_5
- Malaťák, J., & Passian, L. (2011). Heat-emission analysis of small combustion equipments for biomass. *Research in Agricultural Engineering*, 57(2). https://doi.org/10.17221/28/2010-rae
- Manouchehrinejad, M., & Mani, S. (2018). Torrefaction after pelletization (TAP): Analysis of torrefied pellet quality and co-products. *Biomass and Bioenergy*, 118. https://doi.org/10.1016/j.biombioe.2018.08.015
- Mansor, A. M., Lim, J. S., Ani, F. N., Hashim, H., & Ho, W. S. (2018). Ultimate and proximate analysis of Malaysia pineapple biomass from MD2 cultivar for biofuel application. *Chemical Engineering Transactions*, 63. https://doi.org/10.3303/CET1863022
- Matúš, M., Križan, P., Šooš, Ľ., & Beniak, J. (2015). Effects of Initial Moisture Content on the Physical and Mechanical Properties of Norway Spruce Briquettes. *International Journal of Environmental and Ecological Engineering*, 9(10).
- Mechanical durability and combustion characteristics of pellets from biomass blends M.V. Gil, P. Oulego, M.D. Casal, C. Pevida, J.J. Pis, F. Rubiera *. (n.d.). 1–33.
- Medic, D., Darr, M., Shah, A., Potter, B., & Zimmerman, J. (2012). Effects of torrefaction process parameters on biomass feedstock upgrading. *Fuel*, *91*(1). https://doi.org/10.1016/j.fuel.2011.07.019
- Mei, Y., Liu, R., Yang, Q., Yang, H., Shao, J., Draper, C., Zhang, S., & Chen, H. (2015). Torrefaction of cedarwood in a pilot scale rotary kiln and the influence of industrial flue gas. *Bioresource Technology*, 177. https://doi.org/10.1016/j.biortech.2014.10.113
- Mladenović, M., Paprika, M., & Marinković, A. (2018). Denitrification techniques for biomass combustion. In *Renewable and Sustainable Energy Reviews* (Vol. 82). https://doi.org/10.1016/j.rser.2017.10.054
- Moayedi, H., Osouli, A., Bui, D. T., Kok Foong, L., Nguyen, H., & Kalantar, B. (2019). Two novel neural-evolutionary predictive techniques of dragonfly algorithm (DA) and biogeography-based optimization (BBO) for landslide susceptibility analysis. *Geomatics, Natural Hazards and Risk*, 10(1), 2429–2453. https://doi.org/10.1080/19475705.2019.1699608
- Mohamed, S. A. N., Zainudin, E. S., Sapuan, S. M., Deros, M. A. M., & Arifin, A. M. T. (2019). Integration of Taguchi-Grey relational analysis technique in parameter process optimization for rice husk composite. *BioResources*, *14*(1). https://doi.org/10.15376/biores.14.1.1110-1126
- Mohammadi, A., & Anukam, A. I. (2023). *Energy production features of Miscanthus pellets blended with Pine sawdust*. 1–19.

- Moriana, R., Vilaplana, F., & Ek, M. (2015). Forest residues as renewable resources for bio-based polymeric materials and bioenergy: chemical composition, structure and thermal properties. *Cellulose*, *22*(5). https://doi.org/10.1007/s10570-015-0738-4
- Mostafa, M. E., Hu, S., Wang, Y., Su, S., Hu, X., Elsayed, S. A., & Xiang, J. (2019a). The significance of pelletization operating conditions: An analysis of physical and mechanical characteristics as well as energy consumption of biomass pellets. *Renewable and Sustainable Energy Reviews*, 105(January), 332–348. https://doi.org/10.1016/j.rser.2019.01.053
- Mostafa, M. E., Hu, S., Wang, Y., Su, S., Hu, X., Elsayed, S. A., & Xiang, J. (2019b). The significance of pelletization operating conditions: An analysis of physical and mechanical characteristics as well as energy consumption of biomass pellets. *Renewable and Sustainable Energy Reviews*, 105(January), 332–348. https://doi.org/10.1016/j.rser.2019.01.053
- Mostafa, M. E., Xu, J., Zhou, J., Chi, H., Hu, S., Wang, Y., Su, S., Elsayed, S. A., & Xiang, J. (2021a). Optimization and statistical analysis of the effect of main operation conditions on the physical characteristics of solid and hollow cylindrical pellets. *Biomass Conversion and Biorefinery*. https://doi.org/10.1007/s13399-021-01541-7
- Mostafa, M. E., Xu, J., Zhou, J., Chi, H., Hu, S., Wang, Y., Su, S., Elsayed, S. A., & Xiang, J. (2021b). Optimization and statistical analysis of the effect of main operation conditions on the physical characteristics of solid and hollow cylindrical pellets. *Biomass Conversion and Biorefinery*. https://doi.org/10.1007/s13399-021-01541-7
- Mostazur Rahman, M., Aminul Haque, M., Akter, N., Shah Jamal, M., & Hossain, M. (2022). *Production of Biomass Pellets from Sawdust to Enhance Fuel Eciency*. https://doi.org/10.21203/rs.3.rs-1903314/v1
- Mugo Ephantus, Kinyua Robert, & Njogu Paul. (2015). An Analysis of Solid Waste Generation and Characterization in Thika Municipality of Kiambu County, Kenya. *Journal of Environmental Science and Engineering B*, 4(4). https://doi.org/10.17265/2162-5263/2015.04.005
- Mukherjee, A., Okolie, J. A., Niu, C., & Dalai, A. K. (2022). Experimental and Modeling Studies of Torrefaction of Spent Coffee Grounds and Coffee Husk: Effects on Surface Chemistry and Carbon Dioxide Capture Performance. ACS Omega, 7(1). https://doi.org/10.1021/acsomega.1c05270
- Myburg, A. A., Grattapaglia, D., Tuskan, G. A., Hellsten, U., Hayes, R. D., Grimwood, J., Jenkins, J., Lindquist, E., Tice, H., Bauer, D., Goodstein, D. M., Dubchak, I., Poliakov, A., Mizrachi, E., Kullan, A. R. K., Hussey, S. G., Pinard, D., Van Der Merwe, K., Singh, P., ... Schmutz, J. (2014). The genome of Eucalyptus grandis. *Nature*, *510*(7505). https://doi.org/10.1038/nature13308
- Ndibe, C., Maier, J., & Scheffknecht, G. (2014). Combustion, cofiring and emissions characteristics of torrefied biomass in a drop tube reactor. *Biomass and Bioenergy*, 79. https://doi.org/10.1016/j.biombioe.2015.05.010

- Ndindeng, S. A., Mbassi, J. E. G., Mbacham, W. F., Manful, J., Graham-Acquaah, S., Moreira, J., Dossou, J., & Futakuchi, K. (2015). Quality optimization in briquettes made from rice milling by-products. *Energy for Sustainable Development*, 29. https://doi.org/10.1016/j.esd.2015.09.003
- Niedziółka, I., Szpryngiel, M., Kachel-Jakubowska, M., Kraszkiewicz, A., Zawiślak, K., Sobczak, P., & Nadulski, R. (2015). Assessment of the energetic and mechanical properties of pellets produced from agricultural biomass. *Renewable Energy*, 76, 312–317. https://doi.org/10.1016/j.renene.2014.11.040
- Nielsen, S. K., Mandø, M., & Rosenørn, A. B. (2020). Review of die design and process parameters in the biomass pelleting process. *Powder Technology*, *364*, 971–985. https://doi.org/10.1016/j.powtec.2019.10.051
- Nimmanterdwong, P., Chalermsinsuwan, B., & Piumsomboon, P. (2021). Prediction of lignocellulosic biomass structural components from ultimate/proximate analysis. *Energy*, 222, 119945. https://doi.org/10.1016/j.energy.2021.119945
- Nunes, L. J. R., Causer, T. P., & Ciolkosz, D. (2020). Biomass for energy: A review on supply chain management models. *Renewable and Sustainable Energy Reviews*, 120(December 2019), 109658. https://doi.org/10.1016/j.rser.2019.109658
- Nunes, L. J. R., Matias, J. C. O., & Catalão, J. P. S. (2014). A review on torrefied biomass pellets as a sustainable alternative to coal in power generation. *Renewable and Sustainable Energy Reviews*, 40, 153–160. https://doi.org/10.1016/j.rser.2014.07.181
- Nurek, T., Gendek, A., Roman, K., & Dabrowska, M. (2020). The impact of fractional composition on the mechanical properties of agglomerated logging residues. *Sustainability (Switzerland)*, 12(15). https://doi.org/10.3390/su12156120
- Obi, O. F., Pecenka, R., & Clifford, M. J. (2022). A Review of Biomass Briquette Binders and Quality Parameters. *Energies*, 15(7), 1–22. https://doi.org/10.3390/en15072426
- Odhiambo, O. R., Musalagani, A. C., Lyanda, N. J., & Ruth, S. J. (2014). the Plastic Waste Menace in Kenya: a Nairobi City Situation. *International Journal of Current Research*, March 2002.
- Onochie, U., Obanor, A., Aliu, S., & Igbodaro, O. (2017). PROXIMATE AND ULTIMATE ANALYSIS OF FUEL PELLETS FROM OIL PALM RESIDUES. *Nigerian Journal of Technology*, *36*(3). https://doi.org/10.4314/njt.v36i3.44
- Onyenwoke, C., Tabil, L. G., Mupondwa, E., Cree, D., & Adapa, P. (2023). Effect of Torrefaction on the Physiochemical Properties of White Spruce Sawdust for Biofuel Production. *Fuels*, 4(1). https://doi.org/10.3390/fuels4010008
- Ototo, G., & Vlosky, R. P. (2018). Overview of the forest sector in Kenya. In *Forest Products Journal* (Vol. 68, Issue 1). https://doi.org/10.13073/0015-7473.68.1.4
- Park, S., Jeong, H. R., Shin, Y. A., Kim, S. J., Ju, Y. M., Oh, K. C., Cho, L. H., & Kim, D. (2021). Performance optimisation of fuel pellets comprising pepper stem and coffee grounds through mixing ratios and torrefaction. *Energies*, *14*(15). https://doi.org/10.3390/en14154667

- Park, S., Kim, S. J., Oh, K. C., Cho, L. H., & Kim, D. H. (2023). Developing a Proximate Component Prediction Model of Biomass Based on Element Analysis. *Energies*, 16(1), 1–17. https://doi.org/10.3390/en16010509
- Park, S., Kim, S. J., Oh, K. C., Cho, L., Kim, M. J., Jeong, I. S., Lee, C. G., & Kim, D. H. (2020). Investigation of agro-byproduct pellet properties and improvement in pellet quality through mixing. *Energy*, 190. https://doi.org/10.1016/j.energy.2019.116380
- Pellet Fuels Institute Standard Specifications for ResidentialCommercial Densified. (n.d.).
- Peng, J., Wang, J., Bi, X. T., Lim, C. J., Sokhansanj, S., Peng, H., & Jia, D. (2015). Effects of thermal treatment on energy density and hardness of torrefied wood pellets. *Fuel Processing Technology*, 129. https://doi.org/10.1016/j.fuproc.2014.09.010
- Perea-Moreno, M. A., Samerón-Manzano, E., & Perea-Moreno, A. J. (2019). Biomass as renewable energy: Worldwide research trends. *Sustainability (Switzerland)*, 11(3). https://doi.org/10.3390/su11030863
- Perez-Jimenez, J. A. (2015). Gaseous Emissions from the Combustion of Biomass Pellets. https://doi.org/10.2495/978-1-84566-062-8/006
- Picchio, R., Latterini, F., Venanzi, R., Stefanoni, W., Suardi, A., Tocci, D., & Pari, L. (2020a). Pellet production from woody and non-woody feedstocks: A review on biomass quality evaluation. *Energies*, *13*(11), 1–20. https://doi.org/10.3390/en13112937
- Picchio, R., Latterini, F., Venanzi, R., Stefanoni, W., Suardi, A., Tocci, D., & Pari, L. (2020b). Pellet production from woody and non-woody feedstocks: A review on biomass quality evaluation. *Energies*, *13*(11), 1–20. https://doi.org/10.3390/en13112937
- Popa, V. I. (2018). Biomass for Fuels and Biomaterials. In *Biomass as Renewable Raw Material to Obtain Bioproducts of High-Tech Value*. https://doi.org/10.1016/B978-0-444-63774-1.00001-6
- Pradhan, P., Mahajani, S. M., & Arora, A. (2018a). Production and utilization of fuel pellets from biomass: A review. *Fuel Processing Technology*, *181*(September), 215–232. https://doi.org/10.1016/j.fuproc.2018.09.021
- Pradhan, P., Mahajani, S. M., & Arora, A. (2018b). Production and utilization of fuel pellets from biomass: A review. *Fuel Processing Technology*, *181*(September), 215–232. https://doi.org/10.1016/j.fuproc.2018.09.021
- Prapakarn, N., Prapakarn, S., Liplap, P., & Arjharn, W. (2018). Effects of torrefaction temperature and residence time on agricultural residue after pelletization process: Corncobs/ cornhusks, rice straw, and sugarcane trash. *Suranaree Journal of Science and Technology*, 25(4).

- Prasongthum, N., Duangwongsa, N., Khowattana, P., Suemanotham, A., Wongharn, P., Thanmongkhon, Y., Reubroycharoen, P., & Attanatho, L. (2022). Influence of torrefaction on yields and characteristics of densified solid biofuel. *Journal of Physics: Conference Series*, 2175(1). https://doi.org/10.1088/1742-6596/2175/1/012027
- Puig-Arnavat, M., Shang, L., Sárossy, Z., Ahrenfeldt, J., & Henriksen, U. B. (2016). From a single pellet press to a bench scale pellet mill Pelletizing six different biomass feedstocks. *Fuel Processing Technology*, *142*, 27–33. https://doi.org/10.1016/j.fuproc.2015.09.022
- Rabier, F., Temmerman, M., Böhm, T., Hartmann, H., Daugbjerg Jensen, P., Rathbauer, J., Carrasco, J., & Fernández, M. (2006). Particle density determination of pellets and briquettes. *Biomass and Bioenergy*, 30(11). https://doi.org/10.1016/j.biombioe.2006.06.006
- Rahaman, S. A., & Salam, P. A. (2017). Characterization of cold densified rice straw briquettes and the potential use of sawdust as binder. *Fuel Processing Technology*, 158, 9–19. https://doi.org/10.1016/j.fuproc.2016.12.008
- Rajput, S. P., Jadhav, S. V., & Thorat, B. N. (2020). Methods to improve properties of fuel pellets obtained from different biomass sources: Effect of biomass blends and binders. *Fuel Processing Technology*, 199(July 2019). https://doi.org/10.1016/j.fuproc.2019.106255
- Ray, A. E., Li, C., Thompson, V. S., Daubaras, D. L., Nagle, N. J., & Hartley, D. S. (2017). Biomass Blending and Densification: Impacts on Feedstock Supply and Biochemical Conversion Performance. In *Biomass Volume Estimation and Valorization for Energy*. https://doi.org/10.5772/67207
- Rebbling, A., Sundberg, P., Fagerström, J., Carlborg, M., Tullin, C., Boström, D., Öhman, M., Boman, C., & Skoglund, N. (2020). Demonstrating Fuel Design to Reduce Particulate Emissions and Control Slagging in Industrial-Scale Grate Combustion of Woody Biomass. *Energy and Fuels*, 34(2). https://doi.org/10.1021/acs.energyfuels.9b03935
- Ren, S., Lei, H., Wang, L., Bu, Q., Wei, Y., Liang, J., Liu, Y., Julson, J., Chen, S., Wu, J., & Ruan, R. (2012). Microwave torrefaction of douglas fir sawdust pellets. *Energy and Fuels*, 26(9). https://doi.org/10.1021/ef300633c
- Ren, X., Sun, R., Meng, X., Vorobiev, N., Schiemann, M., & Levendis, Y. A. (2017). Carbon, sulfur and nitrogen oxide emissions from combustion of pulverized raw and torrefied biomass. *Fuel*, *188*. https://doi.org/10.1016/j.fuel.2016.10.017
- RESPONSE SURFACE METHODOLOGY. (2010).
- Rezaei, H., Yazdanpanah, F., Lim, C. J., & Sokhansanj, S. (2020). Pelletization properties of refuse-derived fuel Effects of particle size and moisture content. *Fuel Processing Technology*, 205. https://doi.org/10.1016/j.fuproc.2020.106437
- RicharddLSmith, Z., & Xiao-FeiiTian Editors, J. (n.d.). *Biofuels and Biorefi neries 9 Production of Materials from Sustainable Biomass Resources*. http://www.springer.com/series/11687

- Riva, L., Nielsen, H. K., Skreiberg, Ø., Wang, L., Bartocci, P., Barbanera, M., Bidini, G., & Fantozzi, F. (2019). Analysis of optimal temperature, pressure and binder quantity for the production of biocarbon pellet to be used as a substitute for coke. *Applied Energy*, 256. https://doi.org/10.1016/j.apenergy.2019.113933
- Rokni, E., Ren, X., Panahi, A., & Levendis, Y. A. (2018). Emissions of SO2, NOx, CO2, and HCl from Co-firing of coals with raw and torrefied biomass fuels. *Fuel*, *211*. https://doi.org/10.1016/j.fuel.2017.09.049
- Romuli, S., Karaj, S., Correa, C. R., Kruse, A., & Müller, J. (2021). Physico-mechanical properties and thermal decomposition characteristics of pellets from Jatropha curcas L. residues as affected by water addition. *Biofuels*, *12*(9), 1149–1156. https://doi.org/10.1080/17597269.2019.1594596
- Romyen, P., Pianroj, Y., Punvichai, T., Karrila, S., Chotikhun, A., & Jumrat, S. (2023). Utilization of Used Bleaching Clay in Pellet Fuel Production with Torrefied Oil Palm Fronds. *BioResources*, 18(4). https://doi.org/10.15376/biores.18.4.6986-7002
- Rozzi, E., Minuto, F. D., Lanzini, A., & Leone, P. (2020). Green synthetic fuels: Renewable routes for the conversion of non-fossil feedstocks into gaseous fuels and their end uses. *Energies*, 13(2). https://doi.org/10.3390/en13020420
- Ruan, R., Zhang, Y., Chen, P., Liu, S., Fan, L., Zhou, N., Ding, K., Peng, P., Addy, M., Cheng, Y., Anderson, E., Wang, Y., Liu, Y., Lei, H., & Li, B. (2019). Biofuels: Introduction. In *Biomass, Biofuels, Biochemicals: Biofuels: Alternative Feedstocks and Conversion Processes for the Production of Liquid and Gaseous Biofuels* (Issue x). https://doi.org/10.1016/B978-0-12-816856-1.00001-4
- Rudolfsson, M., Borén, E., Pommer, L., Nordin, A., & Lestander, T. A. (2017). Combined effects of torrefaction and pelletization parameters on the quality of pellets produced from torrefied biomass. *Applied Energy*, 191, 414–424. https://doi.org/10.1016/j.apenergy.2017.01.035
- Rudolfsson, M., Stelte, W., & Lestander, T. A. (n.d.). Process optimization of combined biomass torrefaction and pelletization for fuel pellet production A parametric study.
- Said, N., Abdel Daiem, M. M., García-Maraver, A., & Zamorano, M. (2015). Influence of densification parameters on quality properties of rice straw pellets. *Fuel Processing Technology*, *138*. https://doi.org/10.1016/j.fuproc.2015.05.011
- Samal, B., Vanapalli, K. R., Dubey, B. K., Bhattacharya, J., Chandra, S., & Medha, I. (2021). Char from the co-pyrolysis of Eucalyptus wood and low-density polyethylene for use as high-quality fuel: Influence of process parameters. Science of the Total Environment, 794. https://doi.org/10.1016/j.scitotenv.2021.148723
- Sánchez, J., Curt, M. D., Robert, N., & Fernández, J. (2018). Biomass resources. In *The Role of Bioenergy in the Emerging Bioeconomy: Resources, Technologies, Sustainability and Policy*. Elsevier Inc. https://doi.org/10.1016/B978-0-12-813056-8.00002-9

- Santana, H. H. S., Maier, G., & Ródenas, J. (2010). Diametral compression test: Analysing the H/D ratio influence on the mechanical resistance of UO2-green pellets. *Nuclear Instruments and Methods in Physics Research, Section A: Accelerators, Spectrometers, Detectors and Associated Equipment, 619*(1–3). https://doi.org/10.1016/j.nima.2009.10.114
- Sarker, T. R., Azargohar, R., Dalai, A. K., & Meda, V. (2021). Characteristics of torrefied fuel pellets obtained from co-pelletization of agriculture residues with pyrolysis oil. *Biomass and Bioenergy*, *150*. https://doi.org/10.1016/j.biombioe.2021.106139
- Sarker, T. R., Azargohar, R., Stobbs, J., Karunakaran, C., Meda, V., & Dalai, A. K. (2022). Complementary effects of torrefaction and pelletization for the production of fuel pellets from agricultural residues: A comparative study. *Industrial Crops and Products*, 181. https://doi.org/10.1016/j.indcrop.2022.114740
- Sarker, T. R., Nanda, S., Dalai, A. K., & Meda, V. (2021). A Review of Torrefaction Technology for Upgrading Lignocellulosic Biomass to Solid Biofuels. In *Bioenergy Research* (Vol. 14, Issue 2). https://doi.org/10.1007/s12155-020-10236-2
- Sarker, T. R., Nanda, S., Meda, V., & Dalai, A. K. (2023). Densification of waste biomass for manufacturing solid biofuel pellets: a review. In *Environmental Chemistry Letters* (Vol. 21, Issue 1). https://doi.org/10.1007/s10311-022-01510-0
- Serrano, C., Monedero, E., & Portero, H. (2011). Effect of moisture content, particle size and pine addition on quality parameters of barley straw pellets. January 2021. https://doi.org/10.1016/j.fuproc.2010.11.031
- Shang, L., Ahrenfeldt, J., Holm, J. K., Sanadi, A. R., Barsberg, S., Thomsen, T., Stelte, W., & Henriksen, U. B. (2012). Changes of chemical and mechanical behavior of torrefied wheat straw. *Biomass and Bioenergy*, 40, 63–70. https://doi.org/10.1016/j.biombioe.2012.01.049
- Shang, L., Nielsen, N. P. K., Dahl, J., Stelte, W., Ahrenfeldt, J., Holm, J. K., Thomsen, T., & Henriksen, U. B. (2012). Quality effects caused by torrefaction of pellets made from Scots pine. *Fuel Processing Technology*, 101. https://doi.org/10.1016/j.fuproc.2012.03.013
- Shao, J., Cheng, W., Zhu, Y., Yang, W., Fan, J., Liu, H., Yang, H., & Chen, H. (2019). Effects of Combined Torrefaction and Pelletization on Particulate Matter Emission From Biomass Pellet Combustion. *Energy and Fuels*, 33(9), 8777–8785. https://doi.org/10.1021/acs.energyfuels.9b01920
- Sharma, H. K., Xu, C., & Qin, W. (2019). Biological Pretreatment of Lignocellulosic Biomass for Biofuels and Bioproducts: An Overview. In *Waste and Biomass Valorization* (Vol. 10, Issue 2). https://doi.org/10.1007/s12649-017-0059-y

- Shen, G., Tao, S., Wei, S., Zhang, Y., Wang, R., Wang, B., Li, W., Shen, H., Huang, Y., Chen, Y., Chen, H., Yang, Y., Wang, W., Wei, W., Wang, X., Liu, W., Wang, X., & Simonich, S. L. M. (2012). Reductions in emissions of carbonaceous particulate matter and polycyclic aromatic hydrocarbons from combustion of biomass pellets in comparison with raw fuel burning. *Environmental Science and Technology*, 46(11). https://doi.org/10.1021/es300369d
- Silva, D. A. da, Hansted, A. L. S., Nakashima, G. T., Padilla, E. R. D., Pereira, J. C., & Yamaji, F. M. (2021). Volatile matter values change according to the standard utilized? *Research, Society and Development*, 10(12). https://doi.org/10.33448/rsd-v10i12.20476
- Sitek, T., Pospíšil, J., Poláčik, J., & Chýlek, R. (2021). Thermogravimetric analysis of solid biomass fuels and corresponding emission of fine particles. *Energy*, 237. https://doi.org/10.1016/j.energy.2021.121609
- Sivabalan, K., Hassan, S., Ya, H., & Pasupuleti, J. (2021). A review on the characteristic of biomass and classification of bioenergy through direct combustion and gasification as an alternative power supply. *Journal of Physics: Conference Series*, 1831(1). https://doi.org/10.1088/1742-6596/1831/1/012033
- Siyal, A. A., Liu, Y., Mao, X., Ali, B., Husaain, S., Dai, J., Zhang, T., Fu, J., & Liu, G. (2021). Characterization and quality analysis of wood pellets: effect of pelletization and torrefaction process variables on quality of pellets. *Biomass Conversion and Biorefinery*, 11(5). https://doi.org/10.1007/s13399-020-01235-6
- Siyal, A. A., Mao, X., Liu, Y., Ran, C., Fu, J., Kang, Q., Ao, W., Zhang, R., Dai, J., & Liu, G. (2020). Torrefaction subsequent to pelletization: Characterization and analysis of furfural residue and sawdust pellets. *Waste Management*, 113. https://doi.org/10.1016/j.wasman.2020.05.037
- Solid biofuels-Determination of mechanical durability of pellets and briquettes-Part 1:(E) ii COPYRIGHT PROTECTED DOCUMENT. (2015). www.iso.orgiTehSTANDARDPREVIEW
- Song, B., Cooke-Willis, M., Theobald, B., & Hall, P. (2021). Producing a high heating value and weather resistant solid fuel via briquetting of blended wood residues and thermoplastics. *Fuel*, 283. https://doi.org/10.1016/j.fuel.2020.119263
- Stasiak, M., Molenda, M., Bańda, M., Wiącek, J., Parafiniuk, P., & Gondek, E. (2017). Mechanical and combustion properties of sawdust—Straw pellets blended in different proportions. *Fuel Processing Technology*, *156*, 366–375. https://doi.org/10.1016/j.fuproc.2016.09.021
- Stelte, W., Holm, J. K., Sanadi, A. R., Barsberg, S., Ahrenfeldt, J., & Henriksen, U. B. (2011). Fuel pellets from biomass: The importance of the pelletizing pressure and its dependency on the processing conditions. *Fuel*, 90(11). https://doi.org/10.1016/j.fuel.2011.05.011
- Stelte, W., Sanadi, A. R., Shang, L., Holm, J. K., Ahrenfeldt, J., & Henriksen, U. B. (n.d.). *RECENT DEVELOPMENTS IN BIOMASS PELLETIZATION-A REVIEW*.

- Styks, J., Wróbel, M., Fraczek, J., & Knapczyk, A. (2020). Effect of compaction pressure and moisture content on quality parameters of perennial biomass pellets. *Energies*, *13*(8). https://doi.org/10.3390/en13081859
- Suman, S., Mohan Yadav, A., Tomar, N., & Bhushan, A. (2021). Combustion Characteristics and Behaviour of Agricultural Biomass: A Short Review. In *Renewable Energy Technologies and Applications*. https://doi.org/10.5772/intechopen.91398
- Sun, W., Wang, Y., He, H., & Sun, Y. (2023). Compression prediction from single pellet press to industrial production presses. *Powder Technology*, 427. https://doi.org/10.1016/j.powtec.2023.118719
- Teh, J. S., Teoh, Y. H., Idroas, M. Y., & How, H. G. (2022). Estimation of Higher heating Value of Biomass from Proximate and Ultimate Analysis: A Novel Approach. *Journal of Advanced Research in Fluid Mechanics and Thermal Sciences*, 94(2). https://doi.org/10.37934/arfmts.94.2.99109
- Thanapal, S. S., Chen, W., Annamalai, K., Carlin, N., Ansley, R. J., & Ranjan, D. (2014). Carbon dioxide torrefaction of woody biomass. *Energy and Fuels*, 28(2). https://doi.org/10.1021/ef4022625
- Thapa, S., & Engelken, R. (2020). Optimization of pelleting parameters for producing composite pellets using agricultural and agro-processing wastes by Taguchi-Grey relational analysis. *Carbon Resources Conversion*, 3(May), 104–111. https://doi.org/10.1016/j.crcon.2020.05.001
- Thapa, S., Mughal, M. A., Humphrey, K., & Engelken, R. (2018a). Optimization of Process Parameters in the Pelletization of Crop Residues By Taguchi-Grey Relational Analysis. *International Journal of Agriculture, Environment and Bioresearch*, 3(03).
- Thapa, S., Mughal, M. A., Humphrey, K., & Engelken, R. (2018b). Optimization of Process Parameters in the Pelletization of Crop Residues By Taguchi-Grey Relational Analysis. *International Journal of Agriculture, Environment and Bioresearch*, 3(03).
- Tomsej, T., Horak, J., Tomsejova, S., Krpec, K., Klanova, J., Dej, M., & Hopan, F. (2018). The impact of co-combustion of polyethylene plastics and wood in a small residential boiler on emissions of gaseous pollutants, particulate matter, PAHs and 1,3,5- triphenylbenzene. *Chemosphere*, 196. https://doi.org/10.1016/j.chemosphere.2017.12.127
- Tooyserkani, Z., Sokhansanj, S., Bi, X., Lim, C. J., Saddler, J., Lau, A., Melin, S., Lam, P. S., & Kumar, L. (2012). Effect of steam treatment on pellet strength and the energy input in pelleting of softwood particles. *Transactions of the ASABE*, 55(6). https://doi.org/10.13031/2013.42484
- Tu, P., Zhang, G., Wei, G., Li, J., Li, Y., Deng, L., & Yuan, H. (2022). Influence of pyrolysis temperature on the physicochemical properties of biochars obtained from herbaceous and woody plants. *Bioresources and Bioprocessing*, *9*(1). https://doi.org/10.1186/s40643-022-00618-z

- Tumuluru, J. S. (2014). Effect of process variables on the density and durability of the pellets made from high moisture corn stover. *Biosystems Engineering*, 119. https://doi.org/10.1016/j.biosystemseng.2013.11.012
- Tumuluru, J. S. (2019a). Effect of moisture content and hammer mill screen size on the briquetting characteristics of woody and herbaceous biomass. *KONA Powder and Particle Journal*, 36. https://doi.org/10.14356/kona.2019009
- Tumuluru, J. S. (2019b). Pelleting of pine and switchgrass blends: Effect of process variables and blend ratio on the pellet quality and energy consumption. *Energies*, 12(7). https://doi.org/10.3390/en12071198
- Tumuluru, J. S., & Fillerup, E. (2020). Briquetting characteristics of woody and herbaceous biomass blends: Impact on physical properties, chemical composition, and calorific value. *Biofuels, Bioproducts and Biorefining*, *14*(5). https://doi.org/10.1002/bbb.2121
- Tumuluru, J. S., Ghiasi, B., Soelberg, N. R., & Sokhansanj, S. (2021). Biomass Torrefaction Process, Product Properties, Reactor Types, and Moving Bed Reactor Design Concepts. *Frontiers in Energy Research*, 9. https://doi.org/10.3389/fenrg.2021.728140
- Tumuluru, J. S., Hess, J. R., Boardman, R. D., Wright, C. T., & Westover, T. L. (2012). Formulation, pretreatment, and densification options to improve biomass specifications for Co-firing high percentages with coal. In *Industrial Biotechnology* (Vol. 8, Issue 3). https://doi.org/10.1089/ind.2012.0004
- Tumuluru, J. S., Wright, C. T., Hess, J. R., & Kenney, K. L. (2011). A review of biomass densification systems to develop uniform feedstock commodities for bioenergy application. In *Biofuels, Bioproducts and Biorefining* (Vol. 5, Issue 6). https://doi.org/10.1002/bbb.324
- Tumuluru, J., Wright, C., Kenny, K., & Hess, R. (2010). A Riview on Biomass Densification Technologies for Energy Application. *Statewide Agricultural Land Use Baseline 2015*.
- Tursi, A. (2019). A review on biomass: Importance, chemistry, classification, and conversion. *Biofuel Research Journal*, 6(2), 962–979. https://doi.org/10.18331/BRJ2019.6.2.3
- Ungureanu, N., Vladut, V., Voicu, G., Dinca, M. N., & Zabava, B. S. (2018). Influence of biomass moisture content on pellet properties Review. *Engineering for Rural Development*, 17. https://doi.org/10.22616/ERDev2018.17.N449
- Vaish, S., Sharma, N. K., & Kaur, G. (2022). A review on various types of densification/briquetting technologies of biomass residues. *IOP Conference Series: Materials Science and Engineering*, 1228(1), 012019. https://doi.org/10.1088/1757-899x/1228/1/012019
- Valavanidis, A., Iliopoulos, N., Gotsis, G., & Fiotakis, K. (2008). Persistent free radicals, heavy metals and PAHs generated in particulate soot emissions and residue ash from controlled combustion of common types of plastic. *Journal of Hazardous Materials*, 156(1–3). https://doi.org/10.1016/j.jhazmat.2007.12.019

- Valdés, C. F., Marrugo, G., Chejne, F., Cogollo, K., & Vallejos, D. (2018). Pelletization of Agroindustrial Biomasses from the Tropics as an Energy Resource: Implications of Pellet Quality. *Energy and Fuels*, 32(11). https://doi.org/10.1021/acs.energyfuels.8b01673
- van der Stelt, M. J. C., Gerhauser, H., Kiel, J. H. A., & Ptasinski, K. J. (2011). Biomass upgrading by torrefaction for the production of biofuels: A review. In *Biomass and Bioenergy* (Vol. 35, Issue 9). https://doi.org/10.1016/j.biombioe.2011.06.023
- Velusamy, S., Subbaiyan, A., Kandasamy, S., Shanmugamoorthi, M., & Thirumoorthy, P. (2022). Combustion characteristics of biomass fuel briquettes from onion peels and tamarind shells. *Archives of Environmental and Occupational Health*, 77(3). https://doi.org/10.1080/19338244.2021.1936437
- Vinterbäck, J. (2004). Pellets 2002: The first world conference on pellets. *Biomass and Bioenergy*, 27(6). https://doi.org/10.1016/j.biombioe.2004.05.005
- Wang, C., Peng, J., Li, H., Bi, X. T., Legros, R., Lim, C. J., & Sokhansanj, S. (2013). Oxidative torrefaction of biomass residues and densification of torrefied sawdust to pellets. *Bioresource Technology*, 127. https://doi.org/10.1016/j.biortech.2012.09.092
- Wang, C., Zhang, X., Liu, Q., Zhang, Q., Chen, L., & Ma, L. (2020). A review of conversion of lignocellulose biomass to liquid transport fuels by integrated refining strategies. In *Fuel Processing Technology* (Vol. 208). https://doi.org/10.1016/j.fuproc.2020.106485
- Wang, L., Riva, L., Skreiberg, Ø., Khalil, R., Bartocci, P., Yang, Q., Yang, H., Wang, X., Chen, D., Rudolfsson, M., & Nielsen, H. K. (2020). Effect of torrefaction on properties of pellets produced from woody biomass. *Energy and Fuels*, *34*(12), 15343–15354. https://doi.org/10.1021/acs.energyfuels.0c02671
- Wang, Y., Qin, R., Cheng, H., Liang, T., Zhang, K., Chai, N., Gao, J., Feng, Q., Hou, M., Liu, J., Liu, C., Zhang, W., Fang, Y., Huang, J., & Zhang, F. (2022). Can Machine Learning Algorithms Successfully Predict Grassland Aboveground Biomass? *Remote Sensing*, 14(16). https://doi.org/10.3390/rs14163843
- Wang, Z., Lei, T., Chang, X., Shi, X., Xiao, J., Li, Z., He, X., Zhu, J., & Yang, S. (2015). Optimization of a biomass briquette fuel system based on grey relational analysis and analytic hierarchy process: A study using cornstalks in China. *Applied Energy*, 157. https://doi.org/10.1016/j.apenergy.2015.04.079
- Wattana, W., Phetklung, S., Jakaew, W., Chumuthai, S., Sriam, P., & Chanurai, N. (2017). Characterization of Mixed Biomass Pellet Made from Oil Palm and Pararubber Tree Residues. *Energy Procedia*, 138. https://doi.org/10.1016/j.egypro.2017.10.218
- Wei, W., Zhang, W., Hu, D., Ou, L., Tong, Y., Shen, G., Shen, H., & Wang, X. (2012). Emissions of carbon monoxide and carbon dioxide from uncompressed and pelletized biomass fuel burning in typical household stoves in China. *Atmospheric Environment*, 56. https://doi.org/10.1016/j.atmosenv.2012.03.060

- Whittaker, C., & Shield, I. (2017). Factors affecting wood, energy grass and straw pellet durability A review. In *Renewable and Sustainable Energy Reviews* (Vol. 71, pp. 1–11). Elsevier Ltd. https://doi.org/10.1016/j.rser.2016.12.119
- Williams, C. L., Emerson, R. M., & Tumuluru, J. S. (2017). Biomass Compositional Analysis for Conversion to Renewable Fuels and Chemicals. In *Biomass Volume Estimation and Valorization for Energy*. https://doi.org/10.5772/65777
- Williams, C. L., Westover, T. L., Emerson, R. M., Tumuluru, J. S., & Li, C. (2016). Sources of Biomass Feedstock Variability and the Potential Impact on Biofuels Production. In *Bioenergy Research* (Vol. 9, Issue 1). https://doi.org/10.1007/s12155-015-9694-y
- Xing, J., Luo, K., Wang, H., & Fan, J. (2019). Estimating biomass major chemical constituents from ultimate analysis using a random forest model. *Bioresource Technology*, 288. https://doi.org/10.1016/j.biortech.2019.121541
- Xing, J., Luo, K., Wang, H., Gao, Z., & Fan, J. (2019). A comprehensive study on estimating higher heating value of biomass from proximate and ultimate analysis with machine learning approaches. *Energy*, *188*, 116077. https://doi.org/10.1016/j.energy.2019.116077
- Younis, M., Alnouri, S. Y., Abu Tarboush, B. J., & Ahmad, M. N. (2018). Renewable biofuel production from biomass: a review for biomass pelletization, characterization, and thermal conversion techniques. *International Journal of Green Energy*, 15(13), 837–863. https://doi.org/10.1080/15435075.2018.1529581
- Yu, S., Park, J., Kim, M., Kim, H., Ryu, C., Lee, Y., Yang, W., & Jeong, Y. G. (2019). Improving Energy Density and Grindability of Wood Pellets by Dry Torrefaction. *Energy and Fuels*, 33(9). https://doi.org/10.1021/acs.energyfuels.9b01086
- Zabed, H. M., Akter, S., Yun, J., Zhang, G., Zhao, M., Mofijur, M., Awasthi, M. K., Kalam, M. A., Ragauskas, A., & Qi, X. (2023). Towards the sustainable conversion of corn stover into bioenergy and bioproducts through biochemical route: Technical, economic and strategic perspectives. *Journal of Cleaner Production*, 400. https://doi.org/10.1016/j.jclepro.2023.136699
- Zafari, A., & Kianmehr, M. H. (2012). Effect of raw material properties and die geometry on the density of biomass pellets from composted municipal solid waste. *BioResources*, 7(4). https://doi.org/10.15376/biores.7.4.4704-4714
- Zamorano, M., Popov, V., Rodríguez, M. L., & García-Maraver, A. (2011). A comparative study of quality properties of pelletized agricultural and forestry lopping residues. *Renewable Energy*, 36(11). https://doi.org/10.1016/j.renene.2011.03.020
- Zeng, T., Pollex, A., Weller, N., Lenz, V., & Nelles, M. (2018). Blended biomass pellets as fuel for small scale combustion appliances: Effect of blending on slag formation in the bottom ash and pre-evaluation options. *Fuel*, *212*(September 2016), 108–116. https://doi.org/10.1016/j.fuel.2017.10.036

- Zeng, T., Weller, N., Pollex, A., & Lenz, V. (2016). Blended biomass pellets as fuel for small scale combustion appliances: Influence on gaseous and total particulate matter emissions and applicability of fuel indices. *Fuel*, *184*. https://doi.org/10.1016/j.fuel.2016.07.047
- Zepeda-Cepeda, C. O., Goche-Télles, J. R., Palacios-Mendoza, C., Moreno-Anguiano, O., Núñez-Retana, V. D., Heya, M. N., & Carrillo-Parra, A. (2021). Effect of sawdust particle size on physical, mechanical, and energetic properties of pinus durangensis briquettes. *Applied Sciences (Switzerland)*, 11(9). https://doi.org/10.3390/app11093805
- Zhai, J., Burke, I. T., Mayes, W. M., & Stewart, D. I. (2021). New insights into biomass combustion ash categorisation: A phylogenetic analysis. *Fuel*, 287. https://doi.org/10.1016/j.fuel.2020.119469
- Zhang, X., Gao, B., Zhao, S., Wu, P., Han, L., & Liu, X. (2020). Optimization of a "coal-like" pelletization technique based on the sustainable biomass fuel of hydrothermal carbonization of wheat straw. *Journal of Cleaner Production*, 242. https://doi.org/10.1016/j.jclepro.2019.118426

APPENDICES

Appendix 1: Biomass pelleting optimization studies

	Г 1 / 1	D 11 /: / 1 :	G(4' 4' 14 1	0 1:1:	O 1'4 C 11 4	D. C.
Sr. No.	Feedstock	Pelleting technique	Statistical tool	Optimum conditions	Quality of pellet	References
1	Rice straw	Single pellet press (SPP)	Response surface method using multi-objective optimization approach.	72.76 MPa, 110°C, and 7.23% moisture for solid pellets.	Higher pellet quality	(Mostafa et al., 2021a)
2	Rice straw	Flat-die pellet mill	Full factorial design	2% starch additive, 17% moisture content, die temperature<50°C and die size 8/32mm/mm (8mm diameter and 32mm compression length).	and most pellet qualities met set	(Said et al., 2015)
3	Birch, Spruce	SPP	Regression analysis Regression analysis	6.1%moisture, 300MPa and 400MPa. 5.1%moisture, 300MPa	Pellet density, strength and moisture met set standards	(Huang et al., 2017a)
4	Reed canary grass Wheat straw	SPP	Regression analysis Box-Behnken design	5.2% moisture, 300MPa 35 days for <i>Phanerochaete</i> chrysosporium (PC) and 21days for g <i>Trametes</i> versicolor 52J (TV52J) fungal treatments	Pellet density, dimensional integrity and tensile strength met the set standards	(Gao et al., 2017)
5	Biochar, sawdust and water	Pellet mill (unspecified type)	Box-Behnken design	40% biochar, 30% sawdust and 30%moisture	Higher pellet durability and heating value	(Bartocci et al., 2018)

7	Rice straw, wheat straw and cornstover	Flat die pellet mill	Taguchi-grey relational analysis	Order of parameters from those resulting in greatest effect are binder proportion>binder type>residue type>particle size	Improved overall pellet quality	(Thapa et al., 2018a)
8	Corn stalk rinds	SPP	Box-Behnken design	0.5mm particle size, 11.35% moisture, 125.7 ^o C and 154.2MPa	1639.61 kg/m³ Relaxed density, 97.95% durability and 10.18 MPa compressive strength.	(Liu et al., 2023)
9	Bagasse		Box-Behnken design	Biomass composition, molasses concentration and drying time	16.43 MJ kg ⁻¹ higher heating values and 84.2% durability	(Akbar et al., 2021)

Appendix 2: Literature review matrix: Summary and gaps

S. NO.	AUTHOR & YEAR	METHODS	KEY RESULTS OR FINDINGS	GAPS	OBJEC TIVE
1	Bianca M A et al 2022	Flat die pellet mill. Co-pelleting Eucalyptus and corn residues. Proportions of corn residue in the mixture were 0, 20, 25, and 30% (w/w) while that of Kraft lignin 0%,2 and 5%(w/w).	20% of corn residue improved physical and mechanical pellet quality, with or without Kraft lignin addition.	Torrefaction and optimization (variables like corn stover and Kraft lignin). Pellet quality standards.	3, 4 & 5
2	Sunny V et al 2019	Reviewed densification techniques and preptreatment method of solid biomass fuels.	Densification technologies: Screw compaction/extruder, piston press/pump machine, roller press and pellet mills. Pretreatment techniques:Torrefaction, steam explosion, ammonia fiber freeze, grinding and preheating.	Post pelletization processes and pellet quality standards. SPP not used. LLDPE binder not used.	3 & 4
3	Stasiak M et al 2017	Pine sawdust, wheat straw and rapeseed straw blended in different proportions. Starch used as binder.	Mechanical and combustion parameters are proportion-dependent. Durability decreased with increase in starch.Pellet strength decreased with the addition of ground straw. Decrease in heat of combustion with an increase in straw.	Torrefaction and optimization. Pellet standards.	3, 4 & 5
4	Agu O et al 2018	Studied effect of different binders on strength and durability, dimensional stability, and pellet density	Organic and inorganic binders improved pellet quality especially biomass with lower lignin content.	Torrefaction and optimization. Pellet standards.	3, 4 & 5
5	Manar Y. et al 2018	Effect of raw material properties on the pellet's durability and bulk density. Binding mechanisms, types of binders and their effect on the pellet's durability.	Pellet durability above 80% is high and bulk density should be above 500kg/m3.	Torrefaction and optimization. Pellet standards.	3, 4 & 5
6	Rodolfo P et al 2020	Bibliographic analysis of papers on pellet quality evaluation and improvement for five years (2016–2020).	Wood pellets have higher quality than agro- pellets.Blending and using binders improves pellet quality, but their use must be evaluated on a case-by-case basis.	Pellet process parameters. LLDPE.	3

	Xuyang C et al 2021	Co-pelletization technology. Influence of chemical composition on different biomass matrix feedstocks and pelletizing operating parameters.	Natural chemical fraction of biomass influences pelletizing process and fuel quality. Co-pelletizing can be divided into biomass-biomass co-pelletizing and biomass-non-biomass.	Torrefaction and optimization.	3 & 5
	Tumuluru, 2014	Flat die pellet mill; feedstock moisture content in the range of 28-38%.; die speed of 40-60 Hz, and preheating temperatures of 30-110 deg.; particle size 4.8 mm; 8 mm pellet die.		die thickness; pressure gap; feedstock composition; pretreatment/post- treatment; binders; Pellet standards.	3 & 4
	Theerarattanan oon et al., 2011	Ring die pellet mill; effect of moisture content,hammer mill screen size and die thickness on bulk density, true density, and durability of the pellets.	Increased moisture, larger hammer mill screen size (3.2-6.5 mm) and thicker die size (31.8-44.5 mm) resulted in decreased bulk density, true density & durability.	Effect of torrefaction on pellet properties and optimization. Pellet standards.	2 & 4
10	XU et al, 2018	Studied energy consumption, relaxed density, compressive strength, durability, moisture absorption and surface structure of pellets.	Energy used in forming binder-free cornstalks was the lowest at 4.5N per 20MPa increase. Diatomite has a significant effect on the relaxation density test and the compressive strength test	LLDPE binder not tested and post- pelletization processes.	2 & 4
	Obiora et al, 2018	Study of the effect of different binders on different biomass materials pellets.	Combining organic and inorganic binders improves pellet quality. Each binder results in unique physical characteristics when applied with different biomass.	Emissions and optimizations.	3 & 4
	, J., & Lertsatitthanak	Production and investigation of pellet properties from mixing ratio of eucalyptus bark: mangosteen shell: papaya peel and binder.	Mixing ratio had no obvious influence on density and mechanical properties of the pellets. Binders had strong effect on performances of the combustion system.	Torrefaction and optimization. Pellet standards.	2 & 4
	Thapa, S., & Engelken, R. (2020)	Investigation of Moisture, binders, blending ratio, particle size, and principle feedstock material on the effect of physical and thermochemical characteristics of pellets.	Sawdust blended pellets have larger bulk density, durability, diametrical compressive strength (hardness), and heating value.	Review on post pelletization processes and pellet quality standards. LLDPE binder not used.	2

14	Harun, N. Y., & Afzal, M. T. (2016)	Single unit pelletizer and temperature controlled die was employed to produce a blended pellet.	Pellets made from feedstock with lower particle size (150-300 μm) and blends exhibited improved qualities.	No study on pollutant emissions and optimizations.	3 & 4
15	Gil et al, 2010	Pellet blends from pine, chestnut and eucalyptus sawdust, cellulose residue, coffee husks and grape waste and from blends of biomass with two coals, bituminous and semianthracite, were produced from bench-top single pelletizer.	Chestnut and pine sawdust pellets exhibited the highest durability.	No study on pollutant emissions and optimizations. Binder.	3, 4 & 5
16	Tursi, 2019	Biomass classification, chemical characterization and conversion to usefull energy products.	Four major classes of biomass and thermochemical, biochemical, and physicochemical conversion methods.	Proximate and ultimate analysis and conversion of biomass to solid fuels not discussed.	1
17	Adeleke A et al 2021	Torrefaction, torrefaction technologies. The influence of temperature, residence time, particle sizes and gas flow rates on torrefied biomass.	Torrefaction as pretreatment process improves energy density, hydrophobic, moisture content and grindability.	Post pelletization processes and pellet standards. Binder. Torrefaction temperature on mass yield of pellets.	3
18	Djatkov et al., 2018	Particle size, moisture content, wood share, additives and pressing intensity studied.	5% extrusion ratio and 40% wood resulted in maximum quality thresholds. Moisture content influenced bulk density and mechanical durability of cornstover.	Torrefaction. LLDPE.	3
19	Younis et al, 2018	Studied pre-pelletization, pelletization and post-pelletization techniques. Also study of different feedstock conditions on pellet quality and discussion of various binders.	Optimum moisture content was 8-12%, particle size less than 5mm on pellet strength, durability and bulk density. Binders was varied.	Torrefaction as post-pelletization process. Emissions. LLDPE.	2 & 3
20	Pradhan P et al 2018	Review on pellet production procedure, pelletization process parameters and utilization.	Pre-processing techniques are size reduction, torrefaction, steam explosion, hydrothermal carbonation and biological treatment. Pellet process parameters are moisture content, particle size, feedstock composition and machine specific parameters.	Post-pelletization techniques and evaluation against commercial standards. LLDPE binder not studied.	3, 4 & 5

Appendix 3: Using cone and quarter sampling method described above at KIRDI in preparation for proximate analysis



Appendix 4: Using bomb calorimeter to determined HHV



Appendix 5 (a): Pellet particle density results (Y1)

RUN	Trials			Mean Y1	STDEV
NO.:	{Pellet pa	article density	(kg/m^3)		
	1	2	3		
1	966.2581	966.9817	965.3484	966.1961	0.8184
2	938.8534	938.2148	937.8088	938.2923	0.5266
3	933.4631	932.6910	931.7443	932.6328	0.8609
4	945.0816	944.5560	942.2722	943.9699	1.4936
5	985.2603	981.4728	982.5067	983.0799	1.9577
6	963.2021	963.1457	961.1717	962.5065	1.1563
7	945.5948	945.1444	944.4802	945.0731	0.5607
8	930.5273	931.1708	932.6396	931.4459	1.0827
9	928.6016	929.9248	926.6761	928.4008	1.6336
10	956.5375	955.7111	953.4356	955.2281	1.6064
11	943.2912	946.0681	945.3272	944.8955	1.4379
12	894.5304	892.4771	890.8672	892.6249	1.8360
13	833.2010	833.9387	831.1101	832.7499	1.4673
14	832.6210	831.9800	834.9621	833.1877	1.5697
15	826.9100	824.3432	825.9457	825.7330	1.2965
16	960.8576	957.5433	959.1130	959.1713	1.6579
17	951.8005	949.5208	948.7564	950.0259	1.5837
18	865.9221	865.5982	862.3887	864.6363	1.9533
19	866.1009	866.7499	868.2763	867.0424	1.1168
20	859.8909	860.1361	860.5187	860.1819	0.3164
21	993.5583	996.4260	995.4748	995.1530	1.4607
22	946.5011	947.8719	946.9773	947.1168	0.6960
23	901.5746	903.4728	902.9954	902.6809	0.9874
24	891.9513	890.8594	892.2636	891.6915	0.7373
25	892.5911	893.2742	895.7567	893.8740	1.6658
Mean		917.9036			
Minimum		825.7330			
Maximum				995.1530	

Appendix 5 (b): Response Table for Signal to Noise Ratios for pellet particle density

Larger is better

Level	X1	X2	X3
1	59.58	59.69	59.20
2	59.50	59.41	59.06
3	58.74	59.01	59.22
4	59.08	59.01	59.31
5	59.33	59.10	59.43
Delta	0.84	0.69	0.36
Rank	1	2	3

Appendix 5 (c): Response Table for Means for pellet particle density

Level	X1	X2	X3
1	952.8	965.6	913.3
2	944.5	934.6	899.3
3	865.8	892.8	914.9
4	900.2	892.9	924.2
5	926.1	903.6	937.9
Delta	87.0	72.8	38.6
Rank	1	2	3

Appendix 6 (a): Bulk density results (Y2)

RUN	Tri	als	Mean Y2	STDEV
NO.:	{Bulk densi	_		
	1	2		
1	626.0060	628.3312	627.1686	1.6442
2	476.7428	477.8770	477.3099	0.8020
3	603.2196	602.9136	603.0666	0.2164
4	486.5724	488.6895	487.6310	1.4970
5	607.1388	605.5931	606.3660	1.0930
6	584.9800	587.2371	586.1086	1.5960
7	625.6924	623.8801	624.7863	1.2815
8	576.8684	574.2795	575.5740	1.8306
9	551.8400	552.4529	552.1465	0.4334
10	546.7308	547.3475	547.0392	0.4361
11	606.0120	605.1329	605.5725	0.6216
12	543.6620	542.6920	543.1770	0.6859
13	505.3408	505.9753	505.6581	0.4487
14	570.2756	569.9490	570.1123	0.2309
15	501.3324	504.0088	502.6706	1.8925
16	596.0396	596.7720	596.4058	0.5179
17	613.5032	611.1013	612.3023	1.6984
18	606.0840	603.9908	605.0374	1.4801
19	565.0908	566.5670	565.8289	1.0438
20	570.6096	572.1208	571.3652	1.0686
21	612.2892	611.9247	612.1070	0.2577
22	660.9312	662.3032	661.6172	0.9702
23	626.0872	625.9457	626.0165	0.1001
24	608.1916	610.0025	609.0971	1.2805
25	25 551.2708 549.9220		550.5964	0.9537
Mean	•	576.9904		
Minimum			477.3099	
Maximu	m		661.6172	

Appendix 6 (b): Response Table for Signal to Noise Ratios for pellet bulk density

Larger is better

Level	X1	X2	X3
1	54.91	55.64	55.58
2	55.22	55.27	54.79
3	54.71	55.29	55.60
4	55.42	54.89	54.80
5	55.72	54.88	55.21
Delta	1.01	0.76	0.81
Rank	1	3	2

Appendix 6 (c): Response Table for Means for pellet bulk density

Level	X1	X2	X3
1	560.3	605.5	602.2
2	577.1	583.8	551.6
3	545.4	583.1	602.8
4	590.2	557.0	550.7
5	611.9	555.6	577.7
Delta	66.4	49.9	52.1
Rank	1	3	2

Appendix 7 (a): Pellet durability index results (Y3)

RUN		Trials		Mean Y3	STDEV
NO.:	{Pellet durability index (%)}				
	1	2	3		
1	97.0700	96.1289	97.6976	96.9655	0.7896
2	94.7396	94.0928	93.9000	94.2441	0.4398
3	96.2096	95.4918	96.2096	95.9704	0.4145
4	96.2944	96.1965	97.4197	96.6369	0.6797
5	95.7734	97.0734	97.0350	96.6273	0.7397
6	93.8559	95.0360	94.5962	94.4960	0.5964
7	97.3367	97.0351	97.2132	97.1950	0.1516
8	96.6924	96.7375	96.3788	96.6029	0.1954
9	97.8353	97.5228	97.1601	97.5060	0.3379
10	98.2317	97.3986	98.8712	98.1672	0.7384
11	97.7454	96.5077	97.9906	97.4146	0.7949
12	98.2213	97.1965	97.5171	97.6450	0.5243
13	95.9307	96.3199	95.1261	95.7922	0.6089
14	98.5843	97.3529	97.4000	97.7791	0.6978
15	97.2056	95.8022	95.9000	96.3026	0.7835
16	89.7629	88.0401	87.9748	88.5926	1.0141
17	98.7460	98.0025	97.5943	98.1143	0.5839
18	95.6288	96.4794	96.5326	96.2136	0.5071
19	96.5745	97.2630	97.1389	96.9921	0.3669
20	97.6391	97.9133	97.9534	97.8352	0.1711
21	97.8385	98.0819	97.3757	97.7654	0.3587
22	97.8017	98.9942	97.9173	98.2377	0.6577
23	97.7902	98.2938	97.8262	97.9701	0.2809
24	98.6868	97.5326	97.8104	98.0099	0.6024
25	25 96.5294 97.6838 97.5479			97.2537	0.6309
Mean		96.6532			
Minimur	n	88.5926			
Maximu	m	98.2377			

Appendix 7 (b): Response Table for Signal to Noise Ratios for pellet durability index

Larger is better

Level	X1	X2	X3
1	39.65	39.55	39.78
2	39.72	39.74	39.64
3	39.73	39.69	39.76
4	39.60	39.77	39.58
5	39.81	39.76	39.75
Delta	0.21	0.22	0.20
Rank	2	1	3

Appendix 7 (c): Response Table for Means for pellet durability index

Level	X1	X2	X3
1	96.09	95.05	97.47
2	96.79	97.09	96.00
3	96.99	96.51	97.29
4	95.55	97.38	95.35
5	97.85	97.24	97.16
Delta	2.30	2.34	2.13
Rank	2	1	3

Appendix 8 (a): Pellet hardness results (Y4)

RUN		Trials		Mean Y4	STDEV
NO.:	{Pe	llet hardness (N)}		
	1	2	3		
1	996.1610	996.2959	996.3232	996.2601	0.0869
2	577.9680	577.2179	579.8605	578.3488	1.3618
3	586.8555	586.4504	588.1221	587.1427	0.8721
4	627.4675	628.3960	628.4980	628.1205	0.5678
5	918.6295	918.1396	919.7787	918.8493	0.8413
6	922.0315	923.8931	923.4243	923.1163	0.9682
7	747.7440	749.2010	748.6796	748.5415	0.7382
8	754.4240	755.1751	753.4661	754.3551	0.8566
9	704.9215	704.8109	705.2414	704.9913	0.2235
10	595.7515	597.1943	595.8638	596.2699	0.8025
11	696.1635	695.6106	695.2117	695.6619	0.4780
12	590.7655	590.1133	592.0681	590.9823	0.9953
13	586.6720	586.4794	587.4886	586.8800	0.5358
14	541.8075	541.9227	541.7081	541.8128	0.1074
15	571.2485	572.1190	572.9887	572.1187	0.8701
16	560.3115	559.6094	561.9898	560.6369	1.2231
17	586.5295	586.3540	585.8734	586.2523	0.3397
18	740.0345	739.5445	740.9731	740.1840	0.7259
19	598.2620	598.0782	600.2208	598.8537	1.1875
20	574.8390	575.7677	573.9903	574.8656	0.8890
21	915.3270	916.8740	916.9643	916.3884	0.9203
22	954.1270	953.6911	954.6776	954.1652	0.4944
23	771.1235	770.8598	771.5395	771.1743	0.3427
24	734.7135	736.2959	734.7741	735.2612	0.8966
25	631.2915	631.3548	631.6074	631.4179	0.1672
Mean				699.7060	
Minimum				541.8128	
Maximum				996.2601	

Appendix 8 (b): Response Table for Signal to Noise Ratios for pellet hardness

Larger is better

Level	X1	X2	X3
1	57.16	58.07	57.43
2	57.36	56.62	56.60
3	55.50	56.69	56.45
4	55.69	56.10	55.98
5	57.98	56.22	57.24
Delta	2.49	1.97	1.44
Rank	1	2	3

Appendix 8 (c): Response Table for Means for pellet hardness

Level	X1	X2	X3
1	741.7	818.4	765.7
2	745.5	691.7	688.7
3	597.5	687.9	668.3
4	612.2	641.8	633.1
5	801.7	658.7	742.7
Delta	204.2	176.6	132.6
Rank	1	2	3

Appendix 9 (a): Pellet mass yield results (Y5)

RUN		Trials		Mean	STDEV
NO.:	{M	ass yield (%)}	Y5	
	1	2	3		
1	53.3410	55.2760	54.8740	54.4970	1.0211
2	97.8623	97.1237	99.2741	98.0867	1.0926
3	95.7317	97.4511	96.9369	96.7066	0.8826
4	83.3627	84.2858	84.2522	83.9669	0.5236
5	43.8539	44.2625	44.0137	44.0434	0.2059
6	86.3828	86.8261	85.4523	86.2204	0.7011
7	72.1879	72.4109	72.5432	72.3807	0.1795
8	79.5278	79.7307	78.6627	79.3071	0.5672
9	62.8274	63.0942	64.2136	63.3784	0.7355
10	74.9523	74.9724	74.1839	74.7029	0.4495
11	41.2955	40.2994	43.2601	41.6183	1.5065
12	55.2949	55.3803	56.0246	55.5666	0.3989
13	59.9853	61.7820	59.0714	60.2796	1.3790
14	48.8212	47.8392	49.1459	48.6021	0.6803
15	72.0988	72.4995	73.3144	72.6376	0.6194
16	61.1594	61.7675	61.6341	61.5204	0.3196
17	58.7249	58.4429	59.3336	58.8338	0.4552
18	67.3046	69.2427	66.3722	67.6398	1.4643
19	64.1187	65.0504	64.8555	64.6749	0.4914
20	57.5900	56.9240	58.1383	57.5508	0.6081
21	50.1872	49.3567	50.1500	49.8980	0.4691
22	48.7076	49.7349	50.0406	49.4944	0.6983
23	56.4649	58.4383	57.8859	57.5964	1.0180
24	53.0069	52.0535	54.3064	53.1223	1.1308
25	56.2828	56.5178	55.4590	56.0865	0.5560
Mean			64.3365		
Minimum			41.6183		
Maximum			98.0867		

Appendix 9 (b): Response Table for Signal to Noise Ratios for mass yield

Larger is better

Level	X1	X2	X3
1	37.13	35.11	35.28
2	37.48	36.24	37.44
3	34.77	37.02	35.80
4	35.84	35.79	36.42
5	34.51	35.55	34.77
Delta	2.97	1.91	2.66
Rank	1	3	2

Appendix 9 (c): Response Table for Means for mass yield

Level	X1	X2	X3
1	75.46	58.75	58.99
2	75.20	66.87	75.84
3	55.74	72.31	64.28
	62.04	62.75	67.29
5	53.24	61.00	55.29
Delta	22.22	13.56	20.56
Rank	1	3	2

Appendix 10 (a): Pellet's higher heating values results (Y6)

		Trials			
RUN	{Higher hea		es (MJ/kg)}	Mean	
NO.:	1	2	3	Y6	STDEV
1	29.649	28.666	30.088	29.468	0.728
2	24.082	23.832	25.144	24.353	0.697
3	28.784	29.938	28.624	29.115	0.717
4	27.701	27.394	27.450	27.515	0.164
5	29.110	29.272	30.453	29.612	0.733
6	21.708	23.207	22.488	22.468	0.750
7	22.398	21.510	21.920	21.943	0.445
8	25.698	26.059	27.588	26.448	1.003
9	23.889	24.705	24.080	24.225	0.427
10	24.741	24.515	25.559	24.939	0.549
11	23.905	25.482	23.233	24.207	1.155
12	28.863	28.112	30.311	29.095	1.118
13	21.106	20.373	21.751	21.077	0.690
14	29.296	29.049	29.789	29.378	0.377
15	29.524	30.583	31.121	30.409	0.812
16	23.175	22.972	24.372	23.506	0.756
17	27.245	27.029	26.761	27.012	0.243
18	28.699	27.852	29.088	28.546	0.632
19	28.170	29.887	29.506	29.188	0.902
20	27.477	27.731	28.029	27.746	0.276
21	27.291	29.124	28.245	28.220	0.917
22	22.712	22.984	23.629	23.108	0.471
23	26.903	28.230	28.140	27.758	0.742
24	30.502	31.691	31.163	31.119	0.596
25	27.828	28.528	29.076	28.478	0.626
Mean			26.757		
Minimum			21.077		
Maximu	 m			31.119	

Appendix 10 (c): Response Table for Signal to Noise Ratios for HHV(MJ/kg)

Larger is better

Level	X1	X2	X3
1	28.92	28.11	28.61
2	27.59	27.95	28.52
3	28.49	28.44	28.50
4	28.67	29.00	28.61
5	28.82	29.00	28.25
Delta	1.34	1.05	0.37
Rank	1	2	3

Appendix 10 (c): Response Table for Means for HHV(MJ/kg)

Level	X1	X2	X3
1	28.01	25.57	27.09
2	24.00	25.10	26.83
3	26.83	26.59	26.83
	27.20	28.28	27.01
5	27.74	28.24	26.03
Delta	4.01	3.18	1.06
Rank	1	2	3

Appendix 11 (a): Carbon dioxide emissions results (Y7)

	Trials			
RUN	Carbon dioxid			
NO.	1	2	Mean Y7	STDEV
1	2.96	3.02	2.99	0.04
2	1.58	1.70	1.64	0.08
3	2.48	2.52	2.50	0.03
5	1.38	1.44	1.41	0.04
5	1.68	1.81	1.75	0.09
6	1.34	1.46	1.40	0.08
7	1.07	1.22	1.15	0.11
8	5.02	6.37	5.70	0.95
9	6.55	6.97	6.76	0.30
10	6.38	7.44	6.91	0.75
11	0.97	2.99	1.98	1.43
12	1.58	3.14	2.36	1.10
13	2.03	2.16	2.10	0.09
14	1.80	1.92	1.86	0.08
15	1.46	4.22	2.84	1.95
16	3.16	3.46	3.31	0.21
17	2.68	3.24	2.96	0.40
18	2.81	3.33	3.07	0.37
19	3.18	3.67	3.43	0.35
20	1.90	2.44	2.17	0.38
21	3.38	3.47	3.43	0.06
22	1.55	2.50	2.03	0.67
23	4.85	4.89	4.87	0.03
24	3.87	4.32	4.10	0.32
25	4.12	4.18	4.15	0.04
Mean			3.07	
Minimum			1.15	
Maximu	m		6.91	

Appendix 11 (b): Response Table for Signal to Noise Ratios for carbon dioxide emissions

Smaller is better

Level	X1	X2	X3
1	-5.918	-7.892	-9.513
2	-10.519	-5.697	-8.146
3	-6.854	-10.597	-6.808
4	-9.398	-9.582	-9.662
5	-11.036	-9.956	-9.596
Delta	5.118	4.900	2.854
Rank	1	2	3

Appendix 11 (c): Response Table for Means for carbon dioxide emissions

Level	X1	X2	X3
1	2.057	2.621	3.371
	4.382	2.026	2.835
3	2.227	3.646	2.378
4	2.987	3.510	3.385
5	3.713	3.563	3.397
Delta	2.325	1.620	1.019
Rank	1	2	3

Appendix 12: Computation of signal to noise ratios (S/N), Normalized data (Z_{ij}), quality loss (Δ) and grey relational coefficient (GC_{ij}) for pellet particle density (Y1)

SR		Trials		S/N	Zij	Δ	GCij
NO.:	1	2	3				
1	966.26	966.98	965.35	59.7013	0.8418	0.1582	0.8634
2	938.85	938.21	937.81	59.44676	0.6847	0.3153	0.7603
3	933.46	932.69	931.74	59.39421	0.6523	0.3477	0.7420
4	945.08	944.56	942.27	59.49914	0.7171	0.2829	0.7795
5	985.26	981.47	982.51	59.85174	0.9346	0.0654	0.9386
6	963.20	963.15	961.17	59.66806	0.8213	0.1787	0.8484
7	945.59	945.14	944.48	59.50931	0.7233	0.2767	0.7833
8	930.53	931.17	932.64	59.38314	0.6455	0.3545	0.7383
9	928.60	929.92	926.68	59.35468	0.6279	0.3721	0.7288
10	956.54	955.71	953.44	59.60212	0.7806	0.2194	0.8201
11	943.29	946.07	945.33	59.50766	0.7223	0.2777	0.7827
12	894.53	892.48	890.87	59.01334	0.4174	0.5826	0.6319
13	833.20	833.94	831.11	58.41027	0.0453	0.9547	0.5116
14	832.62	831.98	834.96	58.41483	0.0481	0.9519	0.5123
15	826.91	824.34	825.95	58.33677	0.0000	1.0000	0.5000
16	960.86	957.54	959.11	59.6379	0.8027	0.1973	0.8352
17	951.80	949.52	948.76	59.55469	0.7513	0.2487	0.8008
18	865.92	865.60	862.39	58.73663	0.2467	0.7533	0.5703
19	866.10	866.75	868.28	58.76079	0.2616	0.7384	0.5752
20	859.89	860.14	860.52	58.6918	0.2190	0.7810	0.5615
21	993.56	996.43	995.47	59.95778	1.0000	0.0000	1.0000
22	946.50	947.87	946.98	59.52807	0.7349	0.2651	0.7904
23	901.57	903.47	903.00	59.11067	0.4774	0.5226	0.6568
24	891.95	890.86	892.26	59.00429	0.4118	0.5882	0.6296
25	892.59	893.27	895.76	59.0255	0.4249	0.5751	0.6349
			max	59.9578			
			min	58.3368			

Appendix 13: Computation of signal to noise ratios (S/N), Normalized data (Z_{ij}), quality loss (Δ) and grey relational coefficient (GC_{ij}) for bulk density (Y2).

	Tr	ials				
SR NO.:	1	2	S/N	Zij	Δ	GCij
1	626.01	628.33	55.9476	0.8362	0.1638	0.8593
2	476.74	477.88	53.5760	0.0000	1.0000	0.5000
3	603.22	602.91	55.6073	0.7162	0.2838	0.7790
4	486.57	488.69	53.7618	0.0655	0.9345	0.5169
5	607.14	605.59	55.6547	0.7329	0.2671	0.7892
6	584.98	587.24	55.3595	0.6289	0.3711	0.7293
7	625.69	623.88	55.9146	0.8246	0.1754	0.8508
8	576.87	574.28	55.2020	0.5733	0.4267	0.7009
9	551.84	552.45	54.8411	0.4461	0.5539	0.6435
10	546.73	547.35	54.7604	0.4176	0.5824	0.6320
11	606.01	605.13	55.6433	0.7289	0.2711	0.7867
12	543.66	542.69	54.6988	0.3959	0.6041	0.6234
13	505.34	505.98	54.0771	0.1767	0.8233	0.5485
14	570.28	569.95	55.1192	0.5441	0.4559	0.6869
15	501.33	504.01	54.0256	0.1585	0.8415	0.5430
16	596.04	596.77	55.5108	0.6822	0.3178	0.7588
17	613.50	611.10	55.7393	0.7628	0.2372	0.8083
18	606.08	603.99	55.6356	0.7262	0.2738	0.7851
19	565.09	566.57	55.0537	0.5210	0.4790	0.6761
20	570.61	572.12	55.1383	0.5508	0.4492	0.6901
21	612.29	611.92	55.7365	0.7618	0.2382	0.8076
22	660.93	662.30	56.4121	1.0000	0.0000	1.0000
23	626.09	625.95	55.9317	0.8306	0.1694	0.8552
24	608.19	610.00	55.6937	0.7467	0.2533	0.7979
25	551.27	549.92	54.8166	0.4374	0.5626	0.6400
		Max	56.4121			
		Min	53.5760			

Appendix 14: Computation of signal to noise ratios (S/N), Normalized data (Z_{ij}), quality loss (Δ) and grey relational coefficient (GC $_{ij}$) for pellet durability index (Y3).

SR		Trials		S/N	Zij	Δ	GCij
NO.:	1	2	3				
1	97.07	96.13	97.70	39.7318	0.8738	0.1262	0.8879
2	94.74	94.09	93.90	39.4849	0.5990	0.4010	0.7138
3	96.21	95.49	96.21	39.6426	0.7745	0.2255	0.8160
4	96.29	96.20	97.42	39.7024	0.8411	0.1589	0.8629
5	95.77	97.07	97.04	39.7015	0.8400	0.1600	0.8621
6	93.86	95.04	94.60	39.5079	0.6246	0.3754	0.7271
7	97.34	97.04	97.21	39.7529	0.8972	0.1028	0.9068
8	96.69	96.74	96.38	39.6998	0.8381	0.1619	0.8607
9	97.84	97.52	97.16	39.7805	0.9280	0.0720	0.9329
10	98.23	97.40	98.87	39.8388	0.9929	0.0071	0.9930
11	97.75	96.51	97.99	39.7719	0.9184	0.0816	0.9246
12	98.22	97.20	97.52	39.7927	0.9416	0.0584	0.9449
13	95.93	96.32	95.13	39.6263	0.7563	0.2437	0.8041
14	98.58	97.35	97.40	39.8045	0.9547	0.0453	0.9567
15	97.21	95.80	95.90	39.6722	0.8074	0.1926	0.8385
16	89.76	88.04	87.97	38.9468	0.0000	1.0000	0.5000
17	98.75	98.00	97.59	39.8343	0.9879	0.0121	0.9881
18	95.63	96.48	96.53	39.6645	0.7989	0.2011	0.8325
19	96.57	97.26	97.14	39.7346	0.8769	0.1231	0.8904
20	97.64	97.91	97.95	39.8099	0.9607	0.0393	0.9622
21	97.84	98.08	97.38	39.8036	0.9537	0.0463	0.9557
22	97.80	98.99	97.92	39.8452	1.0000	0.0000	1.0000
23	97.79	98.29	97.83	39.8218	0.9740	0.0260	0.9746
24	98.69	97.53	97.81	39.8251	0.9776	0.0224	0.9781
25	96.53	97.68	97.55	39.7578	0.9027	0.0973	0.9113
			max	39.8452			
			min	38.9468			

Appendix 15: Computation of signal to noise ratios (S/N), Normalized data (Z_{ij}), quality loss (Δ) and grey relational coefficient (GC_{ij}) for pellet hardness (Y4).

SR NO.:		Trials		S/N	Zij	Δ	GCij
	1	2	3				
1	996.1610	996.2959	996.3232	59.9675	1.0000	0.0000	1.0000
2	577.9680	577.2179	579.8605	55.2437	0.1071	0.8929	0.5283
3	586.8555	586.4504	588.1221	55.3749	0.1319	0.8681	0.5353
4	627.4675	628.3960	628.4980	55.9609	0.2427	0.7573	0.5690
5	918.6295	918.1396	919.7787	59.2649	0.8672	0.1328	0.8828
6	922.0315	923.8931	923.4243	59.3051	0.8748	0.1252	0.8887
7	747.7440	749.2010	748.6796	57.4843	0.5306	0.4694	0.6806
8	754.4240	755.1751	753.4661	57.5515	0.5433	0.4567	0.6865
9	704.9215	704.8109	705.2414	56.9637	0.4322	0.5678	0.6378
10	595.7515	597.1943	595.8638	55.5088	0.1572	0.8428	0.5427
11	696.1635	695.6106	695.2117	56.8480	0.4104	0.5896	0.6291
12	590.7655	590.1133	592.0681	55.4315	0.1426	0.8574	0.5384
13	586.6720	586.4794	587.4886	55.3710	0.1312	0.8688	0.5351
14	541.8075	541.9227	541.7081	54.6770	0.0000	1.0000	0.5000
15	571.2485	572.1190	572.9887	55.1497	0.0894	0.9106	0.5234
16	560.3115	559.6094	561.9898	54.9736	0.0561	0.9439	0.5144
17	586.5295	586.3540	585.8734	55.3617	0.1294	0.8706	0.5346
18	740.0345	739.5445	740.9731	57.3868	0.5122	0.4878	0.6721
19	598.2620	598.0782	600.2208	55.5464	0.1643	0.8357	0.5448
20	574.8390	575.7677	573.9903	55.1913	0.0972	0.9028	0.5255
21	915.3270	916.8740	916.9643	59.2416	0.8628	0.1372	0.8794
22	954.1270	953.6911	954.6776	59.5925	0.9291	0.0709	0.9338
23	771.1235	770.8598	771.5395	57.7430	0.5795	0.4205	0.7040
24	734.7135	736.2959	734.7741	57.3288	0.5012	0.4988	0.6672
25	631.2915	631.3548	631.6074	56.0063	0.2513	0.7487	0.5718
			max	59.9675			
			min	54.6770			

Appendix 16: Computation of signal to noise ratios (S/N), Normalized data (Z_{ij}), quality loss (Δ) and grey relational coefficient (GC_{ij}) for mass yield (Y5).

SR		Trials		S/N	Zij	Δ	GCij
NO.:	1	2	3				
1	53.34	55.28	54.87	34.7244	0.3151	0.6849	0.5935
2	97.86	97.12	99.27	39.8311	1.0000	0.0000	1.0000
3	95.73	97.45	96.94	39.7084	0.9835	0.0165	0.9838
4	83.36	84.29	84.25	38.4818	0.8190	0.1810	0.8468
5	43.85	44.26	44.01	32.8774	0.0674	0.9326	0.5175
6	86.38	86.83	85.45	38.7116	0.8499	0.1501	0.8695
7	72.19	72.41	72.54	37.1924	0.6461	0.3539	0.7386
8	79.53	79.73	78.66	37.9858	0.7525	0.2475	0.8016
9	62.83	63.09	64.21	36.0377	0.4913	0.5087	0.6628
10	74.95	74.97	74.18	37.4664	0.6829	0.3171	0.7592
11	41.30	40.30	43.26	32.3745	0.0000	1.0000	0.5000
12	55.29	55.38	56.02	34.8958	0.3381	0.6619	0.6017
13	59.99	61.78	59.07	35.5989	0.4324	0.5676	0.6379
14	48.82	47.84	49.15	33.7314	0.1820	0.8180	0.5500
15	72.10	72.50	73.31	37.2226	0.6502	0.3498	0.7408
16	61.16	61.77	61.63	35.7801	0.4567	0.5433	0.6480
17	58.72	58.44	59.33	35.3920	0.4047	0.5953	0.6268
18	67.30	69.24	66.37	36.6000	0.5667	0.4333	0.6977
19	64.12	65.05	64.86	36.2142	0.5149	0.4851	0.6734
20	57.59	56.92	58.14	35.2001	0.3789	0.6211	0.6169
21	50.19	49.36	50.15	33.9609	0.2128	0.7872	0.5595
22	48.71	49.73	50.04	33.8894	0.2032	0.7968	0.5565
23	56.46	58.44	57.89	35.2052	0.3796	0.6204	0.6171
24	53.01	52.05	54.31	34.5016	0.2853	0.7147	0.5832
25	56.28	56.52	55.46	34.9763	0.3489	0.6511	0.6057
			max	39.8311			
			min	32.3745			

Appendix 17: Computation of signal to noise ratios (S/N), Normalized data (Z_{ij}), quality loss (Δ) and grey relational coefficient (GC_{ij}) for pellet's higher heating value (Y6).

SR		Trials		S/N	Zij	Δ	GCij
NO.:	1	2	3				
1	29.6490	28.6660	30.0877	29.3815	0.8597	0.1403	0.8769
2	24.0820	23.8319	25.1442	27.7240	0.3708	0.6292	0.6138
3	28.7840	29.9383	28.6240	29.2773	0.8289	0.1711	0.8539
4	27.7010	27.3936	27.4497	28.7910	0.6855	0.3145	0.7608
5	29.1100	29.2721	30.4525	29.4240	0.8722	0.1278	0.8867
6	21.7080	23.2066	22.4882	27.0214	0.1636	0.8364	0.5445
7	22.3980	21.5095	21.9203	26.8222	0.1049	0.8951	0.5277
8	25.6980	26.0586	27.5880	28.4357	0.5807	0.4193	0.7046
9	23.8890	24.7054	24.0803	27.6826	0.3586	0.6414	0.6092
10	24.7410	24.5153	25.5594	27.9333	0.4325	0.5675	0.6380
11	23.9050	25.4825	23.2327	27.6594	0.3518	0.6482	0.6067
12	28.8630	28.1124	30.3109	29.2639	0.8250	0.1750	0.8511
13	21.1060	20.3728	21.7512	26.4667	0.0000	1.0000	0.5000
14	29.2960	29.0488	29.7895	29.3590	0.8531	0.1469	0.8719
15	29.5240	30.5828	31.1208	29.6538	0.9400	0.0600	0.9434
16	23.1750	22.9722	24.3720	27.4149	0.2797	0.7203	0.5813
17	27.2450	27.0292	26.7605	28.6303	0.6381	0.3619	0.7343
18	28.6990	27.8523	29.0880	29.1067	0.7786	0.2214	0.8188
19	28.1700	29.8872	29.5056	29.2955	0.8343	0.1657	0.8579
20	27.4770	27.7313	28.0289	28.8631	0.7068	0.2932	0.7733
21	27.2910	29.1242	28.2454	29.0020	0.7478	0.2522	0.7986
22	22.7120	22.9843	23.6286	27.2718	0.2374	0.7626	0.5674
23	26.9030	28.2302	28.1397	28.8613	0.7063	0.2937	0.7730
24	30.5020	31.6911	31.1634	29.8573	1.0000	0.0000	1.0000
25	27.8280	28.5285	29.0762	29.0858	0.7725	0.2275	0.8147
			max	29.8573			
			min	26.4667			

Appendix 18: Computation of signal to noise ratios (S/N), Normalized data (Z_{ij}), quality loss (Δ) and grey relational coefficient (GC_{ij}) for pellet's carbon dioxide emissions (Y7).

RUN NO.	Tri	als	S/N	Zij	Δ	GCij
	1	2		_		_
1	2.96	3.02	-9.5139	0.5326	0.4674	0.6815
2	1.58	1.7	-4.3027	0.1990	0.8010	0.5552
3	2.48	2.52	-7.9591	0.4331	0.5669	0.6382
4	1.38	1.44	-2.9863	0.1147	0.8853	0.5304
5	1.68	1.81	-4.8419	0.2335	0.7665	0.5661
6	1.34	1.46	-2.9305	0.1111	0.8889	0.5294
7	1.07	1.22	-1.1947	0.0000	1.0000	0.5000
8	5.02	6.37	-15.1705	0.8947	0.1053	0.9047
9	6.55	6.97	-16.6031	0.9864	0.0136	0.9866
10	6.38	7.44	-16.8150	1.0000	0.0000	1.0000
11	0.97	2.99	-6.9377	0.3677	0.6323	0.6126
12	1.58	3.14	-7.9085	0.4298	0.5702	0.6369
13	2.03	2.16	-6.4279	0.3350	0.6650	0.6006
14	1.8	1.92	-5.3948	0.2689	0.7311	0.5777
15	1.46	4.22	-9.9870	0.5629	0.4371	0.6958
16	3.16	3.46	-10.4055	0.5897	0.4103	0.7091
17	2.68	3.24	-9.4645	0.5294	0.4706	0.6800
18	2.81	3.33	-9.7738	0.5492	0.4508	0.6893
19	3.18	3.67	-10.7154	0.6095	0.3905	0.7192
20	1.9	2.44	-6.7959	0.3586	0.6414	0.6092
21	3.38	3.47	-10.6940	0.6081	0.3919	0.7185
22	1.55	2.5	-6.3611	0.3308	0.6692	0.5991
23	4.85	4.89	-13.7507	0.8038	0.1962	0.8360
24	3.87	4.32	-12.2582	0.7083	0.2917	0.7742
25	4.12	4.18	-12.3612	0.7149	0.2851	0.7781
			-1.1947			
			-16.8150			

Appendix 19: Computation and ranking of grey relational grade from grey relational coefficient of responses

RUN									S/N for	Rank
NO.:	GCijY2	GCijY3	GCijY1	GCijY5	GCijY4	GCijY6	GCijY7	Gi	Gi	rum
	0.0502	0.0050	0.0624	0.5025	1 0000		0.601.5	0.0000	-1.6897	1
1	0.8593	0.8879	0.8634	0.5935	1.0000	0.8769	0.6815	0.8232		
2	0.5000	0.7138	0.7603	1.0000	0.5283	0.6138	0.5552	0.6673	-3.5130	22
3	0.7790	0.8160	0.7420	0.9838	0.5353	0.8539	0.6382	0.7640	-2.3378	9
4	0.5169	0.8629	0.7795	0.8468	0.5690	0.7608	0.5304	0.6952	-3.1580	17
5	0.7892	0.8621	0.9386	0.5175	0.8828	0.8867	0.5661	0.7776	-2.1853	4
6	0.7293	0.7271	0.8484	0.8695	0.8887	0.5445	0.5294	0.7338	-2.6879	12
7	0.8508	0.9068	0.7833	0.7386	0.6806	0.5277	0.5000	0.7125	-2.9439	14
8	0.7009	0.8607	0.7383	0.8016	0.6865	0.7046	0.9047	0.7710	-2.2584	7
9	0.6435	0.9329	0.7288	0.6628	0.6378	0.6092	0.9866	0.7431	-2.5790	10
10	0.6320	0.9930	0.8201	0.7592	0.5427	0.6380	1.0000	0.7693	-2.2785	8
11	0.7867	0.9246	0.7827	0.5000	0.6291	0.6067	0.6126	0.6918	-3.2008	18
12	0.6234	0.9449	0.6319	0.6017	0.5384	0.8511	0.6369	0.6897	-3.2263	19
13	0.5485	0.8041	0.5116	0.6379	0.5351	0.5000	0.6006	0.5911	-4.5667	25
14	0.6869	0.9567	0.5123	0.5500	0.5000	0.8719	0.5777	0.6651	-3.5427	23
15	0.5430	0.8385	0.5000	0.7408	0.5234	0.9434	0.6958	0.6836	-3.3043	20
16	0.7588	0.5000	0.8352	0.6480	0.5144	0.5813	0.7091	0.6495	-3.7479	24
17	0.8083	0.9881	0.8008	0.6268	0.5346	0.7343	0.6800	0.7390	-2.6273	11
18	0.7851	0.8325	0.5703	0.6977	0.6721	0.8188	0.6893	0.7237	-2.8090	13
19	0.6761	0.8904	0.5752	0.6734	0.5448	0.8579	0.7192	0.7053	-3.0328	16
20	0.6901	0.9622	0.5615	0.6169	0.5255	0.7733	0.6092	0.6769	-3.3889	21
21	0.8076	0.9557	1.0000	0.5595	0.8794	0.7986	0.7185	0.8170	-1.7552	2
22	1.0000	1.0000	0.7904	0.5565	0.9338	0.5674	0.5991	0.7782	-2.1785	3
23	0.8552	0.9746	0.6568	0.6171	0.7040	0.7730	0.8360	0.7738	-2.2274	6
24	0.7979	0.9781	0.6296	0.5832	0.6672	1.0000	0.7742	0.7757	-2.2057	5
25	0.6400	0.9113	0.6349	0.6057	0.5718	0.8147	0.7781	0.7081	-2.9985	15

Abbreviations: GCijY1 - grey relational coefficient for computed pellet particle density.

GCijY2-grey relational coefficient for computed pellet bulk density.

GCijY3 - grey relational coefficient for computed pellet durability

index.

GCijY4 - grey relational coefficient for computed pellet hardness.

GCijY5 - grey relational coefficient for computed mass yield.

GCijY6 – grey relational coefficient for higher heating values.

GCijY7 - grey relational coefficient for computed carbon dioxide

emissions.

Gi – grey relational grade

Appendix 20 (a): Computed grey relational grade (Gi) and their signal to noise ratios (S/N)

CD MO	G.	C/NI
SR NO.	Gi	S/N
1	0.8232	-1.6897
2	0.6673	-3.5130
3	0.7640	-2.3378
4	0.6952	-3.1580
5	0.7776	-2.1853
6	0.7338	-2.6879
7	0.7125	-2.9439
8	0.7710	-2.2584
9	0.7431	-2.5790
10	0.7693	-2.2785
11	0.6918	-3.2008
12	0.6897	-3.2263
13	0.5911	-4.5667
14	0.6651	-3.5427
15	0.6836	-3.3043
16	0.6495	-3.7479
17	0.7390	-2.6273
18	0.7237	-2.8090
19	0.7053	-3.0328
20	0.6769	-3.3889
21	0.8170	-1.7552
22	0.7782	-2.1785
23	0.7738	-2.2274
24	0.7757	-2.2057
25	0.7081	-2.9985

Appendix 20 (b): Response Table for Signal to Noise Ratios for Gi

Larger is better

Level	X1	X2	X3
1	-2.577	-2.616	-2.500
2	-2.550	-2.898	-2.953
3	-3.568	-2.840	-2.815
4	-3.121	-2.904	-3.078
5	-2.273	-2.831	-2.743
Delta	1.295	0.287	0.578
Rank	1	3	2

Appendix 20 (c): Response Table for Means for Gi

Level	X1	X2	X3
1	0.7455	0.7431	0.7519
2	0.7460	0.7174	0.7128
3	0.6642	0.7247	0.7242
4	0.6989	0.7169	0.7027
5	0.7706	0.7231	0.7336
Delta	0.1063	0.0262	0.0492
Rank	1	3	2

Appendix 21: Experimental set-up of emissions testing at LEMS



Appendix 22: Combustion of optimized blended pellet in a pellet stove





Appendix 23: Publications

The following articles were as a result of this thesis:

Lazarus Kiprop Limo, Diana Starovoytova Madara, Obadiah Maube

Enhancing herbaceous biomass pellets quality by blending with woody biomass and plastic additives, and post-pelletization torrefaction and optimization processes: A review. https://doi.org/10.7176/jetp/14-2-02

Lazarus Kiprop Limo 1, *, Diana Starovoytova Madara 2, and Jerry Ochola 3Characterization of Corn Stover and Eucalyptus Sawdust for Pellet Productionhttp://dx.doi.org/10.24018/ejenergy.2024.4.2.135

Appendix 23: Antiplagiarism certificate



SR708

ISO 9001:2019 Certified Institution

THESIS WRITING COURSE

PLAGIARISM AWARENESS CERTIFICATE

This certificate is awarded to

LAZARUS KIPROP LIMO

PHD/IE/5312/22

In recognition for passing the University's plagiarism

Awareness test for Thesis entitled: PERFORMANCE OPTIMIZATION OF BLENDED BIOMASS PELLETS FROM CORN STOVER AND EUCALYPTUS SAWDUST USING LINEAR LOW-DENSITY POLYETHYLENE AS A BINDER similarity index of 15% and striving to maintain academic integrity.

Word count:50855 Awarded by

Prof. Anne Syomwene Kisilu

CERM-ESA Project Leader Date: 23/09//2024